

Dissertation zur Erlangung des Doktorgrades

Fakultät für Chemie und Pharmazie

Ludwig-Maximilians-Universität München



**Synthesis and biological evaluation of novel N-substituted
nipecotic acid derivatives with an alkyne, *trans*-alkene or *cis*-alkene
spacer as GABA uptake inhibitors**

Krisztián Csaba Tóth

aus Kerepestarcsa, Ungarn

2018

Erklärung

Diese Dissertation wurde im Sinne von § 7 Abs. 1 bzw. 2 der Promotionsordnung vom
01. August 2013 von Herrn Prof. Dr. Klaus T. Wanner betreut.

Eidesstattliche Versicherung

Diese Dissertation wurde eigenständig und ohne unerlaubte Hilfe erarbeitet.

München, den 20.11.2018

.....
(Krisztián Tóth)

Dissertation eingereicht am	22.11.2018
1. Gutachter	Prof. Dr. Klaus T. Wanner
2. Gutachter	Prof. Dr. Franz Paintner
Mündliche Prüfung am	18.12.2018

Die vorliegende Arbeit entstand in der Zeit von August 2013 bis Dezember 2018
am für Department Pharmazie – Zentrum für Pharmaforschung –
der Ludwig-Maximilians-Universität München auf Anregung und unter Leitung von

Herrn Prof. Dr. Klaus T. Wanner

Für die engagierte, ausgezeichnete und sehr hilfreiche Betreuung und Förderung
meiner Arbeit sowie die hervorragenden Forschungsbedingungen danke ich

Herrn Prof. Dr. Klaus T. Wanner sehr herzlich.

Herrn Prof. Dr. Paintner danke ich herzlich

für die Übernahme des Korreferats.

Danksagung

Ich möchte mich bei meinen Freunden und Kollegen aus dem Arbeitskreis von Professor Dr. Wanner für die freundliche Aufnahme in diese Gruppe, die ausgezeichnete Arbeitsatmosphäre, die gute Zusammenarbeit in der Praktikumsbetreuung und die fröhliche Zeit, die wir neben der Arbeit hatten bedanken.

Besonderer Dank gilt an meinen ehemaligen Laborkollegen Tim Hellenbrand, Davia Prischich, Heinrich Rudy und Janina Andreß für die super Zeit im und rund ums Labor.

Dr. Georg Höfner sowie dem gesamten Team der biologischen Prüfabteilung, insbesondere Silke Duensing-Kropp, Tanja Franz und Miriam Sandner, danke ich sehr für die Testung der von mir synthetisierten Verbindungen.

Dr. Lars Allmendinger und den Mitarbeiterinnen der analytischen Abteilung, insbesondere Claudia Glas und Ursula Groß gilt besonderer Dank für die Messung all meiner IR-, MS- und NMR-Spektren.

Katharina Heimberger und Annerose Kärtner danke ich für die Unterstützung bei allen organisatorischen Aufgaben sowie die Versorgung mit Büro- und Labormaterialien.

Für die Molecular Modeling Präsentationen und die Erläuterungen zum Struktur-basierten Moleküldesign bin ich Herrn Dr. Thomas Wein sehr dankbar.

Für die hervorragende Organisation der von mir betreuten Studentenpraktika möchte ich Herrn Dr. Jörg Pabel und Herrn Dr. Jürgen Krauss herzlich danken. Dr. Jörg Pabel danke ich außerdem für das Korrekturlesen meiner Publikationen.

Ich möchte meiner Familie für die kontinuierliche Unterstützung während meines Studiums danken und dass sie meine Promotion ermöglicht hat.

This cumulative thesis is based on the following original publications and manuscripts:

Reprinted with permission,

Krisztián Tóth, Georg Höfner, Klaus T. Wanner;

Bioorganic & Medicinal Chemistry, **2018**, Volume 26, Issue 12, 3668-3687.

“Synthesis and biological evaluation of novel N-substituted nipecotic acid derivatives with an alkyne spacer as GABA uptake inhibitors”

Krisztián Tóth, Georg Höfner, Klaus T. Wanner;

Bioorganic & Medicinal Chemistry, **2018**, Volume 26, Issue 22, 5944-5961.

“Synthesis and biological evaluation of novel N-substituted nipecotic acid derivatives with a *trans*-alkene spacer as potent GABA uptake inhibitors”

Krisztián Tóth, Georg Höfner, Klaus T. Wanner;

Manuscript to be submitted to Bioorganic & Medicinal Chemistry.

“Synthesis and biological evaluation of novel N-substituted nipecotic acid derivatives with a *cis*-alkene spacer as GABA uptake inhibitors”

Copyright of the publications belong to the publishers.

Table of contents

1. INTRODUCTION	1
1.1. CNS and GABA related diseases.....	2
1.1.1. <i>GABA neurotransmission</i>	3
1.1.2. <i>Treatment possibilities and side effects</i>	4
1.2. GABA transporters	5
1.2.1. <i>GAT subtypes</i>	6
1.2.2. <i>Structure and transport mechanism of SLC6 transporters</i>	7
1.2.3. <i>GATs as drug targets</i>	9
1.2.3.1. mGAT1 selective inhibitors.....	10
1.2.3.2. Selective inhibitors of mGAT2	12
1.2.3.3. mGAT3 and mGAT4 selective inhibitors	13
2. AIMS AND SCOPE	15
2.1. Development of N-substituted nipecotic acid derivatives as selective mGAT4 reuptake inhibitors	15
2.2. Coupling methods.....	17
2.2.1. <i>Iminium salts</i>	17
2.2.2. <i>Hydrozirconation</i>	18
3. SUMMARY OF MANUSCRIPTS AND PUBLISHED RESULTS	19
3.1. First publication: Synthesis and biological evaluation of novel N-substituted nipecotic acid derivatives with an alkyne spacer as GABA uptake inhibitors.....	19
3.2. Second publication: Synthesis and biological evaluation of novel N-substituted nipecotic acid derivatives with a <i>trans</i> -alkene spacer as potent GABA uptake inhibitors	21
3.3. Manuscript of the third publication: Synthesis and biological evaluation of novel N-substituted nipecotic acid derivatives with a <i>cis</i> -alkene spacer as GABA uptake inhibitors.....	23
4. SUMMARY OF THE THESIS	24
5. LIST OF ABBREVIATIONS	26
6. LITERATURE	27
7. PUBLICATIONS AND MANUSCRIPTS	31

1. Introduction

Medicinal chemistry is an important field of research where chemistry and pharmacology are working together to find relations between chemical structures and their biological effect. Chemical structures with pharmacological activity can be naturally occurring and obtained from diverse sources like animal or plant material or can be chemically synthesized. To identify and characterize such active compounds from huge libraries diverse high-throughput screening methods were developed during the last decades. The most promising hits can then be used as a lead structure in the design and development of the following pharmaceutical development. Usually, the identification of the biological target responsible for the pharmacological effect is the first essential step for drug research, which can be an enzyme or a membrane-bound protein like receptors or transporters. In possession of such a protein structure, it is possible to use computer-based screening methods, which are faster and more cost effective.

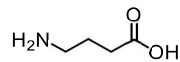
For this purpose, two different strategies can be applied during the screenings. First, if the exact 3D structure of the designated target bound with a ligand is known, usually from X-ray crystallography experiments, then we talk about the “target-based drug design”. By knowing the detailed interactions between the ligand and the binding site we can fit various ligands into the binding pocket (docking) and calculate the binding affinities as docking scores. By comparing these scores, it is possible to create a new structure with possible similar or even better affinity for the target.[1] As the second method, the “ligand-based drug design” can be used, if the target structure is not known. In this case, the design of new active compounds is based on the physiochemical properties of known ligands, from which a pharmacophore model is generated to describe the interactions between ligand and target. Through this model, suitable substance libraries can be screened (*in silico*) to find new active compounds, which can be later synthesized and evaluated in biological tests.[2]

The so discovered most active compounds (hits) can be selected to aid as the parent structure for further optimization (lead structure). Through stepwise chemical modifications and screening of the modified structures, the goal is to find the optimal chemical and physiological properties to acquire more potent and/ or more selective active compounds to the target. The obtained evaluation results can be used to set up a structure-activity relationship (SAR) to support the further optimization of the selected lead structure.

1.1. CNS and GABA related diseases

The central nervous system (CNS) can be involved in a wide-ranging variety of diseases. These neurological disorders can include dementia, depression, epilepsy, multiple sclerosis, neuropathic pain, and Parkinson's disease.[3,4,5,6,7] The most widespread from them is epilepsy, affecting over 50 million patients worldwide.[8] More than 15 different antiepileptic drugs can be used for its treatment, but in many cases the medication is not helping or causing significant side effects, making the research for new, more effective drugs necessary.[9,10]

An important cause of these diseases is a disturbance in the GABAergic neurotransmission in the CNS. The most important inhibitory neurotransmitter in the CNS γ -aminobutyric acid (GABA, **1**) is depicted in Figure 1.[11] Its role, function, and possible ways to influence GABA levels in the CNS will be discussed in the following section.



GABA (**1**)

Figure 1. The γ -aminobutyric acid (GABA) neurotransmitter.

1.1.1. GABA neurotransmission

During the biosynthesis of GABA, glutamate (GLU) is decarboxylated by glutamic acid decarboxylase (GAD) in the presynaptic neuron. The formed GABA is transported and stored into vesicles by the vesicular transporter (VGAT) from where it is released into the synaptic cleft upon depolarization. In the synaptic cleft, GABA can interact with two different GABA receptors at the pre- and post-synaptic side, as it is presented in Figure 2. One type, the ionotropic GABA_A receptors are located on the postsynaptic side and mediate fast signal transduction as ligand controlled chloride channels. The second type, the metabotropic GABA_B receptors, belong to the G-protein coupled receptors (GPCR) and can be found on the pre- and post-synaptic side and on the surrounding glial cells as well.[5,12,13,14]

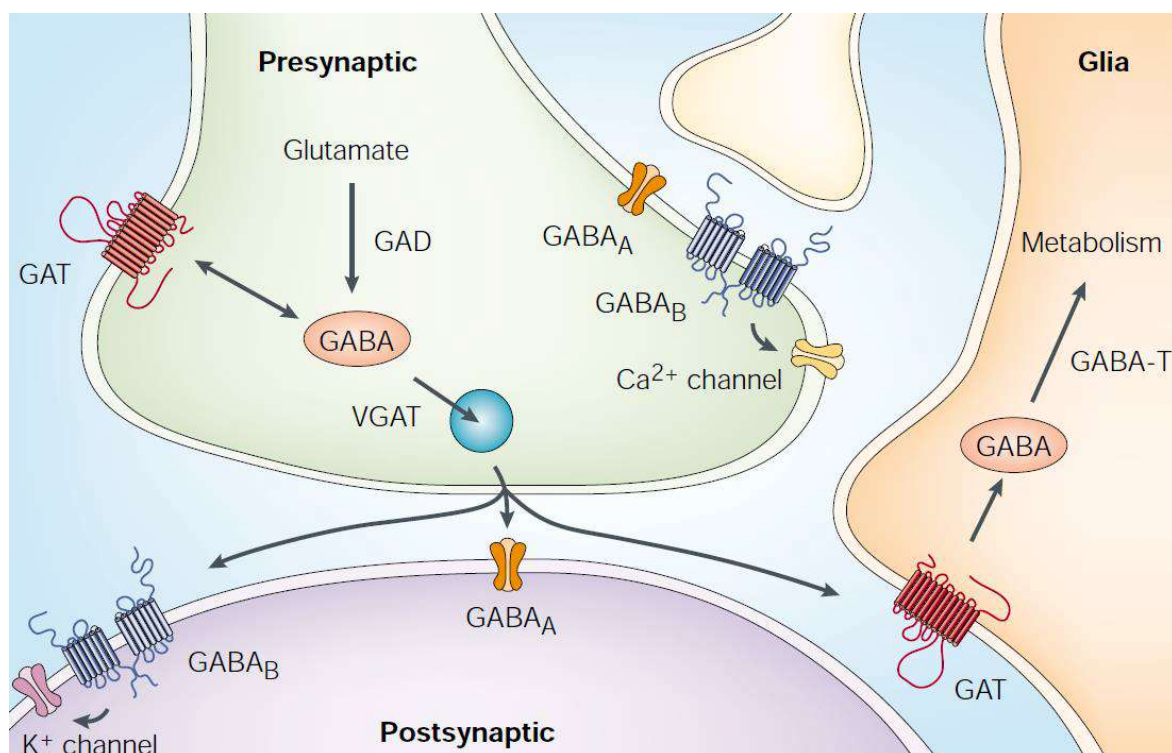


Figure 2. GABA neurotransmission pathways according to literature.[14]

If GABA binds to the GABA_A receptor, the excitability of the neuron is reduced caused by the hyperpolarization of the postsynaptic neuron through the influx of chloride ions. Presynaptic GABA_B receptors play an important negative feedback role to regulate the further release of GABA. Postsynaptic GABA_B receptors affect hyperpolarization through the efflux of potassium.[15]

The GABA transporter proteins (GATs) are responsible for the termination of the GABAergic signaling. They remove the GABA from the synaptic cleft via reuptake into the presynaptic neuron where it is stored in vesicles. Another way is by the uptake into the surrounding glial cells, where it can be broken down into succinic semialdehyde (SSA) by GABA transaminase (GABA-T).[16,17,18]

1.1.2. Treatment possibilities and side effects

An imbalance of the excitatory and inhibitory neurotransmitter levels in the CNS can result from reduced GABAergic signaling which is the main reason for epilepsy and the CNS diseases mentioned before. To increase GABA levels in the CNS, thus restoring the balance between excitatory and inhibitory neurotransmitter, the different GABA receptors, GABA transporters (GATs), and the GABA decomposing transaminase can be targeted with therapeutically active compounds (Figure 3).

Benzodiazepines, like diazepam (**2**), are positive allosteric modulators of the GABA_A receptors. They bind to a specific allosteric side which results in a conformational change of the receptor, thus increasing the opening frequency of the chloride channels.[19,20]

The GABA_B receptors can be influenced by the binding of an agonist molecule, like baclofen (**3**), which increases the GABA neurotransmission.[13] Vigabatrin (**4**) achieves the same effect, through the irreversible inhibition of the GABA transaminase (GABA-T). Most relevant to our work is the inhibition of the GABA transporters (GATs) which results in an increased GABA level since it is not removed from the synaptic cleft. Tiagabine [(*R*)-**5**] acts as a selective inhibitor of the GABA transporter subtype 1 (GAT1) and is the only approved antiepileptic drug on the market from this category.[9]

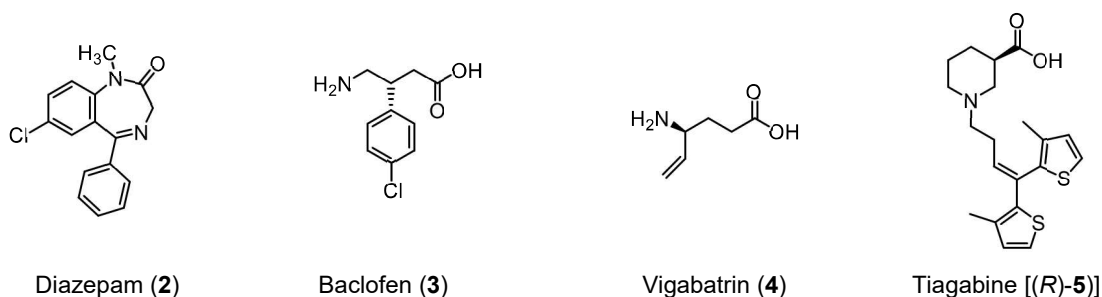


Figure 3. Approved drugs with an influence on GABAergic neurotransmission.

1.2. GABA transporters

Transporters (solute carriers), in general, make the transport of ions and larger molecules like amino acids and neurotransmitters through the cell membrane possible. The GABA transporters (GATs) belong to the solute carrier 6 (SLC6) gene family which includes 20 different transporter subtypes. These, according to their amino acid sequence, can be separated into four main subtypes: monoamine transporters, GABA transporters, and two groups of amino acid transporters as shown in Figure 4.[21]

This class of transporters are also termed the neurotransmitter-sodium symporter (NSS) family or Na^+/Cl^- dependent transporters. They use the co-transport of Na^+ and Cl^- ions in order to transport neurotransmitters into the cells against their concentration gradient.[22]

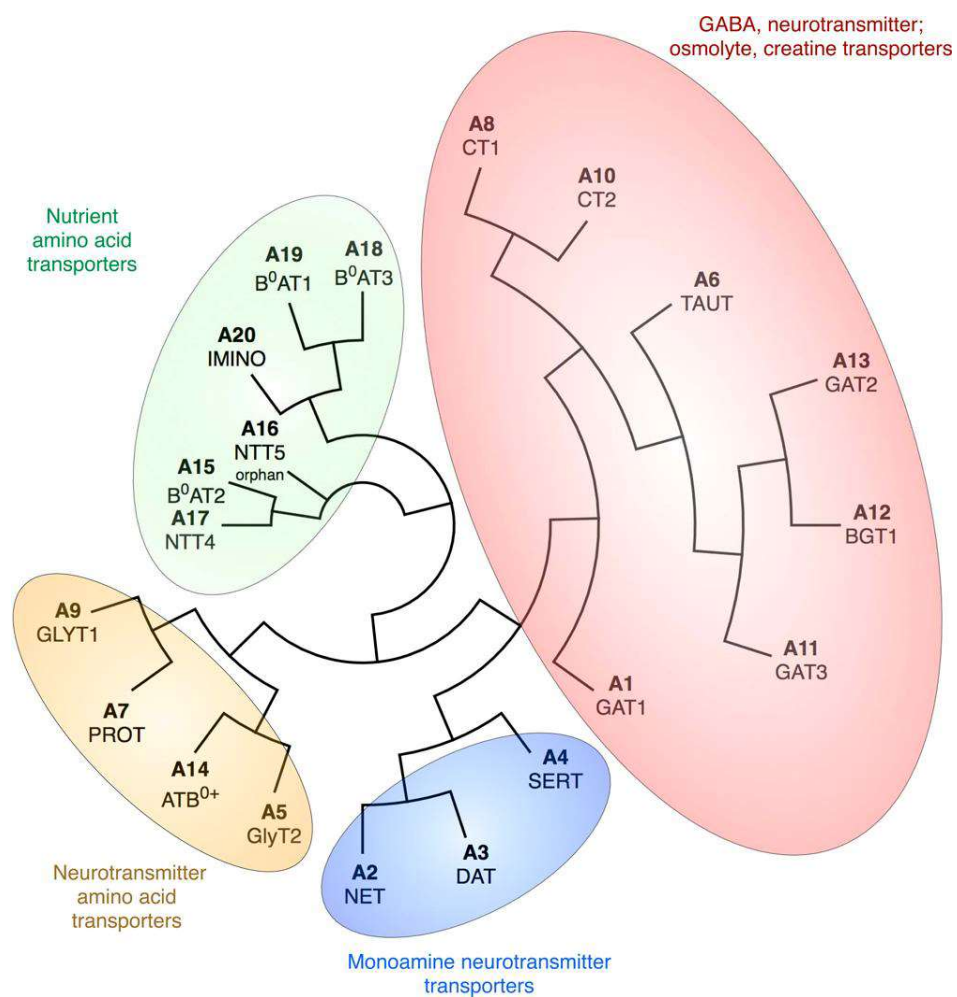


Figure 4. The SLC6 transporter family tree according to literature.[21]

1.2.1. GAT subtypes

The GABA transporters exist in different subtypes and multiple terminologies are applied to name them (Table 1). Within the body, four subtypes can be determined. The origin of the transporter from which animal it was cloned can also play a significant role. Additionally, the “Human Genome Organization” (HUGO) has its own terms for the human transporters, but it is often used for all species. During our research, we used only GAT transporters cloned from mice (mGAT1–mGAT4).[23,24]

Table 1. Different nomenclatures of the GATs.

Source	GAT subtypes			
mouse	mGAT1	mGAT2	mGAT3	mGAT4
human	hGAT-1	hBGT-1	hGAT-2	hGAT-3
HUGO	GAT1	BGT1	GAT2	GAT3

GAT1 is primarily located in the presynaptic neurons of the CNS and plays a crucial role in the transport of GABA. Studies have shown that BGT1 and GAT2 are mainly located in the kidneys and liver, thus playing only a minor function in the GABAergic neurotransmission. Another important subtype is GAT3. It is located on the glial cells surrounding the neurons of the CNS and is responsible for the uptake of GABA into the glial cell where it is metabolized afterwards. [17,25,26]

1.2.2. Structure and transport mechanism of SLC6 transporters

The structure of the NSSs was extensively studied in the last few decades and as a result the isolation, the amino acid sequence analysis, and the cloning of the GAT1 NSS were accomplished.[27] These results and the successful crystallization and X-ray structure analysis of the leucine transporter (LeuT_{Aa}) from the bacteria *Aquifex aeolis* in the presence of the substrate leucine and two sodium ions confirmed the structure of the transporter as illustrated in Figure 5.[28]

However, the overall amino acid sequence of the LeuT_{Aa} compared to the sequence of the eukaryotic SLC6 transporters is only 20% – 25%, but in the region of the substrate binding site, the homology in the sequence is significantly higher 55% – 67%.[29] This fact, in general, makes the use of this structure valid for the understanding of the assembly and purpose of these transporters.

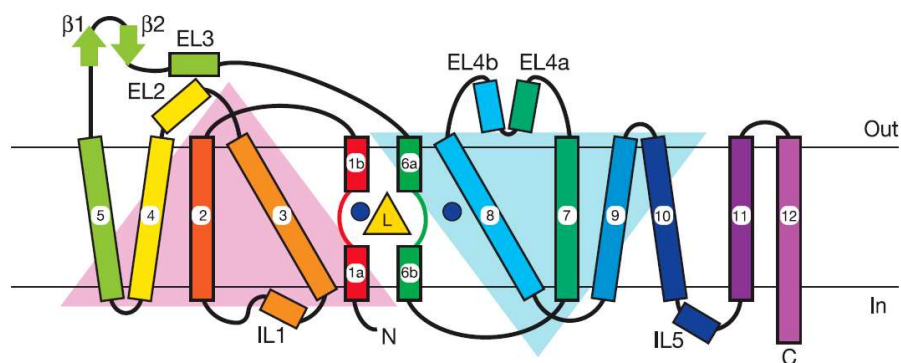


Figure 5. Structure of the LeuT_{Aa} transporter.[28]

The transporter LeuT_{Aa} contains 12 transmembrane helices (TMs) which are connected by corresponding loops both intra- and extracellularly (IL and EL), and the amino- and the carboxyl-terminus is located on the intracellular side (Figure 5). The primary binding site (S1) of leucine and the two sodium ions has a funnel-like structure, consisting from an inner ring formed by TM1, TM3, TM6, and TM8 and an outer ring formed by TM2, TM4, TM5, TM7, TM9, and TM10 (Figure 5). Two transmembrane helices (TM1 and TM6) have an interruption in their helical structures directly at the binding site, thus are divided into two parts (a and b) so the formation of hydrogen and ionic bonds between the exposed amino groups and carbonyl groups is made possible.[28]

The general transport mechanism of the NSSs is described with the “alternating access” Model, in which the transporter goes through several conformational changes.[30] Initially, the transporter is open to the extracellular side and is ready to accept the ligand and ions at the binding site (S1). After the substrate has bound to this “outward-open” conformation, the extracellular gate closes and the conformation changes into the “outward-occluded” state as shown in Figure 6. Subsequently, the intracellular gate opens and the substrate is released into the cytoplasm in the “inward-open” conformation.[31]

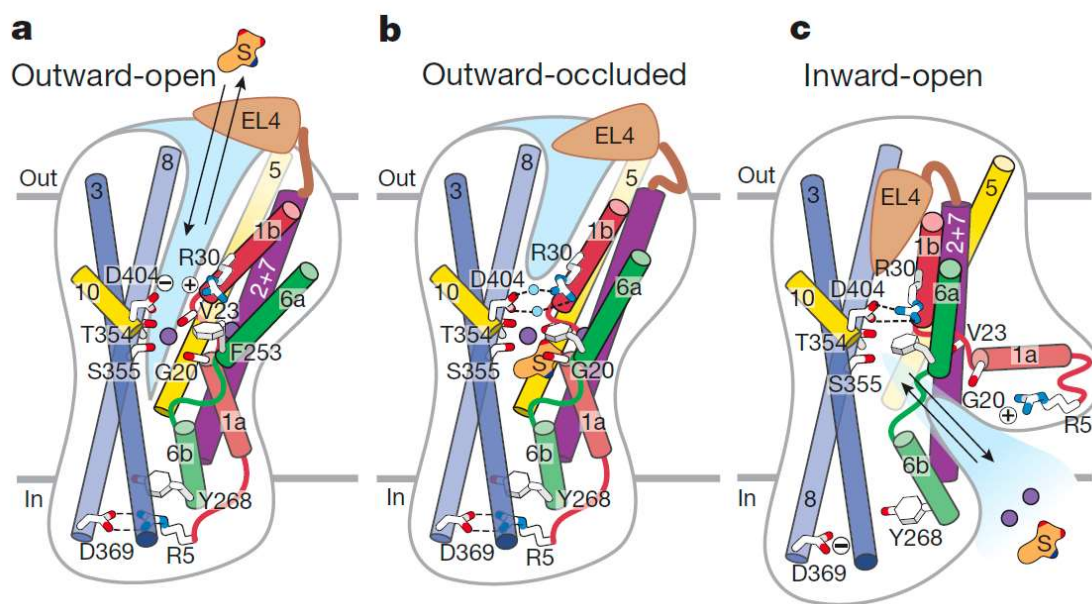


Figure 6. Postulated transport mechanism of the NSSs.[31]

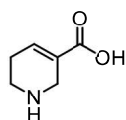
Molecular-dynamic simulations and further studies have shown that a second binding site (S2) located just above the extracellular gate of LeuT exists. It is stated that the occupation of this binding site is necessary for the allosteric release (S1) of the substrate into the cytoplasm.[32] This statement is still debated because others have shown that S2 is rather a binding pocket for non-competitive LeuT inhibitors or detergents, which prevent the conformational change of the transporter.[33,34] Further X-ray crystallographic structures of other NSSs supported the findings of the LeuT results.[35,36] The structure of the eukaryotic dopamine transporter (DAT) bound with the tricyclic antidepressant nortriptyline was isolated from *Drosophila melanogaster* and this was in perfect accordance with the prokaryotic LeuT structure. Similarly, the structure of the human serotonin transporter (SERT) in complex with the antidepressant (S)-citalopram or paroxetine was also published which demonstrates how the binding to the S2 site sterically hinders the release of the ligand from the central binding side.[37]

1.2.3. GATs as drug targets

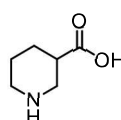
Since the GATs are involved in many neurological disorders mentioned before, their inhibition offers a viable way for a treatment by restoring the physiological neurotransmitter balance in the CNS.

To this end, researchers are looking for compounds that inhibit the GABA uptake effectively, but do not bind to the GABA receptors. First, acyclic analogs of GABA were developed, but these compounds showed no selectivity for any of the GAT subtypes and additionally acted as ligands for the GABA_A receptor. Then, cyclic amino acids like guvacine (**6**) and nipecotic acid (*rac*-**7**) presented more promising results and became a new starting point for GAT inhibitor development.[38] The inhibitory potencies of these compounds (**6** and *rac*-**7**) are similarly high without any pronounced selectivity (Table 2). It is worth to mention that the (*R*)-enantiomer of nipecotic acid [(*R*)-**7**] is significantly more potent than the (*S*)-enantiomer [(*S*)-**7**] at all mGATs. The corresponding pIC₅₀ values are listed in Table 2 and range from 3.13 to as high as 5.12.

Table 2. Small, cyclic amino acids as GABA analogs.



Guvacine (**6**)



Nipecotic acid (*rac*-**7**)

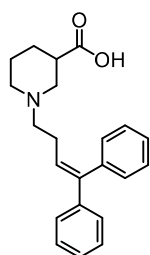
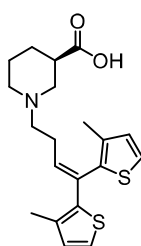
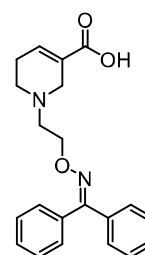
Compound	GABA uptake inhibition (pIC ₅₀ ± SEM) ^a			
	mGAT1	mGAT2	mGAT3	mGAT4
6	4.87 ± 0.06	3.31 ± 0.03	4.59 ± 0.05	4.59 ± 0.05
<i>rac</i> - 7	4.88 ± 0.07	3.10 ± 0.09	4.64 ± 0.07	4.70 ± 0.07
(<i>R</i>)- 7	5.12 ± 0.03	3.40 ± 0.05	4.76 ± 0.05	4.95 ± 0.05
(<i>S</i>)- 7	4.24 ± 0.05	3.13 ± 0.14	3.83 ± 0.04	3.63 ± 0.06

^aFor sake of comparability all listed functional inhibitory potencies (pIC₅₀ values) derive from the biological test of our research group (GABA uptake assay based on HEK293 cells stably expressing the different mGATs).

On the other hand, these compounds are highly polar and under physiological conditions present in a zwitterionic state, making the penetration of the blood-brain-barrier (BBB) extremely difficult. To overcome this problem, lipophilic side chains were introduced at the nitrogen atom of the heterocycles resulting in not only more potent compounds, but also more subtype selective derivatives at the GATs.[39,41,42,51,52] The applied modifications and their results will be discussed in the following part.

1.2.3.1. mGAT1 selective inhibitors

The substitution of the nitrogen atom of the before mentioned heterocyclic amino acids (**6** and *rac-7*) with a linker to a lipophilic moiety, leads to highly potent mGAT1 selective compounds as it is shown in Table 3. The flexible linkers can have a length of four or five atoms with a double bond in it and two aromatic residues at the end. Amongst these compounds, tiagabine [(*R*)-**5**] is used as an add-on treatment of partial epilepsy.[40]

Table 3. Selective inhibitors of mGAT1.SKF-89976A (**8**) [39]Tiagabine [(*R*)-**5**] [41]NO711 (**9**) [42]

Compound	GABA uptake inhibition (pIC ₅₀ ± SEM) ^a			
	mGAT1	mGAT2	mGAT3	mGAT4
8	6.16 ± 0.05	3.43 ± 0.07	3.71 ± 0.04	3.56 ± 0.06
(<i>R</i>)- 5	6.88 ± 0.12	50% ^b	64% ^b	73% ^b
9	6.83 ± 0.06	3.20 ± 0.09	3.62 ± 0.04	3.07 ± 0.05

^aFor sake of comparability all listed functional inhibitory potencies (pIC₅₀ values) derive from the biological test of our research group (GABA uptake assay based on HEK293 cells stably expressing the different mGATs).

^bRemaining ³[H]GABA-Uptake in the presence of 100 μM test compound.

To improve the former results, Andersen conducted a series of SAR studies. This led to the discovery of even more potent inhibitors of GAT1 (Figure 7) which had an ether function in the linker and a 2-biphenyl [(*R*)-**10**] or 2-benzylphenyl [(*R*)-**11**] residue at the end.[43,44]

A recent study demonstrated how the exchange of the alkoxyalkyl spacer of (*R*)-**10** with a but-3-en-1-yl linker resulting in *rac*-**12** delivered a similar inhibitory activity at mGAT1 (Figure 7) which can be viewed as a new parent structure for the further development of mGAT1 inhibitors. However, the same modification applied to (*R*)-**11** caused an order of magnitude drop in the inhibitory potency at mGAT1 for *rac*-**13**.[45]

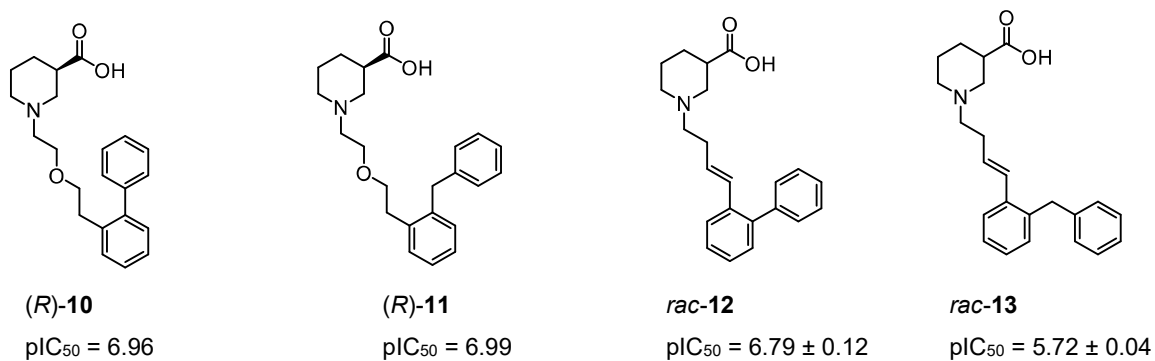


Figure 7. New generation of GAT1 selective inhibitors.[44,45]

1.2.3.2. Selective inhibitors of mGAT2

Contrary to the mGAT1 inhibitors, the today existing mGAT2 inhibitors lack the potency and selectivity for their target. The known best mGAT2 inhibitor NNC05-2090 (**14**, Table 4) [46] is only with a factor of 10 more potent at mGAT2 than at the other GATs. The mixed mGAT1/mGAT2 inhibitor EF1502 (**15**) [47] was derived from the weak mGAT1 inhibitor N-methyl-exo-THPO (**16**), [48] which is slightly more potent at mGAT1 and has no noteworthy inhibition at mGAT3 or at mGAT4.

Interestingly, compared to the potent mGAT1 inhibitors with a cyclic amino acid residue, NNC05-2090 (**14**), as the most potent mGAT2 inhibitor, does not have a carboxylic acid moiety, which implies that the strong binding to mGAT2 is the result of the suitable parent structure of the compound.

Table 4. Selective inhibitors of mGAT2.

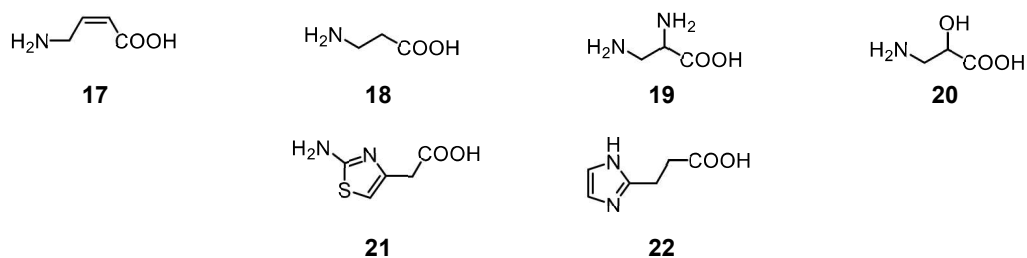
Compound	GABA uptake inhibition (pIC ₅₀)			
	mGAT1	mGAT2	mGAT3	mGAT4
14	4.72 ^a	5.85 ^a	4.39 ^a	4.82 ^a
15	5.15 ^b	4.59 ^b	< 3.52 ^b	< 3.52 ^b
(<i>R</i>)- 16	3.35 ^b	< 2.52 ^b	< 2.52 ^b	< 2.52 ^b

^apK_i values. ^bNo SEM values in the literature.

1.2.3.3. mGAT3 and mGAT4 selective inhibitors

A series of amino acids were tested in our research group for their potency at and selectivity for the mGATs (Table 5).[49] This showed that compound (Z)-4-amino-2-butenoic acid (**17**) is significantly more potent at mGAT3–mGAT4 than at mGAT1–mGAT2. Originating from the known mixed mGAT3–mGAT4 inhibitors beta-alanine (**18**) and 2,3-diaminopropanoic acid (**19**), we managed to find two new potent parent structures. Of these, isoserine (**20**) proved to be one of the most potent and selective mGAT3–mGAT4 inhibitor with a clear subtype selectivity (factor > 400) compared to mGAT1–mGAT2. Furthermore, (2-amino-1,3-thiazol-4-yl)acetic acid (**21**) was found to be the first mGAT3 selective inhibitor despite its low potency ($pIC_{50} = 3.36$). Additionally, 3-imidazol-2-yl-propionic acid (**22**) was found to be even more potent at mGAT3, while having similar subtype selectivity.[50]

Table 5. Amino acids with mGAT3 and mGAT4 selectivity from the literature.[49,50]



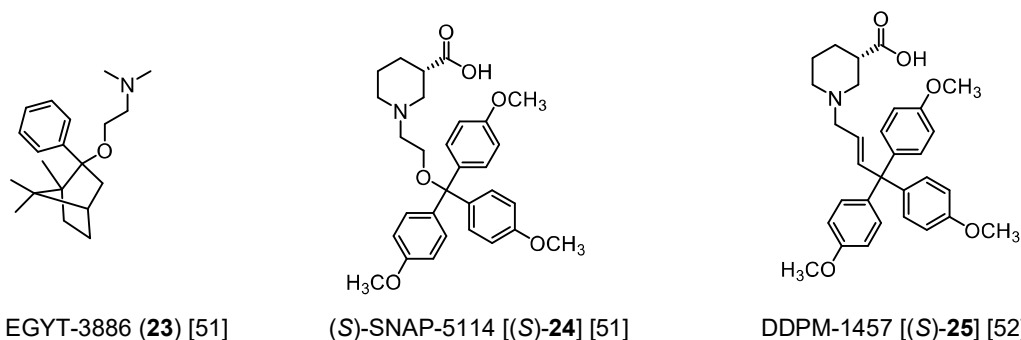
Compound	GABA uptake inhibition ($pIC_{50} \pm SEM$) ^a			
	mGAT1	mGAT2	mGAT3	mGAT4
17	2.99 ± 0.04	3.67 ± 0.08	4.95 ± 0.04	4.93 ± 0.09
18	2.59 ± 0.03	3.48 ± 0.11	4.66 ± 0.06	4.46 ± 0.13
19	3.11 ± 0.02	3.50 ± 0.12	4.66 ± 0.08	5.05 ± 0.02
20	2.33 ± 0.05	3.39 ± 0.11	4.87 ± 0.05	4.78 ± 0.14
21	98% ^b	77% ^b	3.36 ± 0.11	55% ^b
22	63% ^b	3.28 ± 0.12	4.54 ± 0.15	3.51 ± 0.03

^aFor sake of comparability all listed functional inhibitory potencies (pIC_{50} values) derive from the biological test of our research group (GABA uptake assay based on HEK293 cells stably expressing the different mGATs).

^bRemaining ³[H]GABA-Uptake in the presence of 1 mM test compound.

Based on the weak, non-selective GAT inhibitor EGYT-3886 (**23**, Table 6), a series of new compounds was developed, which included the most potent and selective mGAT4 inhibitor (S)-SNAP 5114 [(S)-**24**].[51] From this research, it seemed that the key structural elements needed for the mGAT4 selectivity were a C2-spacer connected via an ether function to a methoxy-substituted trityl residue. Further research conducted in our group resulted in the similarly potent and selective DDPM-1457 [(S)-**25**] in which the ether function of the linker was replaced by a *trans*-alkene unit. This modification additionally significantly increased the compounds chemical stability compared to (S)-SNAP 5114 [(S)-**24**].[52]

Table 6. GABA uptake inhibitors for mGAT3 and mGAT4.



Compound	GABA uptake inhibition (pIC ₅₀ ± SEM)			
	mGAT1	mGAT2	mGAT3	mGAT4
23 ^a	4.59 ^b	4.41 ^c	4.52 ^d	4.34 ^e
(S)- 24 ^f	4.07 ± 0.09	63% ^g	5.29 ± 0.04	5.71 ± 0.20
(S)- 25 ^f	4.40 ± 0.05	4.42 ± 0.11	5.47 ± 0.02	5.87 ± 0.08

^aInhibitory potencies derive from literature [51]; ^bhGAT1; ^chBGT1; ^drGAT2; ^ehGAT3; ^fFor sake of comparability the indicated functional inhibitory potencies (pIC₅₀ values) derive from the biological test of our research group (GABA uptake assay based on HEK293 cells stably expressing the different mGATs); ^gRemaining ³[H]GABA-Uptake in the presence of 100 μM test compound.

2. Aims and scope

Antiepileptic drugs that are currently on the market do not always provide a satisfactory treatment for patients. Hence, there is an urgent need for new, more modern treatment options.[10] The GATs represent a good target for the development of new inhibitors which would selectively target only one of the GAT subtype present in the CNS. This leads to the objective of this study, to find inhibitors of the mGAT4 transporter with high potency and selectivity for its target.

2.1. Development of N-substituted nipecotic acid derivatives as selective mGAT4 reuptake inhibitors

During an earlier study in our group, DDPM-1457 [(S)-**25**] a carba-analog of the known (S)-SNAP-5114 [(S)-**24**] GAT inhibitor with moderately high potency at and selectivity for mGAT4 was discovered.[52] The carba-analog (S)-**25** has a *trans*-alkene moiety in the spacer between the nipecotic acid and the lipophilic residue instead of an ether functionality, compared to (S)-**24**. Additionally to the similar potencies at and selectivity for the mGATs, the new compound exhibited greatly increased chemical stability. This hit compound directed our following research to explore the base structure by its modification in multiple different ways to find even better and more selective inhibitors for mGAT4.

For the first new carba-analog family, the alkyne-analogs (*rac*-**26**, Figure 8), we were interested how the inhibitory potencies and selectivity is influenced if the *trans*-alkene moiety of DDPM-1007 (*rac*-**25**),[52] the racemic analog of the enantiopure DDPM-1457 [(S)-**25**], is converted into a triple bond. Further modifications aimed to introduce a series of different residues, like aromatic and heteroaromatic rings, benzylic residues or sterically less demanding groups at the lipophilic moiety (Figure 8) and to lengthen the spacer by one methylene group on either side of the alkyne unit.

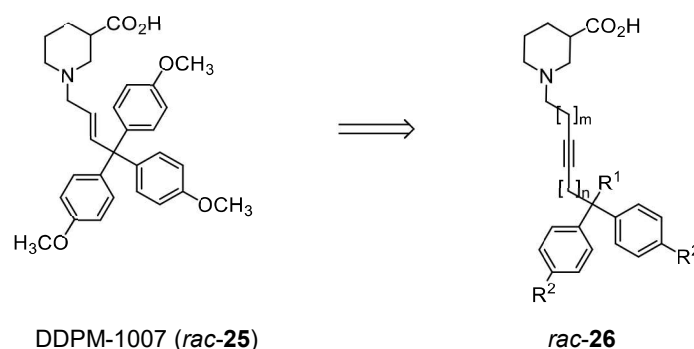


Figure 8. General structure of the alkyne-analogs of DDPM-1007 (*rac*-**25**). For residues R¹, R², m, and n see Publication 1.

During the following project, we applied the identical lipophilic moieties from the alkyne-analogs (*rac-26*, Figure 8) to the original structure with the *trans*-alkene spacer (*rac-25*) to see if it leads to positive results in the biological evaluation of compound *rac-28*. Additionally, while keeping the spacer unmodified, three identical heterocyclic residues were introduced to the lipophilic end (*rac-27*), replacing all of the previous 4-methoxyphenyl residues (Figure 9).

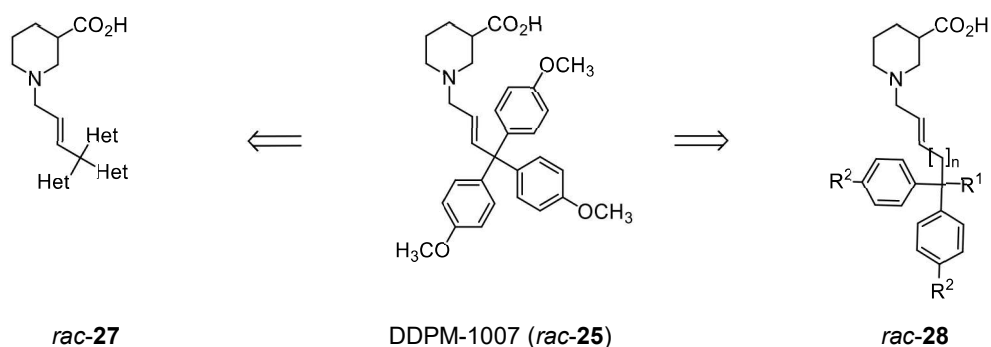


Figure 9. Additional *trans*-alkene analogs. For residues R¹, R², Het, and n see Publication 2.

The topic of the last part included the synthesis and biological evaluation of *cis*-alkene analogs (*rac-29*), in which the alkyne analogs (*rac-26*) were converted via catalytic hydrogenation to the corresponding *cis*-alkene derivatives to complete all of the planned modifications for the carba-analog (*S*)-**25** (Figure 10).

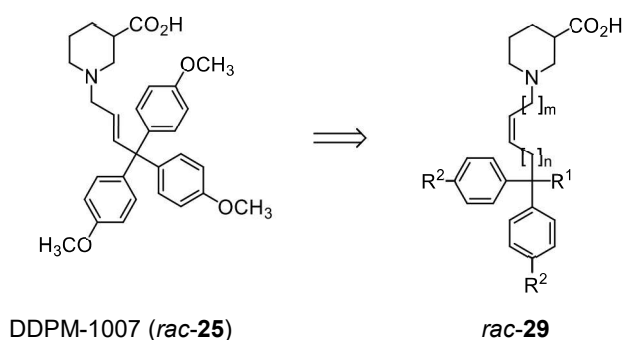


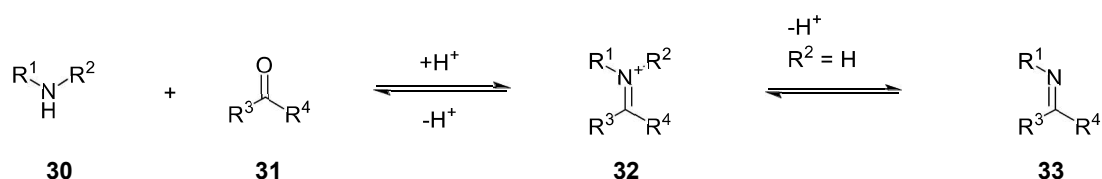
Figure 10. General structure of the *cis*-alkene analogs. For residues R¹, R², m, and n see Publication 3.

2.2. Coupling methods

For the synthesis of the targeted analogs, we utilized the reaction of an iminium salt with diverse organomagnesium or organozirconium reagents. Similar reactions are well reported and known to provide the desired products selectively, under mild conditions, and with high yields.[53,54,55,56,57]

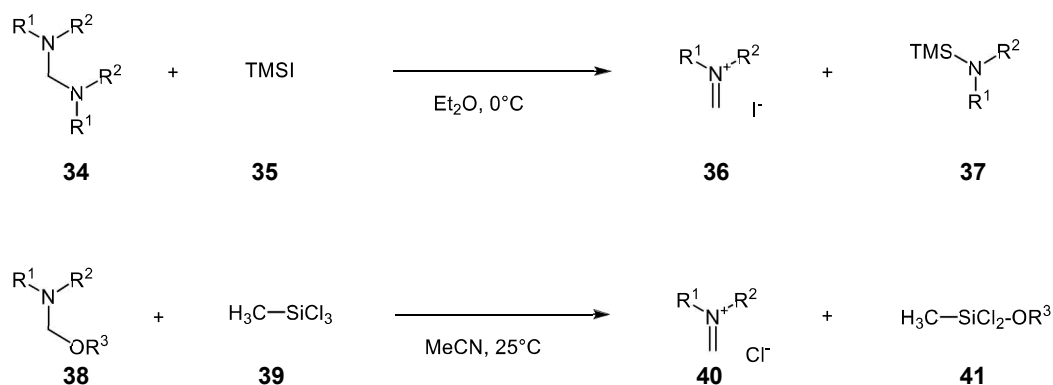
2.2.1. Iminium salts

An iminium salt or iminium cation has the general structure **32** (Scheme 1). The condensation of a primary amine (**30**, $R^2 = H$) with a ketone/ aldehyde (**31**) leads to an equilibrium, in which the imine form (**33**) is generated and under acidic conditions exists as iminium ion (**32**). A secondary amine (**30**, $R^2 \neq H$) can also form with an aldehyde or ketone an iminium ion (**32**) and they can be isolated as salts of strong acids.[58]



Scheme 1. Formation of iminium ions and imines.

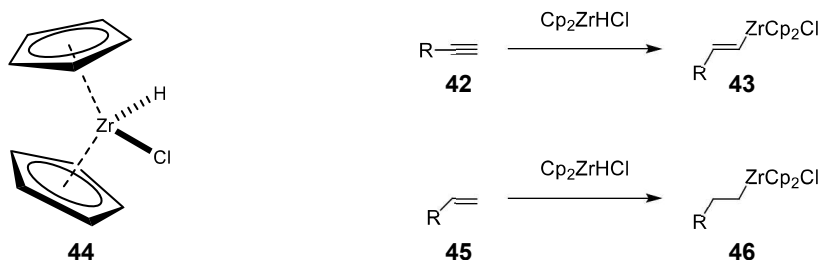
Alternatively, the reaction of aminoacetal **34** with TMSI (**35**) under water-free conditions (Scheme 2) produces iminium salt **36** and TMS-amine **37**.^[59] Additionally, the treatment of *N,O*-acetal **38** with methyltrichlorosilane **39** easily forms iminium salt **40** and silyl ether derivative **41** as a side product.^[60] A similar, alternative method would be more suitable for our conditions, due to the sensitivity of the organometallic reagents planned to be used as nucleophiles.



Scheme 2. Alternative iminium ion formations under water-free conditions.^[59,60]

2.2.2. Hydrozirconation

The addition reaction in which an organozirconium compound is attached across a double or triple bond is the hydrozirconation. The sterically shielded carbon-zirconium bonds of organozirconocenes possess a highly functional group tolerance and can be used for transmetalation reactions.[61] One of the most common methods to generate organozirconocene reagents (**43** and **46**) is the reaction between alkynes **42** or alkenes **45** with Schwartz's reagent **44** (Cp_2ZrHCl , Scheme 3), to give **43** and **46** respectively.[61,62] The ionic character of the C–Zr bond, according to the Pauling electronegativity scale, is almost equivalent to the C–Mg bond, but they exhibit a substantially weaker nucleophilic character due to the steric shielding from the two cyclopentadienyl ligands. For synthetic applications, the most widely used organozirconium compounds are the alkenylzirconocenes **43**. They are easily accessible and their synthesis from alkynes and Schwartz's reagent is fast, regioselective and reasonably functional group tolerant.



Scheme 3. Formation of alkenyl- and alkylzirconocenes by hydrozirconation.

3. Summary of manuscripts and published results

3.1. First publication:

Synthesis and biological evaluation of novel N-substituted nipecotic acid derivatives with an alkyne spacer as GABA uptake inhibitors

In recent years, the search for GABA uptake inhibitors with high affinity and subtype selectivity led to the discovery of the N-substituted nipecotic acid derivative DDPM-1457 [(S)-**25**], which holds good affinity and selectivity for its target mGAT4. As a carba-analog of the known (S)-SNAP-5114 [(S)-**24**], it only differs at its spacer between the nipecotic acid and the lipophilic residue which has a *trans*-alkene unit instead of an ether functionality, respectively.

In this study, we report our efforts to expand the knowledge about the structure-activity relation (SAR) of the carba-analog family of DDPM-1457 [(S)-**25**], in pursuit of finding even more potent and selective inhibitors for mGAT4. To this end, the planned structural modifications of [(S)-**25**] included the replacement of the *trans*-alkene moiety of the spacer with an alkyne unit, increasing the length of the spacer by one methylene group or substituting one aromatic residue at the lipophilic moiety with a heterocyclic, benzylic or sterically less demanding group.

For the synthesis of the targeted compounds, a suitable method was developed involving iminium chemistry. It is well known from the literature that iminium salts readily react with organometallic nucleophiles. Thus, we choose to react the *in situ* generated iminium ion derived from the *N,O*-acetal of nipecotic acid with a series of ethynylmagnesium chloride nucleophiles obtained through the deprotonation of the corresponding terminal alkynes with *n*BuMgCl. The required terminal alkynes were produced by the treatment of triaryl chlorides with ethynylmagnesium bromide or (trimethylsilyl)ethynyllithium reagents. Under the mild coupling conditions (40°C, THF), the yields for the corresponding esters were moderate to good (39% – 85%). After the final hydrolysis of the esters, the obtained free nipecotic acid derivatives were evaluated for their inhibitory potency at and selectivity for the mGATs.

The results of the new alkyne derivatives show, that the introduced small change from a double bond into a triple bond in the linker generally caused a significant drop in the potencies accompanied by a slight shift in the selectivity from mGAT4 to mGAT1. Increasing the spacer length had a similar outcome, potencies and the selectivity got significantly lower than that of the parent structure and were comparable to the result of the alkyne analogs with a shorter spacer. Interestingly, the alkyne analog with a benzothiophene residue instead of a 4-methoxyphenyl ring had a reasonably high affinity for all mGATs ($pIC_{50} \sim 5$), which may indicate that electron rich and planar aryl moieties, similar to a 4-methoxyphenyl residue, can be suitable for interaction with the mGAT proteins.

Declaration of contributions:

Synthesis of the N-substituted nipecotic acid derivatives and all precursor molecules was done by myself including evaluation of the analytical data of all compounds. The practical performance of the biological test of all compounds was carried out by the technical assistants of the group under the supervision of Dr. Georg Höfner.

3.2. Second publication:

Synthesis and biological evaluation of novel N-substituted nipecotic acid derivatives with a *trans*-alkene spacer as potent GABA uptake inhibitors

Our previous discovery of DDPM-1457 [(S)-**25**], a chemically more stable analog of (S)-SNAP-5114 [(S)-**24**], was an important step in the search for new and potent mGAT4 selective inhibitors. Such compounds could provide an additional treatment option for patients with GABAergic disturbances, especially in cases where the currently used medications are not providing the hoped relief.

In this present publication, we focus on broadening the knowledge about this carba-analog family in order to find even better inhibitors for mGAT4. To this end, we modified the parent structure of DDPM-1007 (*rac*-**25**), the racemic analog of the enantiopure DDPM-1457 [(S)-**25**], in the following ways. While keeping the *trans*-alkene spacer unmodified, first, we replaced one aromatic ring of the lipophilic moiety by a series of residues, e.g. aromatic, heteroaromatic or benzylic residues. Furthermore, the length of the spacer was increased by one methylene group by inserting it between the *trans*-alkene moiety and the lipophilic residue to gain an insight on how the spacer length influences the binding affinities. Additional compounds were prepared with three larger and identical aromatic moieties, which were hoped to mimic the original 4-methoxyphenyl residues.

For the synthesis of the esters, we utilized the building blocks from our previous publication, in which we used the coupling reaction of an iminium salt with an organomagnesium species generated from terminal alkynes. Now, we report the coupling reaction between the reported iminium salt and diverse zirconocene reagents, generated through the hydrozirconation of a series of terminal alkynes. Due to the *trans*-selectivity of the hydrozirconation step, this reaction produces the desired esters with the preferred *trans*-alkene spacer. The yields are moderate to good.

After the final hydrolysis of the esters, the obtained free acid derivatives were evaluated for their inhibitory potencies at and selectivities for the mGATs. The results are well comparable with the parent compound DDPM-1007 (*rac*-**25**), however, the new compounds have generally lower potencies at mGAT3–mGAT4 and slightly higher at mGAT1. Amongst them, one of the best mGAT4 inhibitors, which has a benzothiophene residue at the lipophilic moiety, was also synthesized as the pure (*S*)-enantiomer. As it was expected for this enantiomer, the potencies at and selectivities for mGAT3–mGAT4 rose further, making it the most potent compound in our present series. Additionally, the observation was made that the direct analog of DDPM-1007 (*rac*-**25**) with a spacer elongated by one methylene group, by insertion of this group between the *trans*-alkene and the triaryl residue, had a significant lower potency at mGAT4. Another compound having a longer spacer and only two phenyl rings at the lipophilic moiety was found to exhibit a surprisingly high potency at and selectivity for mGAT1. This compound's inhibitory potency ($pIC_{50} = 6.78 \pm 0.09$) was almost as high as that of tiagabine [(*R*)-**5**] ($pIC_{50} = 6.88 \pm 0.12$). Finally, an analog of DDPM-1007 (*rac*-**25**) with three identical benzofuran rings, instead of 4-methoxyphenyl residues, showed a significantly increased binding affinities at all mGATs (pIC_{50} : 5.02 – 5.39), making it an interesting candidate for pharmacological studies.

Declaration of contributions:

Synthesis of the N-substituted nipecotic acid derivatives and all precursor molecules was done by myself including evaluation of the analytical data of all compounds. The practical performance of the biological test of all compounds was carried out by the technical assistants of the group under the supervision of Dr. Georg Höfner.

3.3. Manuscript of the third publication:

Synthesis and biological evaluation of novel N-substituted nipecotic acid derivatives with a *cis*-alkene spacer as GABA uptake inhibitors

In order to discover more potent and selective inhibitors for the murine gamma-aminobutyric acid transporter 4 (mGAT4), the earlier discovered carba-analog family of DDPM-1007 (*rac*-**25**) was subjected to extensive modifications. New mGAT4 inhibitors could be useful in the treatment of complex neurological disorders (depression, epilepsy, and neuropathic pain), and overcome drawbacks (side effects, ineffectiveness in some cases) of the currently used medications. The carba-analog *rac*-**25** having similar potency and additionally significantly increased chemical stability was obtained through the replacement of the ether function in the spacer of the first prototypic mGAT4 inhibitor (S)-SNAP-5114 [(S)-**24**] by a *trans*-alkene moiety. The present work aimed to uncover how the change from a *trans*-double bond to a *cis*-double bond in the spacer would affect the inhibitory potency and subtype selectivity.

For the synthesis of the *cis*-alkene analogs, we utilized the previously reported alkyne-analogs as starting compounds. A catalytic hydrogenation with Lindlar's catalyst produced the desired new analogs in a practical and effective way (49% – 73%). These analogs, compared to DDPM-1007 (*rac*-**25**), have a *cis*-alkene spacer connected to diverse lipophilic moieties, in which, one of the original 4-methoxyphenyl residue is replaced by aromatic and heteroaromatic cycles, benzylic residues or sterically less demanding groups. Additionally, the spacer length was increased by one methylene group either by inserting it between the *cis*-alkene group and the lipophilic residue or between the nipecotic acid and the *cis*-alkene moiety.

The biological evaluation of the structure-activity relation (SAR) study revealed that the obtained compounds generally show slightly decreased potencies at mGAT1–mGAT3 and a significant drop at mGAT4 as compared to the analogous compounds with a *trans*-alkene moiety in the spacer, e.g. DDPM-1007 (*rac*-**25**). Increasing the spacer length of the *cis*-analogs with three aromatic residues further decreased the potency at mGAT4, but it showed different results at mGAT1. If the additional methylene group was placed between the trityl moiety and the *cis*-alkene unit a surprisingly high inhibitory potency at mGAT1 ($pIC_{50} = 6.00 \pm 0.04$) was observed, which was not evident if the additional methylene group was placed between the nipecotic acid and the *cis*-alkene moiety ($pIC_{50} = 4.39$).

Declaration of contributions:

Synthesis of the N-substituted nipecotic acid derivatives and all precursor molecules was done by myself including evaluation of the analytical data of all compounds. The practical performance of the biological test of all compounds was carried out by the technical assistants of the group under the supervision of Dr. Georg Höfner.

4. Summary of the thesis

As more and more people are in desperate need of new treatment options and better medications for disturbances in the GABAergic neurotransmission-related illnesses (epilepsy, Alzheimer's disease, and depression), the search for new inhibitors of the GABA transporter proteins is an ongoing challenge. Our goal was to find potent and selective inhibitors of mGAT4, by exploring new carba-analog families of the previously reported first prototypic mGAT4 inhibitor (S)-SNAP-5114 [(S)-**24**].

Our work was done in three steps resulting in three carba-analog families which most importantly differ in their spacer incorporating an alkyne, *trans*-alkene, or a *cis*-alkene moiety. The structure of these new derivatives is closely related to DDPM-1457 [(S)-**25**], the first carba-analog of (S)-SNAP-5114 [(S)-**24**], in which the ether group of (S)-**24** has been replaced with a *trans*-alkene moiety, making it significantly more chemically stable while retaining good activity and selectivity for mGAT4. The alkyne-analogs were synthesized through the coupling reaction between an iminium ion derived from nipecotic acid and a series of organomagnesium species generated from terminal alkynes. The new analogs, compared to DDPM-1007 (*rac*-**25**), the racemic analog of (S)-**24**, had an alkyne moiety in the spacer and one aromatic residue of the triarylmethyl moiety replaced by a wide range of aryl, heteroaryl, benzyl, or sterically less demanding group. The biological results show that these modifications caused a significant decrease in the mGAT4 potency, of around one log unit, compared to (*rac*-**25**). Similar results could be observed for the alkyne-analogs, which had a by a methylene group longer spacer. Furthermore, one compound having a benzothiophene substituent at the lipophilic moiety exhibited heightened inhibitory potencies at all mGATs ($pIC_{50} = 4.92 - 5.06$), suggesting that the benzothiophene ring being similar in size and shape, but more rigid and electron rich, compared to the original 4-methoxyphenyl moiety, could favor the interaction with the mGAT proteins.

The *trans*-alkene analog family of DDPM-1007 (*rac*-**25**) was broadened with new members. For these analogs, the *trans*-double bond of the spacer was retained while one of the 4-methoxyphenyl rings was replaced by an aromatic, heteroaromatic, benzylic or sterically less demanding group. Additional analogs have their spacer lengthened by one methylene group between the *trans*-alkene moiety and the lipophilic residue, which has three or two 4-methoxyphenyl or phenyl rings. Further derivatives have not only one, but all three of their aromatic moieties replaced by three identical and sterically more demanding heterocyclic residues. The synthesis of the new *trans*-alkene analogs was accomplished through the reaction of the before mentioned iminium salt with a series of alkenylzirconocene reagents generated via the hydrozirconation of the corresponding terminal alkynes. Compared to DDPM-1007 (*rac*-**25**) the new analogs generally have similar or distinctly lower potencies at

mGAT4 and slightly increased potency at mGAT1. Unfortunately, compounds with a longer spacer display an even lower potency at mGAT4. Interestingly, one analog with a longer spacer and only two phenyl rings as the lipophilic moiety exhibited surprisingly high potency at and selectivity for mGAT1 ($pIC_{50} = 6.78 \pm 0.09$) which was well comparable to that of tiagabine ($pIC_{50} = 6.88 \pm 0.12$). Additionally, amongst the products with three identical heterocyclic rings, one analog having three benzofuran moieties had significantly increased potencies at all mGATs (pIC_{50} : 5.02 – 5.39). Consequently, this analog could be used as a pharmacological tool to get a deeper understanding of how the inhibition of multiple GATs at the same time affects the GABA levels of the body.

A further topic of my research was the synthesis of compounds of the *cis*-alkene analog family to compare their biological results with the *trans*-alkene and the alkyne-analogs. It was intended to keep all structural elements identical to the other two analog families, except for the configuration of the double bond in the spacer, to allow an easy side-by-side comparison. In order to gain easy access to the desired *cis*-alkene analogs, I used the alkyne derivatives from our previous work as starting material and subjected them to a partial catalytic hydrogenation reaction with Lindlar's catalyst. The structure-activity relationship (SAR) study of the *cis*-alkene analogs having one 4-methoxyphenyl residue replaced, compared to DDPM-1007 (*rac*-**25**), by aromatic, heteroaromatic, benzylic or sterically less demanding groups revealed, that the inhibitory potency, in general, slightly decreased at mGAT1–mGAT3 and was significantly reduced at mGAT4. Additionally, the potency at mGAT4 got even lower for the *cis*-alkenes with an increased spacer length, regardless of the position of the additional methylene group. Interestingly, if the analog with three phenyl rings at the lipophilic moiety had the additional CH₂-group between the trityl moiety and the *cis*-alkene unit the potency at mGAT1 was significantly higher ($pIC_{50} = 6.00 \pm 0.04$) than if it is between the nipecotic acid residue and the *cis*-alkene group ($pIC_{50} = 4.39$). The reduced inhibitory potencies of the *cis*-alkene derivatives, compared to the *trans*-isomers, show, how important the configuration of only one bond is for the biological activity of these derivatives.

To summarize this work, diverse carba-analog families of the potent and selective mGAT4 inhibitor (S)-SNAP-5114 [(S)-**24**] were extensively explored. New and interesting synthetic methods were developed and the gathered structure-activity relation (SAR) results gave a deeper understanding of how changing individual structural elements affects the binding results. These results contribute to the final goal of finding a potent and selective inhibitor for mGAT4 as treatment option for patients with complex neurological disorders.

5. List of abbreviations

BBB	blood-brain-barrier
CNS	central nervous system
EL	extracellular loop
GABA	gamma-aminobutyric acid
GABA-T	gamma-aminobutyric acid transaminase
GAD	glutamic acid decarboxylase
GAT	GABA transporter
GLU	glutamate
GPCR	G-protein coupled receptors
HUGO	human genome organization
IC ₅₀	half maximal inhibitory concentration
IL	intracellular loop
K _i	inhibition constant
LeuT	leucine transporter
mGAT4	murine gamma-aminobutyric acid transporter subtype 4
NSS	neurotransmitter-sodium-symporters
SAR	structure-activity relationship
SEM	standard error of the mean
SERT	serotonin transporter
SLC6	solute carrier 6
SSA	succinic semialdehyde
TM	transmembrane helix
VGAT	vesicular neurotransmitter transporter

6. Literature

1. D.T. Moustakas, Chapter 9 Application of Docking Methods to Structure-Based Drug Design, Computational and Structural Approaches to Drug Discovery: Ligand-Protein Interactions, *Roy Soc Chem.* **2008**, 155-180.
2. I. Pettersson, T. Balle, T. Liljefors, in *Textbook of Drug Design and Discovery, Vol. 4* (Eds.: P. Krogsgaard-Larsen, K. Stromgaard, U. Madsen), *CRC Press, Boca Raton*, **2010**, 43-57.
3. K.L. Lanctot, N. Herrmann, P. Mazzotta, L.R. Khan, N. Ingber. GABAergic function in Alzheimer's disease: evidence for dysfunction and potential as a therapeutic target for the treatment of behavioural and psychological symptoms of dementia. *Can J Psychiatry.* **2004**, 49, 439-453.
4. A.V. Kalueff, D.J. Nutt. Role of GABA in anxiety and depression. *Depress Anxiety.* **2007**, 24, 495-517.
5. S.R. Kleppner, A.J. Tobin. GABA signalling: therapeutic targets for epilepsy, Parkinson's disease and Huntington's disease. *Expert Opin Ther Tar.* **2001**, 5, 219-239.
6. M.A. Daemen, G. Hoogland, J.M. Cijntje, G.H. Spincemaille. Upregulation of the GABA-transporter GAT-1 in the spinal cord contributes to pain behaviour in experimental neuropathy. *Neurosci Lett.* **2008**, 444, 112-115.
7. K. Ishiwari, S. Mingote, M. Correa, J.T. Trevitt, B.B. Carlson, J.D. Salamone. The GABA uptake inhibitor beta-alanine reduces pilocarpine-induced tremor and increases extracellular GABA in substantia nigra pars reticulata as measured by microdialysis. *J Neurosci Methods.* **2004**, 140, 39-46.
8. P.E. Sanmartin, K. Detyniecki. Cannabidiol for Epilepsy: New Hope on the Horizon? *Clin Ther.* **2018**, 40, 1438-1441.
9. I.E. Leppik, L. Gram, R. Deaton, K.W. Sommerville. Safety of tiagabine: summary of 53 trials. *Epilepsy Res.* **1999**, 33, 235-246.
10. World Health Organization, Media centre: *Epilepsy Fact Sheet*, **2018**. <http://www.who.int/en/news-room/fact-sheets/detail/epilepsy>
11. N.G. Bowery, T.G. Smart. GABA and glycine as neurotransmitters: a brief history. *Br J Pharmacol.* **2006**, 147 Suppl 1, 109-119.
12. F.C. Roth, A. Draguhn. GABA metabolism and transport: effects on synaptic efficacy. *Neural Plast.* **2012**, 2012, 805-830.
13. A.C. Foster, J.A. Kemp. Glutamate- and GABA-based CNS therapeutics. *Curr Opin Pharmacol.* **2006**, 6, 7-17.
14. D.F. Owens, A.R. Kriegstein. Is there more to GABA than synaptic inhibition? *Nat Rev. Neurosci.* **2002**, 3, 715-727.
15. R. W. Olson, in *Neuropsychopharmacology: The fifth Generation of Progress* (Ed.: K. L. Davis), Lippincott Williams & Wilkins, Philadelphia, **2002**, 159-168.
16. V. Eulenburg, J. Gomez. Neurotransmitter transporters expressed in glial cells as regulators of synapse function. *Brain Res Rev.* **2010**, 63, 103-112.

17. N.H. Chen, M.E. Reith, M.W. Quick. Synaptic uptake and beyond: the sodium- and chloride-dependent neurotransmitter transporter family SLC6. *Pflug Arch Eur J Phy.* **2004**, 447, 519-531.
18. X.T. Jin, J.F. Pare, Y. Smith. Differential localization and function of GABA transporters, GAT-1 and GAT-3, in the rat globus pallidus. *Eur J Neurosci.* **2011**, 33, 1504-1518.
19. D.J. Nutt, A.L. Malizia. New insights into the role of the GABAA–benzodiazepine receptor in psychiatric disorder. *Brit J Psychiat.* **2018**, 179, 390-396.
20. K.E. McCarson, S.J. Enna. GABA pharmacology: the search for analgesics. *Neurochem Res.* **2014**, 39, 1948-1963.
21. P.A. Bala, J. Foster, L. Carvelli, L.K. Henry. SLC6 Transporters: Structure, Function, Regulation, Disease Association and Therapeutics. *Mol Aspects Med.* **2013**, 34, 197-219.
22. S. Broer, U. Gether. The solute carrier 6 family of transporters. *Br J Pharmacol.* **2012**, 167, 256-278.
23. K.K. Madsen, H.S. White, A. Schousboe. Neuronal and non-neuronal GABA transporters as targets for antiepileptic drugs. *Pharmacol Ther.* **2010**, 125, 394-401.
24. Q.R. Liu, B. Lopez-Corcuera, S. Mandiyan, H. Nelson, N. Nelson. Cloning and expression of a spinal cord- and brain-specific glycine transporter with novel structural features. *J Biol Chem.* **1993**, 268, 22802-22808.
25. L.A. Borden. GABA transporter heterogeneity: pharmacology and cellular localization. *Neurochem Int.* **1996**, 29, 335-356.
26. Y. Zhou, N.C. Danbolt. GABA and Glutamate Transporters in Brain. *Front Endocrinol (Lausanne).* **2013**, 4, 165.
27. J. Guastella, N. Nelson, H. Nelson, L. Czyzyk, S. Keynan, M.C. Miedel, N. Davidson, H.A. Lester, B.I. Kanner. Cloning and expression of a rat brain GABA transporter. *Science.* **1990**, 249, 1303-1306.
28. A. Yamashita, S.K. Singh, T. Kawate, Y. Jin, E. Gouaux. Crystal structure of a bacterial homologue of Na⁺/Cl⁻-dependent neurotransmitter transporters. *Nature.* **2005**, 437, 215.
29. T. Beuming, L. Shi, J.A. Javitch, H. Weinstein. A comprehensive structure-based alignment of prokaryotic and eukaryotic neurotransmitter/Na⁺ symporters (NSS) aids in the use of the LeuT structure to probe NSS structure and function. *Mol Pharmacol.* **2006**, 70, 1630-1642.
30. O. Jardetzky. Simple allosteric model for membrane pumps. *Nature.* **1966**, 211, 969-970.
31. H. Krishnamurthy, E. Gouaux. X-ray structures of LeuT in substrate-free outward-open and apo inward-open states. *Nature.* **2012**, 481, 469-474.
32. L. Shi, M. Quick, Y. Zhao, H. Weinstein, J.A. Javitch. The mechanism of a neurotransmitter:sodium symporter--inward release of Na⁺ and substrate is triggered by substrate in a second binding site. *Mol Cell.* **2008**, 30, 667-677.
33. Z. Zhou, J. Zhen, N.K. Karpowich, R.M. Goetz, C.J. Law, M.E. Reith, D.N. Wang. LeuT-desipramine structure reveals how antidepressants block neurotransmitter reuptake. *Science.* **2007**, 317, 1390-1393.
34. M. Quick, A.M. Winther, L. Shi, P. Nissen, H. Weinstein, J.A. Javitch. Binding of an octylglucoside detergent molecule in the second substrate (S2) site of LeuT establishes an inhibitor-bound conformation. *P Natl Acad Sci USA.* **2009**, 106, 5563-5568.
35. A. Nyola, N.K. Karpowich, J. Zhen, J. Marden, M.E. Reith, D.N. Wang. Substrate and drug binding sites in LeuT. *Curr Opin Struct Biol.* **2010**, 20, 415-422.

36. H. Wang, E. Gouaux. Substrate binds in the S1 site of the F253A mutant of LeuT, a neurotransmitter sodium symporter homologue. *EMBO Rep.* **2012**, 13, 861-866.
37. J.A. Coleman, E.M. Green, E. Gouaux. X-ray structures and mechanism of the human serotonin transporter. *Nature.* **2016**, 532, 334-339.
38. P. Krosggaard-Larsen. gamma-Aminobutyric acid agonists, antagonists, and uptake inhibitors. Design and therapeutic aspects. *J Med Chem.* **1981**, 24, 1377-1383.
39. F.E. Ali, W.E. Bondinell, P.A. Dandridge, J.S. Frazee, E. Garvey, G.R. Girard, C. Kaiser, T.W. Ku, J.J. Lafferty, G.I. Moonsammy, et al. Orally active and potent inhibitors of gamma-aminobutyric acid uptake. *J Med Chem.* **1985**, 28, 653-660.
40. K. Salat, A. Podkowa, P. Kowalczyk, K. Kulig, A. Dziubina, B. Filipek, T. Librowski. Anticonvulsant active inhibitor of GABA transporter subtype 1, tiagabine, with activity in mouse models of anxiety, pain and depression. *Pharmacol Rep.* **2015**, 67, 465-472.
41. C. Braestrup, E.B. Nielsen, U. Sonnewald, L.J.S. Knutsen, K.E. Andersen, J.A. Jansen, K. Frederiksen, P.H. Andersen, A. Mortensen, P.D. Suzdak. (R)-N-[4,4-Bis(3-Methyl-2-Thienyl)but-3-en-1-yl]Nipicotic Acid Binds with High Affinity to the Brain γ -Aminobutyric Acid Uptake Carrier. *J Neurochem.* **1990**, 54, 639-647.
42. P.D. Suzdak, K. Frederiksen, K.E. Andersen, P.O. Sorensen, L.J. Knutsen, E.B. Nielsen. NNC-711, a novel potent and selective gamma-aminobutyric acid uptake inhibitor: pharmacological characterization. *Eur J Pharmacol.* **1992**, 224, 189-198.
43. K.E. Andersen, J.L. Sorensen, P.O. Huusfeldt, L.J. Knutsen, J. Lau, B.F. Lundt, H. Petersen, P.D. Suzdak, M.D. Swedberg. Synthesis of novel GABA uptake inhibitors. 4. Bioisosteric transformation and successive optimization of known GABA uptake inhibitors leading to a series of potent anticonvulsant drug candidates. *J Med Chem.* **1999**, 42, 4281-4291.
44. K.E. Andersen, J. Lau, B.F. Lundt, H. Petersen, P.O. Huusfeldt, P.D. Suzdak, M.D.B. Swedberg. Synthesis of novel GABA uptake inhibitors. Part 6: Preparation and evaluation of N- Ω asymmetrically substituted nipectic acid derivatives. *Bioorg Med Chem.* **2001**, 9, 2773-2785.
45. M. Petrera, T. Wein, L. Allmendinger, M. Sindelar, J. Pabel, G. Hofner, K.T. Wanner. Development of Highly Potent GAT1 Inhibitors: Synthesis of Nipectic Acid Derivatives by Suzuki-Miyaura Cross-Coupling Reactions. *ChemMedChem.* **2016**, 11, 519-538.
46. C. Thomsen, P.O. Sorensen, J. Egebjerg. 1-(3-(9H-carbazol-9-yl)-1-propyl)-4-(2-methoxyphenyl)-4-piperidinol, a novel subtype selective inhibitor of the mouse type II GABA-transporter. *Br J Pharmacol.* **1997**, 120, 983-985.
47. R.P. Clausen, E.K. Moltzen, J. Perregaard, S.M. Lenz, C. Sanchez, E. Falch, B. Frolund, T. Bolvig, A. Sarup, O.M. Larsson, A. Schousboe, P. Krosggaard-Larsen. Selective inhibitors of GABA uptake: synthesis and molecular pharmacology of 4-N-methylamino-4,5,6,7-tetrahydrobenzo[d]isoxazol-3-ol analogues. *Bioorg Med Chem.* **2005**, 13, 895-908.
48. H.S. White, A. Sarup, T. Bolvig, A.S. Kristensen, G. Petersen, N. Nelson, D.S. Pickering, O.M. Larsson, B. Frolund, P. Krosggaard-Larsen, A. Schousboe. Correlation between anticonvulsant activity and inhibitory action on glial gamma-aminobutyric acid uptake of the highly selective mouse gamma-aminobutyric acid transporter 1 inhibitor 3-hydroxy-4-amino-4,5,6,7-tetrahydro-1,2-benzisoxazole and its N-alkylated analogs. *J Pharmacol Exp Ther.* **2002**, 302, 636-644.
49. A. Kragler, G. Hofner, K.T. Wanner. Novel parent structures for inhibitors of the murine GABA transporters mGAT3 and mGAT4. *Eur J Pharmacol.* **2005**, 519, 43-47.
50. S. Hack, B. Worlein, G. Hofner, J. Pabel, K.T. Wanner. Development of imidazole alkanolic acids as mGAT3 selective GABA uptake inhibitors. *Eur J Med Chem.* **2011**, 46, 1483-1498.

-
51. T.G.M. Dhar, L.A. Borden, S. Tyagarajan, K.E. Smith, T.A. Branchek, R.L. Weinsank, C. Gluchowski. Design, Synthesis and Evaluation of Substituted TriarylNipecotic Acid Derivatives as GABA Uptake Inhibitors: Identification of a Ligand with Moderate Affinity and Selectivity for the Cloned Human GABA Transporter GAT-3. *J Med Chem.* **1994**, 37, 2334-2342.
 52. J. Pabel, M. Faust, C. Prehn, B. Worlein, L. Allmendinger, G. Hofner, K.T. Wanner. Development of an (S)-1-{2-[tris(4-methoxyphenyl)methoxy]ethyl}piperidine-3-carboxylic acid [(S)-SNAP-5114] carba analogue inhibitor for murine gamma-aminobutyric acid transporter type 4. *ChemMedChem.* **2012**, 7, 1245-1255.
 53. N. Millot, C. Piazza, S. Avolio, P. Knochel. Aminomethylation of Functionalized Organozinc Reagents and Grignard Reagents Using Immonium Trifluoroacetates. *Synthesis.* **2000**, 7, 941-948.
 54. N.M. Barl, E. Sansiaume-Dagousset, G. Monzon, A.J. Wagner, P. Knochel. Preparation and reactions of heteroarylmethylzinc reagents. *Org Lett.* **2014**, 16, 2422-2425.
 55. M.S. Cooper, H. Heaney. Mannich reactions of aryl-trialkylstannanes using preformed dialkyl-methyleneiminium salts. *Tetrahedron Lett.* **1986**, 27, 5011-5014.
 56. S. Suga, M. Okajima, J.-i. Yoshida. Reaction of an electrogenerated 'iminium cation pool' with organometallic reagents. Direct oxidative α -alkylation and -arylation of amine derivatives. *Tetrahedron Lett.* **2001**, 42, 2173-2176.
 57. A. Saito, K. Iimura, M. Hayashi, Y. Hanzawa. Catalytic addition of alkenylzirconocene chloride to 3,4-dihydroisoquinoline and its enantioselective reaction. *Tetrahedron Lett.* **2009**, 50, 587-589.
 58. A. Erkkilä, I. Majander, P.M. Pihko. Iminium Catalysis. *Chem Rev.* **2007**, 107, 5416-5470.
 59. T.A. Bryson, G.H. Bonitz, C.J. Reichel, R.E. Dardis. Performed Mannich salts: a facile preparation of dimethyl(methylene)ammonium iodide. *J Org Chem.* **1980**, 45, 524-525.
 60. C. Rochin, O. Babot, J. Dunoguès, F. Duboudin. A New Convenient Synthesis of Dialkyl(methylene)ammonium Chloride. *Synthesis.* **1986**, 1986, 228-229.
 61. P. Wipf, Hydrozirconation and Its Applications, Metallocenes in Regio- and Stereoselective Synthesis: -/-, *Springer Berlin Heidelberg*, Berlin, Heidelberg, **2005**, 1-25.
 62. D.W. Hart, J. Schwartz. Hydrozirconation. Organic synthesis via organozirconium intermediates. Synthesis and rearrangement of alkylzirconium(IV) complexes and their reaction with electrophiles. *J Am Chem Soc.* **1974**, 96, 8115-8116.

7. Publications and Manuscripts

7.1. First publication:

Krisztián Tóth, Georg Höfner, Klaus T. Wanner;

Bioorganic & Medicinal Chemistry, **2018**, Volume 26, Issue 12, 3668-3687.

“Synthesis and biological evaluation of novel N-substituted nipecotic acid derivatives with an alkyne spacer as GABA uptake inhibitors”

7.2. Second publication:

Krisztián Tóth, Georg Höfner, Klaus T. Wanner;

Bioorganic & Medicinal Chemistry, **2018**, Volume 26, Issue 22, 5944-5961.

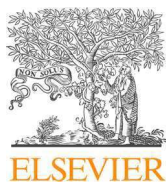
“Synthesis and biological evaluation of novel N-substituted nipecotic acid derivatives with a *trans*-alkene spacer as potent GABA uptake inhibitors”

7.3. Manuscript of the third publication:

Krisztián Tóth, Georg Höfner, Klaus T. Wanner;

Manuscript to be submitted to Bioorganic & Medicinal Chemistry.

“Synthesis and biological evaluation of novel N-substituted nipecotic acid derivatives with a *cis*-alkene spacer as GABA uptake inhibitors”



Contents lists available at ScienceDirect

Bioorganic & Medicinal Chemistry

journal homepage: www.elsevier.com/locate/bmc



Synthesis and biological evaluation of novel *N*-substituted nipecotic acid derivatives with an alkyne spacer as GABA uptake inhibitors



Krisztián Tóth, Georg Höfner, Klaus T. Wanner*

Department of Pharmacy – Center for Drug Research, Ludwig-Maximilians-Universität München, Butenandstr. 5–13, 81377 Munich, Germany

ARTICLE INFO

Keywords:

GABA uptake inhibitor
mGAT4
Nipecotic acid
Iminium ion chemistry

ABSTRACT

In this study, we present the synthesis and structure–activity relationships (SAR) of novel *N*-substituted nipecotic acid derivatives closely related to (*S*)-SNAP-5114 (**2**) in the pursuit of finding new and potent mGAT4 selective inhibitors. By the use of iminium ion chemistry, a series of new *N*-substituted nipecotic acid derivatives containing a variety of heterocycles, and an alkyne spacer were synthesized. Biological evaluation of the prepared compounds showed, how the inhibitory potency and subtype selectivity for the murine GABA transporters (mGATs) were influenced by the performed modifications.

1. Introduction

The major inhibitory neurotransmitter in the central nervous system (CNS) is gamma-aminobutyric acid (GABA).¹ The decrease in the GABAergic neurotransmission can cause severe neurological disorders like epilepsy,^{2,3} Alzheimer's disease,⁴ and depression.⁵ The concentration of GABA in the synaptic cleft is amongst other factors controlled by the GABA transporters (GATs).⁶ These membrane-bound proteins,^{7,8} that exist in four different subtypes, belong to the solute carrier 6 (SLC6) family.^{9,10} The nomenclature for these proteins that vary with regard to their distribution and function depends on the species from which they are cloned. GABA transporters cloned from mice are named as mGAT1, mGAT2, mGAT3, and mGAT4, whereas according to the Human Genome Organization (HUGO), they are denoted as GAT1 (≡mGAT1), BGT-1 (≡mGAT2), GAT2 (≡mGAT3), and GAT3 (≡mGAT4).¹¹ mGAT1 and mGAT4 have been found to be clearly predominating in the CNS.^{7,12} Of these, mGAT1 is mainly responsible for the neuronal uptake of GABA in presynaptic cells. Whereas mGAT4 mediates, in particular, GABA transport from the synaptic cleft into glial cells.^{13,14} mGAT2 and mGAT3 are playing a rather insignificant role in the termination of the GABAergic neurotransmission,¹⁵ but are present at high levels in the kidneys and liver¹⁶ (Fig. 1).

Through the inhibition of mGAT1 and mGAT4, elevated levels of GABA can be achieved in the CNS which offers a treatment for diverse neurological disorders mentioned before. Tiagabine (**1**) is a selective mGAT1 reuptake inhibitor used in the treatment of epilepsy, anxiety disorders, and neuropathic pain, but its main drawbacks are side effects such as dizziness, asthenia, nervousness, tremor, diarrhea, and depression.^{17,18} The selective inhibition of mGAT4 could open up a new

therapeutic approach with less side effects, but selective and potent mGAT4 inhibitors are not available so far.

In addition to highly potent mGAT1 selective reuptake inhibitors such as tiagabine (**1**)^{19,20} also several ligands of the three non-mGAT1 proteins, i.e. mGAT2–mGAT4 have been identified, though for the most part of these compounds the potency and selectivity are far behind that of mGAT1 inhibitors.^{21–25} (*S*)-SNAP-5114 (**2**) represents the first prototypic mGAT4 inhibitor with reasonable potency at and selectivity for this target.²⁶ Later on, carba-analogs of **2** such as DDPM-1457 (**3**) were identified to display similar potencies and subtype selectivities, but to be devoid of the chemical instability encountered for trityl derivative **2**.²⁷ More recently, isatin derivatives have been reported as a new class of hGAT3 (≡mGAT4) inhibitors with compound **4** representing the most potent member.²⁸

In this study, we report on our efforts to broaden the structure-activity relationship of the carba-analogs of (*S*)-SNAP-5114 (**2**) i.e. of compounds such as DDPM-1457 (**3**), at the same time aiming at the identification of more potent and selective inhibitors for mGAT4. To this end, the structure of DDPM-1457 (**3**) has been varied in different respects, as shown in Fig. 2. The first two modifications involved the linker between the nipecotic acid and the aromatic lipophilic residue. Herein as a major modification, instead of a *trans*-moiety as in **3**, an alkyne subunit was implemented resulting as a first representative in *rac*-**5a**. In a second step, one of the aromatic moieties of the lipophilic residue was replaced with a series of new residues (*rac*-**5b–j**), like aromatic and heteroaromatic cycles, benzylic residues or sterically less demanding groups (Table 1). Furthermore, we also increased the length of the alkyne spacer by insertion of one methylene group. This was performed at two different positions, both directly adjacent to the triple

* Corresponding author.

E-mail address: klaus.wanner@cup.uni-muenchen.de (K.T. Wanner).

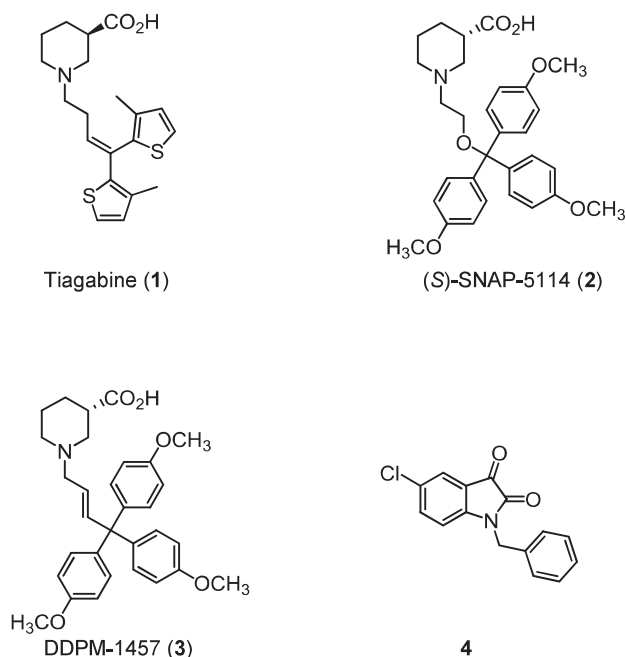


Fig. 1. Selected GABA uptake inhibitors.

bond, either oriented towards the nipecotic acid residue (*rac*-6a, *rac*-6k) or the lipophilic residue (*rac*-7a, *rac*-7k). That way the effect of the linker length on the potency of the test compounds should be elucidated.

2. Results and discussion

2.1. Chemistry

A retrosynthetic analysis for the carboxylic acid ethyl esters of the targeted scaffolds (*rac*-8a–j for *rac*-5a–j; *rac*-11a for *rac*-6a, *rac*-11k for *rac*-6k, *rac*-13a for *rac*-7a, *rac*-13k for *rac*-7k, Fig. 3) led us by disconnecting the linker to following building blocks for the synthesis of the targeted compounds: A common iminium compound *rac*-9 to be trapped with various Grignard reagents (10a–j, 12a, 12k, 14a, 14k). Iminium compound *rac*-9 could be expected to be easily accessible from an *N,O*-acetal derivative *rac*-23 of ethyl nipecotate *rac*-22 (Table 2). The use of iminium ion chemistry for the outlined purpose seemed highly rewarding as only organomagnesium species would have to be varied and only non-toxic and inexpensive chemicals would be involved (Table 2).

2.1.1. Preparation of the alkynes

The synthesis of alkynes **18a–j** required as precursors of the organomagnesium species, that were to be reacted with iminium salt *rac*-9, is summarized in Table 1. In the first step, the alcohols **16a–f** were formed by the reaction of 4,4'-dimethoxybenzophenone (**15**) with the respective organometallic reagent. For the synthesis of **16a–b** and **16f** Grignard reagents, 4-methoxyphenylmagnesium bromide,²⁹ benzo[d][1,3]dioxol-5-ylmagnesium bromide,³⁰ and benzo[b]thiophen-5-ylmagnesium bromide³¹ were employed and for the preparation of alcohols **16c–e** organolithium reagents, i. e. thiazol-2-ylolithium,³² (1-methyl-1H-imidazol-2-yl)lithium,³³ and thiophen-3-ylolithium³² were used, respectively (yields 60%–98%). To obtain chlorides **17a–f**, in the following step alcohols **16a**, **16f** were reacted³⁴ with acetyl chloride (AcCl), alcohols **16b**, **16c**, **16e** with thionyl chloride (SOCl₂),³⁵ and alcohol **16d** with a mixture³⁶ of AcCl and SOCl₂, respectively. As such chlorides are usually unstable due to the ease of carbenium ion formation,³⁷ compounds **17a–f** were used without any further purification. Alkynes **18a–d** were synthesized from chlorides **17a–d** by reaction with ethynylmagnesium bromide in analogy to a literature method,³⁸ in reasonable to excellent yields (42–97%).

Attempts to synthesize **18e–f** by the same protocol, i.e. by reaction of chlorides **17e–f** comprising heterocyclic residues (thiophene or benzothiophene) with ethynylmagnesium bromide failed. Hence a modified method was used. Here, instead of ethynylmagnesium bromide, (trimethylsilyl)ethynyllithium³⁹ was employed which gave the TMS protected alkynes **21e–f** in reasonable yields (52% and 63%). Finally, after removal of the TMS protective group by means of K₂CO₃ in MeOH,⁴⁰ the desired alkynes **18e–f** were obtained in yields of 84% and 95%, respectively. Alkyne **18g** exhibiting a hydroxy function instead of an aromatic moiety was synthesized by addition of ethynylmagnesium bromide to **15** according to a literature procedure.⁴¹

The known TMS diaryl alkyne **21h**⁴² as precursor of the desired alkyne **18h** was synthesized according to a literature method⁴³ from diaryl alcohol **19** via diaryl bromide **20**.⁴⁴ Removal of the TMS group by the treatment with K₂CO₃ in MeOH yielded the diaryl alkyne **18h**. TMS protected alkyne **21h** was further employed for the construction of **18i–j** by the introduction of a benzyl residue in the first step. Treatment⁴⁵ of the alkyne **21h** with *n*BuLi and subsequently with either benzyl bromide or 4-methoxybenzyl chloride⁴⁶ gave TMS protected alkynes **21i–j** (96% and 90%) which after removal of the TMS group delivered alkynes **18i–j** in 77% and 88% yield, respectively.

2.1.2. Synthesis of the *N*-substituted nipecotic acid esters by the coupling of the nipecotic acid derived iminium salt with alkynyl Grignard reagents, and the subsequent hydrolysis to the corresponding acids

Reactions between iminium salts and organometallic nucleophiles are well precedented in the literature.^{47–49} As a source for the iminium ion *rac*-9, we intended to use the *N,O*-acetal derivative *rac*-23. This

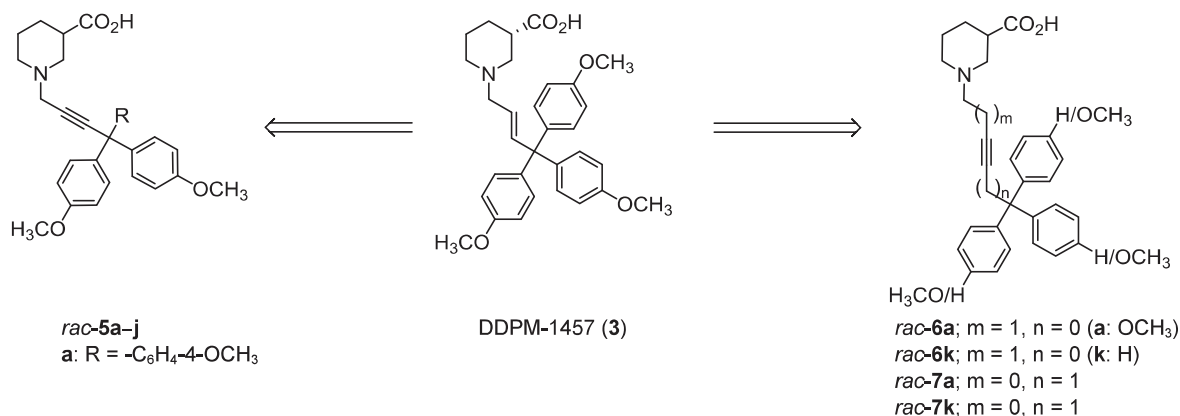
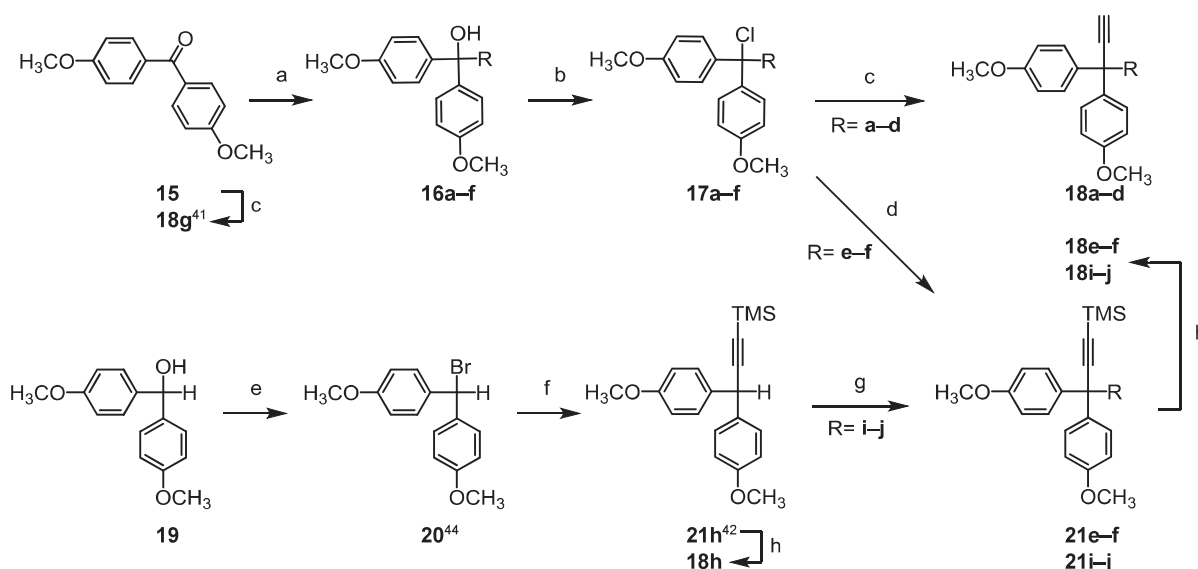
Fig. 2. General structures of targeted *N*-substituted nipecotic acid derivatives *rac*-5a–j, *rac*-6a, *rac*-6k and *rac*-7a, *rac*-7k; for structures of residues R see Table 4.

Table 1
Synthesis of the alkynes **18a–j**.



Entry	R	Alcohols (16)	Yield % ⁱ	Halides (17, 20)	Yield % ^j	TMS Alkynes (21)	Conditions	Yield % ⁱ	Alkynes (18)	Conditions	Yield % ⁱ
1		16a ²⁹	86	17a ³⁴	89	–	–	–	18a ³⁸	c	97
2		16b	98	17b	95	–	–	–	18b	c	97
3		16c	60	17c	99	–	–	–	18c	c	52
4		16d	97	17d	95	–	–	–	18d	c	42
5		16e	95	17e	99	21e	d	52	18e	h	84
6		16f	76	17f	99	21f	d	63	18f	h	95
7	OH	–	–	–	–	–	–	–	18g ⁴¹	c	91
8	H	19	–	20 ⁴⁴	99	21h ⁴²	f	93	18h	h	83
9		–	–	–	–	21i	g	96	18i	h	70
10		–	–	–	–	21j	g	90	18j	h	88

Reagents and conditions: (a) RMgBr or RLi; (b) AcCl or SOCl₂; (c) HC≡CMgBr; (d) TMSC≡CLi; (e) AcBr, toluene; (f) TMSC≡CMgCl, CuBr, THF; (g) *n*BuLi, 4-methoxybenzyl chloride or benzyl bromide, THF, –78 °C; (h) K₂CO₃, MeOH. (i) Yield after chromatography; (j) Yield after removal of the solvents.

compound could be efficiently synthesized by reaction of *rac*-**22** with paraformaldehyde (PFA) in EtOH, the yield amounting to 88% (Table 2).⁵⁰ For the *in situ* generation of iminium salt *rac*-**9** analogously to a literature method,⁵¹ the *N,O*-acetal *rac*-**23** was treated with trimethylsilyl chloride (TMSCl) prior to every coupling reaction. The formation of the expected iminium salt *rac*-**9** has exemplarily been verified in an ¹H NMR experiment. For the coupling reactions, the iminium salt *rac*-**9** was reacted with the respective ethynylmagnesium nucleophiles **10a–j** prepared from alkynes **18a–j** and *n*BuMgCl. This delivered the desired esters *rac*-**8a–j** in moderate to good yields (39%–85%, Table 2). In case of the synthesis of *rac*-**8g** from alkyne **18g**

(Table 2, entry 7), the amount of *n*BuMgCl needed for the deprotonation of **18g** was doubled to account for the acidic property of the hydroxy group also present in the molecule. The chemoselectivity of this reaction deserves extra mentioning. Though highly nucleophilic Grignard reagents were employed in the presence of an ester function at elevated temperatures (40 °C), no significant formation of side products could be observed.

Finally, all of the thus obtained ethyl esters *rac*-**8a–j** were hydrolyzed by treatment with 12 M NaOH in MeOH²² to give after wash up the free acids *rac*-**5a–j** in good to very good yields (79%–98%, Table 2). In case of the diaryl derivative *rac*-**18h** (Table 2, entry 8), an acidic

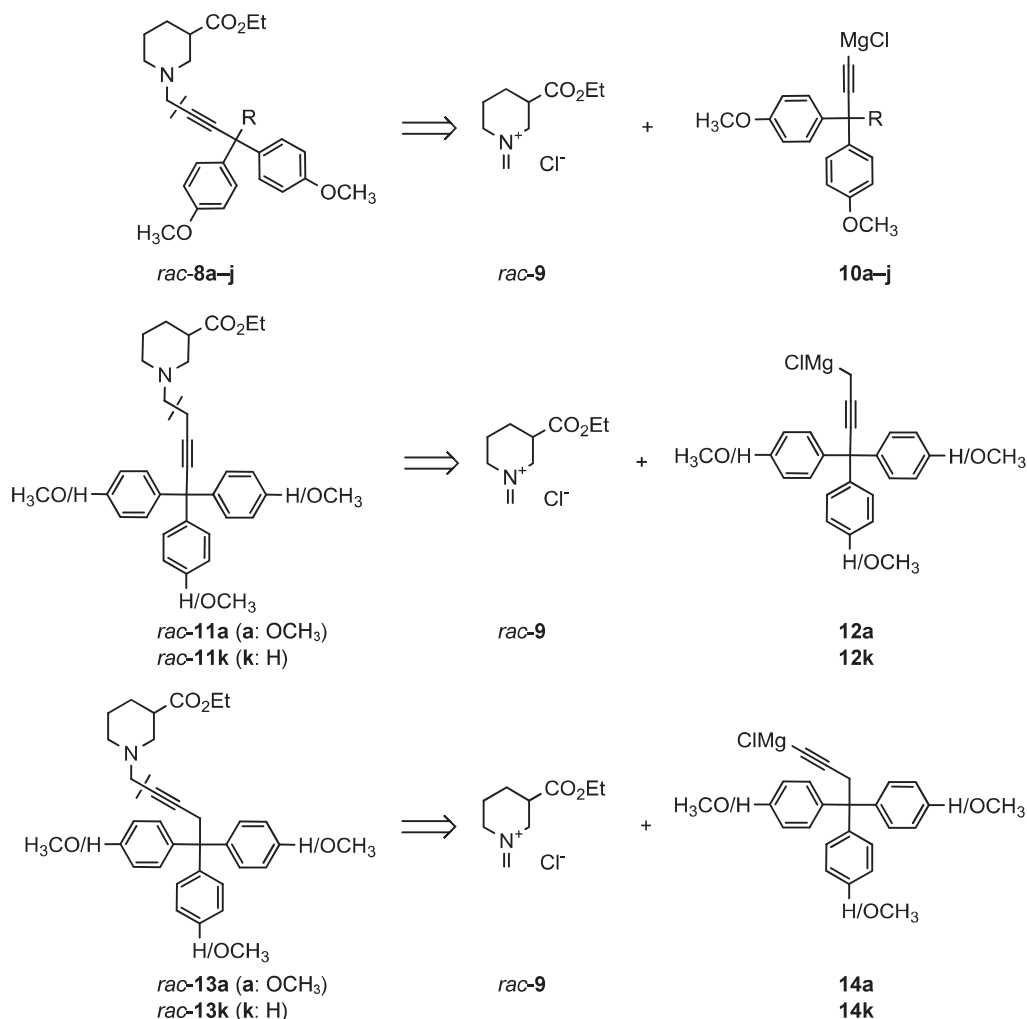


Fig. 3. Retrosynthetic analysis of targeted *N*-substituted nipecotic acid ester analogs *rac*-8a-j, *rac*-11a, *rac*-11k, *rac*-13a, *rac*-13k.

hydrolysis⁵² with 3 M HCl at elevated temperature was performed to obtain *rac*-5h as under basic conditions side reactions leading to an inseparable compound mixture occurred.⁵³

2.1.3. Synthesis of the *N*-substituted nipecotic acid esters with a longer spacer, and subsequent hydrolysis to the corresponding acids

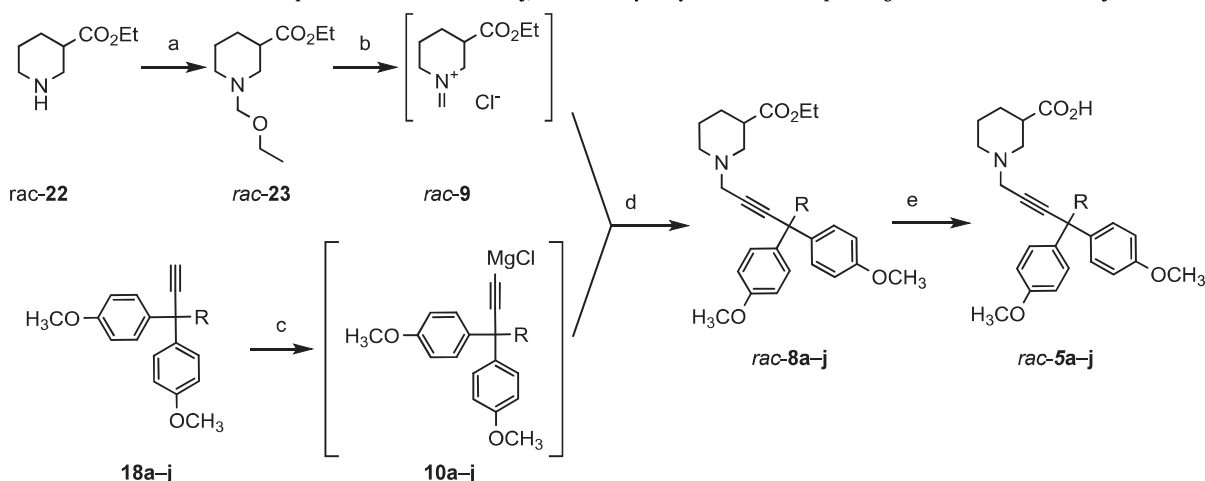
For the synthesis of the desired alkynes exhibiting a longer spacer between the nipecotic acid moiety and the lipophilic residue (Scheme 1), chlorides **17a**, **17k** were reacted with propargylmagnesium bromide⁵⁴ or with lithium chloropropargylide⁵⁵ to get to the targeted alkynes **25a**, **25k** and **26a**, **26k**, respectively. The subsequent coupling reactions in which the iminium salt *rac*-9 was treated either with the Grignard reagents **14a** and **14k** derived from alkynes **25a** and **25k** or with a propargylic Grignard reagent **12a** and **12k** prepared⁵⁶ from the propargyl chlorides **26a** and **26k** yielded the carboxylic esters *rac*-13a, *rac*-13k, *rac*-11a, and *rac*-11k, respectively, with a spacer elongated from three to four carbon atoms. According to literature,⁵⁷ propargylic Grignard reagents like **12a**, **12k** (Scheme 1) can undergo a rearrangement to give allenic isomers. This was also observed in the case of the reaction of the iminium salt *rac*-9 with **12a**, and **12k**, as a side reaction and led to the formation of allenic side products *rac*-27a, *rac*-27k which diminished the yields for the desired compounds *rac*-11a (22%), and *rac*-11k (21%) substantially.

The same standard procedure as employed for the preparation of free acids *rac*-5a-g and *rac*-5i-j (12 M NaOH, MeOH) was used for the hydrolysis of esters *rac*-13a, *rac*-13k, *rac*-11a, and *rac*-11k to obtain

the acids *rac*-6a, *rac*-6k, *rac*-7a, and *rac*-7k (Table 5), respectively in good to very good yields (79%–98%). The *N*-substituted nipecotic acid ester side products with an allenic functionality *rac*-27a and *rac*-27k (Scheme 1) were hydrolyzed under the same conditions giving the *N*-substituted nipecotic acids *rac*-24a and *rac*-24k (Table 5) in 97% and 92% yields, respectively.

2.2. Biological evaluation

The newly synthesized *N*-substituted nipecotic acid derivatives with an alkyne spacer *rac*-5a-j, *rac*-6a, *rac*-6k, *rac*-7a, *rac*-7k and also the *N*-substituted nipecotic acid derivatives with an allenic moiety *rac*-24a, *rac*-24k were evaluated for their inhibitory potencies at mGAT4 and additionally for the non-mGAT4 transporter subtypes mGAT1–mGAT3, using a standardized [³H]GABA uptake assay based on HEK cells developed by our group.⁵⁸ In addition, also binding affinities of these compounds towards mGAT1 (expressed in HEK cells) were determined using a standardized MS Binding Assay.⁵⁹ The measurements were done in triplicates and wherever possible, the potencies of the tested compounds in the uptake assays are given as pIC₅₀ values and the binding affinities as pK_i values. In cases where test compounds at a concentration of 100 μM were not able to reduce [³H]GABA uptake to a value below 50%, which equals pIC₅₀ values ≤ 4.00, only the percent values of the remaining [³H]GABA uptake is given. Analogously, where test compounds applied at 100 μM did not reduce specific MS Marker binding to a value below 50%, only the percentage of remaining MS

Table 2Formation of the *N*-substituted nipecotic acid esters *rac*-**8a–j**, and their hydrolysis to the corresponding acid derivatives *rac*-**5a–j**.

Entry	Alkynes (18)	R	Esters (<i>rac</i> - 8)	Yield % ^f	Acids (<i>rac</i> - 5)	Yield % ^g
1	18a ³⁸		<i>rac</i> - 8a	80	<i>rac</i> - 5a	81
2	18b		<i>rac</i> - 8b	71	<i>rac</i> - 5b	93
3	18c		<i>rac</i> - 8c	85	<i>rac</i> - 5c	95
4	18d		<i>rac</i> - 8d	39	<i>rac</i> - 5d	98
5	18e		<i>rac</i> - 8e	57	<i>rac</i> - 5e	95
6	18f		<i>rac</i> - 8f	62	<i>rac</i> - 5f	85
7	18g ⁴¹	OH	<i>rac</i> - 8g	72 ^h	<i>rac</i> - 5g	83
8	18h	H	<i>rac</i> - 8h	56	<i>rac</i> - 5h	99 ⁱ
9	18i		<i>rac</i> - 8i	57	<i>rac</i> - 5i	90
10	18j		<i>rac</i> - 8j	75	<i>rac</i> - 5j	90

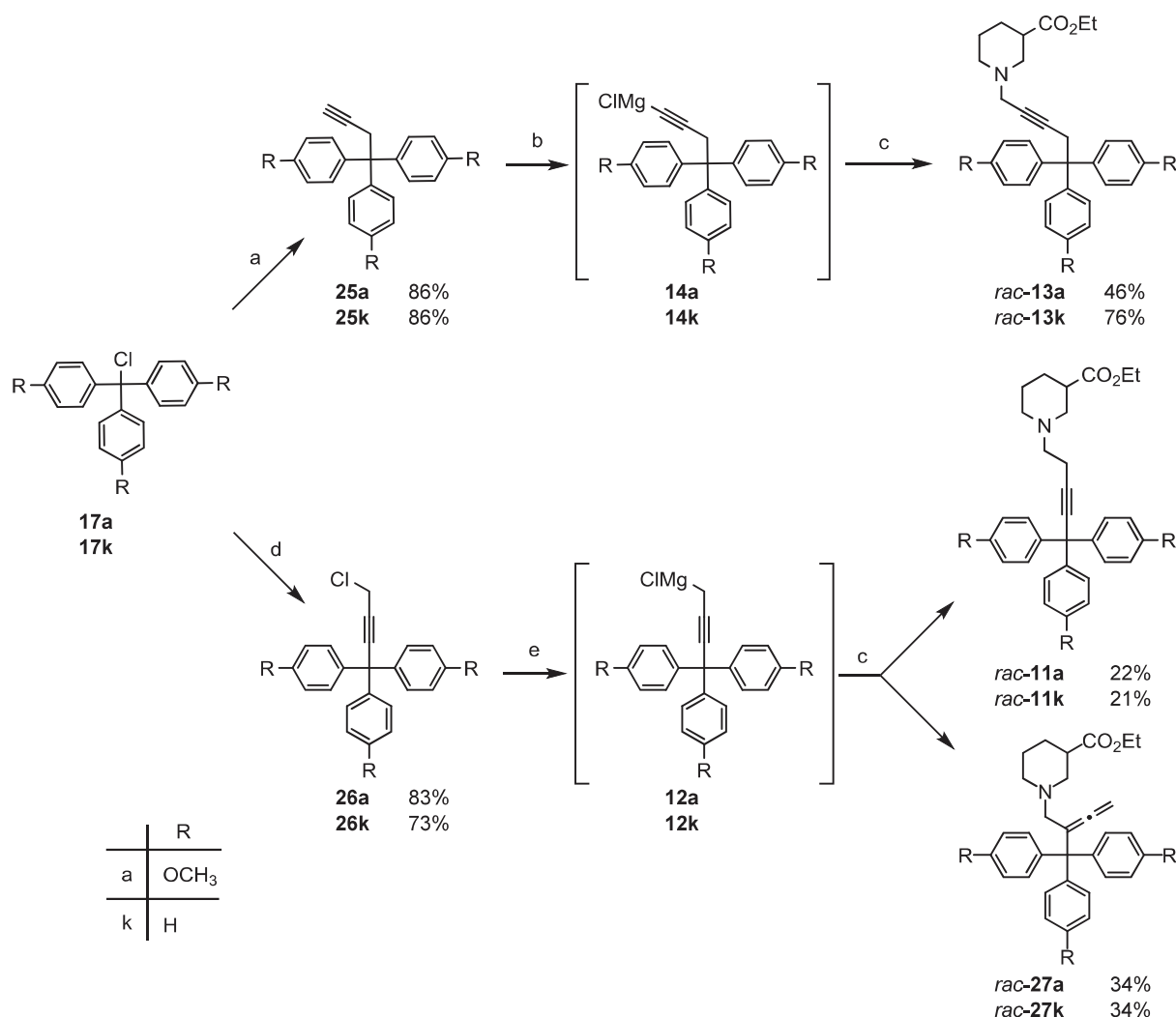
Reagents and conditions: (a) PFA, K₂CO₃, EtOH; (b) TMSCl, THF; (c) *n*BuMgCl, THF; (d) THF, 45 °C; (e) 12 M NaOH, MeOH; (f) Isolated yield after chromatography; (g) Isolated yield after extraction; (h) 2 equiv. *n*BuMgCl was used; (i) Acidic hydrolysis: 3 M HCl, 50 °C, isolated as HCl salt.

Marker bound to the target is given ($\equiv pK_i \leq 4.00$).

Both (*S*)-SNAP-5114 (**2**) and DDPM-1457 (**3**) are enantiopure compounds derived from (*S*)-nipecotic acid which exhibit the same nonpolar residue, but differ with regard to their linker connecting their two subunits. In one case, this is an ethyloxy moiety (*S*)-SNAP-5114, (**2**), in the other a *trans*-configured propenyl chain (DDPM-1457, **3**) and as thus triatomic as the former. These differences in the nature of the linker, an ether function versus a C–C double bond, caused only minor differences in the binding affinities and inhibitory potencies, but led to a distinctly improved stability for DDPM-1457 (**3**, Table 3). Besides, for comparison purposes also DDPM-859 (**29**) and compound **30** have been included in Table 3.²⁷ Both are closely related to (*S*)-SNAP-5114 (**2**) from which they only differ by an additional *ortho*-methyl substituent at either one (**29**) or two (**30**) of the three phenyl residues present in these compounds. Analogue **30**, still being racemic, had a somewhat reduced

mGAT4 inhibitory potency as compared to (*S*)-SNAP-5114 (**2**) whereas its chemical stability was distinctly higher. In contrast, enantiopure DDPM-859 (**29**) was characterized by not only a nominally slightly higher mGAT4 inhibitory potency as compared to **2**, but also a clearly improved subtype selectivity in regard to mGAT3, the chemical stability remained, however, largely unchanged.

For economic reasons, for the synthesis of all compounds listed in Table 4, racemic ethyl nipecotate (*rac*-**22**) has been employed. This also warrants that the biological activity of both enantiomers is reflected in the test data. In general, for mGAT4 inhibitors derived from nipecotic acid, the higher potency resides in the (*S*)-enantiomer. Still, by testing the (*S*)-enantiomers, potent (*R*)-enantiomers might be missed. As for the comparison of the test results obtained for the new compounds, in Table 4, all being racemic, enantiopure mGAT4-selective DDPM-1457 (**3**) seemed less appropriate in these cases, the racemic form, DDPM-



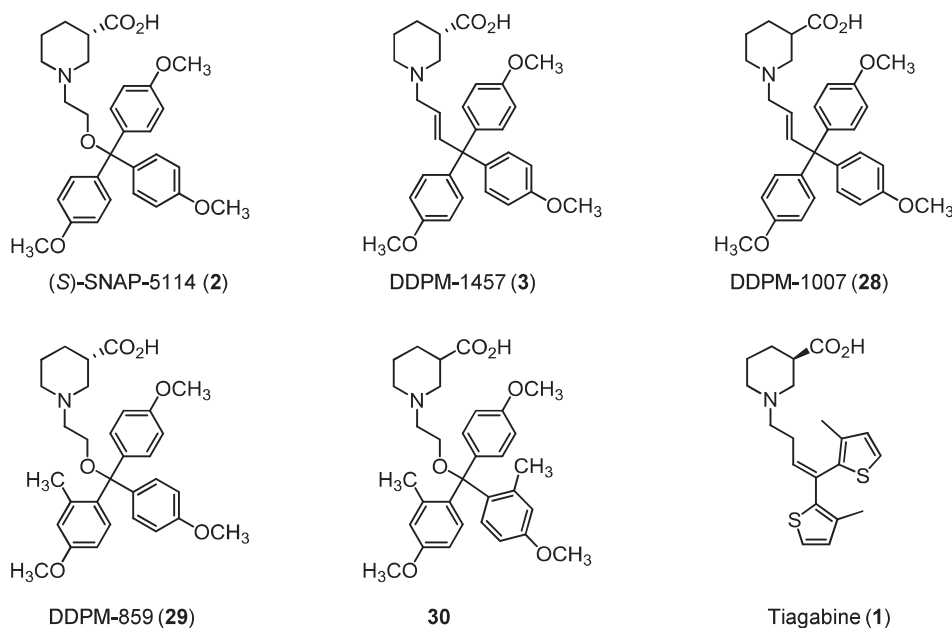
Scheme 1. Synthesis of alkynes **25a**, **25k** and **26a**, **26k**, and the subsequent coupling to the corresponding *N*-substituted nipecotic acid esters with a longer spacer *rac*-**13a**, *rac*-**13k**, *rac*-**11a**, *rac*-**11k**, and the *N*-substituted nipecotic acid esters with an allenic spacer *rac*-**27a**, *rac*-**27k**. Reagents and conditions: (a) $\text{HC}\equiv\text{CCH}_2\text{MgBr}$; (b) $n\text{BuMgCl}$, THF, 45 °C; (c) *rac*-**9**, THF, 45 °C; (d) $\text{ClCH}_2\text{C}\equiv\text{CLi}$, THF, -78 °C; (e) Mg, THF.

1007 (**28**), was used as reference point.^{27,60}

Compound *rac*-**5a** (Table 4) differs from DDPM-1007 (**28**) only by the exchange of the *trans*-configured C–C double bond in the spacer by an alkyne group. This relatively small change resulted in a drop of the potency of *rac*-**5a** at mGAT4 by about one log unit, whereas the potency at mGAT1 was increased by about 0.5 log units (compare Table 4, entry 1 with Table 3, entry 3). Compounds *rac*-**5b** to *rac*-**5g** show the effects the modification of the lipophilic moiety exerts (Table 4), namely the replacement of one aromatic moiety of the triaryl methyl residue with a heterocyclic or heteroaromatic (*rac*-**5b–f**) or benzylic group (*rac*-**5i–j**) or by a hydrogen atom or hydroxyl group (*rac*-**5g–h**). Compound *rac*-**5b** with an additional oxygen-containing ring shows nominally slightly lower potencies on all mGATs except for mGAT2 for which they remain the same. Compounds *rac*-**5c–d** with a thiazole or imidazole residue similarly to *rac*-**5g** possessing only a hydroxy group instead of one of the three 4-methoxyphenyl moieties, in *rac*-**5a**, were devoid of any reasonable activity at the mGATs ($\text{pIC}_{50} = 4.00$; Table 4, entries 3, 4, and 7). The potency displayed at mGAT4 of the thiophene ring containing *rac*-**5e** was similar to that of *rac*-**5a**, whereas the mGAT1–3 values were nominally slightly lower (Table 4, entry 5). Interestingly, *rac*-**5f** bearing a benzothiophene ring has higher potencies at all mGATs than *rac*-**5a**, but possesses no reasonable selectivity for either of the four subtypes. In case of *rac*-**5h**, where one of the three aromatic residues of

5a had been omitted, the potency at mGAT4 remained unchanged, but the potency at and selectivity for mGAT1 was somewhat higher, whereas at mGAT3, it was lower and at mGAT2 practically inactive (Table 4, entry 8). Compounds *rac*-**5i–j** with a benzylic moiety showed slightly reduced potencies at mGAT2–4 whereas at mGAT1, it was nominally similar to *rac*-**5i** or slightly improved (*rac*-**5j**), (Table 4, entry 9–10).

Finally, we turned our attention toward compounds with an, as compared to *rac*-**5a**, by one carbon extended spacer. The results for the respective compounds *rac*-**6a**, *rac*-**6k**, *rac*-**7a**, and *rac*-**7k** as well as for *rac*-**24a** and *rac*-**24k** containing an allene subunit are shown in Table 5. For compounds *rac*-**6a** and *rac*-**7a** differing from *rac*-**5a** by formal insertion of one methylene group adjacent to the nipecotic acid or the trityl residue the potencies at all transporters remains very similar (Table 5, entry 1 and 3). The corresponding compounds without methoxy groups in the *para*-position of the phenyl rings, (*rac*-**6k**, and *rac*-**7k**, Table 5, entry 2 and 4) had, as compared to *rac*-**6a** and *rac*-**7a**, distinctly lower potencies at mGAT3–4, and significantly increased at mGAT1. This was especially true for *rac*-**6k** having a pIC_{50} of 6.37 ± 0.09 at mGAT1 (Table 5, entry 2). Compounds **24a**, and *rac*-**24k** exhibiting an allene functionality were found to neither possess any reasonable potency at or selectivity for mGAT1–4 (Table 5, entry 5–6).

Table 3Binding affinities and inhibitory potencies of reference compounds **2**, **3**, **28**, **29**, **30**, and **1** from the literature.

Entry	Compound	pK _i ^a	pIC ₅₀ ^b			
			mGAT1	mGAT2	mGAT3	mGAT4
1	(S)-SNAP-5114 (2) ^c	4.56 ^c ± 0.02	4.07 ± 0.09	56%	5.29 ± 0.04	5.71 ± 0.07
2	DDPM-1457 (3) ^c	4.33 ^c ± 0.06	4.40 ± 0.05	4.42 ± 0.11	5.47 ± 0.02	5.87 ± 0.08
3	DDPM-1007 (28) ^c	4.83 ^c ± 0.04	4.32 ± 0.05	4.68 ± 0.09	5.19 ± 0.06	5.67 ± 0.06
4	DDPM-859 (29) ^c	59% ^e	4.19 ± 0.07	4.12 ± 0.08	4.85 ± 0.04	5.78 ± 0.03
5	30 ^c	4.42 ^c ± 0.02	4.17 ± 0.02	4.49 ± 0.09	4.54 ± 0.10	5.07 ± 0.09
6	Tiagabine (1) ^d	7.43 ± 0.11	6.88 ± 0.12	50%	64%	73%

^a Results of MS Binding Assay results are given as pK_i ± SEM. Percentages represent remaining specific NO711 binding in presence of 100 μM test compound.

^b Results of [³H]GABA uptake assays results are given as pIC₅₀ ± SEM. Percentages represent remaining [³H]GABA uptake in presence of 100 μM test compound.

^c Reference literature.²⁷

^d Reference literature.⁶⁰

^e pK_i results were determined in our group from compounds synthesized according to literature.^{26,27}

The binding affinities at mGAT1 determined for the compounds listed in Tables 4 and 5 in MS Binding Assays and given as pK_i values were all in the same range as the corresponding potencies, pIC₅₀ values, for the same transporters. Thereby, all of the pK_i values tend to be higher than the corresponding pIC₅₀ data up to about a half log unit. This is a general phenomenon which has been reported already earlier.^{21,59}

3. Conclusion

For the development of new mGAT4 inhibitors, the structure of DDPM-1457 (**3**), a carba-analogue of prototypic mGAT4 inhibitor (S)-SNAP-5114 (**2**) has been extensively varied. For the construction of the new compounds, iminium ion chemistry involving addition reaction of organomagnesium reagents to a nipecotic acid derived iminium ion, *rac*-**9**, was found to be well suited. As a major modification, to further increase the rigidity of the linker, the linker double bond was replaced by a triple bond. Furthermore, this new linker was elongated by one carbon atom by introduction of a CH₂ moiety on either side of the triple bond. In any case, a significant decrease in mGAT4 potency, of about one log unit, as compared to DDPM-1457 (**3**), resulted.

Additionally, the structure of the triarylmethyl moiety of *rac*-**5a**, the direct alkyne analogue of DDPM-1457 (**3**), was modified by replacing one of the three aryl residues by different aryl, heteroaryl, and benzyl groups. As compared to the parent compound *rac*-**5a**, the mGAT4

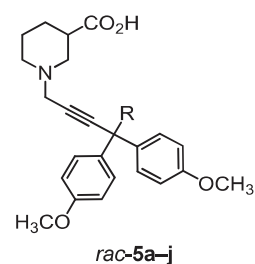
potency remained mostly unaltered. Only for the benzothiophene derivative *rac*-**5f**, a reasonable increase in mGAT4 potency occurred. With the benzothiophene residue being similar in size and shape to the 4-methoxyphenyl moiety present in the parent compound *rac*-**5a**, but more rigid, this may indicate that especially electron rich and planar aryl moieties are particularly suitable for interaction with mGAT4 proteins.

4. Experimental section

4.1. Chemistry

Reactions were carried out in vacuum dried glassware under argon atmosphere. Tetrahydrofuran (THF) and diethyl ether (Et₂O) were distilled from sodium benzophenone ketyl. Dichloromethane (DCM) was distilled from CaH₂. All commercially available starting materials were used without further purification and solvents were distilled before use. As petroleum ether (PE) the fraction 40–60 °C was used. Flash chromatography was performed on silica gel (Merck 60F-254, 0.040–0.063 mm). HRMS data were obtained with JMS-GCmate II (EI, Jeol) or Thermo Finnigan LTQ FT Ultra (ESI, Thermo Finnigan). NMR spectra were recorded with a J NMR-GX (JEOL 400 or 500 MHz) or Bruker BioSpin Avance III HD (400 or 500 MHz). As an internal standard, the known chemical shift of solvent traces were used to reference the spectra. Spectra were processed using the software MestReNova. All

Table 4
Binding affinities and inhibitory potencies of the *N*-substituted nipecotic acids *rac*-5a–j.



Entry	Compound	R	pK _i ^a	pIC ₅₀ ^b			
				mGAT1	mGAT2	mGAT3	mGAT4
1	<i>rac</i> -5a		5.36 ± 0.02	4.84	4.36	4.61	4.53
2	<i>rac</i> -5b		5.31 ± 0.04	4.64	4.38	4.22	4.29
3	<i>rac</i> -5c		4.11	68%	84%	82%	79%
4	<i>rac</i> -5d		83%	80%	106%	103%	91%
5	<i>rac</i> -5e		5.28 ± 0.12	4.60	70%	4.37	4.46
6	<i>rac</i> -5f		5.72 ± 0.11	4.96	4.93	5.06 ± 0.04	4.92
7	<i>rac</i> -5g	OH	59%	66%	72%	74%	69%
8	<i>rac</i> -5h	H	5.96 ± 0.05	5.43 ± 0.09	80%	4.02	4.63
9	<i>rac</i> -5i		5.72 ± 0.09	4.88	53%	4.38	4.44
10	<i>rac</i> -5j		5.67 ± 0.06	5.08 ± 0.08	67%	4.41	4.38

^a Results of MS Binding Assay results are given as pK_i ± SEM. For low pK_i values only one measurement was performed in triplicate, therefore no SEM could be calculated. Percentages represent remaining specific NO711 binding in presence of 100 μM test compound.

^b Results of [³H]GABA uptake assays results are given as pIC₅₀ ± SEM. For low pIC₅₀ values only one measurement was performed in triplicate, therefore no SEM could be calculated. Percentages represent remaining [³H]GABA uptake in presence of 100 μM test compound.

melting points are uncorrected and were determined using an Electrothermal IA9100 apparatus. For IR spectroscopy, a Perkin Elmer FT-IR Spectrometer 1600 was used.

4.2. General procedures

4.2.1. Synthesis of the Grignard reagents from aryl, or alkyl halides (**GP 1**)

Magnesium turnings (1.3 equiv) were suspended in THF (2 mL) and 1,2-dibromoethane (0.1 equiv) was added. The suspension was heated to 60 °C for 15 min. After cooling to 25 °C the solution of the appropriate aryl, or alkyl halide (1.1 equiv) in THF (2 mL/mmol) was added dropwise, and after the exothermic reaction was finished the mixture was heated to 60 °C for 1 h. The slightly colored mixture was cooled to 25 °C to obtain the corresponding Grignard reagent.

4.2.2. Synthesis of the triaryl alcohols from a Grignard reagent and ketone **15** (**GP 2**)

The appropriate Grignard reagent (1.3 equiv) generated according

to **GP 1** was added to ketone **15** (1.0 equiv) suspended in THF (2 mL/mmol) and heated to 60 °C for 2 h. At 25 °C the mixture was quenched with saturated aqueous NH₄Cl solution and extracted with Et₂O. The organic phases were dried over Na₂SO₄ and concentrated under reduced pressure. The crude product was purified by recrystallization or by column chromatography over silica gel.

4.2.3. Synthesis of the triaryl chlorides with acetyl chloride (**GP 3**)

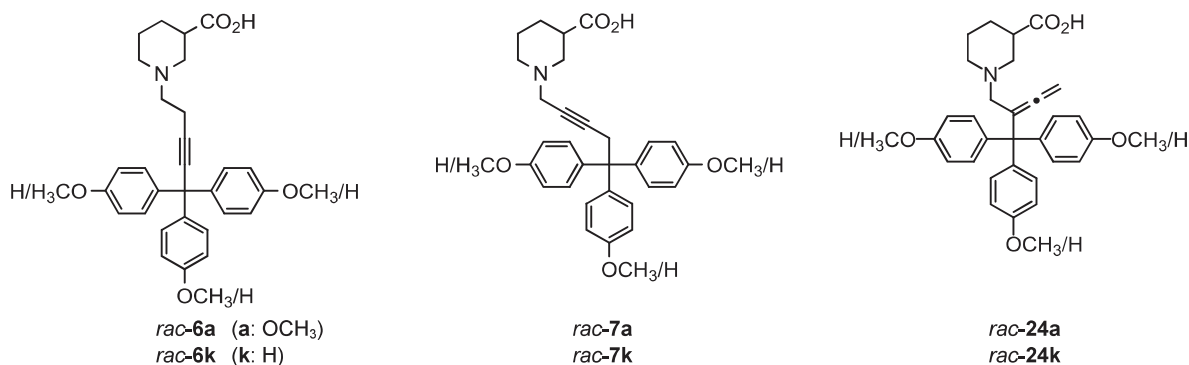
AcCl (3 equiv) was added to the appropriate alcohol (1 equiv) dissolved in toluene (2 mL/mmol) and the mixture was heated to 100 °C. After 2 h, the volatiles were removed under reduced pressure and the solid was dissolved in dry toluene (4 mL/mmol) and evaporated to dryness three times. The crude product was used without any further purification.

4.2.4. Synthesis of the triaryl chlorides with thionyl chloride (**GP 4**)

The appropriate alcohol (1 equiv) and DMF (0.02 equiv) was dissolved in SOCl₂ (5 equiv) at 0 °C and stirred for 4 h at 25 °C. The

Table 5

Binding affinities and inhibitory potencies of the *N*-substituted nipecotic acids with a longer spacer *rac*-6a, *rac*-6k, *rac*-7a, *rac*-7k, and the *N*-substituted nipecotic acids with an allenic spacer *rac*-24a, *rac*-24k.



Entry	Compound	Residue	pK _i ^a	pIC ₅₀ ^b			
				mGAT1	mGAT2	mGAT3	mGAT4
1	<i>rac</i> -6a	OCH ₃	5.56 ± 0.03	4.80	4.45	4.38	4.59
2	<i>rac</i> -6k	H	7.04 ± 0.11	6.37 ± 0.09	66%	61%	64%
3	<i>rac</i> -7a	OCH ₃	4.43	4.28	4.47	4.55	4.76
4	<i>rac</i> -7k	H	4.84	4.45 ± 0.03	66%	50%	4.15
5	<i>rac</i> -24a	OCH ₃	57%	69%	77%	4.37	4.31
6	<i>rac</i> -24k	H	70%	62%	87%	80%	54%

^a Results of MS Binding Assay results are given as pK_i ± SEM. For low pK_i values only one measurement was performed in triplicate, therefore no SEM could be calculated. Percentages represent remaining specific NO711 binding in presence of 100 μM test compound.

^b Results of [³H]GABA uptake assays results are given as pIC₅₀ ± SEM. For low pIC₅₀ values only one measurement was performed in triplicate, therefore no SEM could be calculated. Percentages represent remaining [³H]GABA uptake in presence of 100 μM test compound.

volatiles were removed under reduced pressure and the residue was taken up in DCM (4 mL/mmol) and evaporated to dryness three times. The crude product was used without any further purification.

4.2.5. Synthesis of the alkynes from triaryl chlorides and ethynylmagnesium bromide (GP 5)

Ethynylmagnesium bromide (2 equiv, 0.5 M in THF) was added to a stirred solution of the appropriate triaryl chloride (1 equiv) in toluene (2 mL/mmol) at 0 °C.³⁸ After 15 min, the mixture was heated to 60 °C for 2 h, then allowed to cool to 25 °C, quenched with saturated aqueous NH₄Cl, and extracted with Et₂O three times. The combined organic phases were dried over Na₂SO₄ and concentrated under reduced pressure to get the crude product. This crude product was then purified by column chromatography over silica gel.

4.2.6. Synthesis of the alkynes from triaryl chlorides and (trimethylsilyl) ethynyllithium (GP 6)

*n*BuLi (1.1 equiv, 2.5 M in hexanes) was added to ethynyltrimethylsilane (1.1 equiv) in THF (2 mL/mmol) at 0 °C. After stirring for 1 h at 0 °C, this solution was added to the appropriate triaryl chloride (1 equiv) in THF (2 mL/mmol) cooled to −78 °C and stirred for 1 h. Finally, the mixture was warmed to 0 °C, stirred for 1 h and then quenched with saturated aqueous NH₄Cl solution. The aqueous layer was separated and extracted three times with Et₂O. The combined organic fractions were washed with brine, dried over Na₂SO₄ and concentrated under reduced pressure. The crude product was purified by flash chromatography over silica gel.

4.2.7. Deprotection of the TMS protected alkynes (GP 7)

K₂CO₃ (3 equiv) was added to a stirred solution of the appropriate TMS alkyne (1 equiv) in MeOH (4 mL/mmol) at 0 °C. The mixture was stirred for 1 h at 0 °C and for further 3–5 h at 25 °C until TLC showed complete conversion. The mixture was quenched with H₂O at 0 °C and

extracted with Et₂O three times. The combined organic phases were dried over Na₂SO₄ and concentrated under reduced pressure to get the crude product. This crude product was purified by column chromatography over silica gel.

4.2.8. Coupling of the *N,O*-acetal *rac*-23 with alkynes to form the *N*-substituted nipecotic acid esters (GP 8)

TMSCl (1.15 equiv) was added to a stirred solution of *N,O*-acetal *rac*-23 (1.15 equiv) in THF (3 mL/mmol) at 0 °C. After 15 min, the solution was warmed to 25 °C and stirred for further 3 h at 25 °C to form a white suspension. *n*BuMgCl (1.05 equiv, 2 M in THF) was added in a separate Schlenk tube to a stirred solution of the appropriate alkyne (1 mmol) in THF (1 mL/mmol) at 0 °C and stirred for 1 h at 25 °C. To complete the deprotonation, the solution was stirred for another 1 h at 45 °C to form a slightly colored solution. To perform the coupling reaction, the solution of the deprotonated alkyne was added dropwise to the suspension of the iminium salt at 0 °C. After 1 h at 0 °C, a clear solution was formed and it was then heated at 45 °C for 1 h. The mixture was quenched with H₂O and extracted with Et₂O three times. The combined organic phases were dried over Na₂SO₄ and concentrated under reduced pressure to get the crude product. This crude product was purified by flash chromatography on silica gel with DCM/MeOH (99:1).

4.2.9. Hydrolysis of the *N*-substituted nipecotic acid esters (GP 9)

NaOH (5 equiv., 12 M in H₂O) was added dropwise to the appropriate ester (1 equiv) dissolved in MeOH (1 mL/mmol) at 0 °C. The mixture was stirred at 25 °C for 3–6 h until the hydrolysis was complete (TLC). The mixture was diluted with H₂O, stirred for 1 h at 25 °C and extracted with Et₂O. The water phase was collected and pH = 6.0 was set by adding HCl (5 equiv., 6 M in H₂O), and phosphate buffer (pH = 6.0). This mixture was extracted with DCM. The combined organic layers were dried over Na₂SO₄ and concentrated under reduced

pressure to get the pure product as an oil. To get the *N*-substituted nipecotic acid as a solid, the oil was dissolved in DCM (0.1 mL), H₂O (2 mL) was added and an emulsion was prepared by sonication. This emulsion was freeze-dried to obtain a white, amorphous solid.

4.3. Synthesized compounds

4.3.1. Ethyl 1-(ethoxymethyl)piperidine-3-carboxylate, (*rac*-**23**)

K₂CO₃ (4.2 g, 30 mmol) was added to a solution of ethyl nipecotate (*rac*-**22**) (4.9 g, 30 mmol, 4.9 mL) in EtOH (5.52 g, 120 mmol, 7.01 mL) at 0 °C. Paraformaldehyde (PFA) (0.98 g, 30 mmol) was added after 15 min and the mixture was stirred at 25 °C for 6 h. The mixture was diluted with Et₂O and filtered. The filtrate was concentrated under reduced pressure. The crude product was purified by distillation (Kugelrohr distillation) at 130 °C (0.4 Torr) to obtain the product *N,O*-acetal (*rac*-**23**) as a colorless oil (5.6 g, 88%).

IR (Film): $\tilde{\nu}$ = 2975, 2940, 2862, 1733, 1465, 1447, 1375, 1355, 1312, 1273, 1231, 1174, 1159, 1091, 1069, 1035, 981, 863, 796, 669 cm⁻¹. ¹H NMR (500 MHz, CD₂Cl₂) δ = 1.15 (t, *J* = 7.0 Hz, 3H), 1.23 (t, *J* = 7.2 Hz, 3H), 1.40–1.55 (m, 2H), 1.67–1.73 (m, 1H), 1.84–1.91 (m, 1H), 2.40–2.52 (m, 2H), 2.55–2.61 (m, 1H), 2.72–2.80 (m, 1H), 2.96–3.01 (m, 1H), 3.45 (q, *J* = 7.0 Hz, 2H), 4.03 (s, 2H), 4.09 (q, *J* = 7.1 Hz, 2H) ppm. ¹³C NMR (126 MHz, CD₂Cl₂) δ = 14.58, 15.67, 25.24, 27.38, 42.59, 50.59, 52.74, 60.69, 64.41, 89.24, 174.54 ppm. HRMS (EI): [M]⁺ calcd. for C₁₁H₂₁NO₃, 215.1521; found: 215.1518.

4.3.2. 3-(Ethoxycarbonyl)-1-methylenepiperidin-1-ium chloride, (*rac*-**9**)

TMSCl (60 mg, 0.50 mmol, 68 μ L) was added to a stirred solution of *N,O*-acetal *rac*-**23** (113 mg, 0.50 mmol) in THF (1.5 mL) at 0 °C. After 15 min the solution was warmed to 25 °C and stirred for further 3 h at 25 °C to form a white suspension. The volatiles were removed under vacuum to obtain a white residue (95 mg, 92%).

IR (KBr): $\tilde{\nu}$ = 3084, 2962, 2868, 2637, 2532, 1731, 1678, 1454, 1390, 1368, 1331, 1301, 1208, 1151, 1135, 1113, 1046, 923, 867, 850, 769, 726, 673, 584, 563, 511, 470 cm⁻¹. ¹H NMR (500 MHz, CD₂Cl₂) δ = 1.71 (dtd, *J* = 14.1, 10.1, 4.1 Hz, 1H), 1.83–1.97 (m, 2H), 2.05–2.12 (m, 2H), 2.96 (tt, *J* = 9.7, 4.2 Hz, 1H), 3.37–3.44 (m, 1H), 3.50–3.56 (m, 1H), 3.75 (d, *J* = 12.4 Hz, 1H), 3.88 (d, *J* = 12.2 Hz, 1H), 4.13 (q, *J* = 7.1 Hz, 2H), 7.42 (s, 2H) ppm. ¹³C NMR (126 MHz, CD₂Cl₂) δ = 14.43, 24.07, 25.96, 41.02, 54.97, 56.10, 61.58, 132.36, 172.36 ppm. HRMS (ESI): [M–Cl]⁺ calcd. for C₉H₁₆O₂N, 170.1175; found: 170.1176.

4.3.3. Tris(4-methoxyphenyl)methanol, (**16a**)

According to **GP2**: Magnesium turnings (370 mg, 15.0 mmol), 4-bromoanisole (2.5 g, 13 mmol, 1.7 mL), and ketone **15** (2.5 g, 10 mmol). The crude product was recrystallized from EtOAc/PE. White solid (2.6 g, 74%).

Mp: 80 °C. IR (KBr): $\tilde{\nu}$ = 3541, 3074, 3014, 2956, 2894, 2835, 2545, 2361, 2038, 1908, 1773, 1608, 1581, 1508, 1459, 1442, 1412, 1329, 1295, 1247, 1171, 1154, 1112, 1026, 948, 903, 826, 725, 638, 584 cm⁻¹. ¹H NMR (500 MHz, CD₂Cl₂) δ = 2.75 (s, 1H), 3.78 (s, 9H), 6.79–6.86 (m, 6H), 7.10–7.18 (m, 6H) ppm. ¹³C NMR (126 MHz, CD₂Cl₂) δ = 55.77, 81.49, 113.57, 129.50, 140.32, 159.21 ppm. HRMS (EI): [M]⁺ calcd. for C₂₂H₂₂O₄, 350.1518; found: 350.1500.

Analytical data corresponds with the known literature.²⁹ Additional data is shown above.

4.3.4. 4,4',4''-(chloromethanetriyl)tris(methoxybenzene), (**17a**)

According to **GP3**: AcCl (1.4 g, 18 mmol, 1.3 mL) and alcohol **16a** (2.1 g, 6.0 mmol). Red solid (1.9 g, 90%).

Mp: 142–144 °C. IR (KBr): $\tilde{\nu}$ = 3015, 2962, 2931, 2840, 2554, 2035, 1909, 1780, 1607, 1579, 1508, 1459, 1442, 1414, 1364, 1305, 1290, 1252, 1178, 1149, 1117, 1091, 1024, 943, 905, 829, 809, 774, 708, 629, 604, 577 cm⁻¹. ¹H NMR (500 MHz, CD₂Cl₂) δ = 3.85 (s, 9H),

6.86–6.92 (m, 6H), 7.17–7.23 (m, 6H) ppm. ¹³C NMR (126 MHz, CD₂Cl₂) δ = 55.77, 56.11, 113.89, 133.12, 137.59, 161.26 ppm. HRMS (EI): [M–Cl]⁺ calcd. for C₂₂H₂₁O₃, 333.1491; found: 333.1522.

Analytical data corresponds with the known literature.⁶¹

4.3.5. 4,4',4''-(Prop-2-yne-1,1,1-triyl)tris(methoxybenzene), (**18a**)

According to **GP5**: Alcohol **17a** (1.2 g, 3.0 mmol) and ethynylmagnesium bromide (12 mL, 6.0 mmol, 0.5 M in THF). The crude product was purified by flash chromatography over silica gel with PE/EtOAc (95:5). White solid (1.0 g, 97%).

Mp: 128–130 °C. IR (KBr): $\tilde{\nu}$ = 3277, 2954, 2935, 2839, 1606, 1582, 1507, 1459, 1447, 1415, 1293, 1251, 1176, 1117, 1030, 828, 679 cm⁻¹. ¹H NMR (500 MHz, CD₂Cl₂) δ = 2.74 (s, 1H), 3.78 (s, 9H), 6.79–6.84 (m, 6H), 7.13–7.18 (m, 6H) ppm. ¹³C NMR (126 MHz, CD₂Cl₂) δ = 54.03, 55.79, 73.55, 90.71, 113.74, 130.47, 137.95, 159.02 ppm. (HRMS (EI): [M]⁺ calcd. for C₂₄H₂₂O₃, 358.1569; found: 358.1564.

Analytical data corresponds with the known literature.³⁸ Additional data is shown above.

4.3.6. Benzo[d][1,3]dioxol-5-ylbis(4-methoxyphenyl)methanol, (**16b**)

According to **GP2**: Magnesium turnings (305 mg, 12.5 mmol), 1-bromo-3,4-(methylenedioxy)benzene (2.4 g, 11.5 mmol, 1.4 mL), ketone **15** (2.5 g, 10 mmol) The crude product was purified by flash chromatography over silica gel with DCM. Violet oil (3.6 g, 98%).

IR (Film): $\tilde{\nu}$ = 3490, 3000, 2955, 2933, 2900, 2836, 1608, 1582, 1507, 1484, 1463, 1435, 1298, 1246, 1116, 1089, 1036, 932, 860, 828, 810, 731, 668 cm⁻¹. ¹H NMR (500 MHz, CDCl₃) δ = 2.68 (s, 1H), 3.80 (s, 6H), 5.94 (s, 2H), 6.68 (dd, *J* = 8.1, 1.8 Hz, 1H), 6.72 (d, *J* = 8.1 Hz, 1H), 6.80 (d, *J* = 1.8 Hz, 1H), 6.81–6.85 (m, 4H), 7.15–7.19 (m, 4H) ppm. ¹³C NMR (126 MHz, CDCl₃) δ = 55.40, 81.47, 101.21, 107.47, 108.91, 113.31, 121.45, 129.18, 139.58, 141.78, 146.68, 147.48, 158.78 ppm. HRMS (EI): [M]⁺ calcd. for C₂₂H₂₀O₅, 364.1311; found: 364.1305.

4.3.7. 5-[Chlorobis(4-methoxyphenyl)methyl]benzo[d][1,3]dioxole, (**17b**)

According to **GP4**: Alcohol **16b** (0.2 g, 0.5 mmol), DMF (10 μ L, 0.05 mmol) and SOCl₂ (375 mg, 6.0 mmol, 230 μ L). The mixture was stirred at 45 °C for 2 h. Brown oil (190 mg, 99%).

IR (Film): $\tilde{\nu}$ = 3088, 2844, 1579, 1505, 1484, 1451, 1374, 1358, 1314, 1274, 1165, 1144, 1125, 1107, 1031, 1009, 917, 853, 812, 763, 734, 686 cm⁻¹. ¹H NMR (500 MHz, CDCl₃) δ = 3.88 (s, 6H), 6.05 (s, 2H), 6.70 (dd, *J* = 8.1, 1.8 Hz, 1H), 6.80 (d, *J* = 8.2 Hz, 1H), 6.91 (d, *J* = 1.7 Hz, 1H), 6.93 (d, *J* = 8.4 Hz, 4H), 7.23–7.29 (m, 4H) ppm. ¹³C NMR (126 MHz, CDCl₃) δ = 55.91, 102.10, 107.68, 113.88, 127.00, 133.66, 136.75, 138.82, 148.04, 149.74, 161.63 ppm. HRMS (EI): [M–Cl]⁺ calcd. for C₂₂H₁₉O₄, 347.1283; found: 347.1277.

4.3.8. 5-[1,1-Bis(4-methoxyphenyl)prop-2-yn-1-yl]benzo[d][1,3]dioxole, (**18b**)

According to **GP5**: Chloride **17b** (0.2 g, 0.5 mmol), and ethynylmagnesium bromide (1.0 mmol, 0.5 M in THF). The crude product was purified by flash chromatography over silica gel with PE/EtOAc (98:2). Slightly red solid (180 mg, 97%).

Mp: 114–116 °C. IR (KBr): $\tilde{\nu}$ = 2930, 2835, 1606, 1506, 1481, 1437, 1298, 1248, 1177, 1115, 1094, 1036, 932, 855, 811, 760, 739, 719, 657, 635, 600, 574, 547 cm⁻¹. ¹H NMR (500 MHz, CDCl₃) δ = 2.68 (s, 1H), 3.80 (s, 6H), 5.94 (s, 2H), 6.66 (dd, *J* = 8.2, 1.9 Hz, 1H), 6.70 (d, *J* = 8.2 Hz, 1H), 6.80–6.84 (m, 5H), 7.15–7.20 (m, 4H) ppm. ¹³C NMR (126 MHz, CDCl₃) δ = 54.01, 55.41, 73.11, 90.31, 101.27, 107.52, 110.03, 113.44, 122.40, 130.15, 137.38, 139.59, 146.51, 147.60, 158.53 ppm. HRMS (EI): [M]⁺ calcd. for C₂₄H₂₀O₄, 372.1362; found: 372.1361.

4.3.9. *Bis(4-methoxyphenyl)(thiazol-2-yl)methanol*, (**16c**)

*n*BuLi (3.45 mmol, 2.5 M in hexane) was added to 2-bromothiazole (602 mg, 3.60 mmol, 331 μ L) dissolved in Et₂O (6 mL) at -78°C . After 1 h this solution was cannulated to ketone **15** (0.74 g, 3.05 mmol) suspended in Et₂O (5 mL) at -78°C and stirred for 1 h. After 1 h at 25°C , the mixture was quenched with saturated aqueous NH₄Cl solution and extracted with DCM. The organic phases were dried over Na₂SO₄, filtered and concentrated under reduced pressure. The crude product was purified by flash chromatography over silica gel with DCM/MeOH (99:1). Brown solid (580 mg, 60%).

Mp: 146–148 $^{\circ}\text{C}$. IR (KBr): $\tilde{\nu}$ = 3271, 3128, 3060, 3013, 2961, 2929, 2898, 2832, 2035, 1605, 1583, 1508, 1459, 1436, 1415, 1381, 1303, 1250, 1210, 1194, 1169, 1135, 1108, 1056, 1044, 1029, 934, 913, 897, 871, 828, 812, 804, 768, 757, 726, 684, 637, 611, 577, 562, 537 cm^{-1} . ¹H NMR (500 MHz, CD₂Cl₂) δ = 3.79 (s, 6H), 4.18 (s, 1H), 6.82–6.87 (m, 4H), 7.25–7.30 (m, 4H), 7.34 (d, J = 3.3 Hz, 1H), 7.76 (d, J = 3.2 Hz, 1H) ppm. ¹³C NMR (126 MHz, CD₂Cl₂) δ = 55.79, 80.59, 113.76, 120.47, 129.21, 138.41, 143.13, 159.79, 178.49 ppm. HRMS (EI): [M]⁺ calcd. for C₁₈H₁₇O₃NS, 327.0929; found: 327.0932.

4.3.10. *2-[Chlorobis(4-methoxyphenyl)methyl]thiazole*, (**17c**)

According to **GP4**: Alcohol **16c** (2.0 g, 6.0 mmol, 1.2 equiv), DMF (10 μ L, 0.12 mmol), and SOCl₂ (3.8 g, 30 mmol, 2.3 mL). Brown oil (2.07 g, 99%).

IR (Film): $\tilde{\nu}$ = 3120, 3042, 3005, 2960, 2936, 2837, 1907, 1607, 1583, 1558, 1510, 1462, 1418, 1387, 1372, 1303, 1255, 1178, 1118, 1031, 865, 828, 734, 698 cm^{-1} . ¹H NMR (500 MHz, CDCl₃) δ = 3.82 (s, 6H), 6.86–6.91 (m, 4H), 7.27–7.32 (m, 4H), 7.62 (d, J = 3.5 Hz, 1H), 8.11 (d, J = 3.3 Hz, 1H) ppm. ¹³C NMR (126 MHz, CDCl₃) δ = 55.55, 75.58, 114.10, 122.32, 130.22, 133.49, 139.51, 160.38, 177.94 ppm. HRMS (EI): [M–Cl]⁺ calcd. for C₁₈H₁₆NO₂S, 310.0902; found: 310.0901.

4.3.11. *2-[1,1-Bis(4-methoxyphenyl)prop-2-yn-1-yl]thiazole*, (**18c**)

According to **GP5**: Chloride **17c** (2.0 g, 5.5 mmol), and ethynylmagnesium bromide (8.25 mmol, 0.5 M in THF). The crude product was purified by flash chromatography over silica gel with DCM. Brown solid (950 mg, 52%).

Mp: 103–105 $^{\circ}\text{C}$. IR (KBr): $\tilde{\nu}$ = 3285, 3108, 3078, 3001, 2956, 2930, 2900, 2835, 1606, 1582, 1508, 1461, 1441, 1014, 1300, 1251, 1178, 1112, 1032, 885, 861, 822, 791, 757, 731, 648, 601, 581, 547 cm^{-1} . ¹H NMR (400 MHz, CD₂Cl₂) δ = 2.92 (s, 1H), 3.79 (s, 6H), 6.81–6.86 (m, 4H), 7.27–7.32 (m, 4H), 7.33 (d, J = 3.3 Hz, 1H), 7.77 (d, J = 3.3 Hz, 1H) ppm. ¹³C NMR (101 MHz, CD₂Cl₂) δ = 53.86, 55.82, 75.76, 87.81, 113.90, 120.46, 130.04, 136.20, 143.63, 159.53, 175.13 ppm. HRMS (EI): [M]⁺ calcd. for C₂₀H₁₇O₂NS, 335.0980; found: 335.0966.

4.3.12. *Bis(4-methoxyphenyl)(1-methyl-1H-imidazol-2-yl)methanol*, (**16d**)

*n*BuLi (17.3 mmol, 2.5 M in hexanes) was added to a solution of 1-methylimidazole (1.4 g, 16.5 mmol, 1.3 mL) in THF (16 mL) at -78°C and stirred for 1 h, then cannulated slowly to a solution of ketone **15** (3.7 g, 15.3 mmol) in THF (15 mL) at -78°C . The mixture was then stirred for 2 h at this temperature, then further 2 h at 25°C . The mixture was quenched with saturated aqueous NH₄Cl, extracted with DCM, dried over Na₂SO₄, and concentrated under reduced pressure. The crude product was recrystallized from DCM/PE. White solid (4.7 g, 97%).

Mp: 158–160 $^{\circ}\text{C}$. IR (KBr): $\tilde{\nu}$ = 3196, 2954, 2913, 2835, 1703, 1609, 1586, 1511, 1468, 1445, 1415, 1359, 1297, 1283, 1249, 1175, 1132, 1030, 1009, 943, 925, 898, 838, 821, 795, 755, 738, 693, 613, 583, 562, 540, 506 cm^{-1} . ¹H NMR (500 MHz, CD₂Cl₂) δ = 3.20 (s, 3H), 3.79 (s, 6H), 4.66 (s, 1H), 6.82–6.86 (m, 4H), 6.86 (d, J = 1.1 Hz, 1H), 6.89 (d, J = 1.2 Hz, 1H), 7.08–7.14 (m, 4H) ppm. ¹³C NMR (126 MHz, CD₂Cl₂) δ = 35.23, 55.79, 78.27, 113.78, 123.74, 126.22, 129.41,

137.31, 151.53, 159.63 ppm. HRMS (EI): [M]⁺ calcd. for C₁₉H₂₀N₂O₃, 324.1474; found: 324.1473.

4.3.13. *2-[Chlorobis(4-methoxyphenyl)methyl]-1-methyl-1H-imidazole*, (**17d**)

Alcohol **16d** (2 g, 6 mmol) was treated with SOCl₂ (4.2 g, 36 mmol, 2.6 mL) and AcCl (1.9 g, 24 mmol, 1.7 mL) at 0°C . The mixture was stirred at 25°C for 2 h and then heated at 50°C for 1 h. The volatiles were evaporated under vacuum; toluene (5 mL) was added and removed under reduced pressure three times. The crude product was used without further purification. Grey gum (2.3 g, 99%).

IR (KBr): $\tilde{\nu}$ = 2954, 2835, 1608, 1582, 1511, 1461, 1417, 1372, 1301, 1254, 1177, 1106, 1027, 911, 828, 793, 761, 731, 612, 581 cm^{-1} . ¹H NMR (400 MHz, CDCl₃) δ = 3.65 (s, 3H), 3.82 (s, 6H), 6.89–6.96 (m, 4H), 7.06–7.13 (m, 4H), 7.47 (s, 1H), 7.62 (s, 1H), 14.68 (s, 1H) ppm. ¹³C NMR (101 MHz, CDCl₃) δ = 37.54, 55.68, 71.06, 114.84, 120.15, 125.95, 129.95, 145.80, 160.89 ppm. HRMS (ESI): [M–Cl]⁺ calcd. for C₁₉H₁₉O₂N₂, 307.1446; found: 307.1443.

4.3.14. *2-[1,1-Bis(4-methoxyphenyl)prop-2-yn-1-yl]-1-methyl-1H-imidazole*, (**18d**)

According to **GP5**: Chloride **17d** (2.3 g, 5.6 mmol) and ethynylmagnesium bromide (17 mmol, 0.5 M in THF, 34 mL). The crude product was purified by flash chromatography over silica gel with Et₂O/PE (80:20). Yellow oil (560 mg, 30%).

IR (KBr): $\tilde{\nu}$ = 3282, 3002, 2954, 2835, 1606, 1583, 1508, 1460, 1298, 1279, 1250, 1177, 1134, 1116, 1084, 1031, 824, 745, 685, 603, 585, 541 cm^{-1} . ¹H NMR (500 MHz, CDCl₃) δ = 2.77 (s, 1H), 3.45 (s, 3H), 3.79 (s, 6H), 6.83–6.87 (m, 4H), 6.88 (d, J = 1.3 Hz, 1H), 6.97 (d, J = 1.3 Hz, 1H), 7.16–7.21 (m, 4H) ppm. ¹³C NMR (126 MHz, CDCl₃) δ = 35.00, 49.86, 55.34, 74.64, 85.82, 113.68, 123.03, 127.01, 129.52, 134.41, 148.49, 158.79 ppm. HRMS (EI): [M]⁺ calcd. for C₂₁H₂₀O₂N₂, 332.1525; found: 332.1522.

4.3.15. *Bis(4-methoxyphenyl)(thiophen-3-yl)methanol*, (**16e**)

*n*BuLi (12 mmol, 1.6 M in hexanes) was added to 3-bromothiophene (1.9 g, 11.5 mmol, 1.1 mL) in Et₂O (12 mL) at -78°C . After 1 h, this mixture was added to a suspension of ketone **15** (2.5 g, 10.3 mmol) in Et₂O (12 mL) at -78°C . After 1 h, the mixture was allowed to warm to room temperature and was stirred for further 3 h. Finally, the mixture was heated for 1 h at 50°C , then quenched with saturated aqueous NH₄Cl solution. The aqueous layer was separated and extracted three times with Et₂O. The combined organic fractions were washed with brine, dried over Na₂SO₄, and concentrated under reduced pressure. The crude product was purified by flash chromatography over silica gel with PE/Et₂O (60:40). Yellow oil (3.1 g, 95%).

IR (Film): $\tilde{\nu}$ = 3448, 2835, 1608, 1508, 1458, 1299, 1248, 1175, 1033, 829, 795, 771, 651 cm^{-1} . ¹H NMR (400 MHz, CD₂Cl₂) δ = 2.80 (s, 1H), 3.79 (s, 6H), 6.81–6.86 (m, 4H), 6.93 (dd, J = 3.0, 1.4 Hz, 1H), 6.95 (dd, J = 5.1, 1.4 Hz, 1H), 7.18–7.23 (m, 4H), 7.31 (dd, J = 5.1, 3.1 Hz, 1H) ppm. ¹³C NMR (101 MHz, CD₂Cl₂) δ = 55.78, 79.75, 113.66, 123.46, 126.21, 128.34, 129.02, 139.86, 149.89, 159.35 ppm. HRMS (EI): [M]⁺ calcd. for C₁₉H₁₈O₃S, 326.0977; found: 326.0971.

4.3.16. *3-[Chlorobis(4-methoxyphenyl)methyl]thiophene*, (**17e**)

According to **GP4**: Alcohol **16e** (0.7 g, 2.1 mmol), DMF (10 μ L), and SOCl₂ (750 mg, 6.30 mmol, 460 μ L). The mixture was stirred at 45°C for 4 h. Brown gum (720 mg, 95%).

IR (KBr): $\tilde{\nu}$ = 3097, 3004, 2966, 2933, 2840, 2044, 1900, 1607, 1580, 1459, 1508, 1459, 1415, 1384, 1306, 1292, 1250, 1177, 1136, 1078, 1026, 831, 798, 783, 770, 753, 703, 646, 631, 614, 589, 564, 533 cm^{-1} . ¹H NMR (500 MHz, CD₂Cl₂) δ = 3.83 (s, 6H), 6.81 (dd, J = 2.9, 1.3 Hz, 1H), 6.85–6.90 (m, 4H), 7.12 (dd, J = 5.1, 1.4 Hz, 1H), 7.20–7.24 (m, 4H), 7.38 (dd, J = 5.1, 3.0 Hz, 1H) ppm. ¹³C NMR (126 MHz, CD₂Cl₂) δ = 56.02, 85.95, 113.77, 126.60, 127.37, 130.38, 131.84, 137.49, 147.68, 160.70 ppm. HRMS (EI): [M–Cl]⁺ calcd. for

C₁₉H₁₇O₂S, 309.0949; found: 309,0924.

4.3.17. [3,3-Bis(4-methoxyphenyl)-3-(thiophen-3-yl)prop-1-yn-1-yl]trimethylsilane, (21e)

According to **GP6**: Ethynyltrimethylsilane (261 mg, 2.40 mmol, 375 μ L), *n*BuLi (2.4 mmol, 2.5 M in hexanes) chloride **17e** (0.7 g, 2.0 mmol). The crude product was purified by flash chromatography over silica gel with PE/DCM (80:20). Colorless oil (420 mg, 53%).

IR (Film): $\tilde{\nu}$ = 3000, 2956, 2901, 2834, 2167, 1606, 1581, 1507, 1462, 1441, 1414, 1298, 1250, 1114, 1066, 1035, 842, 828, 793, 771, 759, 697, 646 cm⁻¹. ¹H NMR (400 MHz, CD₂Cl₂) δ = 0.23 (s, 9H), 3.78 (s, 6H), 6.78 (dd, *J* = 3.7, 1.1 Hz, 1H), 6.80–6.84 (m, 4H), 7.00 (d, *J* = 3.7 Hz, 1H), 7.16–7.21 (m, 4H), 7.29 (dd, *J* = 5.1, 3.0 Hz, 1H) ppm. ¹³C NMR (101 MHz, CD₂Cl₂) δ = 0.23, 52.33, 55.80, 89.50, 111.54, 113.80, 123.68, 126.04, 129.41, 129.98, 137.81, 147.29, 159.09 ppm. HRMS (EI): [M]⁺ calcd. for C₂₄H₂₆O₂SSi, 406.1423; found: 406.1418.

4.3.18. 3-[1,1-Bis(4-methoxyphenyl)prop-2-yn-1-yl]thiophene, (18e)

According to **GP7**: TMS alkyne **21e** (0.5 g, 1.2 mmol) was dissolved in MeOH/ THF (2 mL/1 mL), and K₂CO₃ (0.8 g, 6.0 mmol). The crude product was purified by flash chromatography over silica gel with PE/EtOAc (98:2). White solid (320 mg, 80%).

Mp: 122–124 °C. IR (KBr): $\tilde{\nu}$ = 3265, 3108, 3016, 2951, 2835, 1605, 1582, 1507, 1463, 1438, 1415, 1365, 1307, 1294, 1175, 1080, 1035, 1021, 910, 829, 810, 793, 780, 773, 694, 676, 653, 603, 579, 541 cm⁻¹. ¹H NMR (400 MHz, CD₂Cl₂) δ = 2.76 (s, 1H), 3.78 (s, 6H), 6.79–6.85 (m, 5H), 7.00 (dd, *J* = 5.1, 1.4 Hz, 1H), 7.17–7.23 (m, 4H), 7.30 (dd, *J* = 5.0, 3.0 Hz, 1H) ppm. ¹³C NMR (101 MHz, CD₂Cl₂) δ = 51.42, 55.81, 73.60, 89.49, 113.84, 123.81, 126.19, 129.27, 129.95, 137.49, 147.00, 159.17 ppm. HRMS (EI): [M]⁺ calcd. for C₂₁H₁₈O₂S, 334.1028; found: 334.1023.

4.3.19. Benzo[b]thiophen-5-ylbis(4-methoxyphenyl)methanol, (16f)

According to **GP 2**: Magnesium turnings (440 mg, 18.0 mmol), 1,2-dibromomethane (25 μ L), 5-bromobenzo(b)thiophene (3.7 g, 17.3 mmol) ketone **15** (3.7 g, 15.3 mmol). The crude product was purified by recrystallization (Et₂O/PE). White solid (4300 mg, 76%).

Mp: 168–170 °C. IR (KBr): $\tilde{\nu}$ = 3560, 3092, 3058, 3005, 2963, 2929, 2899, 2836, 2029, 1903, 1772, 1653, 1604, 1581, 1456, 1438, 1409, 1331, 1295, 1251, 1176, 1160, 1138, 1117, 1089, 1049, 1023, 960, 943, 913, 899, 886, 868, 835, 808, 791, 767, 721, 712, 683, 643, 634, 612, 583, 561, 550, 507, 491 cm⁻¹. ¹H NMR (500 MHz, CD₂Cl₂) δ = 2.87 (s, 1H), 3.79 (s, 6H), 6.82–6.86 (m, 4H), 7.17–7.22 (m, 4H), 7.27 (dd, *J* = 5.4, 0.7 Hz, 1H), 7.30 (dd, *J* = 8.5, 1.9 Hz, 1H), 7.46 (d, *J* = 5.5 Hz, 1H), 7.69 (d, *J* = 1.7 Hz, 1H), 7.82 (d, *J* = 8.5 Hz, 1H) ppm. ¹³C NMR (126 MHz, CD₂Cl₂) δ = 55.79, 81.94, 113.65, 122.31, 123.15, 124.73, 125.16, 127.40, 129.64, 139.00, 139.83, 140.11, 144.59, 159.32 ppm. HRMS (EI): [M]⁺ calcd. for C₂₃H₂₀O₃S, 376.1133; found: 376.1124.

4.3.20. 5-[Chlorobis(4-methoxyphenyl)methyl]benzo[b]thiophene, (17f)

According to **GP3**: Alcohol **16f** (2 g, 5 mmol), and AcCl (3.3 g, 41 mmol, 3.0 mL). Red solid (2 g, 99%).

Mp: 165–167 °C. IR (KBr): $\tilde{\nu}$ = 3099, 3060, 3012, 2957, 2933, 2902, 2836, 1604, 1576, 1508, 1457, 1439, 1409, 1330, 1307, 1296, 1255, 1223, 1177, 1130, 1117, 1089, 1049, 1029, 964, 913, 897, 866, 847, 825, 810, 790, 778, 762, 711, 678, 634, 624, 593, 565, 550, 516, 490 cm⁻¹. ¹H NMR (500 MHz, CD₂Cl₂) δ = 3.82 (s, 6H), 6.82–6.86 (m, 4H), 7.15–7.19 (m, 4H), 7.26 (dd, *J* = 5.5, 0.7 Hz, 1H), 7.40 (dd, *J* = 8.6, 2.0 Hz, 1H), 7.49 (d, *J* = 5.4 Hz, 1H), 7.52 (d, *J* = 1.9 Hz, 1H), 7.85 (d, *J* = 8.6 Hz, 1H) ppm. ¹³C NMR (126 MHz, CD₂Cl₂) δ = 55.90, 84.81, 113.51, 122.30, 124.81, 125.07, 127.16, 127.82, 131.73, 138.12, 139.50, 139.80, 142.72, 159.91 ppm. HRMS (ESI): [M – Cl]⁺ calcd. for C₂₃H₁₉O₂S, 359.1105; found: 359.1101.

4.3.21. (3-(Benzo[b]thiophen-5-yl)-3,3-bis(4-methoxyphenyl)prop-1-yn-1-yl)trimethylsilane, (21f)

According to **GP7**: Ethynyltrimethylsilane (45 mg, 0.44 mmol, 64 μ L), *n*BuLi (0.46 mmol, 2 M in hexanes), chloride **17f** (0.17 g, 0.40 mmol). The crude product was purified by flash chromatography over silica gel with PE/EtOAc (95:5). White solid (115 mg, 63%).

Mp: 159–161 °C. IR (KBr): $\tilde{\nu}$ = 3102, 3006, 2955, 2932, 2898, 2836, 2172, 2039, 1892, 1769, 1646, 1606, 1580, 1508, 1463, 1440, 1413, 1296, 1252, 1176, 1117, 1089, 1074, 1049, 1031, 956, 914, 893, 841, 830, 808, 791, 756, 706, 693, 630, 613, 591, 574, 557, 534, 479 cm⁻¹. ¹H NMR (400 MHz, CD₂Cl₂) δ = 0.24 (s, 9H), 3.79 (s, 6H), 6.79–6.85 (m, 4H), 7.15–7.20 (m, 4H), 7.24 (dd, *J* = 5.5, 0.7 Hz, 1H), 7.35 (ddd, *J* = 8.6, 1.9, 0.5 Hz, 1H), 7.43–7.47 (m, 1H), 7.57 (d, *J* = 1.6 Hz, 1H), 7.80 (dt, *J* = 8.6, 0.7 Hz, 1H) ppm. ¹³C NMR (101 MHz, CD₂Cl₂) δ = 0.22, 55.57, 55.80, 89.79, 112.86, 113.77, 122.39, 124.17, 124.67, 126.48, 127.39, 130.65, 137.98, 138.71, 139.94, 142.85, 159.03 ppm. HRMS (EI): [M]⁺ calcd. for C₂₈H₂₈O₂SSi, 456.1579; found: 456.1574.

4.3.22. 5-[1,1-Bis(4-methoxyphenyl)prop-2-yn-1-yl]benzo[b]thiophene, (18f)

According to **GP7**: TMS alkyne **21f** (0.7 g, 1.5 mmol) was dissolved in MeOH/THF (6 mL/6 mL), and K₂CO₃ (0.6 g, 4.4 mmol). The crude product was recrystallized from DCM. White solid (560 mg, 99%).

Mp: 192–194 °C. IR (KBr): $\tilde{\nu}$ = 3255, 2933, 2839, 1603, 1579, 1507, 1458, 1437, 1410, 1295, 1250, 1178, 1117, 1088, 1052, 1030, 895, 866, 831, 807, 790, 760, 696, 635, 602, 581, 552, 490 cm⁻¹. ¹H NMR (400 MHz, CD₂Cl₂) δ = 0.24 (s, 9H), 3.79 (s, 6H), 6.79–6.85 (m, 4H), 7.15–7.20 (m, 4H), 7.24 (dd, *J* = 5.5, 0.7 Hz, 1H), 7.35 (ddd, *J* = 8.6, 1.9, 0.5 Hz, 1H), 7.43–7.47 (m, 1H), 7.57 (d, *J* = 1.6 Hz, 1H), 7.80 (dt, *J* = 8.6, 0.7 Hz, 1H) ppm. ¹³C NMR (101 MHz, CD₂Cl₂) δ = 0.22, 55.57, 55.80, 89.79, 112.86, 113.77, 122.39, 124.17, 124.67, 126.48, 127.39, 130.65, 137.98, 138.71, 139.94, 142.85, 159.03 ppm. HRMS (EI): [M]⁺ calcd. for C₂₅H₂₀O₂S, 384.1184; found: 384.1179.

4.3.23. 1,1-Bis(4-methoxyphenyl)prop-2-yn-1-ol, (18g)

Ethynylmagnesium bromide (4 mmol, 0.5 M in THF) was added to the suspension of ketone **15** (0.5 g, 2.0 mmol) in THF (2 mL) at 25 °C. The mixture was then stirred at 60 °C for 2 h and then quenched with saturated aqueous NH₄Cl solution. The aqueous layer was separated and extracted three times with Et₂O. The combined organic fractions were washed with brine, dried over Na₂SO₄ and concentrated under reduced pressure. The crude product was recrystallized from Et₂O/PE. White solid (490 mg, 91%).

Mp: 90–91 °C. IR (KBr): $\tilde{\nu}$ = 3472, 3245, 3004, 2959, 2932, 2836, 2545, 2102, 2039, 1933, 1902, 1886, 1870, 1683, 1635, 1607, 1584, 1506, 1464, 1455, 1440, 1415, 1350, 1305, 1295, 1251, 1241, 1199, 1180, 1164, 1199, 1180, 1164, 1119, 1062, 1025, 991, 967, 930, 897, 842, 882, 815, 782, 764, 732, 715, 685, 633, 627, 587, 526, 510, 488 cm⁻¹. ¹H NMR (500 MHz, CDCl₃) δ 2.79 (s, 1H), 2.86 (s, 1H), 3.79 (s, 6H), 6.83–6.89 (m, 4H), 7.47–7.53 (m, 4H) ppm. ¹³C NMR (126 MHz, CDCl₃) δ 55.42, 73.76, 75.22, 86.92, 113.68, 127.46, 137.06, 159.26 ppm. HRMS (EI): [M]⁺ calcd. for C₁₇H₁₆O₃, 268.1099; found: 268.1096.

Analytical data corresponds with the known literature.⁶² Additional data is shown above.

4.3.24. 4,4'-(Bromomethylene)bis(methoxybenzene), (20)

Acetyl bromide (AcBr) (3.9 g, 30.0 mmol, 2.4 mL) was added to a stirred solution of alcohol **19** (2.5 g, 10 mmol) in toluene (15 mL) at 0 °C and stirred for 2 h at 25 °C. The volatiles were removed under reduced pressure. The remaining mixture was diluted with toluene (10 mL) and evaporated under reduced pressure three times. The obtained red solid was used without any further purification. Red solid (3 g, 99%).

Mp: 71–72 °C. IR (KBr): $\tilde{\nu}$ = 3011, 2960, 2928, 1603, 1582, 1458, 1440, 1417, 1313, 1300, 1253, 1238, 1198, 1172, 1112, 1024, 852,

822, 808, 757, 721, 698, 615, 580, 545 cm⁻¹. ¹H NMR (400 MHz, CDCl₃) δ = 3.80 (s, 6H), 6.31 (s, 1H), 6.84–6.89 (m, 4H), 7.35–7.41 (m, 4H) ppm. ¹³C NMR (101 MHz, CDCl₃) δ = 55.48, 56.07, 113.97, 129.83, 133.70, 159.37 ppm. HRMS (EI): [M]⁺ calcd. for C₁₅H₁₅O₂Br, 306.0255; found: 306.0248.

Analytical data corresponds with the known literature.⁴⁴

4.3.25. 3,3-Bis(4-methoxyphenyl)prop-1-yn-1-yltrimethylsilane, (21 h)

nBuMgCl (10 mmol, 2 M in THF, 5 mL) was added to a stirred solution of ethynyltrimethylsilane (982 mg, 10.0 mmol) in THF (15 mL) at 0 °C and stirred for 1 h at 45 °C. CuBr (180 mg, 1.25 mmol) was added at 25 °C and stirred for 30 min. Finally, the solution of bromide **20** (1.5 g, 5.0 mmol) in THF (20 mL) was added at 0 °C and stirred for 2 h at 60 °C. The mixture was quenched with saturated aqueous NH₄Cl solution and extracted with Et₂O three times. The combined organic phases were dried over Na₂SO₄ and concentrated under reduced pressure to get the crude product. This was then purified by flash chromatography over silica gel with PE/EtOAc (98:2). Yellow oil (1.5 g, 93%)

Note: CuBr (black, discolored) was purified⁶³ by rinsing it with AcOH, EtOH and Et₂O under argon to get an off white powder.

IR (Film): ν̄ = 3001, 2958, 2902, 2836, 2170, 1609, 1585, 1463, 1442, 1419, 1327, 1302, 1247, 1174, 1034, 1011, 846, 809, 761, 699, 668, 633 cm⁻¹. ¹H NMR (400 MHz, CD₂Cl₂) δ = 0.21 (s, 9H), 3.77 (s, 6H), 4.93 (s, 1H), 6.81–6.86 (m, 4H), 7.24–7.29 (m, 4H) ppm. ¹³C NMR (101 MHz, CD₂Cl₂) δ = 0.31, 42.97, 55.79, 89.09, 107.82, 114.42, 129.17, 134.64, 159.12 ppm. HRMS (EI): [M]⁺ calcd. for C₂₀H₂₄O₂Si, 324.1546; found: 324.1541.

Analytical data corresponds with the known literature.⁴² Additional data is shown above.

4.3.26. 4,4'-(Prop-2-yne-1,1-diyl)bis(methoxybenzene), (18 h)

According to GP7: TMS alkyne **21 h** (0.32 g, 1.0 mmol), and K₂CO₃ (0.2 g, 1.5 mmol). The crude product was purified by flash chromatography over silica gel with PE/EtOAc (97:3). White solid (210 mg, 83%).

Mp: 69–70 °C. IR (KBr): ν̄ = 3257, 3035, 3011, 2958, 2907, 2835, 2053, 2012, 1884, 1607, 1584, 1506, 1464, 1441, 1417, 1327, 1300, 1254, 1239, 1175, 1108, 1033, 986, 930, 865, 843, 830, 804, 766, 721, 700, 670, 631, 590, 570, 538, 510 cm⁻¹. ¹H NMR (500 MHz, CD₂Cl₂) δ = 2.52 (d, J = 2.7 Hz, 1H), 3.77 (s, 6H), 4.92 (d, J = 2.6 Hz, 1H), 6.82–6.86 (m, 4H), 7.25–7.30 (m, 4H) ppm. ¹³C NMR (126 MHz, CD₂Cl₂) δ = 41.76, 55.79, 72.90, 85.65, 114.45, 129.15, 134.27, 159.19 ppm. HRMS (EI): [M]⁺ calcd. for C₁₇H₁₆O₂, 252.1150; found: 252.1142.

4.3.27. Trimethyl[3,3,4-tris(4-methoxyphenyl)but-1-yn-1-yl]silane, (21i)

nBuLi (2.3 mmol, 2.5 M in hexanes) was added to the solution of TMS alkyne **21 h** (0.66 mg, 2.0 mmol) in THF (7 mL) at –78 °C. The resulting mixture was stirred at –78 °C for 1 h. 4-Methoxybenzyl chloride (0.4 g, 2.4 mmol) was added and the mixture was stirred at 0 °C for 1 h. Finally, the mixture was heated to 40 °C for 1 h and quenched with saturated aqueous NH₄Cl solution. The aqueous layer was separated and extracted three times with DCM. The combined organic fractions were washed with brine, dried over Na₂SO₄, and concentrated under reduced pressure. The crude product was purified by flash chromatography over silica gel with PE/EtOAc (98:2). White solid (855 mg, 96%).

Mp: 79–82 °C. IR (KBr): ν̄ = 2995, 2955, 2835, 2171, 1699, 1653, 1610, 1577, 1558, 1540, 1508, 1457, 1437, 1417, 1301, 1249, 1178, 1112, 1074, 1035, 887, 832, 759, 669, 606, 585, 516, 485 cm⁻¹. ¹H NMR (500 MHz, CD₂Cl₂) δ = 0.19 (s, 9H), 3.44 (s, 2H), 3.73 (s, 3H), 3.78 (s, 6H), 6.61–6.66 (m, 2H), 6.78–6.84 (m, 6H), 7.26–7.31 (m, 4H) ppm. ¹³C NMR (126 MHz, CD₂Cl₂) δ = 0.24, 46.88, 50.82, 55.55, 55.74, 91.73, 110.73, 112.91, 113.74, 129.22, 129.84, 132.54, 137.72, 158.77 ppm. HRMS (EI): [M]⁺ calcd. for C₂₈H₃₂O₃Si, 444.2121; found: 444.2113.

4.3.28. 4,4',4''-(But-3-yne-1,2,2-triyl)tris(methoxybenzene), (18i)

According to GP7: TMS alkyne **21 i** (0.81 g, 1.7 mmol) dissolved in MeOH/THF (3 mL/3 mL), K₂CO₃ (1.2 g, 8.7 mmol). The crude product was purified by flash chromatography over silica gel with PE/Et₂O (85:15). White solid (450 mg, 70%).

Mp: 142–145 °C. IR (KBr): ν̄ = 3284, 2932, 2834, 1609, 1582, 1509, 1463, 1300, 1249, 1178, 1110, 1034, 828, 784, 737, 650, 601, 581, 548 cm⁻¹. ¹H NMR (500 MHz, CD₂Cl₂) δ = 2.63 (s, 1H), 3.49 (s, 2H), 3.73 (s, 3H), 3.78 (s, 6H), 6.63–6.67 (m, 2H), 6.79–6.84 (m, 6H), 7.28–7.32 (m, 4H) ppm. ¹³C NMR (126 MHz, CD₂Cl₂) δ = 46.69, 49.83, 55.53, 55.75, 75.64, 88.49, 113.08, 113.81, 129.20, 129.69, 132.39, 137.61, 158.79, 158.85 ppm. HRMS (EI): [M]⁺ calcd. for C₂₅H₂₄O₃, 372.1725; found: 372.1719.

4.3.29. 3,3-Bis[4-methoxyphenyl]-4-phenylbut-1-yn-1-yltrimethylsilane, (21j)

nBuLi (2.7 mmol, 2.5 M in hexanes) was added to the solution of TMS alkyne **21 h** (803 mg, 2.45 mmol) in THF (6 mL) at –78 °C. The resulting mixture was stirred at –78 °C for 1 h. Benzyl bromide (0.5 g, 2.9 mmol) was added and the mixture was stirred at 0 °C for 1 h. Finally, the mixture was heated to 40 °C for 1 h and quenched with saturated aqueous NH₄Cl solution. The aqueous layer was separated and extracted three times with DCM. The combined organic fractions were washed with brine, dried over Na₂SO₄ and concentrated under reduced pressure. The crude product was purified by flash chromatography over silica gel with PE/EtOAc (98:2). White solid (915 mg, 90%).

Mp: 103–104 °C. IR (KBr): ν̄ = 3031, 3005, 2958, 2899, 2835, 2166, 1607, 1580, 1508, 1461, 1438, 1414, 1315, 1294, 1260, 1245, 1182, 1116, 1090, 1030, 995, 913, 881, 835, 800, 758, 737, 700 cm⁻¹. ¹H NMR (400 MHz, CD₂Cl₂) δ = 0.18 (s, 9H), 3.50 (s, 2H), 3.77 (s, 6H), 6.77–6.82 (m, 4H), 6.88–6.92 (m, 2H), 7.06–7.15 (m, 3H), 7.26–7.31 (m, 4H) ppm. ¹³C NMR (101 MHz, CD₂Cl₂) δ = 0.20, 47.71, 50.66, 55.75, 91.91, 110.52, 113.76, 126.73, 127.53, 129.20, 131.65, 137.68, 137.86, 158.80 ppm. HRMS (EI): [M]⁺ calcd. for C₂₇H₃₀O₂Si, 414.2015; found: 414.2008.

4.3.30. 4,4'-(1-Phenylbut-3-yne-2,2-diyl)bis(methoxybenzene), (18j)

According to GP7: TMS alkyne **21 j** (891 mg, 2.15 mmol) dissolved in MeOH/ THF (3 mL/3 mL), K₂CO₃ (0.9 g, 6.5 mmol). The crude product was purified by flash chromatography over silica gel with PE/Et₂O (90:10). White solid (650 mg, 88%).

Mp: 107–109 °C. IR (KBr): ν̄ = 3287, 3031, 3001, 2932, 2835, 1607, 1582, 1508, 1455, 1441, 1417, 1290, 1250, 1179, 1119, 1084, 1034, 827, 758, 730, 700, 650, 607, 584, 565, 546 cm⁻¹. ¹H NMR (500 MHz, CD₂Cl₂) δ = 2.45 (s, 1H), 3.36 (s, 2H), 3.60 (s, 6H), 6.61–6.65 (m, 4H), 6.70–6.73 (m, 2H), 6.90–6.98 (m, 3H), 7.08–7.14 (m, 4H) ppm. ¹³C NMR (126 MHz, CD₂Cl₂) δ = 47.50, 49.67, 55.76, 75.75, 88.31, 113.82, 126.80, 127.70, 129.17, 131.49, 137.55, 137.76, 158.88 ppm. HRMS (EI): [M]⁺ calcd. for C₂₄H₂₂O₂, 342.1620; found: 342.1615.

4.3.31. 4,4',4''-(But-3-yne-1,1,1-triyl)tris(methoxybenzene), (25a)

Propargyl bromide (4.6 mmol, 80% in toluene) was added dropwise to a suspension of magnesium turnings (0.12 g, 4.8 mmol) and HgCl₂ (11 mg, 0.04 mmol) in Et₂O (5 mL) at 25 °C. This mixture was stirred at 25 °C for 1 h, cooled to 0 °C and a solution of chloride **17 a** (1.5 g, 4.0 mmol) in toluene (10 mL) was added. After 1 h at 25 °C, it was heated at 40 °C for 1 h. The mixture was quenched with saturated aqueous NH₄Cl solution, extracted with Et₂O and dried over Na₂SO₄ to get the crude product. The crude product was purified by flash chromatography over silica gel with PE/EtOAc (96:4). White solid (1.3 g, 86%).

Mp: 91–92 °C. IR (KBr): ν̄ = 3293, 2997, 2956, 2931, 2910, 2837, 1605, 1577, 1508, 1440, 1297, 1248, 1180, 1121, 1033, 827, 729, 668, 641, 599, 575 cm⁻¹. ¹H NMR (500 MHz, CD₂Cl₂) δ = 1.96 (t, J = 2.7 Hz, 1H), 3.42 (d, J = 2.7 Hz, 2H), 3.78 (s, 9H), 6.76–6.84 (m,

6H), 7.04–7.15 (m, 6H) ppm. ^{13}C NMR (126 MHz, CD_2Cl_2): δ = 33.07, 54.57, 55.70, 72.13, 83.48, 113.49, 130.58, 139.76, 158.49 ppm. HRMS (EI): $[\text{M}]^+$ calcd. for $\text{C}_{25}\text{H}_{24}\text{O}_3$, 372.1726; found: 372.1725.

4.3.32. But-3-yne-1,1,1-triyltribenzene, (25k)

Propargyl bromide (4.6 mmol, 80% in toluene) was added dropwise to magnesium turnings (0.13 g, 5.0 mmol) suspended in Et_2O (5 mL) with HgCl_2 (12 mg, 0.05 mmol) while maintaining a temperature below 25 °C. After 1 h, a solution of chloride **17k** (1.16 g, 4.12 mmol) in toluene (5 mL) was added. The mixture was heated to 50 °C and stirred for 1 h. After cooling to 25 °C, it was quenched with saturated aqueous NH_4Cl solution, extracted with Et_2O , the organic layer was dried over Na_2SO_4 , and concentrated under reduced pressure. The crude product was purified by flash chromatography over silica gel with PE/ EtOAc (99:1). White solid (1.0 g, 86%).

Mp: 82–83 °C. IR (KBr): $\tilde{\nu}$ = 3285, 3048, 3019, 2930, 2900, 1955, 1890, 1816, 1772, 1718, 1683, 1656, 1591, 1488, 1443, 1420, 1310, 1269, 1310, 1269, 1186, 1154, 1080, 1029, 997, 970, 908, 878, 843, 802, 760, 745, 698, 668, 654, 636, 589 cm^{-1} . ^1H NMR (500 MHz, CD_2Cl_2) δ = 1.95 (t, J = 2.6 Hz, 1H), 3.52 (d, J = 2.6 Hz, 2H), 7.20–7.26 (m, 9H), 7.26–7.32 (m, 6H) ppm. ^{13}C NMR (126 MHz, CD_2Cl_2) δ = 32.69, 56.51, 72.30, 83.08, 126.92, 128.35, 129.70, 147.10 ppm. HRMS (EI): $[\text{M}]^+$ calcd. for $\text{C}_{22}\text{H}_{18}$, 282.1409; found: 282.1396.

4.3.33. 4,4',4''-(4-Chlorobut-2-yne-1,1,1-triyl)tris(methoxybenzene), (26a)

$n\text{BuLi}$ (6.9 mmol, 2.5 M in hexanes) was added to propargyl chloride (0.55 g, 7.20 mmol) dissolved in Et_2O (6 mL) cooled to –78 °C. After 20 min at –78 °C a solution of chloride **17a** (2.3 g, 6.0 mmol) in toluene (20 mL) was added and the mixture was stirred at –60 °C for 2 h, then brought to 25 °C. After 2 h the mixture was quenched with H_2O and extracted with Et_2O and dried. The crude product was purified by flash chromatography over silica gel with PE/ EtOAc (90:10). Yellow solid (2.0 g, 82%).

Mp: 93–94 °C. IR (KBr): $\tilde{\nu}$ = 3016, 2999, 2963, 2926, 2902, 2831, 2219, 2035, 1893, 1605, 1583, 1506, 1461, 1440, 1412, 1298, 1248, 1177, 1111, 1028, 902, 826, 784, 683, 636 cm^{-1} . ^1H NMR (400 MHz, CD_2Cl_2) δ 3.78 (s, 9H), 4.35 (s, 2H), 6.74–6.88 (m, 6H), 7.04–7.19 (m, 6H) ppm. ^{13}C NMR (101 MHz, CD_2Cl_2) δ 31.97, 54.15, 55.80, 80.08, 93.60, 113.79, 130.46, 137.88, 159.07 ppm. HRMS (EI): $[\text{M}]^+$ calcd. for $\text{C}_{25}\text{H}_{23}\text{O}_3\text{Cl}$, 406.1336; found: 406.1337.

4.3.34. (4-Chlorobut-2-yne-1,1,1-triyl)tribenzene, (26k)

$n\text{BuLi}$ (5.75 mmol, 2.5 M in hexanes) was added to propargyl chloride (0.5 g, 6.0 mmol) dissolved in Et_2O (8 mL) cooled to –78 °C. After 20 min at –78 °C, a solution of chloride **17k** (1.5 g, 5.0 mmol) in toluene (10 mL) was added and the mixture was stirred at –60 °C for 2 h, then brought to 25 °C. After 2 h, the mixture was quenched with H_2O and extracted with Et_2O and dried. The crude product was purified by flash chromatography over silica gel with PE/ EtOAc (99:1). Yellow solid (1.2 g, 76%).

Mp: 141–142 °C. IR (KBr): $\tilde{\nu}$ = 2057, 3019, 2234, 1954, 1899, 1812, 1775, 1689, 1592, 1488, 1445, 1321, 1261, 1198, 1179, 1156, 1129, 1076, 1031, 1001, 928, 890, 845, 760, 748, 698, 637, 530, 516 cm^{-1} . ^1H NMR (500 MHz, CD_2Cl_2) δ = 4.37 (s, 2H), 7.22–7.33 (m, 15H) ppm. ^{13}C NMR (126 MHz, CD_2Cl_2) δ = 31.85, 56.18, 80.74, 92.95, 127.56, 128.62, 129.56, 145.26 ppm. HRMS (EI): $[\text{M}]^+$ calcd. for $\text{C}_{22}\text{H}_{17}\text{Cl}$, 316.1019; found: 316.1016.

4.3.35. Ethyl 1-[4,4,4-tris(4-methoxyphenyl)but-2-yn-1-yl]piperidine-3-carboxylate, (rac-8a)

According to **GP8**: *N,O*-acetal *rac*-**23** (230 mg, 1.05 mmol), TMSCl (112 mg, 1.00 mmol, 130 μL), alkyne **18a** (330 mg, 0.90 mmol) and $n\text{BuMgCl}$ (0.9 mmol, 2 M in THF). The crude product was purified by flash chromatography over silica gel with DCM/ MeOH (99:1). Yellow

oil (380 mg, 80%).

IR (Film): $\tilde{\nu}$ = 2938, 2836, 2803, 1729, 1606, 1583, 1506, 1464, 1442, 1297, 1250, 1176, 1152, 1092, 1034, 825 cm^{-1} . ^1H NMR (500 MHz, CD_2Cl_2) δ = 1.21 (t, J = 7.1 Hz, 3H), 1.33–1.47 (m, 1H), 1.50–1.64 (m, 1H), 1.68–1.78 (m, 1H), 1.84–1.92 (m, 1H), 2.24 (td, J = 10.9, 3.1 Hz, 1H), 2.40 (t, J = 10.5 Hz, 1H), 2.55 (tt, J = 10.4, 3.9 Hz, 1H), 2.76 (d, J = 11.2 Hz, 1H), 3.00 (d, J = 11.0 Hz, 1H), 3.45 (s, 2H), 3.78 (s, 9H), 4.04–4.15 (m, 2H), 6.78–6.83 (m, 6H), 7.12–7.17 (m, 6H) ppm. ^{13}C NMR (126 MHz, CD_2Cl_2) δ = 14.58, 25.12, 27.08, 42.49, 48.35, 53.10, 54.26, 55.08, 55.77, 60.74, 80.86, 91.87, 113.65, 130.53, 138.69, 158.89, 174.35 ppm. HRMS (ESI): $[\text{M}+\text{H}]^+$ calcd. for $\text{C}_{33}\text{H}_{38}\text{O}_5\text{N}$, 528.2744; found: 528.2752.

4.3.36. 1-[4,4,4-Tris(4-methoxyphenyl)but-2-yn-1-yl]piperidine-3-carboxylic acid, (rac-5a)

According to **GP9**: The ester *rac*-**8a** (54 mg, 0.1 mmol) with NaOH (0.5 mmol, 12 M in H_2O) was hydrolyzed to get the pure product. White solid (40 mg, 80%).

Mp: 86–94 °C. IR (KBr): $\tilde{\nu}$ = 3428, 2998, 2934, 2834, 1715, 1606, 1582, 1507, 1463, 1441, 1297, 1250, 1175, 1111, 1033, 903, 824, 784, 725, 635 cm^{-1} . ^1H NMR (400 MHz, MeOD) δ = 1.23–1.39 (m, 1H), 1.58 (qt, J = 13.2, 3.7 Hz, 1H), 1.68–1.78 (m, 1H), 1.98 (d, J = 13.0 Hz, 1H), 2.18 (td, J = 11.8, 2.5 Hz, 1H), 2.33 (t, J = 10.8 Hz, 1H), 2.34–2.46 (m, 1H), 2.91 (d, J = 11.2 Hz, 1H), 3.17 (d, J = 10.1 Hz, 1H), 3.47 (dd, J = 20.5, 16.5 Hz, 2H), 3.78 (s, 9H), 6.79–6.85 (m, 6H), 7.07–7.14 (m, 6H) ppm. ^{13}C NMR (101 MHz, MeOD) δ = 25.91, 29.07, 46.38, 53.68, 55.00, 55.82, 57.27, 80.45, 93.38, 114.16, 131.15, 139.37, 159.74, 182.52 ppm. HRMS (ESI): $[\text{M}+\text{H}]^+$ calcd. for $\text{C}_{31}\text{H}_{34}\text{O}_5\text{N}$, 500.2431; found: 500.2430.

4.3.37. Ethyl 1-[4-(benzo[d][1,3]dioxol-5-yl)-4,4-bis(4-methoxyphenyl)but-2-yn-1-yl]piperidine-3-carboxylate, (rac-8b)

According to **GP8**: *N,O*-acetal *rac*-**23** (172 mg, 0.75 mmol), TMSCl (79 mg, 0.71 mmol, 92 μL), alkyne **18b** (0.25 g, 0.65 mmol), $n\text{BuMgCl}$ (0.68 mmol, 2 M in THF). The crude product was purified by flash chromatography over silica gel with DCM/ MeOH (99:1). Yellow oil (250 mg, 72%).

IR (Film): $\tilde{\nu}$ = 2938, 2905, 2836, 2802, 1729, 1607, 1582, 1506, 1482, 1440, 1298, 1248, 1177, 1152, 1132, 1112, 1093, 1036, 933, 856, 824, 808, 714, 637 cm^{-1} . ^1H NMR (500 MHz, CD_2Cl_2) δ 1.21 (t, J = 7.1 Hz, 3H), 1.33–1.47 (m, 1H), 1.51–1.63 (m, 1H), 1.68–1.78 (m, 1H), 1.84–1.92 (m, 1H), 2.24 (td, J = 10.9, 3.1 Hz, 1H), 2.40 (t, J = 10.5 Hz, 1H), 2.55 (tt, J = 10.4, 3.8 Hz, 1H), 2.76 (d, J = 11.2 Hz, 1H), 2.99 (d, J = 11.0 Hz, 1H), 3.45 (d, J = 0.9 Hz, 2H), 3.78 (s, 6H), 4.09 (qd, J = 7.1, 1.9 Hz, 2H), 5.93 (s, 2H), 6.66 (dd, J = 8.2, 1.9 Hz, 1H), 6.70 (d, J = 8.2 Hz, 1H), 6.77 (d, J = 1.8 Hz, 1H), 6.79–6.83 (m, 4H), 7.13–7.18 (m, 4H) ppm. ^{13}C NMR (126 MHz, CD_2Cl_2) δ = 14.57, 25.12, 27.08, 42.48, 48.34, 53.12, 54.68, 55.08, 55.78, 60.74, 81.08, 91.70, 101.86, 107.68, 110.31, 113.68, 122.72, 130.54, 138.44, 140.73, 146.87, 148.03, 158.97, 174.34 ppm. HRMS (EI): $[\text{M}]^+$ calcd. for $\text{C}_{34}\text{H}_{37}\text{NO}_5$, 539.2672; found: 539.2675.

4.3.38. 1-[4-(Benzo[d][1,3]dioxol-5-yl)-4,4-bis(4-methoxyphenyl)but-2-yn-1-yl]piperidine-3-carboxylic acid, (rac-5b)

According to **GP9**: Ester *rac*-**8b** (40 mg, 0.07 mmol), NaOH (0.36 mmol, 12 M in H_2O) was hydrolyzed to get the pure product. White solid (35 mg, 93%).

Mp: 95–101 °C. IR (KBr): $\tilde{\nu}$ = 3421, 2941, 2837, 1717, 1607, 1582, 1507, 1481, 1437, 1340, 1298, 1247, 1177, 1145, 1114, 1035, 929, 857, 826, 808, 669, 637, 595, 575 cm^{-1} . ^1H NMR (400 MHz, MeOD) δ 1.23–1.39 (m, 1H), 1.50–1.67 (m, 1H), 1.68–1.78 (m, J = 13.7, 3.0 Hz, 1H), 1.98 (d, J = 13.0 Hz, 1H), 2.18 (td, J = 11.8, 2.9 Hz, 1H), 2.33 (t, J = 10.9 Hz, 1H), 2.40 (tt, J = 11.1, 3.1 Hz, 1H), 2.91 (d, J = 11.2 Hz, 1H), 3.16 (d, J = 10.3 Hz, 1H), 3.47 (dd, J = 21.7, 16.5 Hz, 2H), 3.78 (s, 6H), 5.92 (s, 2H), 6.62 (dd, J = 8.1, 1.9 Hz, 1H), 6.68 (d, J = 1.8 Hz, 1H), 6.70 (d, J = 8.2 Hz, 1H), 6.80–6.85 (m, 4H), 7.08–7.14 (m, 4H)

ppm. ^{13}C NMR (101 MHz, MeOD) δ = 25.91, 29.06, 46.36, 48.44, 53.69, 55.41, 55.83, 57.29, 80.70, 93.16, 102.47, 108.16, 110.76, 114.20, 123.39, 131.15, 139.10, 141.37, 147.69, 148.78, 159.83, 182.48 ppm. HRMS (ESI): $[\text{M}+\text{H}]^+$ calcd. for $\text{C}_{31}\text{H}_{32}\text{O}_6\text{N}$, 514.2223; found: 514.2218.

4.3.39. Ethyl 1-[4,4-bis(4-methoxyphenyl)-4-(thiazol-2-yl)but-2-yn-1-yl]piperidine-3-carboxylate, (rac-8c)

According to **GP8**: *N,O*-acetal *rac*-**23** (340 mg, 1.49 mmol), TMSCl (158 mg, 1.43 mmol, 185 μL), alkyne **18c** (0.46 g, 1.3 mmol), *n*BuMgCl (1.37 mmol, 2 M in THF). The crude product was purified by flash chromatography over silica gel with DCM/MeOH (99:1). Yellow oil (556 mg, 85%).

IR (Film): $\tilde{\nu}$ = 2939, 2835, 2805, 1728, 1606, 1580, 1507, 1464, 1440, 1366, 1300, 1251, 1179, 1151, 1133, 1109, 1091, 1032, 893, 858, 817, 790, 741, 719, 683, 648 cm^{-1} . ^1H NMR (400 MHz, CD_2Cl_2) δ = 1.22 (t, J = 7.1 Hz, 3H), 1.37–1.48 (m, 1H), 1.52–1.64 (m, 1H), 1.71–1.79 (m, 1H), 1.84–1.93 (m, 1H), 2.29 (td, J = 10.8, 3.1 Hz, 1H), 2.45 (t, J = 10.4 Hz, 1H), 2.57 (tt, J = 10.3, 3.8 Hz, 1H), 2.80 (dt, J = 11.1, 3.9 Hz, 1H), 3.03 (d, J = 10.9 Hz, 1H, 1H), 3.50 (s, 2H), 3.78 (s, 6H), 4.09 (q, J = 7.1 Hz, 2H), 6.80–6.85 (m, 4H), 7.27–7.31 (m, 4H), 7.31 (d, J = 3.3 Hz, 1H), 7.75 (d, J = 3.3 Hz, 1H) ppm. ^{13}C NMR (101 MHz, CD_2Cl_2) δ = 14.59, 25.13, 27.04, 42.49, 48.27, 53.12, 54.09, 55.09, 55.80, 60.76, 83.60, 89.25, 113.79, 120.23, 130.06, 136.86, 143.51, 159.36, 174.30, 176.00 ppm. HRMS (EI): $[\text{M}]^+$ calcd. for $\text{C}_{29}\text{H}_{32}\text{O}_4\text{N}_2\text{S}$, 504.2083; found: 504.2044.

4.3.40. 1-[4,4-Bis(4-methoxyphenyl)-4-(thiazol-2-yl)but-2-yn-1-yl]piperidine-3-carboxylic acid, (rac-5c)

According to **GP9**: Ester *rac*-**8c** (57 mg, 0.11 mmol) NaOH (0.55 mmol, 12 M in H_2O) was hydrolyzed to get the pure product. White solid (50 mg, 95%).

Mp: 85–95 °C. IR (KBr): $\tilde{\nu}$ = 3422, 1072, 2995, 2935, 2835, 1717, 1606, 1583, 1508, 1463, 1411, 1346, 1300, 1252, 1179, 1112, 1032, 820, 786, 732, 580 cm^{-1} . ^1H NMR (400 MHz, MeOD) δ 1.33 (qd, J = 12.7, 4.1 Hz, 1H), 1.59 (qt, J = 13.1, 4.0 Hz, 1H), 1.69–1.79 (m, 1H), 1.99 (d, J = 13.1 Hz, 1H), 2.23 (td, J = 11.7, 2.9 Hz, 1H), 2.33–2.46 (m, 2H), 2.92 (d, J = 11.3 Hz, 1H), 3.18 (d, J = 7.9 Hz, 1H), 3.51 (dd, J = 19.9, 16.6 Hz, 2H), 3.79 (s, 6H), 6.84–6.89 (m, 4H), 7.20–7.29 (m, 4H), 7.53 (d, J = 3.4 Hz, 1H), 7.75 (d, J = 3.4 Hz, 1H) ppm. ^{13}C NMR (101 MHz, MeOD) δ = 25.94, 29.02, 46.42, 48.36, 53.75, 54.82, 55.85, 57.35, 83.25, 90.22, 114.48, 121.59, 130.68, 137.31, 143.65, 160.40, 177.86, 182.45 ppm. HRMS (ESI): $[\text{M}+\text{H}]^+$ calcd. for $\text{C}_{27}\text{H}_{29}\text{O}_4\text{N}_2\text{S}$, 477.1842; found: 477.1843.

4.3.41. Ethyl 1-[4,4-bis(4-methoxyphenyl)-4-(1-methyl-1H-imidazol-2-yl)but-2-yn-1-yl]piperidine-3-carboxylate, (rac-8d)

According to **GP8**: *N,O*-acetal *rac*-**23** (162 mg, 0.72 mmol), TMSCl (75 mg, 0.68 mmol, 88 μL), alkyne **18d** (0.21 g, 0.62 mmol) and *n*BuMgCl (0.65 mmol, 2 M in THF). The crude product was purified by flash chromatography over silica gel with DCM/MeOH (99:1). Yellow oil (120 mg, 39%).

IR (Film): $\tilde{\nu}$ = 2939, 2836, 2794, 1728, 1607, 1508, 1298, 1279, 1250, 1177, 1152, 1134, 1109, 1092, 1032, 823, 744, 682, 668, 634 cm^{-1} . ^1H NMR (400 MHz, CD_2Cl_2) δ 1.21 (t, J = 7.1 Hz, 3H), 1.35–1.47 (m, 1H), 1.50–1.65 (m, 2H), 1.69–1.79 (m, 1H), 1.84–1.93 (m, 1H), 2.24 (td, J = 10.8, 3.1 Hz, 1H), 2.39 (t, J = 10.4 Hz, 1H), 2.55 (tt, J = 10.4, 3.8 Hz, 1H), 2.76 (d, J = 11.2 Hz), 3.00 (d, J = 11.0 Hz, 1H), 3.44 (s, 3H), 3.48 (s, 2H), 3.78 (s, 6H), 4.09 (qd, J = 7.1, 1.1 Hz, 2H), 6.81–6.85 (m, 5H), 6.90 (d, J = 1.2 Hz, 1H), 7.12–7.18 (m, 4H) ppm. ^{13}C NMR (101 MHz, CD_2Cl_2) δ = 14.58, 25.11, 27.06, 35.20, 42.45, 48.28, 50.55, 55.17, 55.77, 60.78, 82.69, 87.18, 113.78, 123.46, 126.70, 129.98, 135.85, 149.31, 159.20, 174.25 ppm. HRMS (ESI): $[\text{M}+\text{H}]^+$ calcd. for $\text{C}_{30}\text{H}_{36}\text{O}_4\text{N}_3$; 502.2700; found: 502.2706.

4.3.42. 1-[4,4-Bis(4-methoxyphenyl)-4-(1-methyl-1H-imidazol-2-yl)but-2-yn-1-yl]piperidine-3-carboxylic acid, (rac-5d)

According to **GP9**: Ester *rac*-**8d** (41 mg, 0.08 mmol) with NaOH (0.4 mmol, 12 M in H_2O) was hydrolyzed to get the pure product. White solid (37 mg, 98%).

Mp: 94–105 °C. IR (KBr): $\tilde{\nu}$ = 3425, 2938, 2836, 1709, 1607, 1584, 1508, 1465, 1299, 1251, 1178, 1136, 1112, 1091, 1033, 823, 748, 730, 686, 583 cm^{-1} . ^1H NMR (500 MHz, MeOD) δ 1.31 (qd, J = 12.8, 4.2 Hz, 1H), 1.59 (qt, J = 12.9, 3.9 Hz, 1H), 1.74 (dt, J = 13.4, 3.5 Hz, 1H), 1.99 (dd, J = 13.1, 2.7 Hz, 1H), 2.17 (td, J = 11.9, 2.9 Hz, 1H), 2.31 (t, J = 11.1 Hz, 1H), 2.40 (tt, J = 11.6, 3.6 Hz, 1H), 2.91 (d, J = 11.2 Hz, 1H), 3.16 (d, J = 10.3 Hz, 1H), 3.48 (s, 3H), 3.51 (d, J = 2.1 Hz, 2H), 3.79 (s, 6H), 6.79 (d, J = 1.3 Hz, 1H), 6.85–6.90 (m, 4H), 7.08 (d, J = 1.3 Hz, 1H), 7.10–7.14 (m, 4H) ppm. ^{13}C NMR (126 MHz, MeOD) δ = 25.92, 29.04, 35.54, 46.37, 48.31, 51.25, 53.85, 55.85, 57.38, 82.90, 88.30, 114.59, 124.69, 126.49, 130.58, 135.91, 135.93, 150.18, 160.27, 182.41 ppm. HRMS (ESI): $[\text{M}+\text{H}]^+$ calcd. for $\text{C}_{28}\text{H}_{32}\text{O}_4\text{N}_3$, 474.2387; found: 474.2386.

4.3.43. Ethyl 1-[4,4-bis(4-methoxyphenyl)-4-(thiophen-3-yl)but-2-yn-1-yl]piperidine-3-carboxylate, (rac-8e)

According to **GP8**: *N,O*-acetal *rac*-**23** (122 mg, 0.54 mmol), TMSCl (60 mg, 0.52 mmol, 70 μL), alkyne **18e** (0.16 g, 0.45 mmol) and *n*BuMgCl (0.47 mmol, 2 M in THF). The crude product was purified by flash chromatography over silica gel with DCM/MeOH (99:1). Yellow oil (128 mg, 57%).

IR (Film): $\tilde{\nu}$ = 2937, 2835, 2800, 1729, 1606, 1582, 1507, 1464, 1437, 1364, 1299, 1250, 1177, 1151, 1109, 1091, 1033, 827, 791, 771, 650 cm^{-1} . ^1H NMR (400 MHz, CD_2Cl_2) δ 1.22 (t, J = 7.1 Hz, 3H), 1.33–1.48 (m, 1H), 1.49–1.63 (m, 1H), 1.69–1.78 (m, 1H), 1.81–1.93 (m, 1H), 2.23 (td, J = 10.8, 3.1 Hz, 1H), 2.40 (t, J = 10.4 Hz, 1H), 2.55 (tt, J = 10.3, 3.8 Hz, 1H), 2.76 (dt, J = 10.4, 3.7 Hz, 1H), 2.99 (d, J = 11.2 Hz, 1H), 3.44 (s, 2H), 3.78 (s, 6H), 4.09 (qd, J = 7.1, 1.2 Hz, 2H), 6.77 (dd, J = 3.0, 1.4 Hz, 1H), 6.79–6.84 (m, 4H), 6.99 (dd, J = 5.1, 1.4 Hz, 1H), 7.17–7.22 (m, 4H), 7.29 (dd, J = 5.0, 3.0 Hz, 1H) ppm. ^{13}C NMR (101 MHz, CD_2Cl_2) δ = 14.59, 25.11, 27.07, 42.48, 48.32, 51.69, 53.11, 55.08, 55.79, 80.94, 90.64, 113.75, 123.54, 126.00, 129.46, 130.00, 138.22, 147.81, 159.04, 174.33 ppm. HRMS (EI): $[\text{M}]^+$ calcd. for $\text{C}_{30}\text{H}_{33}\text{NO}_4\text{S}$, 503.2130; found: 503.2101.

4.3.44. 1-[4,4-Bis(4-methoxyphenyl)-4-(thiophen-3-yl)but-2-yn-1-yl]piperidine-3-carboxylic acid, (rac-5e)

According to **GP9**: Ester *rac*-**8e** (41 mg, 0.08 mmol) and NaOH (0.4 mmol, 12 M in H_2O) was hydrolyzed to get the pure product. White solid (36 mg, 95%).

Mp: 80–100 °C. IR (KBr): $\tilde{\nu}$ = 3432, 2932, 2835, 1717, 1606, 1582, 1507, 1464, 1441, 1299, 1250, 1177, 1112, 1034, 827, 792, 770, 668, 648, 595, 578, 535 cm^{-1} . ^1H NMR (400 MHz, MeOD) δ 1.25–1.38 (m, 1H), 1.58 (qt, J = 12.9, 3.9 Hz, 1H), 1.67–1.79 (m, 1H), 1.99 (dd, J = 12.9, 2.6 Hz, 1H), 2.17 (td, J = 11.8, 2.9 Hz, 1H), 2.27–2.37 (m, 1H), 2.40 (tt, J = 11.3, 3.3 Hz, 1H), 2.91 (d, J = 11.2 Hz, 1H), 3.17 (d, J = 10.5 Hz, 1H), 3.46 (dd, J = 20.0, 16.4 Hz, 2H), 3.78 (s, 6H), 6.74 (dd, J = 3.0, 1.3 Hz, 1H), 6.80–6.85 (m, 4H), 6.97 (dd, J = 5.1, 1.3 Hz, 1H), 7.13–7.18 (m, 4H), 7.35 (dd, J = 5.1, 3.1 Hz, 1H) ppm. ^{13}C NMR (101 MHz, MeOD) δ = 25.92, 29.07, 46.39, 52.42, 53.71, 55.81, 57.29, 80.57, 92.14, 114.24, 123.90, 126.47, 129.99, 130.63, 138.92, 148.47, 159.89, 182.48 ppm. HRMS (ESI): $[\text{M}+\text{H}]^+$ calcd. for $\text{C}_{28}\text{H}_{30}\text{O}_4\text{NS}$, 476.1889; found: 476.1893.

4.3.45. Ethyl 1-[4-(benzo[b]thiophen-5-yl)-4,4-bis(4-methoxyphenyl)but-2-yn-1-yl]piperidine-3-carboxylate, (rac-8f)

According to **GP8**: *N,O*-acetal *rac*-**23** (121 mg, 0.55 mmol), TMSCl (62 mg, 0.55 mmol, 72 μL), alkyne **18f** (0.2 g, 0.5 mmol), *n*BuMgCl (0.52 mmol, 2 M in THF). The crude product was purified by flash chromatography over silica gel with DCM/MeOH (99:1). Yellow oil (170 mg, 62%).

IR (Film): $\tilde{\nu}$ = 2937, 2835, 1728, 1606, 1582, 1507, 1463, 1439, 1299, 1250, 1177, 1132, 1090, 1033, 827, 805, 790, 756, 701 cm^{-1} . ^1H NMR (400 MHz, CD_2Cl_2) δ 1.20 (t, J = 7.1 Hz, 3H), 1.33–1.49 (m, 1H), 1.51–1.64 (m, 1H), 1.68–1.78 (m, 1H), 1.82–1.93 (m, 1H), 2.26 (td, J = 10.8, 3.1 Hz, 1H), 2.44 (t, J = 10.4 Hz, 1H), 2.56 (tt, J = 10.3, 3.8 Hz, 1H), 2.77 (dt, J = 11.1, 3.9 Hz, 1H), 3.02 (d, J = 10.8 Hz, 1H), 3.48 (s, 2H), 3.79 (s, 6H), 4.03–4.14 (m, 2H), 6.79–6.84 (m, 4H), 7.16–7.21 (m, 4H), 7.25 (dd, J = 5.5, 0.8 Hz, 1H), 7.35 (ddd, J = 8.5, 1.9, 0.5 Hz, 1H), 7.45 (dd, J = 5.5, 0.3 Hz, 1H), 7.62 (d, J = 1.9 Hz, 1H), 7.79 (dt, J = 8.5, 0.7 Hz, 1H) ppm. ^{13}C NMR (101 MHz, CD_2Cl_2) δ = 14.57, 25.14, 27.10, 42.51, 48.38, 53.13, 54.95, 55.10, 55.79, 60.75, 81.27, 91.83, 113.72, 122.34, 124.17, 124.68, 126.55, 127.37, 130.68, 138.42, 138.65, 139.96, 143.23, 158.99, 174.35 ppm. HRMS (ESI): $[\text{M} + \text{H}]^+$ calcd. for $\text{C}_{34}\text{H}_{36}\text{O}_4\text{NS}$, 554.2359; found: 554.2364.

4.3.46. 1-[4-(Benzo[b]thiophen-5-yl)-4-bis(4-methoxyphenyl)but-2-yn-1-yl]piperidine-3-carboxylic acid, (rac-5f)

According to **GP9**: Ester *rac-8f* (55 mg, 0.1 mmol) NaOH (0.5 mmol, 12 M in H_2O) was hydrolyzed to get the pure product. White solid (40 mg, 85%).

Mp: 102–111 °C. IR (KBr): $\tilde{\nu}$ = 2933, 2834, 1710, 1605, 1581, 1507, 1462, 1438, 1413, 1298, 1250, 1177, 1112, 1089, 1033, 865, 826, 805, 790, 755, 701, 636, 596, 578, 555 cm^{-1} . ^1H NMR (400 MHz, MeOD) δ 1.23–1.39 (m, 1H), 1.50–1.67 (m, 1H), 1.72 (dt, J = 13.2, 3.0 Hz, 1H), 1.98 (d, J = 13.1 Hz, 1H), 2.20 (td, J = 11.8, 2.9 Hz, 1H), 2.31–2.46 (m, 2H), 2.92 (d, J = 11.3 Hz, 1H), 3.19 (d, J = 8.5 Hz, 1H), 3.49 (dd, J = 20.0, 16.5 Hz, 2H), 3.78 (s, 6H), 6.81–6.86 (m, 4H), 7.11–7.18 (m, 4H), 7.24 (dd, J = 5.5, 0.8 Hz, 1H), 7.31 (dd, J = 8.6, 1.9 Hz, 1H), 7.53 (d, J = 5.9 Hz, 1H), 7.54 (d, J = 1.5 Hz, 1H), 7.80 (dt, J = 8.5, 0.7 Hz, 1H) ppm. ^{13}C NMR (101 MHz, MeOD) δ = 25.92, 29.09, 46.38, 48.46, 53.71, 55.67, 55.83, 57.30, 80.87, 93.32, 114.25, 122.72, 124.64, 125.13, 127.10, 128.04, 131.28, 139.09, 139.50, 140.78, 143.85, 159.85, 182.50 ppm. HRMS (ESI): $[\text{M} + \text{H}]^+$ calcd. for $\text{C}_{32}\text{H}_{32}\text{O}_4\text{NS}$, 526.2046; found: 526.2056.

4.3.47. Ethyl 1-[4-hydroxy-4,4-bis(4-methoxyphenyl)but-2-yn-1-yl]piperidine-3-carboxylate, (rac-8g)

According to the modified **GP8**: *N,O*-acetal *rac-23* (142 mg, 0.66 mmol), TMSCl (72 mg, 0.66 mmol, 84 μL), alkyne **18g** (0.16 g, 0.60 mmol) and *n*BuMgCl (1.2 mmol, 2 M in THF). The crude product was purified by flash chromatography over silica gel with DCM/MeOH (98:2). Yellow oil (170 mg, 72%).

IR (Film): $\tilde{\nu}$ = 3462, 3073, 2940, 1836, 2043, 1895, 1729, 1608, 1585, 1506, 1464, 1455, 1368, 1302, 1249, 1173, 1131, 1105, 1032, 1007, 906, 830, 784, 735, 668 cm^{-1} . ^1H NMR (500 MHz, CDCl_3) δ 1.24 (t, J = 7.1 Hz, 3H), 1.35–1.46 (m, 1H), 1.53–1.65 (m, 1H), 1.69–1.78 (m, 1H), 1.88–1.96 (m, 1H), 2.22 (td, J = 10.8, 2.6 Hz, 1H), 2.39 (t, J = 10.7 Hz, 1H), 2.57 (tt, J = 10.6, 3.9 Hz, 1H), 2.77 (d, J = 11.0 Hz, 1H), 3.00 (d, J = 10.5 Hz, 1H), 3.06–3.23 (m, 1H), 3.37–3.50 (m, 2H), 3.78 (s, 6H), 4.12 (qd, J = 7.1, 2.1 Hz, 2H), 6.80–6.87 (m, 4H), 7.44–7.54 (m, 4H) ppm. ^{13}C NMR (126 MHz, CDCl_3) δ = 14.35, 24.55, 26.59, 41.89, 47.84, 52.53, 54.47, 55.41, 60.52, 73.92, 82.09, 88.85, 113.57, 113.65, 127.43, 127.48, 137.84, 159.08, 174.03 ppm. HRMS (ESI): $[\text{M} + \text{H}]^+$ calcd. for $\text{C}_{26}\text{H}_{32}\text{O}_5\text{N}$, 438.2274; found: 438.2277.

4.3.48. 1-[4-Hydroxy-4,4-bis(4-methoxyphenyl)but-2-yn-1-yl]piperidine-3-carboxylic acid, (rac-5g)

According to **GP9**: Ester *rac-8g* (22 mg, 0.05 mmol) with NaOH (0.25 mmol, 12 M in H_2O) was hydrolyzed to get the pure product. White solid (17 mg, 83%).

Mp: 82–102 °C. IR (KBr): $\tilde{\nu}$ = 3422, 2950, 2837, 1717, 1700, 1684, 1653, 1607, 1585, 1559, 1540, 1508, 1457, 1395, 1301, 1250, 1174, 1110, 1032, 906, 829, 768, 680, 654, 592 cm^{-1} . ^1H NMR (500 MHz, MeOD) δ = 1.56–1.77 (m, 2H), 1.81–1.97 (m, 2H), 2.57–2.66 (m, 1H), 2.70–2.84 (m, 1H), 2.88–3.01 (m, 1H), 3.02–3.11 (m, 1H), 3.23 (d, J = 11.6 Hz, 1H), 3.71–3.79 (m, 6H), 3.83 (d, J = 6.0 Hz, 2H),

6.80–6.93 (m, 4H), 7.37–7.52 (m, 4H) ppm. ^{13}C NMR (126 MHz, MeOD) δ = 23.86, 27.01, 42.44, 47.68, 53.52, 55.35, 55.73, 74.48, 78.52, 93.29, 114.34, 128.51, 139.02, 160.49, 178.33 ppm. HRMS (ESI): $[\text{M} + \text{H}]^+$ calcd. for $\text{C}_{24}\text{H}_{28}\text{O}_5\text{N}$, 410.1961; found: 410.1963.

4.3.49. Ethyl 1-[4,4-bis(4-methoxyphenyl)but-2-yn-1-yl]piperidine-3-carboxylate, (rac-8h)

According to **GP8**: *N,O*-acetal *rac-23* (230 mg, 1.05 mmol), TMSCl (111 mg, 1.00 mmol, 130 μL), alkyne **18h** (0.23 g, 0.90 mmol) and *n*BuMgCl (0.9 mmol, 2 M in THF). The crude product was purified by flash chromatography over silica gel with DCM/MeOH (99:1). Yellow oil (210 mg, 56%).

IR (Film): $\tilde{\nu}$ = 2939, 2836, 1731, 1699, 1683, 1652, 1608, 1584, 1558, 1508, 1456, 1302, 1294, 1175, 1152, 1103, 1033, 820, 766, 668 cm^{-1} . ^1H NMR (400 MHz, CD_2Cl_2) δ 1.22 (t, J = 7.1 Hz, 3H), 1.35–1.48 (m, 1H), 1.50–1.67 (m, 1H), 1.68–1.80 (m, 1H), 1.83–1.94 (m, 1H), 2.21 (td, J = 10.9, 3.1 Hz, 1H), 2.37 (t, J = 10.5 Hz, 1H), 2.55 (tt, J = 10.4, 3.9 Hz, 1H), 2.76 (dt, J = 10.8, 3.7 Hz, 1H), 2.99 (d, J = 11.4 Hz, 1H), 3.38 (d, J = 2.2 Hz, 2H), 3.76 (s, 6H), 4.09 (qd, J = 7.1, 0.8 Hz, 2H), 4.93 (t, J = 1.8 Hz, 1H), 6.80–6.86 (m, 4H), 7.24–7.29 (m, 4H) ppm. ^{13}C NMR (101 MHz, CD_2Cl_2) δ = 14.58, 25.13, 27.12, 42.14, 42.49, 48.29, 53.03, 55.02, 55.78, 60.76, 80.19, 86.48, 114.37, 129.16, 135.14, 159.06, 174.40 ppm. HRMS (ESI): $[\text{M} + \text{H}]^+$ calcd. for $\text{C}_{26}\text{H}_{32}\text{O}_4\text{N}$, 422.2325; found: 422.2329.

4.3.50. 1-[4,4-Bis(4-methoxyphenyl)but-2-yn-1-yl]piperidine-3-carboxylic acid, (rac-5h)

The ester *rac-8h* (30 mg, 0.07 mmol) was dissolved in HCl (500 μL , 6 M in H_2O) and H_2O (500 μL). The solution was stirred at 50 °C for 3 h. After extraction with DCM the organic layer was dried with Na_2SO_4 , filtered, and evaporated to get the pure product. White solid (30 mg, 99%).

Mp: 70–85 °C. IR (KBr): $\tilde{\nu}$ = 2930, 2837, 2528, 1724, 1607, 1584, 1509, 1455, 1418, 1303, 1249, 1176, 1146, 1110, 1031, 952, 823, 769, 733, 668 cm^{-1} . ^1H NMR (500 MHz, MeOD) δ 1.32 (qd, J = 13.0, 4.2 Hz, 1H), 1.58 (qt, J = 13.2, 4.0 Hz, 1H), 1.70–1.76 (m, 1H), 1.98 (d, J = 13.0 Hz, 1H), 2.16 (td, J = 11.9, 2.9 Hz, 1H), 2.30 (t, J = 11.2 Hz, 1H), 2.39 (tt, J = 11.7, 3.6 Hz, 1H), 2.89 (d, J = 11.3 Hz, 1H), 3.14 (d, J = 10.9 Hz, 1H), 3.39 (t, J = 2.0 Hz, 2H), 3.76 (s, 6H), 4.95 (s, 1H), 6.82–6.86 (m, 4H), 7.23–7.27 (m, 4H) ppm. ^{13}C NMR (126 MHz, MeOD) δ = 25.84, 29.02, 42.60, 46.34, 48.36, 53.58, 55.85, 57.07, 79.79, 88.05, 114.84, 129.77, 135.88, 159.76, 182.62 ppm. HRMS (ESI): $[\text{M} + \text{H}]^+$ calcd. for $\text{C}_{24}\text{H}_{28}\text{O}_4\text{N}$, 394.2012; found: 394.2017.

4.3.51. Ethyl 1-[4,4,5-tris(4-methoxyphenyl)pent-2-yn-1-yl]piperidine-3-carboxylate, (rac-8i)

According to **GP8**: *N,O*-acetal *rac-23* (135 mg, 0.57 mmol), TMSCl (62 mg, 0.55 mmol, 72 μL), alkyne **18i** (0.19 g, 0.50 mmol), *n*BuMgCl (0.52 mmol, 2 M in THF). The crude product was purified by flash chromatography over silica gel with DCM/MeOH (99:1). Yellow oil (154 mg, 57%).

IR (Film): $\tilde{\nu}$ = 2937, 2835, 1729, 1609, 1583, 1511, 1464, 1440, 1369, 1300, 1249, 1179, 1153, 1130, 1111, 1091, 1035, 829, 748, 733, 651 cm^{-1} . ^1H NMR (400 MHz, CD_2Cl_2) δ 1.22 (t, J = 7.1 Hz, 3H), 1.39 (qd, J = 11.7, 3.8 Hz, 1H), 1.49–1.61 (m, 1H), 1.64–1.77 (m, 1H), 1.84–1.93 (m, 1H), 2.12 (td, J = 10.9, 3.1 Hz, 1H), 2.31 (t, J = 10.5 Hz, 1H), 2.53 (tt, J = 10.4, 3.8 Hz, 1H), 2.70 (dt, J = 11.1, 3.7 Hz, 1H), 2.96 (d, J = 10.8 Hz, 1H), 3.37 (s, 2H), 3.46 (s, 2H), 3.72 (s, 3H), 3.77 (s, 6H), 4.10 (qd, J = 7.1, 1.3 Hz, 2H), 6.61–6.66 (m, 2H), 6.75–6.82 (m, 6H), 7.26–7.31 (m, 4H) ppm. ^{13}C NMR (101 MHz, CD_2Cl_2) δ = 14.59, 25.14, 27.10, 42.52, 46.94, 48.30, 50.11, 53.03, 55.09, 55.51, 55.75, 60.75, 82.98, 89.42, 113.07, 113.72, 129.24, 129.26, 130.06, 132.35, 138.38, 138.43, 158.72, 174.37 ppm. HRMS (ESI): $[\text{M} + \text{H}]^+$ calcd. for $\text{C}_{34}\text{H}_{40}\text{O}_5\text{N}$, 542.2900; found: 542.2907.

4.3.52. 1-[4,4,5-Tris(4-methoxyphenyl)pent-2-yn-1-yl]piperidine-3-carboxylic acid, (rac-5i)

According to **GP9**: Ester *rac-8i* (45 mg, 0.08 mmol) with NaOH (0.4 mmol, 12 M in H₂O) was hydrolyzed to get the pure product. White solid (37 mg, 90%).

Mp: 84–91 °C. IR (KBr): $\tilde{\nu}$ = 2934, 2835, 1717, 1609, 1582, 1511, 1464, 1441, 1300, 1249, 1179, 1112, 1034, 829, 668, 653, 617, 599, 580, 548, 518 cm⁻¹. ¹H NMR (400 MHz, MeOD) δ 1.30 (qd, *J* = 12.7, 4.1 Hz, 1H), 1.47–1.63 (m, 1H), 1.65–1.72 (m, 1H), 1.98 (d, *J* = 12.7 Hz, 1H), 2.04 (td, *J* = 11.8, 3.0 Hz, 1H), 2.28 (t, *J* = 11.1 Hz, 1H), 2.38 (tt, *J* = 11.5, 3.5 Hz, 1H), 2.81 (d, *J* = 11.4 Hz, 1H), 3.11 (d, *J* = 11.0 Hz, 1H), 3.38 (dd, *J* = 31.7, 16.4 Hz, 2H), 3.45 (s, 2H), 3.71 (s, 3H), 3.77 (s, 6H), 6.60–6.65 (m, 2H), 6.72–6.77 (m, 2H), 6.79–6.84 (m, 4H), 7.25–7.30 (m, 4H) ppm. ¹³C NMR (101 MHz, MeOD) δ = 25.90, 29.04, 46.32, 47.58, 50.87, 53.53, 54.82, 55.67, 55.80, 57.30, 82.63, 91.04, 113.62, 114.20, 129.96, 129.99, 130.87, 132.94, 139.10, 139.16, 159.52, 182.50 ppm. HRMS (ESI): [M+H]⁺ calcd. for C₃₂H₃₆N₂O₅, 514.2587; found: 514.2588.

4.3.53. Ethyl 1-[4,4-bis(4-methoxyphenyl)-5-phenylpent-2-yn-1-yl]piperidine-3-carboxylate, (rac-8j)

According to **GP8**: *N,O*-acetal *rac-23* (175 mg, 0.77 mmol), TMSCl (84 mg, 0.75 mmol, 98 μ L), alkyne **18j** (0.24 g, 0.70 mmol), *n*BuMgCl (0.73 mmol, 2 M in THF). The crude product was purified by flash chromatography over silica gel with DCM/MeOH (99:1). Yellow oil (270 mg, 75%).

IR (Film): $\tilde{\nu}$ = 3030, 2936, 2835, 1729, 1607, 1582, 1455, 1292, 1249, 1179, 1152, 1132, 1110, 1092, 1033, 829, 757, 728, 700 cm⁻¹. ¹H NMR (500 MHz, CD₂Cl₂) δ 1.23 (t, *J* = 7.1 Hz, 3H), 1.34–1.44 (m, 1H), 1.48–1.60 (m, 1H), 1.65–1.75 (m, 1H), 1.82–1.92 (m, 1H), 2.11 (td, *J* = 10.9, 3.1 Hz, 1H), 2.29 (t, *J* = 10.5 Hz, 1H), 2.52 (tt, *J* = 10.5, 3.9 Hz, 1H), 2.68 (dt, *J* = 11.1, 3.7 Hz, 1H), 2.94 (d, *J* = 11.2 Hz, 1H), 3.36 (s, 2H), 3.53 (s, 2H), 3.78 (s, 6H), 4.05–4.15 (m, 3H), 6.78–6.82 (m, 4H), 6.86–6.89 (m, 2H), 7.07–7.14 (m, 3H), 7.27–7.32 (m, 4H) ppm. ¹³C NMR (126 MHz, CD₂Cl₂) δ = 14.60, 25.13, 27.09, 42.52, 47.78, 48.28, 49.96, 53.02, 55.07, 55.74, 60.74, 83.14, 89.24, 113.73, 126.69, 127.69, 129.22, 131.46, 138.13, 138.34, 138.37, 158.75, 174.36 ppm. HRMS (ESI): [M+H]⁺ calcd. for C₃₃H₃₈O₄N, 512.2795; found: 512.2781.

4.3.54. 1-[4,4-Bis(4-methoxyphenyl)-5-phenylpent-2-yn-1-yl]piperidine-3-carboxylic acid, (rac-5j)

According to **GP9**: Ester *rac-8j* (42 mg, 0.08 mmol) with NaOH (0.4 mmol, 12 M in H₂O) was hydrolyzed to get the pure product. White solid (35 mg, 91%).

Mp: 79–93 °C. IR (KBr): $\tilde{\nu}$ = 3030, 2933, 2861, 1711, 1607, 1582, 1508, 1436, 1453, 1442, 1391, 1292, 1250, 1180, 1113, 1034, 830, 817, 757, 729, 701, 583, 564 cm⁻¹. ¹H NMR (400 MHz, MeOD) δ = 1.30 (qd, *J* = 12.8, 4.1 Hz, 1H), 1.54 (qt, *J* = 12.6, 3.7 Hz, 1H), 1.63–1.74 (m, 1H), 1.92–2.08 (m, 2H), 2.27 (t, *J* = 11.2 Hz, 1H), 2.38 (tt, *J* = 11.6, 3.6 Hz, 1H), 2.80 (d, *J* = 11.3 Hz, 1H), 3.10 (d, *J* = 10.7 Hz, 1H), 3.33–3.44 (m, 2H), 3.52 (s, 2H), 3.77 (s, 6H), 6.78–6.86 (m, 6H), 7.03–7.11 (m, 3H), 7.25–7.31 (m, 4H) ppm. ¹³C NMR (101 MHz, MeOD) δ = 25.89, 29.02, 46.34, 48.41, 48.47, 50.74, 53.56, 55.77, 57.29, 82.77, 90.89, 114.21, 127.23, 128.18, 129.94, 129.97, 132.01, 138.77, 139.05, 139.09, 159.56, 182.47 ppm. HRMS (ESI): [M+H]⁺ calcd. for C₃₁H₃₄O₄N 484.2482; found 484.2485.

4.3.55. Ethyl 1-[5,5,5-tris(4-methoxyphenyl)pent-2-yn-1-yl]piperidine-3-carboxylate, (rac-13a)

According to **GP8**: *N,O*-acetal *rac-23* (268 mg, 1.20 mmol), TMSCl (128 mg, 1.15 mmol, 150 μ L), alkyne **25a** (0.4 g, 1.0 mmol), *n*BuMgCl (1.1 mmol, 2 M in THF). The crude product was purified by flash chromatography over silica gel with DCM/MeOH (99:1). Yellow oil (251 mg, 47%)

IR (Film): $\tilde{\nu}$ = 3037, 2936, 2836, 1731, 1608, 1581, 1514, 1504,

1463, 1455, 1443, 1415, 1368, 1294, 1251, 1183, 1153, 1131, 1090, 1037, 983, 957, 916, 829, 768, 735, 701 cm⁻¹. ¹H NMR (400 MHz, CD₂Cl₂) δ = 1.22 (t, *J* = 7.2 Hz, 3H), 1.25–1.32 (m, 1H), 1.33–1.49 (m, 1H), 1.51–1.62 (m, 1H), 1.73–1.83 (m, 2H), 2.08 (t, *J* = 10.5 Hz, 1H), 2.35 (d, *J* = 11.0 Hz, 1H), 2.41 (tt, *J* = 10.5, 3.9 Hz, 1H), 2.69 (d, *J* = 11.1 Hz, 1H), 3.04–3.17 (m, 2H), 3.41 (t, *J* = 2.2 Hz, 2H), 3.77 (s, 9H), 4.09 (q, *J* = 7.1 Hz, 2H), 6.74–6.86 (m, 6H), 7.04–7.16 (m, 6H) ppm. ¹³C NMR (101 MHz, CD₂Cl₂) δ = 14.58, 25.08, 26.88, 33.50, 42.44, 48.03, 52.20, 54.58, 54.83, 55.67, 60.68, 79.33, 84.22, 113.46, 130.66, 140.08, 158.41, 174.38 ppm. HRMS (EI): [M]⁺ calcd. for C₃₄H₃₉O₅N, 541.2828; found: 541.2819.

4.3.56. 1-[5,5,5-Tris(4-methoxyphenyl)pent-2-yn-1-yl]piperidine-3-carboxylic acid, (rac-7a)

According to **GP9**: Ester *rac-13a* (44 mg, 0.08 mmol) with NaOH (0.4 mmol, 12 M in H₂O) was hydrolyzed to get the pure product. White solid (40 mg, 97%).

Mp: 83–96 °C. IR (KBr): $\tilde{\nu}$ = 3423, 2998, 2934, 2835, 1718, 1608, 1579, 1509, 1464, 1441, 1292, 1250, 1183, 1118, 1090, 1035, 829, 727, 595, 576 cm⁻¹. ¹H NMR (500 MHz, MeOD) δ 1.21 (qd, *J* = 12.5, 3.9 Hz, 1H), 1.41 (qt, *J* = 12.8, 3.9 Hz, 1H), 1.50–1.58 (m, 1H), 1.65 (td, *J* = 11.8, 2.9 Hz, 1H), 1.90 (d, *J* = 13.1 Hz, 1H), 2.13 (t, *J* = 11.2 Hz, 1H), 2.28 (tt, *J* = 11.7, 3.7 Hz, 1H), 2.40 (d, *J* = 11.3 Hz, 1H), 2.87 (d, *J* = 11.1 Hz, 1H), 3.04 (dt, *J* = 16.4, 2.1 Hz, 1H), 3.16 (dt, *J* = 16.6, 2.2 Hz, 1H), 3.43 (t, *J* = 2.2 Hz, 2H), 3.77 (s, 9H), 6.78–6.83 (m, 6H), 7.07–7.11 (m, 6H) ppm. ¹³C NMR (126 MHz, MeOD) δ = 25.84, 28.78, 33.99, 46.19, 48.18, 52.63, 55.46, 55.77, 56.87, 78.92, 85.92, 114.01, 131.30, 140.96, 159.23, 182.44 ppm. HRMS (ESI): [M+H]⁺ calcd. for C₃₂H₃₆O₅N, 514.2587; found: 514.2584.

4.3.57. Ethyl 1-(5,5,5-triphenylpent-2-yn-1-yl)piperidine-3-carboxylate, (rac-13k)

According to **GP8**: *N,O*-acetal *rac-23* (170 mg, 0.80 mmol), TMSCl (85 mg, 0.8 mmol, 100 μ L), alkyne **25 k** (0.2 g, 0.7 mmol) and *n*BuMgCl (0.74 mmol, 2 M in THF). The crude product was purified by flash chromatography over silica gel with DCM/MeOH (99:1). Yellow oil (241 mg, 76%).

IR (Film): $\tilde{\nu}$ = 3086, 3058, 3031, 2938, 2854, 2807, 1954, 1731, 1597, 1494, 1467, 1446, 1368, 1317, 1223, 1181, 1152, 1131, 1090, 1034, 1001, 867, 803, 754, 701, 648 cm⁻¹. ¹H NMR (500 MHz, CD₂Cl₂) δ 1.23 (t, *J* = 7.1 Hz, 2H), 1.24–1.32 (m, 1H), 1.34–1.45 (m, 1H), 1.52–1.62 (m, 1H), 1.71–1.83 (m, 2H), 2.01 (t, *J* = 10.6 Hz, 1H), 2.33 (d, *J* = 11.0 Hz, 1H), 2.39 (tt, *J* = 10.6, 3.9 Hz, 1H), 2.64 (d, *J* = 11.1 Hz, 1H), 3.02–3.13 (m, 2H), 3.52 (t, *J* = 2.2 Hz, 2H), 4.09 (qd, *J* = 7.1, 1.0 Hz, 2H), 7.18–7.25 (m, 9H), 7.25–7.31 (m, 6H) ppm. ¹³C NMR (126 MHz, CD₂Cl₂) δ = 14.60, 25.07, 26.87, 33.14, 42.46, 47.98, 52.23, 54.48, 56.77, 60.67, 79.57, 83.81, 126.79, 128.31, 129.79, 147.41, 174.36 ppm. HRMS (ESI): [M+H]⁺ calcd. for C₃₁H₃₄O₂N, 452.2583; found: 452.2579.

4.3.58. 1-(5,5,5-Triphenylpent-2-yn-1-yl)piperidine-3-carboxylic acid, (rac-7k)

According to **GP9**: Ester *rac-13 k* (32 mg, 0.07 mmol) with NaOH (0.4 mmol, 12 M in H₂O) was hydrolyzed to get the pure product. White solid (29 mg, 98%).

Mp: 93–108 °C. IR (KBr): $\tilde{\nu}$ = 3447, 3057, 3030, 2937, 2863, 1717, 1653, 1636, 1584, 1559, 1493, 1446, 1388, 1362, 1306, 1272, 1219, 1192, 1155, 1119, 1089, 1036, 1001, 976, 900, 870, 829, 796, 757, 701, 646, 614, 594, 512, 485 cm⁻¹. ¹H NMR (500 MHz, MeOD) δ 1.21 (qd, *J* = 12.7, 4.0 Hz, 1H), 1.41 (qt, *J* = 12.8, 3.9 Hz, 1H), 1.51–1.58 (m, 1H), 1.66 (td, *J* = 11.8, 2.9 Hz, 1H), 1.89 (d, *J* = 12.9 Hz, 1H), 2.06 (t, *J* = 11.3 Hz, 1H), 2.27 (tt, *J* = 11.9, 3.8 Hz, 1H), 2.40 (d, *J* = 11.4 Hz, 1H), 2.80–2.87 (m, 1H), 3.00–3.14 (m, 2H), 3.54 (t, *J* = 2.1 Hz, 2H), 7.16–7.23 (m, 9H), 7.23–7.30 (m, 6H) ppm. ¹³C NMR (126 MHz, MeOD) δ = 25.84, 28.77, 33.59, 46.22, 48.16, 52.79, 54.82, 56.78, 57.38, 79.18, 85.49, 127.39, 128.82, 130.38, 148.24,

182.41 ppm. HRMS (ESI): $[M+H]^+$ calcd. for $C_{29}H_{30}O_2N$, 424.2170; found: 424.2273.

4.4. Ethyl 1-[5,5,5-tris(4-methoxyphenyl)pent-3-yn-1-yl]piperidine-3-carboxylate, (*rac-11a*)

N,O-acetal *rac-23* (0.52 g, 2.30 mmol) in THF (6 mL) was treated with TMSCl (243 mg, 2.20 mmol, 285 μ L) at 0 °C. After 15 min, the solution was heated to 25 °C and stirred for 3 h to get a thick, white suspension. Meanwhile, a Grignard reagent was prepared (**GP 1**) from chloride **26a** (0.83 g, 2.0 mmol) and magnesium turnings (64 mg, 2.6 mmol) in THF (2 mL). This solution was added to the white suspension from before at 0 °C. After 1 h, the mixture was heated to 25 °C, stirred for 1 h, and for a further 1 h at 45 °C. This solution was quenched with H₂O and extracted with Et₂O three times. The organic fractions were dried over Na₂SO₄, filtered, and evaporated to dryness under reduced pressure. The crude product was purified by flash chromatography on silica gel with PE/EtOAc/MeOH (78:20:2), yielding a yellow oil *rac-11a* (240 mg, 22%) and a colorless oil *rac-27a* (370 mg, 34%).

IR (Film): $\tilde{\nu}$ = 2946, 2835, 1729, 1606, 1464, 1442, 1370, 1298, 1249, 1176, 1152, 1134, 1110, 1034, 825 cm⁻¹. ¹H NMR (500 MHz, CD₂Cl₂) δ 1.21 (t, *J* = 7.1 Hz, 3H, OCH₂CH₃), 1.38–1.47 (m, 1H), 1.49–1.59 (m, 1H), 1.67–1.74 (m, 1H), 1.86–1.93 (m, 1H), 2.07 (td, *J* = 10.9, 3.0 Hz, 1H), 2.23 (t, *J* = 10.6 Hz, 1H), 2.48–2.55 (m, 3H), 2.60–2.66 (m, 2H), 2.77 (dt, *J* = 11.1, 3.6 Hz, 1H), 2.98 (d, *J* = 11.4 Hz, 1H), 3.77 (s, 9H), 4.07 (qd, *J* = 7.1, 1.0 Hz, 2H), 6.77–6.82 (m, 6H), 7.12–7.18 (m, 6H) ppm. ¹³C NMR (126 MHz, CD₂Cl₂) δ = 14.57, 18.01, 25.28, 27.48, 42.56, 53.97, 54.20, 55.77, 55.86, 58.16, 60.71, 84.13, 87.56, 113.58, 130.50, 139.02, 158.81, 174.50 ppm. HRMS (EI): $[M]^+$ calcd. for $C_{34}H_{39}O_5N$, 541.2828; found 541.2832.

4.4.1. 1-[5,5,5-Tris(4-methoxyphenyl)pent-3-yn-1-yl]piperidine-3-carboxylic acid, (*rac-6a*)

According to **GP9**: Ester *rac-11a* (39 mg, 0.07 mmol) with NaOH (0.35 mmol, 12 M in H₂O) was hydrolyzed to get the pure product. White solid (32 mg, 89%).

Mp: 82–92 °C. IR (KBr): $\tilde{\nu}$ = 3432, 2934, 2834, 2035, 1986, 1717, 1606, 1582, 1507, 1463, 1442, 1298, 1249, 1175, 1111, 1034, 826, 785, 588 cm⁻¹. ¹H NMR (400 MHz, MeOD) δ = 1.33 (qd, *J* = 13.0, 4.5 Hz, 1H), 1.56 (qt, *J* = 12.9, 3.8 Hz, 1H), 1.64–1.72 (m, 1H), 1.99 (td, *J* = 11.8, 3.0 Hz, 2H), 2.11 (t, *J* = 11.3 Hz, 1H), 2.38 (tt, *J* = 11.8, 3.8 Hz, 1H), 2.52–2.61 (m, 2H), 2.60–2.72 (m, 2H), 2.93 (d, *J* = 11.3 Hz, 1H), 3.11 (d, *J* = 11.0 Hz, 1H), 3.77 (s, 9H), 6.78–6.83 (m, 6H), 7.06–7.11 (m, 6H) ppm. ¹³C NMR (101 MHz, MeOD) δ = 17.54, 25.95, 29.35, 46.36, 54.56, 54.76, 55.82, 57.85, 58.92, 83.85, 88.88, 114.07, 131.08, 139.73, 159.64, 182.72 ppm. HRMS (ESI): $[M+H]^+$ calcd. for $C_{32}H_{36}O_5N$, 514.2587; found: 514.2582.

4.4.2. Ethyl 1-[2-(tris(4-methoxyphenyl)methyl)buta-2,3-dien-1-yl]piperidine-3-carboxylate, (*rac-27a*)

N,O-acetal *rac-23* (0.52 g, 2.30 mmol) in THF (6 mL) was treated with TMSCl (243 mg, 2.20 mmol, 285 μ L) at 0 °C. After 15 min, the solution was heated to 25 °C and stirred for 3 h to get a thick, white suspension. Meanwhile, a Grignard reagent was prepared (**GP 1**) from chloride **26a** (0.83 g, 2.0 mmol) and magnesium turnings (64 mg, 2.6 mmol) in THF (2 mL). This solution was added to the white suspension from before at 0 °C. After 1 h the mixture was heated to 25 °C, stirred for 1 h and for a further 1 h at 45 °C. This solution was quenched with H₂O and extracted with Et₂O three times. The organic fractions were dried over Na₂SO₄, filtered, and evaporated to dryness under reduced pressure. The crude product was purified by flash chromatography on silica gel with PE/EtOAc/MeOH (78:20:2), yielding a yellow oil *rac-11a* (240 mg, 22%) and a colorless oil *rac-27a* (370 mg, 34%).

IR (Film): $\tilde{\nu}$ = 3034, 2936, 2834, 1949, 1728, 1606, 1581, 1507, 1463, 1441, 1299, 1249, 1179, 1153, 1116, 1091, 1035, 823, 735,

668 cm⁻¹. ¹H NMR (500 MHz, CD₂Cl₂) δ 1.22 (t, *J* = 7.1 Hz, 3H), 1.29 (td, *J* = 12.2, 4.0 Hz, 1H), 1.34–1.44 (m, 1H), 1.53–1.62 (m, 1H), 1.77 (td, *J* = 11.2, 2.9 Hz, 1H), 1.78–1.86 (m, 1H), 1.89 (t, *J* = 10.7 Hz, 1H), 2.35 (tt, *J* = 10.8, 3.8 Hz, 1H), 2.64–2.69 (m, 1H), 2.68–2.76 (m, 2H), 2.86 (d, *J* = 11.2 Hz, 1H), 3.77 (s, 9H), 4.03–4.10 (m, 2H), 4.77 (t, *J* = 3.0 Hz, 2H), 6.75–6.80 (m, 6H), 7.19–7.24 (m, 6H) ppm. ¹³C NMR (126 MHz, CD₂Cl₂) δ = 14.59, 25.16, 27.55, 42.49, 54.30, 55.67, 56.22, 59.61, 60.58, 61.30, 79.72, 108.83, 113.06, 131.99, 138.15, 158.20, 174.59, 209.42 ppm. HRMS (EI): $[M]^+$ calcd. for $C_{34}H_{39}O_5N$, 541.2828; found: 541.2822.

4.4.3. 1-[2-[Tris(4-methoxyphenyl)methyl]buta-2,3-dien-1-yl]piperidine-3-carboxylic acid, (*rac-24a*)

According to **GP9**: Ester *rac-27a* (49 mg, 0.09 mmol) with NaOH (0.43 mmol, 12 M in H₂O) was hydrolyzed to get the pure product. White solid (43 mg, 97%).

Mp: 85–98 °C. IR (KBr): $\tilde{\nu}$ = 3433, 3034, 2997, 2934, 2834, 1950, 1718, 1606, 1581, 1506, 1463, 1441, 1299, 1250, 1179, 1117, 1034, 910, 822, 733, 604, 580, 530 cm⁻¹. ¹H NMR (400 MHz, MeOD) δ 1.25 (qd, *J* = 12.6, 4.6 Hz, 1H), 1.40–1.62 (m, 2H), 1.68 (td, *J* = 11.6, 2.9 Hz, 1H), 1.88 (t, *J* = 11.2 Hz, 1H), 1.91–1.96 (m, 1H), 2.33 (tt, *J* = 11.8, 3.7 Hz, 1H), 2.62 (dt, *J* = 15.1, 3.5 Hz, 1H), 2.74 (dt, *J* = 15.1, 3.6 Hz, 1H), 2.82 (d, *J* = 11.0 Hz, 1H), 3.15 (d, *J* = 10.6 Hz, 1H), 3.77 (s, 9H), 4.84 (ddt, *J* = 22.9, 10.6, 3.2 Hz, 2H), 6.74–6.84 (m, 6H), 7.14–7.25 (m, 6H) ppm. ¹³C NMR (101 MHz, MeOD) δ = 25.87, 29.51, 46.33, 55.41, 55.76, 58.97, 60.35, 61.73, 81.48, 109.02, 113.66, 132.63, 138.69, 159.08, 183.15, 209.05 ppm. HRMS (ESI): $[M+H]^+$ calcd. for $C_{32}H_{36}O_5N$, 514.2587; found: 514.2586.

4.4.4. Ethyl 1-(5,5,5-triphenylpent-3-yn-1-yl)piperidine-3-carboxylate, (*rac-11k*)

N,O-acetal *rac-23* (0.5 g, 2.30 mmol) in THF (6 mL) was treated with TMSCl (238 mg, 2.20 mmol, 280 μ L) at 0 °C. After 15 min, the solution was heated to 25 °C and stirred for 3 h to get a thick, white suspension. Meanwhile, a Grignard reagent was prepared (**GP 1**) from chloride **26k** (0.64 g, 2.0 mmol) and magnesium turnings (35 mg, 2.2 mmol) in THF (2 mL). This solution was added to the white suspension from before at 0 °C. After 1 h, the mixture was heated to 25 °C, stirred for 1 h and for a further 1 h at 45 °C. This solution was quenched with H₂O and extracted with Et₂O three times. The organic fractions were dried over Na₂SO₄, filtered, and evaporated to dryness under reduced pressure. The crude product was purified by flash chromatography on silica gel with PE/EtOAc/MeOH (94:5:1), yielding a yellow oil *rac-11k* (190 mg, 21%) and a colorless oil *rac-27k* (305 mg, 34%).

IR (Film): $\tilde{\nu}$ = 3060, 3031, 2941, 2859, 2805, 2776, 1729, 1597, 1490, 1446, 1372, 1307, 1213, 1180, 1152, 1133, 1097, 1074, 1032, 890, 861, 747, 698, 639 cm⁻¹. ¹H NMR (500 MHz, CD₂Cl₂) δ 1.22 (t, *J* = 7.2 Hz, 3H), 1.39–1.48 (m, 1H), 1.50–1.60 (m, 1H), 1.66–1.76 (m, 1H), 1.87–1.94 (m, 1H), 2.09 (td, *J* = 10.9, 3.0 Hz, 1H), 2.25 (t, *J* = 10.5 Hz, 1H), 2.49–2.57 (m, 3H), 2.63–2.69 (m, 2H), 2.79 (dt, *J* = 11.6, 4.0 Hz, 1H), 3.00 (d, *J* = 11.0 Hz, 1H), 4.08 (qd, *J* = 7.2, 0.9 Hz, 2H), 7.21–7.33 (m, 15H) ppm. ¹³C NMR (126 MHz, CD₂Cl₂) δ = 14.58, 18.05, 25.28, 27.48, 42.56, 53.98, 55.85, 56.11, 58.07, 60.70, 84.94, 86.98, 127.19, 128.41, 129.63, 146.35, 174.49 ppm. HRMS (ESI): $[M+H]^+$ calcd. for $C_{31}H_{34}O_2N$, 452.2583; found 452.2587.

4.4.5. 1-(5,5,5-Triphenylpent-3-yn-1-yl)piperidine-3-carboxylic acid, (*rac-6k*)

According to **GP9**: Ester *rac-11k* (55 mg, 0.12 mmol) with NaOH (0.6 mmol, 12 M in H₂O) was hydrolyzed to get the pure product. White solid (40 mg, 79%).

Mp: 82–91 °C. IR (KBr): $\tilde{\nu}$ = 3422, 3057, 3019, 2940, 2859, 2811, 1713, 1595, 1490, 1446, 1389, 1219, 1183, 1150, 1100, 1077, 1032, 1000, 890, 748, 698, 638 cm⁻¹. ¹H NMR (400 MHz, MeOD) δ 1.33 (qd, *J* = 12.7, 4.2 Hz, 1H), 1.56 (qt, *J* = 12.9, 3.9 Hz, 1H), 1.63–1.73 (m,

1H), 2.00 (td, $J = 11.8, 3.1$ Hz, 2H), 2.11 (t, $J = 11.3$ Hz, 1H), 2.38 (tt, $J = 11.9, 3.7$ Hz, 1H), 2.52–2.63 (m, 2H), 2.63–2.74 (m, 2H), 2.94 (d, $J = 11.4$ Hz, 1H), 3.11 (d, $J = 11.1$ Hz, 1H), 7.17–7.30 (m, 15H) ppm. ^{13}C NMR (101 MHz, MeOD) $\delta = 17.57, 25.99, 29.37, 46.40, 54.58, 56.82, 57.88, 58.84, 84.69, 88.28, 127.76, 128.85, 130.17, 147.03, 182.68$ ppm. HRMS (ESI): $[\text{M} + \text{H}]^+$ calcd. for $\text{C}_{29}\text{H}_{30}\text{O}_2\text{N}$, 424.2270; found: 424.2271.

4.4.6. Ethyl 1-(2-tritylbuta-2,3-dien-1-yl)piperidine-3-carboxylate, (rac-27k)

N,O-acetal *rac*-**23** (0.5 g, 2.3 mmol) in THF (6 mL) was treated with TMSCl (238 mg, 2.2 mmol, 280 μL) at 0 °C. After 15 min, the solution was heated to 25 °C and stirred for 3 h to get a thick, white suspension. Meanwhile, a Grignard reagent was prepared (**GP 1**) from chloride **26 k** (640 mg, 2.0 mmol) and magnesium turnings (35 mg, 2.2 mmol) in THF (2 mL). This solution was added to the white suspension from before at 0 °C. After 1 h, the mixture was heated to 25 °C, stirred for 1 h and for a further 1 h at 45 °C. This solution was quenched with H_2O and extracted with Et_2O three times. The organic fractions were dried over Na_2SO_4 , filtered and evaporated to dryness under reduced pressure. The crude product was purified by flash chromatography on silica gel with PE/ EtOAc/MeOH (94:5:1), yielding a yellow oil *rac*-**11k** (190 mg, 21%), and a colorless oil *rac*-**27k** (305 mg, 34%).

IR (Film): $\tilde{\nu} = 3056, 3031, 2939, 2853, 2804, 2764, 1951, 1731, 1596, 1491, 1466, 1447, 1393, 1368, 1352, 1311, 1181, 1153, 1092, 1033, 1001, 899, 839, 797, 745, 702, 669, 646, 631$ cm^{-1} . ^1H NMR (500 MHz, CD_2Cl_2) $\delta = 1.22$ (t, $J = 7.1$ Hz, 3H), 1.28 (td, $J = 12.3, 3.9$ Hz, 1H), 1.31–1.44 (m, 1H), 1.52–1.60 (m, 1H), 1.74 (td, $J = 11.1, 2.8$ Hz, 1H), 1.76–1.85 (m, 1H), 1.86 (t, $J = 10.7$ Hz, 1H), 2.33 (tt, $J = 10.8, 3.8$ Hz, 1H), 2.63 (d, $J = 11.4$ Hz, 1H), 2.69–2.82 (m, 2H), 2.83 (d, $J = 11.2$ Hz, 1H), 4.01–4.11 (m, 2H), 4.81 (t, $J = 3.0$ Hz, 2H), 7.15–7.20 (m, 3H), 7.22–7.28 (m, 6H), 7.33–7.38 (m, 6H) ppm. ^{13}C NMR (126 MHz, CD_2Cl_2) $\delta = 14.59, 25.12, 27.51, 42.46, 54.19, 56.12, 59.46, 60.58, 63.40, 80.04, 108.25, 126.52, 127.92, 131.12, 145.58, 174.56, 209.52$ ppm. HRMS (EI): $[\text{M}]^+$ calcd. for $\text{C}_{31}\text{H}_{33}\text{O}_2\text{N}$, 451.2511; found: 451.2539.

4.4.7. 1-(2-Tritylbuta-2,3-dien-1-yl)piperidine-3-carboxylic acid, (rac-24k)

According to **GP9**: Ester *rac*-**27 k** (46 mg, 0.1 mmol) with NaOH (0.5 mmol, 12 M in H_2O) was hydrolyzed to get the pure product. White solid (39 mg, 92%).

MP: 84–94 °C. IR (KBr): $\tilde{\nu} = 3423, 3055, 3025, 2938, 2859, 2805, 1950, 1717, 1595, 1491, 1447, 1395, 1349, 1301, 1270, 1187, 1156, 1089, 1033, 1001, 844, 745, 702, 668, 646, 630$ cm^{-1} . ^1H NMR (500 MHz, MeOD) $\delta = 1.23$ (qd, $J = 12.8, 4.5$ Hz, 1H), 1.41–1.58 (m, 2H), 1.64 (td, $J = 11.5, 2.9$ Hz, 1H), 1.86 (t, $J = 11.3$ Hz, 1H), 1.89–1.94 (m, 1H), 2.31 (tt, $J = 11.8, 3.7$ Hz, 1H), 2.64 (dt, $J = 15.1, 3.5$ Hz, 1H), 2.74–2.82 (m, 2H), 3.13 (d, $J = 11.0$ Hz, 1H), 4.82–4.91 (m, 2H), 7.13–7.19 (m, 3H), 7.21–7.27 (m, 6H), 7.30–7.35 (m, 6H) ppm. ^{13}C NMR (126 MHz, MeOD) $\delta = 25.86, 29.49, 46.32, 55.24, 58.92, 60.18, 63.81, 81.72, 108.40, 127.19, 128.45, 131.70, 146.08, 183.09, 209.21$ ppm. HRMS (ESI): $[\text{M} + \text{H}]^+$ calcd. for $\text{C}_{29}\text{H}_{30}\text{O}_2\text{N}$, 424.2270; found: 424.2271.

4.5. Biological evaluation

4.5.1. MS binding assays

The MS Binding Assays were performed with mGAT1 membrane preparations obtained from a stable HEK293 cell line and NO711 as non-labeled marker in competitive binding experiments as described previously.⁵⁹

4.5.2. GABA uptake assay

The [^3H]GABA uptake assays were performed in a 96-well plate

format with intact HEK293 cells stably expressing mGAT1, mGAT2, mGAT3, mGAT4 as described earlier.⁵⁸

References

- Krogsgaard-Larsen P. GABA synaptic mechanisms: stereochemical and conformational requirements. *Med Res Rev.* 1988;8:27–56.
- Treiman DM. GABAergic mechanisms in epilepsy. *Epilepsia.* 2001;42:8–12.
- Dalby NO. Inhibition of gamma-aminobutyric acid uptake: anatomy, physiology and effects against epileptic seizures. *Eur J Pharmacol.* 2003;479:127–137.
- Lancot KL, Herrmann N, Mazzotta P, Khan LR, Ingber N. GABAergic function in Alzheimer's disease: evidence for dysfunction and potential as a therapeutic target for the treatment of behavioural and psychological symptoms of dementia. *Can J Psychiatry.* 2004;49:439–453.
- Kalueff AV, Nutt DJ. Role of GABA in anxiety and depression. *Depress Anxiety.* 2007;24:495–517.
- Cherubini E. Generating diversity at GABAergic synapses. *Trends Neurosci.* 2001;24:155–162.
- Borden LA. GABA transporter heterogeneity: pharmacology and cellular localization. *Neurochem Int.* 1996;29:335–356.
- Conti F, Minelli A, Melone M. GABA transporters in the mammalian cerebral cortex: localization, development and pathological implications. *Brain Res Rev.* 2004;45:196–212.
- Masson J, Sagne C, Hamon M, El Mestikawy S. Neurotransmitter transporters in the central nervous system. *Pharmacol Rev.* 1999;51:439–464.
- Kristensen AS, Andersen J, Jorgensen TN, et al. SLC6 neurotransmitter transporters: structure, function, and regulation. *Pharmacol Rev.* 2011;63:585–640.
- Madsen KK, Clausen RP, Larsson OM, Krogsgaard-Larsen P, Schousboe A, White HS. Synaptic and extrasynaptic GABA transporters as targets for anti-epileptic drugs. *J Neurochem.* 2009;109:139–144.
- Palacin M, Estevez R, Bertran J, Zorzano A. Molecular biology of mammalian plasma membrane amino acid transporters. *Physiol Rev.* 1998;78:969–1054.
- Minelli A, DeBiasi S, Brecha NC, Zuccarello LV, Conti F. GAT-3, a high-affinity GABA plasma membrane transporter, is localized to astrocytic processes, and it is not confined to the vicinity of GABAergic synapses in the cerebral cortex. *J Neurosci.* 1996;16:6255–6264.
- Jin XT, Galvan A, Wichmann T, Smith Y. Localization and Function of GABA Transporters GAT-1 and GAT-3 in the Basal Ganglia. *Front Syst Neurosci.* 2011;5:63.
- Kempson SA, Zhou Y, Danbolt NC. The betaine/GABA transporter and betaine: roles in brain, kidney, and liver. *Front Physiol.* 2014;5:159.
- Zhou Y, Holmseth S, Hua R, et al. The betaine-GABA transporter (BGT1, slc6a12) is predominantly expressed in the liver and at lower levels in the kidneys and at the brain surface. *Am J Physiol Renal Physiol.* 2012;302:F316–328.
- Leppik IE. Tiagabine: the safety landscape. *Epilepsia.* 1995;36:S10–S13.
- Fijalkowski L, Salat K, Podkova A, Zareba P, Nowaczyk A. Potential role of selected antiepileptics used in neuropathic pain as human GABA transporter isoform 1 (GAT1) inhibitors-Molecular docking and pharmacodynamic studies. *Eur J Pharm Sci.* 2017;96:362–372.
- Nielsen EB, Suzdak PD, Andersen KE, Knutsen LJ, Sonnewald U, Braestrup C. Characterization of tiagabine (NO-328), a new potent and selective GABA uptake inhibitor. *Eur J Pharmacol.* 1991;196:257–266.
- Andersen KE, Braestrup C, Groenwald FC, et al. The synthesis of novel GABA uptake inhibitors. 1. Elucidation of the structure-activity studies leading to the choice of (R)-1-[4,4-bis(3-methyl-2-thienyl)-3-butenyl]-3-piperidinecarboxylic acid (Tiagabine) as an anticonvulsant drug candidate. *J Med Chem.* 1993;36:1716–1725.
- Steffan T, Renukappa-Gutke T, Höfner G, Wanner KT. Design, synthesis and SAR studies of GABA uptake inhibitors derived from 2-substituted pyrrolidine-2-yl-acetic acids. *Bioorg Med Chem.* 2015;23:1284–1306.
- Hellenbrand T, Höfner G, Wein T, Wanner KT. Synthesis of 4-substituted nipecotic acid derivatives and their evaluation as potential GABA uptake inhibitors. *Bioorg Med Chem.* 2016;24:2072–2096.
- Vogensen SB, Jorgensen L, Madsen KK, et al. Structure activity relationship of selective GABA uptake inhibitors. *Bioorg Med Chem.* 2015;23:2480–2488.
- Vogensen SB, Jorgensen L, Madsen KK, et al. Selective mGAT2 (BGT-1) GABA uptake inhibitors: design, synthesis, and pharmacological characterization. *J Med Chem.* 2013;56:2160–2164.
- Kerschler-Hack S, Renukappa-Gutke T, Höfner G, Wanner KT. Synthesis and biological evaluation of a series of N-alkylated imidazole alkanic acids as mGAT3 selective GABA uptake inhibitors. *Eur J Med Chem.* 2016;124:852–880.
- Dhar TGM, Borden LA, Tyagarajan S, et al. Design, Synthesis and Evaluation of Substituted Triaryl Nipecotic Acid Derivatives as GABA Uptake Inhibitors: Identification of a Ligand with Moderate Affinity and Selectivity for the Cloned Human GABA Transporter GAT-3. *J Med Chem.* 1994;37:2334–2342.
- Pabel J, Faust M, Prehn C, et al. Development of an (S)-1-(2-[tris(4-methoxyphenyl)methoxy]ethyl)piperidine-3-carboxylic acid [(S)-SNAP-5114] carba analogue inhibitor for murine gamma-aminobutyric acid transporter type 4. *ChemMedChem.* 2012;7:1245–1255.
- Damgaard M, Al-Khawaja A, Vogensen SB, et al. Identification of the First Highly Subtype-Selective Inhibitor of Human GABA Transporter GAT3. *ACS Chem Neurosci.* 2015;6:1591–1599.
- Horn M, Mayr H. Stabilities of trityl-protected substrates: the wide mechanistic spectrum of trityl ester hydrolyses. *Chemistry.* 2010;16:7469–7477.
- Cho SJ, Ahn YH, Maiti KK, et al. Combinatorial synthesis of a triphenylmethine

- library and their application in the development of surface enhanced Raman scattering (SERS) probes. *Chem Commun (Camb)*. 2010;46:722–724.
31. Rocco VP, Spinazze PG, Kohn TJ, et al. Advances toward new antidepressants beyond SSRIs: 1-aryloxy-3-piperidinylpropan-2-ols with dual 5-HT1A receptor antagonism/SSRI activities. Part 4. *Bioorg Med Chem Lett*. 2004;14:2653–2656.
 32. Liu B, Fan Y, Lv X, Liu X, Yang Y, Jia Y. Generation and reactions of heteroaromatic lithium compounds by using in-line mixer in a continuous flow microreactor system at mild conditions. *Org Process Res Dev*. 2013;17:133–137.
 33. Shirley DA, Alley PW. The metalation of 1-Methyl-, 1-Benzyl- and 1-phenylimidazole with n-Butyllithium. *J Am Chem Soc*. 1957;79:4922–4927.
 34. Guieu S, Rocha J, Silva AMS. Synthesis, crystal structure, and luminescence of tetrakis(4-methoxyphenyl)methane. *Tetrahedron Lett*. 2013;54:2870–2873.
 35. Brogi S, Brindisi M, Joshi BP, et al. Exploring clotrimazole-based pharmacophore: 3D-QSAR studies and synthesis of novel antiparasitic agents. *Bioorg Med Chem Lett*. 2015;25:5412–5418.
 36. Ruda GF, Nguyen C, Ziemkowski P, et al. Modified 5'-trityl nucleosides as inhibitors of *Plasmodium falciparum* dUTPase. *ChemMedChem*. 2011;6:309–320.
 37. Wada M, Mishima H, Watanabe T, et al. Triarylcarbenium salts highly reducible by primary alcohols. *J Chem Soc Chem Commun*. 1993;1462.
 38. Jones PD, Glass TE. Exploring the effects of cooperative interactions on affinity using a pinwheel sensor system. *Tetrahedron*. 2004;60:11057–11065.
 39. Nakazaki A, Mori A, Kobayashi S, Nishikawa T. Diastereoselective synthesis of 3,3-disubstituted oxindoles from atropisomeric N-aryl oxindole derivatives. *Tetrahedron Lett*. 2012;53:7131–7134.
 40. Maraval V, Duhayon C, Coppel Y, Chauvin R. The intricate assembling of gem-diphenylpropargylic units. *Eur J Org Chem*. 2008;2008:5144–5156.
 41. Lichtenheldt M, Kress S, Blechert S. Synthesis of electronically modified Ru-based neutral 16 VE allenylidene olefin metathesis precatalysts. *Molecules*. 2012;17:5177–5186.
 42. Srihari P, Reddy J, Mandal S, Satyanarayana K, Yadav J. PMA-silica gel catalyzed propargylation of aromatic compounds with arylpropargyl alcohols under solvent-free conditions. *Synthesis*. 2008;2008:1853–1860.
 43. Porter NA, Hogenkamp DJ, Khouri FF. Allene/haloolefin electrocyclic reactions: a new route to stable triarylmethyl radicals. *J Am Chem Soc*. 1990;112:2402–2407.
 44. Nolte C, Ammer J, Mayr H. Nucleofugality and nucleophilicity of fluoride in protic solvents. *J Org Chem*. 2012;77:3325–3335.
 45. Dem'yanov P, Boche G, Marsch M, Harms K, Fyodorova G, Petrosyan V. Crystal Structure of η^3 -lithio-1,3,3-triphenylpropyne-(diethyl ether)₂ and [1-lithio-1-(2-methoxyphenyl)-3,3-diphenylallene-diethyl ether]₂: Propargyl- versus allenyl-type structures. *Liebigs Ann*. 1995;1995:457–460.
 46. Libman NM. *J Org Chem USSR (English Translation)*. 1979;15:1243–1247.
 47. Cooper MS, Heaney H. Mannich reactions of aryl-trialkylstannanes using preformed dialkyl-methyleneiminium salts. *Tetrahedron Lett*. 1986;27:5011–5014.
 48. Suga S, Okajima M, Yoshida J-I. Reaction of an electrogenerated 'iminium cation pool' with organometallic reagents. Direct oxidative α -alkylation and -arylation of amine derivatives. *Tetrahedron Lett*. 2001;42:2173–2176.
 49. Werner V, Ellwart M, Wagner AJ, Knochel P. Preparation of tertiary amines by the reaction of iminium ions derived from unsymmetrical aminals with zinc and magnesium organometallics. *Org Lett*. 2015;17:2026–2029.
 50. Rochin C, Babot O, Dunoguès J, Duboudin F. A new convenient synthesis of dialkyl (methylene)ammonium chloride. *Synthesis*. 1986;1986:228–229.
 51. Heaney H, Papageorgiou G, Wilkins RF. The generation of iminium ions using chlorosilanes and their reactions with electron rich aromatic heterocycles. *Tetrahedron*. 1997;53:2941–2958.
 52. Andersen KE, Begtrup M, Chorghade MS, et al. The synthesis of novel GABA uptake inhibitors. Part 2. Synthesis of 5-hydroxytiagabine, a human metabolite of the GABA reuptake inhibitor tiagabine. *Tetrahedron*. 1994;50:8699–8710.
 53. Steinmetz MG, Mayes RT. Mechanisms for interconversions among C₃H₄ hydrocarbons: deuterium isotope effects and independent generation of vinylmethylene intermediates in photoisomerizations of allenes and cyclopropenes. *J Am Chem Soc*. 1985;107:2111–2121.
 54. Marshall JA, Robinson ED, Lebreton J. Synthesis of the tumor-inhibitory tobacco constituents. α - and β -2,7,11-cembratriene-4,6-diol by diastereoselective [2,3] Wittig ring contraction. *J Org Chem*. 1990;55:227–239.
 55. Zweifel G, Backlund SJ, Leung T. Synthesis of homopropargylic and α -allenic alcohols from lithium chloropropargylide, trialkylboranes, and aldehydes. *J Am Chem Soc*. 1978;100:5561–5562.
 56. Baker KV, Brown JM, Hughes N, Skarnulis AJ, Sexton A. Mechanical activation of magnesium turnings for the preparation of reactive Grignard reagents. *J Org Chem*. 1991;56:698–703.
 57. Eckenberg P, Groth U, Köhler T. Stereoselective synthesis of steroids and related compounds. IV. Addition of cerium reagents derived from (Trimethylsilyl)propargyl bromide to aldehydes. *Liebigs Ann Chem*. 1994;1994:673–677.
 58. Kragler A, Höfner G, Wanner KT. Synthesis and biological evaluation of amino-methylphenol derivatives as inhibitors of the murine GABA transporters mGAT1-mGAT4. *Eur J Med Chem*. 2008;43:2404–2411.
 59. Zepperitz C, Höfner G, Wanner KT. MS-binding assays: kinetic, saturation, and competitive experiments based on quantitation of bound marker as exemplified by the GABA transporter mGAT1. *ChemMedChem*. 2006;1:208–217.
 60. Petrerá M, Wein T, Allmendinger L, et al. Development of highly potent GAT1 inhibitors: synthesis of nipecotic acid derivatives by Suzuki-miyaura cross-coupling reactions. *ChemMedChem*. 2016;11:519–538.
 61. Nösel P, Moghimi S, Hendrich C, et al. Oxidative gold catalysis meets photochemistry – synthesis of benzo[a]fluorenones from diynes. *Adv Synth Cat*. 2014;356:3755–3760.
 62. Gabbutt CD, Heron BM, Instone AC, Thomas DA, Partington SM, Hursthouse MB, Gelbrich T. Observations on the synthesis of photochromic Naphthopyrans. *Eur J Org Chem*. 2003;2003:1220–1230.
 63. Nicolas J, San Miguel V, Mantovani G, Haddleton DM. Fluorescently tagged polymer bioconjugates from protein derived macroinitiators. *Chem Commun (Camb)*. 2006;4697–4699.



Synthesis and biological evaluation of novel N-substituted nipecotic acid derivatives with a *trans*-alkene spacer as potent GABA uptake inhibitors



Krisztián Tóth, Georg Höfner, Klaus T. Wanner*

Department of Pharmacy – Center for Drug Research, Ludwig-Maximilians-Universität München, Butenandstr. 5–13, 81377 Munich, Germany

ARTICLE INFO

Keywords:

GABA uptake inhibitor
mGAT4
Nipecotic acid
Iminium ion chemistry
Hydrozirconation

ABSTRACT

Our study presents the synthesis and structure-activity relationship (SAR) of novel N-substituted nipecotic acid derivatives closely related to DDPM-1457 [(S)-**2a**], a chemically stable analog of (S)-SNAP-5114 (**1**), in the pursuit of finding new and potent mGAT4 selective inhibitors. Iminium ion chemistry served as key step for the preparation of the desired, new N-substituted nipecotic acid derivatives containing a variety of different heterocycles attached to the nipecotic acid moiety via a *trans*-alkene spacer. The target compounds were characterized with regard to their potency at and subtype selectivity for the GABA transporters mGAT1–mGAT4.

1. Introduction

The decrease in the GABAergic neurotransmission, with gamma-aminobutyric acid (GABA) as the major inhibitory neurotransmitter in the central nervous system (CNS),¹ can cause severe neurological disorders including Alzheimer's disease,² depression,³ and epilepsy.^{4,5} The GABA transporters (GATs), amongst other factors, are responsible for the regulation of the GABA concentration in the synaptic cleft in the CNS.⁶ Four different subtypes of these membrane-bound transporter proteins,^{7,8} which belong to the solute carrier 6 (SLC6) family, are known.^{9,10} Depending on the species they are cloned from, different nomenclatures are used. GABA transporters originating from mice are named as mGAT1, mGAT2, mGAT3, and mGAT4. Alternatively, according to the Human Genome Organization (HUGO) they are also denoted as GAT1 (≡mGAT1), BGT-1 (≡mGAT2), GAT2 (≡mGAT3), and GAT3 (≡mGAT4).¹¹ Most importantly, mGAT1 and mGAT4 have been found to be clearly predominating in the CNS.¹² Of these, mGAT1 is mainly located in the presynaptic neurons where it is responsible for the uptake of GABA in neurons, whereas GABA transport from the synaptic cleft into the surrounding glial cells is mediated by mGAT4.^{13,14} The other two subtypes, mGAT2 and mGAT3 are mainly observed in the kidneys and liver¹⁵ and are thought not to play any significant role in the termination of GABAergic neurotransmission in the CNS under normal conditions.¹⁶

As increased levels of GABA in the synaptic cleft can be achieved by inhibitors of mGAT1 and mGAT4, inhibitors of these proteins are considered useful for the treatment of neurological disorders related to a hypofunction of GABA neurotransmission, some of which have been

mentioned above. New GAT inhibitors with high potency at and subtype selectivity for mGAT4 that have not been identified so far might allow an improved treatment of some of the aforementioned complex neurological diseases. At the same time, new mGAT1 inhibitors might show less side effects (asthenia, depression, diarrhea, dizziness, nervousness, and tremor)¹⁷ as found for example for tiagabine (**4**, Fig. 1), an mGAT1 inhibitor in medical use. Additionally to many highly potent and selective mGAT1 inhibitors such as tiagabine (**4**),^{18,19} also a large number of inhibitors for mGAT2–mGAT4 have been identified, but the potency and selectivity of the latter regarding their targets are in general far from being satisfying.^{20–24} DDPM-1457 [(S)-**2a**],²⁵ a carba-analogue of the earlier discovered mGAT4 inhibitor (S)-SNAP-5114 (**1**)²⁶ has a reasonable potency at and selectivity for its target, and furthermore, it has increased chemical stability compared to trityl-ether derivative (S)-SNAP-5114 (**1**), the most prototypic mGAT4 inhibitor. In our previous work, we described a new series of analogues of (S)-**2a** in which the spacer was modified from a *trans*-double bond to a triple bond resulting in compound **3** (Fig. 1) as the closest structural analogue. However, these compounds showed in general lower potencies at mGAT2–mGAT4 and marginally higher at mGAT1 than (S)-**2a**.²⁷ Additionally, a former study reported various isatin derivatives as a new class of hGAT3 (≡mGAT4) inhibitors with compound **5** representing the most potent and selective member.²⁸

The goal of this study was to further explore the carba-analogue family of DDPM-1457 [(S)-**2a**] for more potent and selective inhibitors for mGAT4 with increased chemical stability compared to (S)-SNAP-5114 (**1**). To this end, the structure of DDPM-1457 [(S)-**2a**] has been varied. To be more precise, the variation refers actually to DDPM-1007

* Corresponding author.

E-mail address: klaus.wanner@cup.uni-muenchen.de (K.T. Wanner).

<https://doi.org/10.1016/j.bmc.2018.11.002>

Received 7 September 2018; Received in revised form 31 October 2018; Accepted 2 November 2018

Available online 03 November 2018

0968-0896/ © 2018 Elsevier Ltd. All rights reserved.

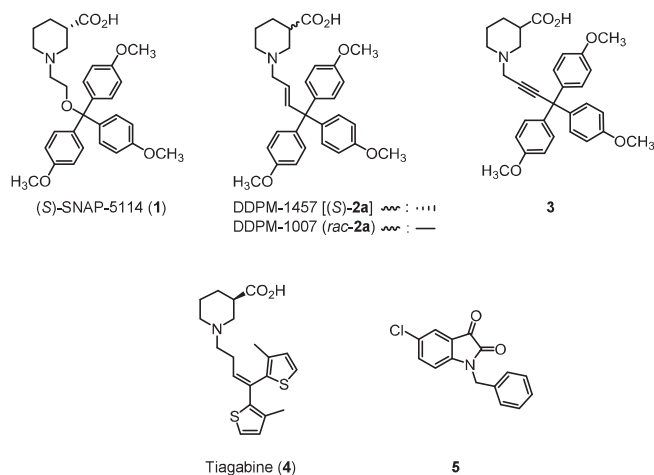


Fig. 1. Selected GABA uptake inhibitors from the literature.

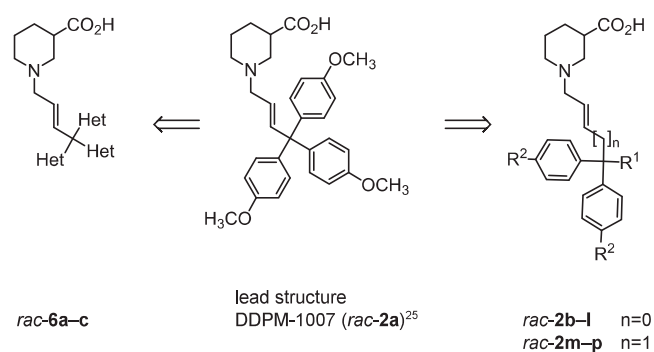


Fig. 2. General structures of targeted *N*-substituted nipecotic acid derivatives *rac*-6a–c, and *rac*-2b–p.

(*rac*-2a),²⁵ the racemic form of (*S*)-2a, which is to be considered the better reference compound as the target compounds have been made only as racemates in this study. Anyway, the potencies of *rac*-2a differ only slightly from those of (*S*)-2a. For mGAT1, mGAT3, and mGAT4, they are somewhat lower and for mGAT2 somewhat higher. Variations performed in this study are indicated in Fig. 2. As a major modification one of the aromatic moieties of the lipophilic residue was replaced with a series of new residues, e.g. aromatic, heteroaromatic, and benzylic residues (*rac*-2b–j, Table 1). Furthermore, for compounds *rac*-2k–l (Table 1, entry 12 and 13) not only one, but all three aromatic moieties were replaced by three identical phenyl or 4-methylphenyl residues, respectively.

In addition, the spacer was extended by one methylene group between the *trans*-double bond and the lipophilic residue (*rac*-2m–p, Table 1), to explore the influence of the linker length on the biological activity. Finally, also compounds *rac*-6a–c exhibiting three identical but sterically more demanding heterocyclic residues than in *rac*-2a have been synthesized.

2. Results and discussion

2.1. Chemistry

For the construction of the ethyl esters *rac*-7a–p, as precursors for the synthesis of the free nipecotic acid derivatives *rac*-2a–p, we intended to react iminium ion *rac*-8, which should be accessible from *N,O*-acetal *rac*-10 (Table 1),²⁷ with zirconocene reagents **9a–p** (Fig. 3). The zirconocene reagents **9a–p** should be generated by hydrozirconation²⁹ of alkynes **11a–p** and their reaction with iminium ion *rac*-8 lead to esters *rac*-7a–p with a *trans*-configured double bond.

2.1.1. Preparation of the alkynes

The alkynes **11a–p** needed for the synthesis of the target compounds are shown in Table 1. Alkynes **11a–f**, **11h–j**, **11m–n** were synthesized as described earlier by us,²⁷ and alkynes **11k**³⁰ and **11l**³¹ according to literature. Alkyne **11g** was prepared from alkyne **12g**²⁷ by the protection of the free hydroxy group with a TMS group (Table 1).³²

Alkynes **11o–p** with a longer carbon chain were obtained through the reaction of diaryl bromides **13o–p** with $\text{TMSC}\equiv\text{CCH}_2\text{MgBr}$ and the subsequent removal of the TMS group as shown in Scheme 1.²⁷ As a side product, allenenes **15o–p** were formed, a result observed before for similar reactions.^{27,33,34}

2.1.2. Synthesis of the *N*-substituted nipecotic acid esters by the coupling of iminium salt *rac*-8 with zirconocene reagents, and subsequent hydrolysis to the corresponding acids.

When treated with trimethylsilyl chloride (TMSCl) in tetrahydrofuran (THF), the *N,O*-acetal *rac*-10 yields the iminium salt *rac*-8 as a white slurry.²⁷ To warrant a homogenous reaction mixture in the present study, dichloromethane (DCM) was used as a solvent (Table 1). A ¹H NMR spectrum of the resulting homogenous solution revealed, when the reaction was repeated in DCM-*d*₂ that the educt **10** had been completely transformed into the iminium salt *rac*-8. The most characteristic ¹H NMR signal of the iminium salt being found at 7.42 ppm (s, 2H) resulting from the exocyclic CH₂ moiety.²⁷

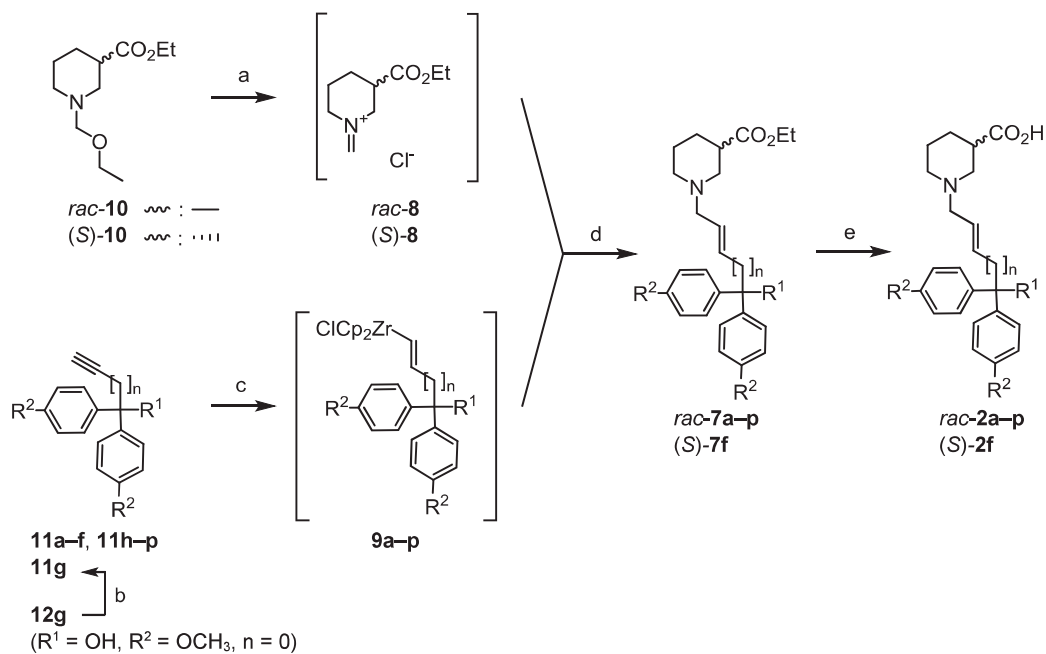
Iminium salts similar to *rac*-8 are known to efficiently add organometallic reagents under mild conditions.^{36–41} Hence, it appeared reasonable to assume that also the organometallic species **9a–p** (Table 1), that should form by reaction of alkynes **11a–p** with Schwartz's reagent (Cp_2ZrHCl),²⁹ would undergo an addition to iminium salt *rac*-8 to give *rac*-7a–p. Considering the *trans*-stereochemistry of the hydrozirconation product of alkynes **11a–p**, also the alkene moiety of the addition products, *rac*-7a–p can be expected to possess the desired *trans*-configuration. To study the feasibility of this approach at first the synthesis of ester *rac*-7a,²⁵ the preparation of which by a different route has been reported before, was attempted. Employing alkyne **11a** to hydrozirconation and reaction with *rac*-8 gave *rac*-7a in 45% yield (Table 1, entry 1) demonstrating the validity of this method. Analogously, after hydrozirconation of the respective alkynes **11b–p** with Cp_2ZrHCl (DCM, 25 °C) and reaction of the resulting organometallic reagents with *in situ* generated iminium salt *rac*-8, the nipecotic acid ester derivatives *rac*-7b–p could be obtained, with the alkene moiety exhibiting the desired *trans*-configuration.^{42–44} Yields were moderate to good (48%–84%, Table 1), except for *rac*-7b and *rac*-7f, where they amounted to 24% and 23% only (Table 1, entry 2 and 6). In many cases medium to large amounts of the individual unreacted starting alkyne **11a–p** could be recovered. The low yields might be due to the high steric demand of the triaryl moiety of the alkynes used, which could hamper the hydrozirconation step. According to literature, the sterically less demanding alkyne 3,3-dimethyl-1-butyne (**11q**) reacts well with Cp_2ZrHCl to give the corresponding hydrozirconation product.⁴⁵ When this alkyne **11q** was employed in the above reaction sequence with iminium salt *rac*-8 as electrophilic, the corresponding ester *rac*-7q was obtained in a yield of 87%. This suggests that the low yields partly observed in the preparation of *rac*-7a–p are related to steric hindrance arising from the alkyne in the hydrozirconation step.

Additionally, we employed the enantiomerically pure *N,O*-acetal (*S*)-**10** in this reaction sequence, to synthesize the enantiomerically pure ester (*S*)-**7f** and the corresponding free acid (*S*)-**7f** (Table 1, entry 7, yield 17% and 88%) having a benzothiophene residue at the triaryl center. By doing so, we expected that the potency at and selectivity for mGAT4 of this compound would increase as (*S*)-enantiomers of nipecotic acid derivatives are known²⁵ to be in general more potent than mGAT4 than their racemates.²⁷

Lastly, the esters *rac*-7a–p and (*S*)-**7f** were hydrolyzed with NaOH (12 M in MeOH) which gave the free acids *rac*-2a–p and (*S*)-**2f** with good to excellent yields (61%–97%, Table 1).²⁷ In case of *rac*-7g during

Table 1

Formation of the N-substituted nipecotic acid esters *rac*-7a–p and (S)-7f, and their hydrolysis to the free acids *rac*-2a–p and (S)-2f.



Entry	Alkynes (11)	R ¹	R ²	n	Esters (7)	Yield % ^e	Acids (2)	Yield % ^f
1	11a		OCH ₃	0	<i>rac</i> -7a ²⁵	45	<i>rac</i> -2a ²⁵	86
2	11b		OCH ₃	0	<i>rac</i> -7b	24	<i>rac</i> -2b	91
3	11c		OCH ₃	0	<i>rac</i> -7c	51	<i>rac</i> -2c	97
4	11d		OCH ₃	0	<i>rac</i> -7d	58	<i>rac</i> -2d	91
5	11e		OCH ₃	0	<i>rac</i> -7e	49	<i>rac</i> -2e	89
6	11f		OCH ₃	0	<i>rac</i> -7f	23	<i>rac</i> -2f	85
7	11f		OCH ₃	0	(S)-7f	16	(S)-2f	88
8	11g	OTMS/OH ^g	OCH ₃	0	<i>rac</i> -7g	59	<i>rac</i> -2g ^g	61
9	11h	H	OCH ₃	0	<i>rac</i> -7h	77	<i>rac</i> -2h	91
10	11i		OCH ₃	0	<i>rac</i> -7i	84	<i>rac</i> -2i	94
11	11j		OCH ₃	0	<i>rac</i> -7j	83	<i>rac</i> -2j	93
12	11k		H	0	<i>rac</i> -7k	55	<i>rac</i> -2k	95
13	11l		CH ₃	0	<i>rac</i> -7l	48	<i>rac</i> -2l	91

(continued on next page)

Table 1 (continued)

Entry	Alkynes (11)	R ¹	R ²	n	Esters (7)	Yield % ^e	Acids (2)	Yield % ^f
14	11m		OCH ₃	1	<i>rac</i> -7m	57	<i>rac</i> -2m	80
15	11n		H	1	<i>rac</i> -7n	71	<i>rac</i> -2n	88
16	11o	H	OCH ₃	1	<i>rac</i> -7o	78	<i>rac</i> -2o	93
17	11p	H	H	1	<i>rac</i> -7p	70	<i>rac</i> -2p	83

Reagents and conditions: (a) TMSCl, DCM; (b) Formation of **11g** from **12g**: TMSCl, DMAP, TEA, THF; (c) Cp₂ZrHCl, DCM; (d) DCM, 25 °C; (e) 12 M NaOH, MeOH; ^eIsolated yield after chromatography; ^fIsolated yield after extraction; ^gTMS group was cleaved during the hydrolysis; R¹ = OH.

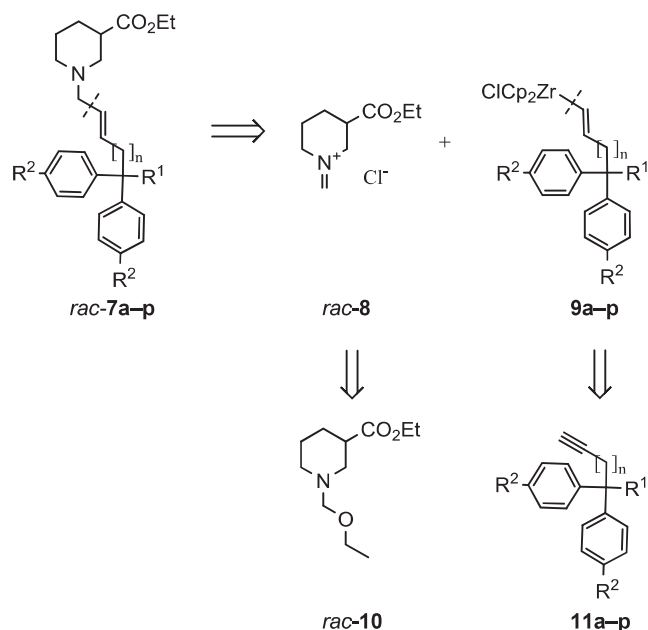


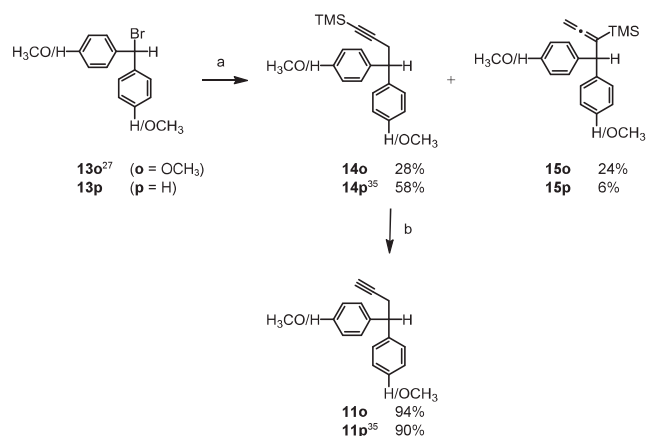
Fig. 3. Retrosynthetic analysis of targeted *N*-substituted nipecotic acid ester analogs *rac*-7a–p.

ester hydrolysis also the TMS ether function was cleaved leading to *rac*-2g exhibiting a hydroxy group in vicinity to the lipophilic moiety (Table 1, entry 8).

2.1.3. Synthesis of the *N*-substituted nipecotic acid esters, having three identical heterocycles, by the coupling of the iminium salt with alkenyl zirconocene reagents, and the subsequent hydrolysis to the corresponding acids

For the synthesis of the nipecotic acid derivatives *rac*-6a–c with a *trans*-configured alkene spacer and three identical heterocycles forming the lipophilic domain, first, the tertiary alcohols **17a–c** had to be prepared. The synthesis of these compounds was accomplished analogously to literature⁴⁶ by reacting the Grignard reagents formed from the heterocyclic bromides **16a–c** with diethyl carbonate as shown in Table 2 (**17a–c**, yields 48%–89%). Subsequent treatment²⁷ of the alcohols **17a–c** with acetyl chloride (AcCl) yielded chloride derivatives **18a–c**. These delivered alkynes **20a–b** from chlorides **18a–b** upon reaction²⁷ with trimethylsilyl ethynyllithium (\rightarrow **19a–b**) and subsequent removal of the TMS group (\rightarrow **20a–b**) and alkyne **20c** by treating **18c** with ethynylmagnesium bromide.²⁷

The synthesis of the targeted esters *rac*-21a–c by coupling the hydrozirconation products **22a–c** of alkynes **20a–c** with iminium salt *rac*-8 was accomplished analogously to the above-described preparation of *rac*-7a–p. Considering the high steric demand of the triaryl moiety present in alkynes **20a–c**, the yields for the coupling products *rac*-21a–c were not unexpectedly low (15%–28%, Table 3).



Scheme 1. Synthesis of the diaryl alkyne derivatives **11o–p**. Reagents and conditions: (a) TMSCl, CuBr, THF; (b) K₂CO₃, MeOH.

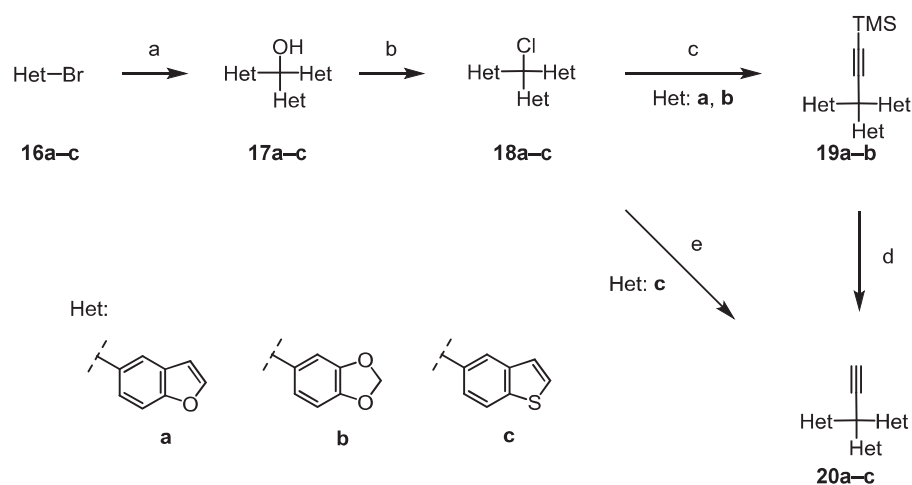
Hydrolysis of esters *rac*-21a–c under the previously described conditions (12 M NaOH in MeOH)²⁷ led finally to the free nipecotic acid derivatives *rac*-6a–c having different, but each three identical heterocycles at their lipophilic termini (66%–91%, Table 3).

2.2. Biological evaluation

The synthesized *N*-substituted nipecotic acid derivatives with a *trans*-alkene spacer *rac*-2b–p and *rac*-6a–c were evaluated for their inhibitory potencies at mGAT4 and additionally for the other murine GABA transporter subtypes mGAT1–mGAT3 in a standardized [³H]GABA uptake assay based on HEK cells developed by our group.⁴⁷ Binding affinities of these compounds towards mGAT1 (expressed in HEK cells) were also determined using a standardized MS Binding Assay.⁴⁸ The measurements were done in triplicates and wherever possible, the potencies of the tested compounds in the uptake assays are given as pIC₅₀ values. In cases where test compounds at a concentration of 100 μM were not able to reduce [³H]GABA uptake to a value of below 50%, which equals pIC₅₀ values ≤ 4.00, only the percent values of the remaining [³H]GABA uptake is given.

The results of the binding and uptake assays at mGAT1–mGAT4 for the chemically more stable DDPM-1457 [(*S*)-**2a**] show only minor differences as compared to the chemically labile (*S*)-SNAP-5114 (**1**, Table 4, entry 1 and 2). Also the racemic analog of (*S*)-**2a** DDPM-1007 (*rac*-**2a**), (Table 4, entry 3)²⁵ shows compared to **1**, only slightly lower binding affinities and inhibitory potencies. Hence, we considered it convenient to focus in this study, at least at first, on the racemic nipecotic acid derivatives. This way the synthesis will be more economical while at the same time the biological activity of both enantiomers of the final compounds will be reflected in the data from the biological testing. In a former study in *rac*-**2a**, the *trans*-C–C double bond moiety

Table 2
Synthesis of the heterocyclic alkynes **20a–c**.



Entry	Alcohols (17)	Het	Yield % ^f	Halides (18)	Yield % ^g	TMS-Alkynes (19)	Conditions	Yield % ^f	Alkynes (20)	Conditions	Yield % ^f
1	17a		67	18a	99	19a	c	35	20a	d	77
2	17b		89	18b	97	19b	c	53	20b	d	88
3	17c		48	18c	95	-	-	-	20c	e	54

Reagents and conditions: (a) 1) Mg, 2) diethyl carbonate, THF; (b) AcCl, toluene; (c) TMS≡CLi; (d) K₂CO₃, MeOH; (e) HC≡CMgBr. ^fYield after chromatography; ^gYield after removal of the solvents.

in the spacer has been replaced by a triple bond resulting in compound **3** (Table 4, entry 4). This derivative, which as a close structural analog of (*S*)-**2a** and *rac*-**2a** is a further helpful reference compound from the literature, shows a significant decrease in the inhibitory potency at mGAT4 of more than one log unit as compared to (*S*)-**2a** and *rac*-**2a** (Table 4, entry 2 and 3). Additionally, for comparison purposes also tiagabine (**4**) as a potent and selective mGAT1 inhibitor – in contrary to DDPM-1457 [(*S*)-**2a**] which is most potent at mGAT3–mGAT4 – has been included in Table 4.⁴⁹

In the first series of new analogs, as compared to *rac*-**2a** (Table 4, entry 3), one aromatic residue of the lipophilic moiety was replaced by a new heteroaromatic (*rac*-**2b–f**), OH or H (*rac*-**2g–h**) or benzylic substituent (*rac*-**2i–j**). The data from the biological evaluation of these compounds are given in Table 5. The introduction of a 1,3-benzodioxole ring in compound *rac*-**2b**, a thiophene ring (*rac*-**2e**), or a benzothio-*phene* ring (*rac*-**2f**) had only minor consequences. As compared to *rac*-**2a**, the potencies at mGAT2–mGAT4 were nominally somewhat lower and at the same time at mGAT1 slightly higher. Derivatives with a thiazole ring (*rac*-**2c**), imidazole ring (*rac*-**2d**), or a free hydroxy group (*rac*-**2g**) instead of an aromatic moiety exhibited very low activity at all mGATs. In case of *rac*-**2h**, where one of the 4-methoxyphenyl residues in *rac*-**2a** has been replaced by a hydrogen, potencies were lower at mGAT2–mGAT4 and slightly higher at mGAT1. A similar trend applies to *rac*-**2i–j** exhibiting benzylic moieties, but with still lower potencies at mGAT4. Compound *rac*-**2k**, in which the three methoxy groups in *para*-position of the triaryl moiety had been omitted (R₂ = H), is more or less devoid of any activity at mGAT2–mGAT4, but has similar potency at mGAT1 as *rac*-**2a**. For compound *rac*-**2l** with a methyl instead of methoxy group in the *para*-position of the phenyl rings in *rac*-**2a** potencies at all four mGATs are similar, but at mGAT1 the potency is somewhat higher and at mGAT4 lower as compared to *rac*-**2a**.

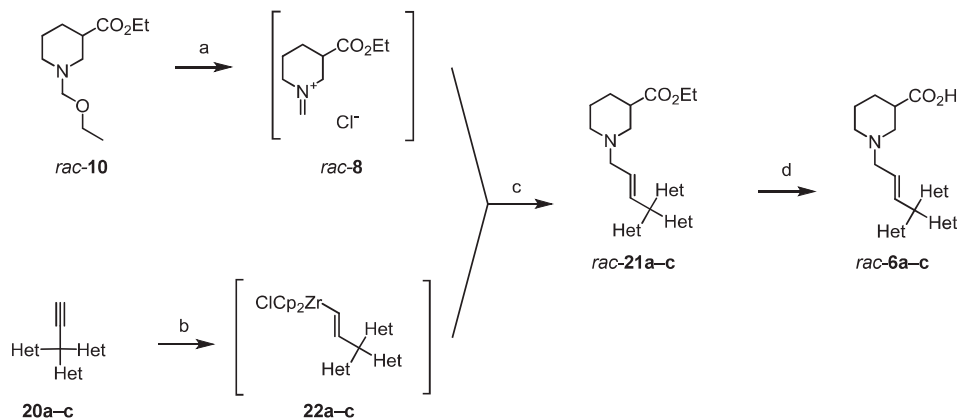
Compound *rac*-**2m** (Table 5, entry 13) that is directly delineated from *rac*-**2a** with an additional methylene group between the triaryl and the alkene moiety and hence possessing a longer spacer as it is also the case for *rac*-**2n–p**, the potency at mGAT3–mGAT4 dropped by more than one log unit whereas the decrease at mGAT2 was small and at mGAT1 insignificant. For *rac*-**2n** missing the three methoxy groups on the phenyl rings present in *rac*-**2m**, the potencies at mGAT2–mGAT4 remained almost the same as for *rac*-**2m**, but slightly increased for mGAT1. Compounds *rac*-**2o–p** with only two aromatic residues, two phenyl or two 4-methoxyphenyl rings, present in the lipophilic domain showed only low to marginal potencies at mGAT2–mGAT4. Interestingly, whereas the potency at mGAT1 was still low for *rac*-**2o** (pIC₅₀ = 4,87, Table 5, entry 15), it rose by almost two log units upon transition to *rac*-**2p** (pIC₅₀ = 6.78 ± 0.09, Table 5, entry 16), that is devoid of two methoxy substituents present in *rac*-**2o**. Thereby, *rac*-**2p** reaches a potency at mGAT1 (pIC₅₀ = 6.78 ± 0.09, Table 5, entry 16) that is almost as high as that of tiagabine (pIC₅₀ = 6.88 ± 0.12, Table 4, entry 5).

As a final point, we evaluated the enantiomerically pure compound (*S*)-**2f** (Table 5, entry 6) to see if it holds higher potency and better selectivity for mGAT4 as it was expected for this enantiomer.²⁵ Our expectations were only partly fulfilled. Compared to *rac*-**2f** (Table 5, entry 5), the potencies at mGAT1 got slightly lower, at mGAT2 almost unchanged, at mGAT3 significantly, and at mGAT4 marginally better. However, these changes were not as distinct as we hoped for, amongst our present derivatives, compound (*S*)-**2f** is still the most potent inhibitor of mGAT3–mGAT4.

Because of the promising mGAT4 results of (*S*)-**2f**, additionally to the pIC₅₀ values at mGAT1–mGAT4, for compound (*S*)-**2f** also the inhibitory potency at hGAT3 (≡mGAT4) was determined in our group with a previously reported assay.⁵⁰ The results show that the potency at

Table 3

Formation of the *N*-substituted nipecotic acid esters *rac*-21a–c, and their hydrolysis to the free acids *rac*-6a–c.



Entry	Alkynes (20)	Het	Esters (<i>rac</i> -21)	Yield % ^e	Acids (<i>rac</i> -6)	Yield % ^f
1	20a		<i>rac</i> -21a	28	<i>rac</i> -6a	66
2	20b		<i>rac</i> -21b	15	<i>rac</i> -6b	91
3	20c		<i>rac</i> -21c	20	<i>rac</i> -6c	87

Reagents and conditions: (a) TMSCl, DCM; (b) Cp₂ZrHCl, DCM; (c) DCM, 25 °C; (d) 12 M NaOH, MeOH; ^eIsolated yield after chromatography; ^fIsolated yield after extraction.

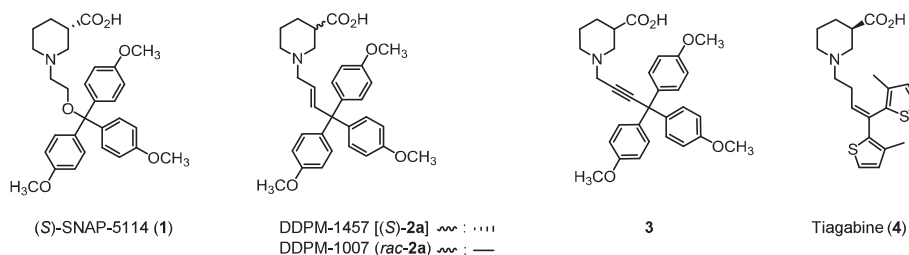
hGAT3 for (*S*)-2f with pIC₅₀: 5.73 ± 0.12 compared to the previously published value of (*S*)-SNAP-5114 (1, pIC₅₀: 5.4 ± 0.1)⁵⁰ is similar or even slightly better.

For compounds *rac*-6a–c, as close analogs of *rac*-2a with all three 4-methoxyphenyl residues being replaced with three identical benzo annelated heterocyclic residues, the heterocyclic part thought to mimic the methoxy function in *rac*-2a, the following results were found (Table 6). Analog *rac*-6a having three benzofuran moieties displays

similar potencies at all four mGATs. With the pIC₅₀ values being between 5.02 and 5.39, this compound shows distinctly increased potencies at mGAT1 and mGAT2, a slight increase at mGAT3 and a clear decrease at mGAT4 compared to *rac*-2a. For compounds *rac*-6b–c, characterized by the presence of three 1,3-benzodioxole and benzothiophene units, respectively, the potencies at all four mGATs were lower as these for *rac*-6a and within a range of about 4.0–4.8 (Table 6, entry 2 and 3).

Table 4

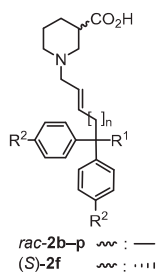
Binding affinities and inhibitory potencies of reference compounds 1, (*S*)-2a, *rac*-2a, 3, and 4 from the literature.



Entry	Compound	conf.	pK _i ^a	pIC ₅₀ ^b			
				mGAT1	mGAT2	mGAT3	mGAT4
1	(<i>S</i>)-SNAP-5114 (1) ^c	<i>S</i>	4.56 ^e ± 0.02	4.07 ± 0.09	56%	5.29 ± 0.04	5.71 ± 0.07
2	DDPM-1457 [(<i>S</i>)-2a] ^c	<i>S</i>	4.33 ^e ± 0.06	4.40 ± 0.05	4.42 ± 0.11	5.47 ± 0.02	5.87 ± 0.08
3	DDPM-1007 (<i>rac</i> -2a) ^c	<i>rac</i>	4.83 ^e ± 0.04	4.32 ± 0.05	4.68 ± 0.09	5.19 ± 0.06	5.67 ± 0.06
4	3 ^c	<i>rac</i>	5.36 ± 0.02	4.84	4.36	4.61	4.53
5	Tiagabine (4) ^c	<i>R</i>	7.43 ± 0.11	6.88 ± 0.12	50%	64%	73%

^a Results of the MS Binding Assays are given as pK_i ± SEM; ^bResults of the [³H]GABA uptake assays are given as pIC₅₀ ± SEM. Percentages represent remaining [³H]GABA uptake in presence of 100 μM test compound; ^cReference literature.²⁷

Table 5
Binding affinities and inhibitory potencies of the *N*-substituted nipecotic acids with a *trans*-alkene spacer *rac*-2b–p and (*S*)-2f.



Entry	Compound (2)	R ¹	R ²	n	pK _i ^a	pIC ₅₀ ^b			
						mGAT1	mGAT2	mGAT3	mGAT4
1	<i>rac</i> -2b		OCH ₃	0	5.06 ± 0.03	4.55	53%	4.99	5.50 ± 0.13
2	<i>rac</i> -2c		OCH ₃	0	4.47	65%	78%	82%	49%
3	<i>rac</i> -2d		OCH ₃	0	62%	70%	72%	83%	83%
4	<i>rac</i> -2e		OCH ₃	0	4.89	4.41	53%	4.37	5.12 ± 0.06
5	<i>rac</i> -2f		OCH ₃	0	5.48 ± 0.09	4.99 ± 0.08	4.60 ± 0.07	4.70 ± 0.04	5.45 ± 0.07
6	(<i>S</i>)-2f		OCH ₃	0	5.14 ± 0.02	4.85	4.63	5.55 ± 0.10	5.54 ± 0.12
7	<i>rac</i> -2g	OH	OCH ₃	0	54%	4.15	69%	66%	4.35
8	<i>rac</i> -2h	H	OCH ₃	0	5.43 ± 0.02	4.85	51%	4.27	4.50
9	<i>rac</i> -2i		OCH ₃	0	5.51 ± 0.04	4.95 ± 0.04	60%	53%	4.18
10	<i>rac</i> -2j		OCH ₃	0	5.33 ± 0.05	4.80	92%	66%	69%
11	<i>rac</i> -2k		H	0	5.08 ± 0.08	4.39	108%	103%	89%
12	<i>rac</i> -2l		CH ₃	0	5.26 ± 0.09	4.69	4.85	4.80	4.97 ± 0.03
13	<i>rac</i> -2m		OCH ₃	1	4.46	4.26	66%	4.07	4.38
14	<i>rac</i> -2n		H	1	5.01 ± 0.01	4.67	55%	56%	4.13
15	<i>rac</i> -2o	H	OCH ₃	1	5.49 ± 0.06	4.87	96%	71%	84%
16	<i>rac</i> -2p	H	H	1	7.51 ± 0.07	6.78 ± 0.09	96%	69%	82%

^a Results of the MS Binding Assays are given as pK_i ± SEM. For low pK_i values only one measurement was performed in triplicate, therefore no SEM could be calculated. Percentages represent remaining specific NO711 binding in presence of 100 μM test compound; ^bResults of the [³H]GABA uptake assays are given as pIC₅₀ ± SEM. For low pIC₅₀ values only one measurement was performed in triplicate, therefore no SEM could be calculated. Percentages represent remaining [³H]GABA uptake in presence of 100 μM test compound.

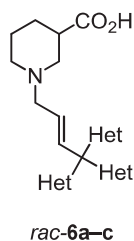
Compounds addressing GAT1 and BGT1 with moderate affinity could be shown to exert synergistic anticonvulsant effects making these compounds important pharmacological tools.^{51,52} Therefore, it may be worth subjecting also non-subtype selective GAT inhibitors such as *rac*-6a to a detailed pharmacological characterization, as addressing

different GAT subtypes with similar potency may result in a promising pharmacological profile.

The binding affinities of *rac*-6a–b and *rac*-2b–p determined in binding assays for mGAT1 and given as pK_i values were also in the same range as the corresponding potencies in uptake assays (pIC₅₀ values) for

Table 6

Binding affinities and inhibitory potencies of the *N*-substituted nipecotic acids with a *trans*-alkene spacer *rac*-6a–c.



Entry	Compound (<i>rac</i> -6)	Het	pK_i^a	pIC_{50}^b			
				mGAT1	mGAT2	mGAT3	mGAT4
1	<i>rac</i> -6a		5.67 ± 0.02	5.39 ± 0.10	5.02 ± 0.09	5.26 ± 0.10	5.23 ± 0.03
2	<i>rac</i> -6b		5.20 ± 0.06	4.75	4.05	4.61	4.82
3	<i>rac</i> -6c		54%	50%	4.47	4.28	4.70

^a Results of the MS Binding Assays are given as $pK_i \pm SEM$. For low pK_i values only one measurement was performed in triplicate, therefore no SEM could be calculated. Percentages represent remaining specific NO711 binding in presence of 100 μM test compound.

^b Results of the [³H]GABA uptake assays are given as $pIC_{50} \pm SEM$. For low pIC_{50} values only one measurement was performed in triplicate, therefore no SEM could be calculated. Percentages represent remaining [³H]GABA uptake in presence of 100 μM test compound.

the same transporter. As a general phenomenon, also here the pK_i values were found to be about a half log unit higher as the corresponding pIC_{50} values, which is already well known from literature.^{20,27,48}

3. Conclusion

DDPM-1457 [(*S*)-2a] being a potent and selective mGAT4 inhibitor was subjected to structural variations with the aim to identify new and preferentially more potent and selective mGAT4 inhibitors. For the synthesis of the *N*-substituted nipecotic acid esters – of the compounds the study aimed at – the addition of zirconocene reagents to an iminium salt *rac*-8 derived from ethyl nipecotate was utilized as a key step. As a major modification, the structure of the triarylmethyl moiety of the known DDPM-1007 (*rac*-2a), the racemic analogue of DDPM-1457 [(*S*)-2a], was modified by replacing one of the three aryl residues by diverse aryl, heteroaryl, or benzyl groups. These new compounds, *rac*-2b–l compared to the parent compound *rac*-2a, show similar or even distinctly lower potencies at mGAT4, while at mGAT1 generally a slight increase can be observed. Furthermore, the increase of the spacer length of DDPM-1007 (*rac*-2a) led to a large decrease of the potency at mGAT4. However, in one case, compound *rac*-2p, possessing an extended spacer, but only two instead of three phenyl rings forming the lipophilic domain a notable increase of the inhibitory potency at and binding affinity for mGAT1 occurred. The binding affinity and inhibitory potency of this compound were similar to that of tiagabine (4), as was the subtype selectivity in favor of mGAT1.

Additionally, derivatives with three identical heterocycles, replacing the 4-methoxyphenyl rings of DDPM-1007 (*rac*-2a), were synthesized. Amongst these, compound *rac*-6a bearing three benzofuran moieties showed similar potencies at all four mGATs (pIC_{50} : 5.02–5.39), which was a significant improvement compared to the analogs with three 1,3-benzodioxole or benzothiophene units. Such a reasonably potent and unselective inhibitor could be useful as a pharmacological tool to acquire a deeper understanding of how inhibition of multiple GATs at the same time influences GABA levels in the body.

4. Experimental section

4.1. Chemistry

Reactions were carried out in vacuum dried glassware under argon atmosphere. Tetrahydrofuran (THF) and diethyl ether (Et₂O) were distilled from sodium benzophenone ketyl. Dichloromethane (DCM) was distilled from CaH₂. All commercially available starting materials were used without further purification and solvents were distilled before use. As petroleum ether (PE) the fraction 40–60 °C was used. Flash chromatography was performed on silica gel (Merck 60F-254, 0.040–0.063 mm). Medium pressure liquid chromatography (MPLC) was performed using a Büchi instrument (C-605 binary pump system, C-630 UV detector at 254 nm, and C-660 fraction collector) and a Sepacore glass column B-685 (26*230 mm) equipped with silica gel (YMC Gel SIL-HG, 12 nm, S-20 μm). HRMS data were obtained with JMS-GCmate II (EI, Jeol) or Thermo Finnigan LTQ FT Ultra (ESI, Thermo Finnigan). NMR spectra were recorded with a JNMR-GX (JEOL 400 or 500 MHz) or Bruker BioSpin Avance III HD (400 or 500 MHz). As an internal standard, the known chemical shift of solvent traces was used to reference the spectra. Spectra were processed using the software MestReNova. All melting points are uncorrected and were determined using a Büchi B-540 apparatus. For IR spectroscopy, a Perkin Elmer FT-IR Spectrometer 1600 was used.

4.2. General procedures

4.2.1. Coupling of the *N,O*-acetal *rac*-10 with alkynes to form the *N*-substituted nipecotic acid esters (GP 1)

TMSCl (1 equiv.) was added to a stirred solution of *N,O*-acetal *rac*-10 (1 equiv.) in DCM (3 mL/mmol) at 0 °C. After 15 min the solution was warmed to 25 °C and was stirred for further 3 h at 25 °C to form a colorless solution. In a separate Schlenk tube DCM (6 mL/mmol) was added to the appropriate alkyne (2 equiv.) and Schwartz's reagent (Cp₂ZrHCl) (2 equiv.) at 0 °C and stirred for 3 h at 25 °C to form a slightly colored solution. To perform the coupling, the solution of the

iminium salt was cooled to 0 °C and the solution of the alkyne with Cp_2ZrHCl was added dropwise. After 24 h at 25 °C a clear, slightly colored solution formed. The mixture was quenched with concentrated aqueous NaHCO_3 solution and extracted with Et_2O three times. The combined organic phases were dried over Na_2SO_4 and concentrated under reduced pressure. The crude product was purified by flash chromatography on silica gel with DCM/MeOH (99:1) or with $\text{Et}_2\text{O}/\text{PE}/\text{MeOH}$ (50:50:1).

4.2.2. Hydrolysis of the *N*-substituted nipecotic acid esters (GP 2)

The ester (1 equiv.) was dissolved in MeOH (1 mL/mmol), then an excess of NaOH (5 equiv., 12 M in H_2O) was added dropwise at 0 °C. The mixture was stirred at 25 °C for 3–6 h until the hydrolysis was complete (TLC). The mixture was diluted with H_2O , stirred for 1 h at 25 °C and extracted with Et_2O . The water phase was collected and pH = 6.0 was set by adding HCl (5 equiv., 6 M in H_2O) and phosphate buffer (pH = 6.0, 1.0 M). This solution was extracted with DCM. The combined organic layers were dried over Na_2SO_4 and concentrated under reduced pressure to get the pure product as a thick oil. To get the *N*-substituted nipecotic acid as a solid, the oil was dissolved in DCM (0.1 mL), H_2O (2 mL) was added and an emulsion was prepared by sonication. This emulsion was freeze-dried to obtain a white, amorphous solid.

4.2.3. Synthesis of the heterocyclic alcohols (GP 3)

Dibromoethane (0.05 equiv.) was added to a suspension of magnesium turnings (3.5 equiv.) in THF (5 mL) and heated to 60 °C for 15 min. A solution of the corresponding heterocyclic bromide (3.3 equiv.) in THF (3 mL/mmol) was added dropwise to the mixture at 25 °C. After the initial exothermic reaction, the mixture was heated at 65 °C for 1 h. Finally, diethyl carbonate (1.0 equiv.) was added at 25 °C and it was heated at 65 °C for 2 h. The mixture was quenched with saturated aqueous NH_4Cl solution at 25 °C and extracted with EtOAc. The organic fractions were dried with Na_2SO_4 and concentrated under vacuum. The crude product was purified by flash chromatography.

4.2.4. Synthesis of the heterocyclic chlorides (GP 4)

AcCl (5 equiv.) was added to a solution of the corresponding heterocyclic alcohol (1 equiv.) in toluene (3 mL/mmol) and the mixture was heated at 65 °C for 4 h to obtain a deeply colored (red to violet) mixture. The volatiles were removed and the residue was taken up in toluene and evaporated to dryness, this procedure was repeated three times. This crude product was used without any further purification.

4.3. Synthesized compounds

4.3.1. (*E*)-1-[4,4,4-Tris(4-methoxyphenyl)but-2-en-1-yl]piperidine-3-carboxylic acid, (rac-2a)

According to GP2: Ester *rac-7a* (70 mg, 0.13 mmol) with NaOH (0.65 mmol, 12 M in H_2O) was hydrolyzed to get the pure product. White solid (56 mg, 86%).

The characterization data are in agreement with previously published data.²⁵

4.3.2. (*E*)-1-[4-(Benzo[d][1,3]dioxol-5-yl)-4-bis(4-methoxyphenyl)but-2-en-1-yl]piperidine-3-carboxylic acid, (rac-2b)

According to GP2: Ester *rac-7b* (40 mg, 0.070 mmol), NaOH (0.35 mmol, 12 M in H_2O) was hydrolyzed to get the pure product. White solid (33 mg, 91%).

IR (KBr): $\tilde{\nu}$ = 2935, 2905, 2835, 2047, 1711, 1607, 1580, 1507, 1484, 1464, 1439, 1395, 1346, 1296, 1249, 1180, 1119, 1097, 1036, 994, 933, 862, 829, 809, 737, 639 cm^{-1} . ^1H NMR (400 MHz, MeOD) δ 1.33 (qd, J = 12.3, 3.7 Hz, 1H), 1.55 (qt, J = 12.7, 3.7 Hz, 1H), 1.69 (d, J = 13.4 Hz, 1H), 1.92 (td, J = 12.0, 3.0 Hz, 1H), 1.98 (d, J = 11.6 Hz, 1H), 2.04 (t, J = 11.4 Hz, 1H), 2.37 (tt, J = 12.0, 3.8 Hz, 1H), 2.86 (d, J = 11.4 Hz, 1H), 3.12 (d, J = 11.0 Hz, 1H), 3.16 (d, J = 6.7 Hz, 2H),

3.78 (s, 6H), 5.33 (dt, J = 15.5, 6.8 Hz, 1H), 5.90 (s, 2H), 6.49 (d, J = 1.9 Hz, 1H), 6.52 (dd, J = 8.2, 1.9 Hz, 1H), 6.63 (d, J = 15.5 Hz, 1H), 6.70 (d, J = 8.1 Hz, 1H), 6.79–6.84 (m, 4H), 6.94–6.99 (m, 4H) ppm. ^{13}C NMR (101 MHz, MeOD) δ 25.87, 29.42, 46.44, 54.77, 55.73, 58.15, 60.43, 62.38, 102.32, 108.05, 111.78, 114.00, 124.30, 128.41, 132.16, 139.64, 142.00, 143.24, 147.29, 148.60, 159.47, 182.71 ppm. HRMS (ESI): $[\text{M}+\text{H}]^+$ calcd. for $\text{C}_{31}\text{H}_{34}\text{O}_6\text{N}$, 516.2380; found: 516.2380.

4.3.3. (*E*)-1-[4,4-Bis(4-methoxyphenyl)-4-(thiazol-2-yl)but-2-en-1-yl]piperidine-3-carboxylic acid, (rac-2c)

According to GP2: Ester *rac-7c* (46 mg, 0.090 mmol) NaOH (0.45 mmol, 12 M in H_2O) was hydrolyzed to get the pure product. White solid (42 mg, 97%).

IR (KBr): $\tilde{\nu}$ = 3406, 2995, 2933, 2835, 1722, 1710, 1658, 1606, 1580, 1509, 1462, 1442, 1408, 1349, 1297, 1251, 1179, 1133, 1115, 1031, 988, 866, 826, 725, 573 cm^{-1} . ^1H NMR (400 MHz, MeOD) δ 1.34 (qd, J = 12.7, 4.0 Hz, 1H), 1.55 (qt, J = 12.9, 3.9 Hz, 1H), 1.64–1.75 (m, 1H), 1.89–2.02 (m, 2H), 2.06 (t, J = 11.4 Hz, 1H), 2.37 (tt, J = 11.8, 3.7 Hz, 1H), 2.87 (d, J = 10.9 Hz, 1H), 3.13 (d, J = 11.5 Hz, 1H), 3.18 (dd, J = 6.8, 1.1 Hz, 2H), 3.78 (s, 6H), 5.38 (dt, J = 15.5, 6.8 Hz, 1H), 6.78 (d, J = 15.5 Hz, 1H), 6.82–6.89 (m, 4H), 6.99–7.06 (m, 4H), 7.50 (d, J = 3.4 Hz, 1H), 7.80 (d, J = 3.4 Hz, 1H) ppm. ^{13}C NMR (101 MHz, MeOD) δ 25.89, 29.39, 46.44, 54.84, 55.77, 58.23, 60.61, 62.10, 114.30, 120.92, 130.17, 131.80, 138.07, 141.00, 143.28, 160.17, 180.29, 182.66 ppm. HRMS (ESI): $[\text{M}+\text{H}]^+$ calcd. for $\text{C}_{27}\text{H}_{31}\text{O}_4\text{N}_2\text{S}$, 479.1998; found: 479.2007.

4.3.4. (*E*)-1-[4,4-Bis(4-methoxyphenyl)-4-(1-methyl-1H-imidazol-2-yl)but-2-en-1-yl]piperidine-3-carboxylic acid, (rac-2d)

According to GP2: Ester *rac-7d* (45 mg, 0.090 mmol) with NaOH (0.45 mmol, 12 M in H_2O) was hydrolyzed to get the pure product. White solid (39 mg, 91%).

IR (KBr): $\tilde{\nu}$ = 3428, 2939, 2836, 1710, 1607, 1582, 1509, 1464, 1397, 1344, 1296, 1252, 1180, 1137, 1032, 983, 831, 744, 686, 591, 576, 541 cm^{-1} . ^1H NMR (400 MHz, MeOD) δ 1.32 (qd, J = 12.7, 4.2 Hz, 1H), 1.45–1.62 (m, 1H), 1.63–1.74 (m, 1H), 1.85–1.99 (m, 2H), 2.03 (t, J = 11.4 Hz, 1H), 2.35 (tt, J = 11.8, 3.7 Hz, 1H), 2.84 (d, J = 11.5 Hz, 1H), 3.00 (s, 3H), 3.07 (d, J = 11.9 Hz, 1H), 3.14 (d, J = 6.9 Hz, 2H), 3.79 (s, 6H), 5.18 (dt, J = 15.5, 6.8 Hz, 1H), 6.63 (d, J = 15.7 Hz, 1H), 6.86–6.91 (m, 4H), 6.92 (d, J = 1.3 Hz, 1H), 6.94–7.00 (m, 4H), 7.05 (d, J = 1.3 Hz, 1H) ppm. ^{13}C NMR (101 MHz, MeOD) δ 25.82, 29.33, 35.66, 46.43, 54.71, 55.85, 57.61, 58.17, 61.93, 114.62, 124.39, 126.60, 127.08, 131.46, 131.49, 135.62, 141.15, 152.18, 159.93, 182.75 ppm. HRMS (ESI): $[\text{M}+\text{H}]^+$ calcd. for $\text{C}_{28}\text{H}_{34}\text{O}_4\text{N}_3$, 476.2543; found: 476.2542.

4.3.5. (*E*)-1-[4,4-Bis(4-methoxyphenyl)-4-(thiophen-3-yl)but-2-en-1-yl]piperidine-3-carboxylic acid, (rac-2e)

According to GP2: Ester *rac-7e* (41 mg, 0.080 mmol) and NaOH (0.4 mmol, 12 M in H_2O) was hydrolyzed to get the pure product. White solid (34 mg, 89%).

IR (KBr): $\tilde{\nu}$ = 3423, 2997, 2934, 1711, 1606, 1580, 1508, 1463, 1441, 1390, 1365, 1296, 1250, 1179, 1116, 1033, 991, 829, 795, 777, 733, 674, 650, 591 cm^{-1} . ^1H NMR (400 MHz, MeOD) δ 1.33 (qd, J = 12.6, 4.0 Hz, 1H), 1.55 (qt, J = 13.0, 3.8 Hz, 1H), 1.63–1.75 (m, 1H), 1.92 (td, J = 11.9, 2.8 Hz, 1H), 1.94–2.01 (m, 1H), 2.04 (t, J = 11.4 Hz, 1H), 2.36 (tt, J = 11.8, 3.7 Hz, 1H), 2.86 (d, J = 11.4 Hz, 1H), 3.11 (d, J = 11.4 Hz, 1H), 3.15 (d, J = 6.8 Hz, 2H), 3.77 (s, 6H), 5.32 (dt, J = 15.5, 6.8 Hz, 1H), 6.61 (d, J = 15.5 Hz, 1H), 6.69 (dd, J = 3.1, 1.3 Hz, 1H), 6.77–6.86 (m, 5H), 6.94–7.02 (m, 4H), 7.35 (dd, J = 5.0, 3.0 Hz, 1H) ppm. ^{13}C NMR (101 MHz, MeOD) δ 25.83, 29.38, 46.41, 54.73, 55.77, 58.03, 58.08, 62.26, 114.06, 124.19, 125.81, 128.02, 130.74, 131.62, 139.54, 142.72, 149.49, 159.50, 182.78 ppm. HRMS (ESI): $[\text{M}+\text{H}]^+$ calcd. for $\text{C}_{28}\text{H}_{32}\text{O}_4\text{NS}$, 478.2046; found: 478.2048.

4.3.6. (*E*)-1-[4-(Benzo[*b*]thiophen-5-yl)-4,4-bis(4-methoxyphenyl)but-2-en-1-yl]piperidine-3-carboxylic acid, (*rac*-2*f*)

According to **GP2**: Ester *rac*-7*f* (37 mg, 0.060 mmol) NaOH (0.3 mmol, 12 M in H₂O) was hydrolyzed to get the pure product. White solid (29 mg, 85%).

IR (KBr): $\tilde{\nu}$ = 3423, 3034, 2997, 2935, 2834, 1711, 1606, 1580, 1508, 1462, 1439, 1411, 1390, 1343, 1296, 1250, 1180, 1117, 1090, 1034, 994, 896, 869, 830, 808, 756, 737, 704, 592, 554 cm⁻¹. ¹H NMR (500 MHz, MeOD) δ 1.36 (qd, *J* = 12.9, 4.0 Hz, 1H), 1.57 (qt, *J* = 13.0, 3.8 Hz, 1H), 1.67–1.74 (m, 1H), 1.95 (td, *J* = 12.2, 2.8 Hz, 1H), 2.00 (d, *J* = 12.4 Hz, 1H), 2.07 (t, *J* = 11.5 Hz, 1H), 2.38 (tt, *J* = 12.0, 3.7 Hz, 1H), 2.88 (d, *J* = 11.4 Hz, 1H), 3.16 (d, *J* = 11.0 Hz, 1H), 3.15–3.26 (m, 2H), 3.80 (s, 6H), 5.37 (dt, *J* = 15.5, 6.8 Hz, 1H), 6.77 (d, *J* = 15.5 Hz, 1H), 6.82–6.87 (m, 4H), 6.99–7.05 (m, 4H), 7.13 (dd, *J* = 8.6, 1.8 Hz, 1H), 7.24 (d, *J* = 5.5 Hz, 1H), 7.48 (d, *J* = 1.7 Hz, 1H), 7.52 (d, *J* = 5.4 Hz, 1H), 7.79 (d, *J* = 8.6 Hz, 1H) ppm. ¹³C NMR (126 MHz, MeOD) δ 25.88, 29.42, 46.46, 54.85, 55.71, 58.13, 60.66, 62.42, 114.04, 122.29, 125.22, 125.69, 127.61, 128.36, 128.66, 132.26, 139.06, 139.65, 140.85, 143.37, 144.36, 159.49, 182.67 ppm. HRMS (ESI): [M+H]⁺ calcd. for C₃₂H₃₄O₄N₂S, 528.2202; found: 528.2205.

4.3.7. (*S,E*)-1-[4-(Benzo[*b*]thiophen-5-yl)-4,4-bis(4-methoxyphenyl)but-2-en-1-yl]piperidine-3-carboxylic acid, [(*S*)-2*f*]

According to **GP2**: Ester (*S*)-7*f* (34 mg, 0.060 mmol) NaOH (0.3 mmol, 12 M in H₂O) was hydrolyzed to get the pure product. White solid (28 mg, 88%).

Analytical data correspond to those of *rac*-2*f* except [α]_D²⁰ = -14.5 (c = 0.6, DCM).

4.3.8. (*E*)-1-[4-Hydroxy-4,4-bis(4-methoxyphenyl)but-2-en-1-yl]piperidine-3-carboxylic acid, (*rac*-2*g*)

According to **GP2**: The ester *rac*-7*g* (30 mg, 0.060 mmol) with NaOH (0.6 mmol, 12 M in H₂O) was hydrolyzed to get the pure product. White solid (15 mg, 61%).

IR (KBr): $\tilde{\nu}$ = 3421, 2933, 2829, 1700, 1607, 1582, 1559, 1541, 1508, 1457, 1388, 1301, 1249, 1175, 1102, 1033, 987, 830, 802, 768, 694, 586, 513, 486 cm⁻¹. ¹H NMR (500 MHz, MeOD) δ 1.34 (qd, *J* = 12.9, 4.1 Hz, 1H), 1.56 (qt, *J* = 13.0, 3.8 Hz, 1H), 1.67–1.73 (m, 1H), 1.92 (td, *J* = 12.1, 2.9 Hz, 1H), 1.98 (d, *J* = 12.8 Hz, 1H), 2.04 (t, *J* = 11.4 Hz, 1H), 2.37 (tt, *J* = 11.9, 3.7 Hz, 1H), 2.88 (d, *J* = 11.4 Hz, 1H), 3.10 (dd, *J* = 6.9, 1.2 Hz, 2H), 3.13 (d, *J* = 10.8 Hz, 1H), 3.77 (s, 6H), 5.60 (dt, *J* = 15.4, 6.9 Hz, 1H), 6.27 (dt, *J* = 15.4, 1.2 Hz, 1H), 6.81–6.87 (m, 4H), 7.21–7.26 (m, 4H) ppm. ¹³C NMR (126 MHz, MeOD) δ 25.85, 29.37, 46.35, 54.69, 55.76, 58.02, 61.78, 79.41, 114.14, 114.22, 126.39, 129.40, 129.45, 140.04, 140.06, 142.21, 159.92, 159.93, 182.75 ppm. HRMS (ESI): [M+H]⁺ calcd. for C₂₄H₃₀NO₅, 412.2118; found 412.2120.

4.3.9. (*E*)-1-[4,4-Bis(4-methoxyphenyl)but-2-en-1-yl]piperidine-3-carboxylic acid, (*rac*-2*h*)

According to **GP2**: Ester *rac*-7*h* (43 mg, 0.10 mmol) with NaOH (0.5 mmol, 12 M in H₂O) was hydrolyzed to get the pure product. White solid (36 mg, 91%).

IR (KBr): $\tilde{\nu}$ = 3421, 2997, 2935, 2834, 1710, 1608, 1583, 1509, 1463, 1440, 1389, 1301, 1247, 1175, 1110, 1032, 979, 855, 829, 772, 725, 663, 627, 580, 556 cm⁻¹. ¹H NMR (400 MHz, MeOD) δ 1.33 (qd, *J* = 12.6, 3.9 Hz, 1H), 1.55 (qt, *J* = 12.9, 3.8 Hz, 1H), 1.63–1.75 (m, 1H), 1.89 (td, *J* = 11.9, 2.9 Hz, 1H), 1.97 (d, *J* = 8.8 Hz, 1H), 2.02 (t, *J* = 11.4 Hz, 1H), 2.37 (tt, *J* = 11.8, 3.7 Hz, 1H), 2.86 (d, *J* = 11.4 Hz, 1H), 3.05 (d, *J* = 6.9 Hz, 2H), 3.12 (d, *J* = 11.6 Hz, 1H), 3.76 (s, 6H), 4.64 (d, *J* = 7.4 Hz, 1H), 5.45 (dtd, *J* = 15.1, 6.9, 1.2 Hz, 1H), 6.09 (dd, *J* = 15.3, 7.2 Hz, 1H), 6.79–6.87 (m, 4H), 7.03–7.10 (m, 4H) ppm. ¹³C NMR (101 MHz, MeOD) δ 25.85, 29.41, 46.41, 53.49, 54.64, 55.75, 58.02, 62.06, 114.77, 128.01, 130.42, 137.42, 137.47, 139.27, 159.49, 182.78 ppm. HRMS (ESI): [M+H]⁺ calcd. for C₂₄H₃₀O₄N, 396.2169; found: 396.2170.

4.3.10. (*E*)-1-[4,4,5-Tris(4-methoxyphenyl)pent-2-en-1-yl]piperidine-3-carboxylic acid, (*rac*-2*i*)

According to **GP2**: Ester *rac*-7*i* (75 mg, 0.14 mmol) with NaOH (0.7 mmol, 12 M in H₂O) was hydrolyzed to get the pure product. White solid (66 mg, 95%).

IR (KBr): $\tilde{\nu}$ = 3434, 2997, 2933, 2833, 1713, 1609, 1581, 1510, 1463, 1299, 1248, 1179, 1110, 1033, 829, 778, 732, 590, 546, 505 cm⁻¹. ¹H NMR (400 MHz, MeOD) δ 1.32 (qd, *J* = 12.8, 4.0 Hz, 1H), 1.52 (qt, *J* = 12.7, 3.5 Hz, 1H), 1.62–1.73 (m, 1H), 1.86 (td, *J* = 11.9, 2.8 Hz, 1H), 1.92–2.04 (m, 2H), 2.34 (tt, *J* = 11.8, 3.7 Hz, 1H), 2.80 (d, *J* = 11.4 Hz, 1H), 3.01 (d, *J* = 6.8 Hz, 2H), 3.09 (d, *J* = 10.9 Hz, 1H), 3.45 (s, 2H), 3.70 (s, 3H), 3.77 (s, 6H), 5.03 (dt, *J* = 15.6, 6.9 Hz, 1H), 6.14 (d, *J* = 15.7 Hz, 1H), 6.57–6.67 (m, 4H), 6.77–6.85 (m, 4H), 7.01–7.10 (m, 4H) ppm. ¹³C NMR (101 MHz, MeOD) δ 25.82, 29.41, 46.36, 47.62, 54.08, 54.68, 55.61, 55.73, 58.04, 62.46, 113.79, 114.07, 114.08, 127.70, 131.05, 131.13, 133.02, 140.26, 142.99, 159.23, 159.42, 182.77 ppm. HRMS (ESI): [M+H]⁺ calcd. for C₃₂H₃₈NO₅, 516.2744; found: 516.2752.

4.3.11. (*E*)-1-[4,4-Bis(4-methoxyphenyl)-5-phenylpent-2-en-1-yl]piperidine-3-carboxylic acid, (*rac*-2*j*)

According to **GP2**: Ester *rac*-7*j* (42 mg, 0.080 mmol) with NaOH (0.4 mmol, 12 M in H₂O) was hydrolyzed to get the pure product. White solid (36 mg, 93%).

IR (KBr): $\tilde{\nu}$ = 3420, 3030, 3000, 2934, 2863, 2835, 1711, 1607, 1581, 1509, 1454, 1384, 1345, 1289, 1250, 1180, 1151, 1120, 1033, 1002, 958, 830, 809, 756, 739, 702, 640, 601, 575 cm⁻¹. ¹H NMR (400 MHz, MeOD) δ 1.32 (qd, *J* = 12.8, 4.3 Hz, 1H), 1.52 (qt, *J* = 13.0, 3.8 Hz, 1H), 1.63–1.72 (m, 1H), 1.85 (td, *J* = 11.9, 2.9 Hz, 1H), 1.98 (t, *J* = 11.5 Hz, 2H), 2.34 (tt, *J* = 11.8, 3.7 Hz, 1H), 2.80 (d, *J* = 11.4 Hz, 1H), 3.01 (d, *J* = 6.9 Hz, 2H), 3.09 (d, *J* = 11.2 Hz, 1H), 3.52 (s, 2H), 3.78 (s, 6H), 5.04 (dt, *J* = 15.6, 6.9 Hz, 1H), 6.14 (d, *J* = 15.6 Hz, 1H), 6.69–6.77 (m, 2H), 6.79–6.84 (m, 4H), 7.01–7.10 (m, 7H) ppm. ¹³C NMR (101 MHz, MeOD) δ 25.84, 29.42, 46.39, 48.50, 54.04, 54.71, 55.70, 58.07, 62.45, 114.08, 127.04, 127.87, 128.35, 131.12, 132.15, 139.13, 140.17, 142.79, 159.29, 182.72 ppm. HRMS (ESI): [M+H]⁺ calcd. for C₃₁H₃₆O₄N, 486.2638; found 486.2639.

4.3.12. (*E*)-1-(4,4,4-Triphenylbut-2-en-1-yl)piperidine-3-carboxylic acid, (*rac*-2*k*)

According to **GP2**: Ester *rac*-7*k* (22 mg, 0.050 mmol) with NaOH (0.25 mmol, 12 M in H₂O) was hydrolyzed to get the pure product. White solid (20 mg, 97%).

IR (KBr): $\tilde{\nu}$ = 3083, 3060, 3030, 2924, 2854, 2793, 2760, 2739, 1952, 1679, 1582, 1491, 1464, 1443, 1397, 1365, 1345, 1305, 1365, 1345, 1305, 1269, 1241, 1203, 1180, 1147, 1138, 1116, 1090, 1031, 1001, 990, 974, 957, 936, 908, 787, 772, 755, 739, 711, 700, 668, 654 cm⁻¹. ¹H NMR (400 MHz, MeOD) δ 1.41–1.55 (m, 1H), 1.53–1.69 (m, 1H), 1.70–1.82 (m, 1H), 1.95 (d, *J* = 12.9 Hz, 1H), 2.21–2.36 (m, 1H), 2.38–2.49 (m, 2H), 2.93 (d, *J* = 12.1 Hz, 1H), 3.13 (d, *J* = 7.6 Hz, 1H), 3.38 (d, *J* = 5.9 Hz, 2H), 5.38 (dt, *J* = 15.6, 7.0 Hz, 1H), 6.86 (d, *J* = 15.5 Hz, 1H), 7.05–7.11 (m, 6H), 7.18–7.32 (m, 9H) ppm. ¹³C NMR (101 MHz, MeOD) δ 24.93, 28.58, 45.15, 54.80, 57.33, 61.62, 62.07, 126.80, 127.54, 128.82, 131.26, 144.90, 147.05, 181.60 ppm. HRMS (ESI): [M+H]⁺ calcd. for C₂₈H₃₀O₂N, 412.2270; found 412.2272.

4.3.13. (*E*)-1-(4,4,4-Tri-*p*-tolylbut-2-en-1-yl)piperidine-3-carboxylic acid, (*rac*-2*l*)

According to **GP2**: Ester *rac*-7*l* (40 mg, 0.080 mmol) with NaOH (0.4 mmol, 12 M in H₂O) was hydrolyzed to get the pure product. White solid (33 mg, 91%).

IR (KBr): $\tilde{\nu}$ = 3022, 2921, 2859, 2519, 2284, 1722, 1508, 1452, 1402, 1310, 1275, 1189, 1145, 1120, 1071, 1038, 1020, 991, 952, 811, 784, 731, 567 cm⁻¹. ¹H NMR (400 MHz, MeOD) δ 1.33 (qd, *J* = 12.6, 3.9 Hz, 1H), 1.54 (dddd, *J* = 16.8, 13.0, 8.4, 3.9 Hz, 1H), 1.64–1.73 (m, 1H), 1.91 (td, *J* = 12.0, 3.0 Hz, 1H), 1.97 (d, *J* = 13.0 Hz, 1H), 2.04 (t,

$J = 11.4$ Hz, 1H), 2.30 (s, 9H), 2.35 (tt, $J = 12.3$, 3.9 Hz, 1H), 2.85 (d, $J = 11.4$ Hz, 1H), 3.11 (d, $J = 11.1$ Hz, 1H), 3.15 (d, $J = 6.8$ Hz, 2H), 5.31 (dt, $J = 15.5$, 6.8 Hz, 1H), 6.66 (d, $J = 15.5$ Hz, 1H), 6.87–6.97 (m, 6H), 7.02–7.08 (m, 6H) ppm. ^{13}C NMR (101 MHz, MeOD) δ 25.94, 30.83, 34.40, 51.42, 59.70, 63.12, 65.94, 67.43, 133.44, 134.24, 136.12, 141.91, 148.19, 149.63, 187.76 ppm. HRMS (ESI): $[\text{M} + \text{H}]^+$ calcd. for $\text{C}_{31}\text{H}_{36}\text{O}_2\text{N}$, 454.2739; found 454.2739.

4.3.14. (*E*)-1-[5,5,5-Tris(4-methoxyphenyl)pent-2-en-1-yl]piperidine-3-carboxylic acid, (*rac*-2m)

According to **GP2**: Ester *rac*-7m (42 mg, 0.080 mmol) with NaOH (0.4 mmol, 12 M in H_2O) was hydrolyzed to get the pure product. White solid (31 mg, 80%).

IR (KBr): $\tilde{\nu} = 3423$, 2025, 2997, 2934, 2834, 2054, 1709, 1607, 1580, 1508, 1462, 1441, 1389, 1294, 1249, 1181, 1119, 1034, 976, 824, 729, 628, 576 cm^{-1} . ^1H NMR (400 MHz, MeOD) δ 1.26 (qd, $J = 12.7$, 3.9 Hz, 1H), 1.36–1.52 (m, 1H), 1.52–1.63 (m, 2H), 1.93 (t, $J = 11.5$ Hz, 2H), 2.32 (tt, $J = 11.6$, 3.7 Hz, 1H), 2.51 (d, $J = 11.2$ Hz, 1H), 2.71 (dd, $J = 12.9$, 6.5 Hz, 1H), 2.89 (dd, $J = 12.9$, 5.5 Hz, 1H), 2.99 (d, $J = 11.4$ Hz, 1H), 3.26 (dd, $J = 14.5$, 6.5 Hz, 1H), 3.37 (dd, $J = 14.7$, 5.2 Hz, 1H), 3.76 (s, 9H), 5.35–5.54 (m, 2H), 6.76–6.84 (m, 6H), 7.02–7.13 (m, 6H) ppm. ^{13}C NMR (101 MHz, MeOD) δ 25.84, 29.43, 45.50, 46.38, 53.98, 55.74, 58.17, 62.30, 114.01, 129.68, 131.38, 133.63, 141.19, 159.02, 182.71 ppm. HRMS (ESI): $[\text{M} + \text{H}]^+$ calcd. for $\text{C}_{32}\text{H}_{38}\text{O}_5\text{N}$, 516.2744; found: 516.2743.

4.3.15. (*E*)-1-[5,5,5-Triphenylpent-2-en-1-yl]piperidine-3-carboxylic acid, (*rac*-2n)

According to **GP2**: The ester *rac*-7n (36 mg, 0.080 mmol) with NaOH (0.4 mmol, 12 M in H_2O) was hydrolyzed to get the pure product. White solid (30 mg, 88%).

IR (KBr): $\tilde{\nu} = 3424$, 3055, 3030, 2938, 2862, 1594, 1493, 1446, 1390, 1082, 1035, 1001, 977, 761, 703, 640, 614 cm^{-1} . ^1H NMR (400 MHz, MeOD) δ 1.16–1.31 (m, 1H), 1.37–1.49 (m, 1H), 1.57 (t, $J = 11.4$ Hz, 2H), 1.83–1.95 (m, 2H), 2.29 (tt, $J = 11.8$, 3.8 Hz, 1H), 2.49 (d, $J = 11.0$ Hz, 1H), 2.70 (dd, $J = 12.8$, 5.2 Hz, 1H), 2.82–2.94 (m, 2H), 3.38 (dd, $J = 14.6$, 5.0 Hz, 1H), 3.45 (dd, $J = 14.6$, 4.4 Hz, 1H), 5.37–5.46 (m, 2H), 7.14–7.28 (m, 15H) ppm. ^{13}C NMR (101 MHz, MeOD) δ 25.74, 29.34, 44.94, 46.37, 54.83, 57.70, 57.92, 62.17, 127.08, 128.82, 129.97, 130.43, 133.13, 148.46, 182.86 ppm. HRMS (ESI): $[\text{M} + \text{H}]^+$ calcd. for $\text{C}_{29}\text{H}_{32}\text{O}_2\text{N}$, 426.2427; found 426.2431.

4.3.16. (*E*)-1-[5,5-Bis(4-methoxyphenyl)pent-2-en-1-yl]piperidine-3-carboxylic acid, (*rac*-2o)

According to **GP2**: The ester *rac*-7o (74 mg, 0.17 mmol) with NaOH (0.85 mmol, 12 M in H_2O) was hydrolyzed to get the pure product. White solid (63 mg, 93%).

IR (KBr): $\tilde{\nu} = 3443$, 2996, 2934, 2835, 1713, 1608, 1582, 1509, 1463, 1442, 1302, 1247, 1176, 1145, 1034, 976, 863, 827, 767, 743, 668, 560 cm^{-1} . ^1H NMR (500 MHz, MeOD) δ 1.26 (qd, $J = 12.8$, 4.0 Hz, 1H), 1.43 (qt, $J = 13.1$, 4.0 Hz, 1H), 1.53–1.61 (m, 2H), 1.89–2.00 (m, 2H), 2.32 (tt, $J = 11.8$, 3.8 Hz, 1H), 2.50 (d, $J = 10.8$ Hz, 1H), 2.69–2.79 (m, 3H), 2.91 (dd, $J = 12.9$, 6.1 Hz, 1H), 3.00 (d, $J = 11.6$ Hz, 1H), 3.74 (s, 6H), 3.90 (t, $J = 7.9$ Hz, 1H), 5.43 (dt, $J = 15.4$, 6.6 Hz, 1H), 5.50 (dt, $J = 15.4$, 6.5 Hz, 1H), 6.79–6.83 (m, 4H), 7.11–7.16 (m, 4H) ppm. ^{13}C NMR (126 MHz, MeOD) δ 25.85, 29.42, 40.17, 46.34, 50.93, 53.84, 55.70, 55.73, 58.05, 62.08, 114.72, 114.73, 128.48, 129.76, 129.96, 134.88, 138.38, 138.60, 159.30, 159.31, 182.76 ppm. HRMS (ESI): $[\text{M} + \text{H}]^+$ calcd. for $\text{C}_{25}\text{H}_{32}\text{O}_4\text{N}$, 410.2325; found 410.2320.

4.3.17. (*E*)-1-[5,5-Diphenylpent-2-en-1-yl]piperidine-3-carboxylic acid, (*rac*-2p)

According to **GP2**: The ester *rac*-7p (38 mg, 0.10 mmol) with NaOH (0.5 mmol, 12 M in H_2O) was hydrolyzed to get the pure product. White solid (29 mg, 83%).

IR (KBr): $\tilde{\nu} = 3426$, 3057, 3025, 2939, 2865, 1583, 1494, 1450, 1388, 1309, 1147, 1072, 1032, 975, 958, 756, 737, 701, 669, 636, 583, 536, 487, 475 cm^{-1} . ^1H NMR (400 MHz, MeOD) δ 1.25 (qd, $J = 12.5$, 3.9 Hz, 1H), 1.42 (qt, $J = 12.6$, 3.6 Hz, 1H), 1.51–1.63 (m, 2H), 1.89 (t, $J = 11.5$ Hz, 1H), 1.92 (d, $J = 12.5$ Hz, 1H), 2.29 (tt, $J = 11.8$, 3.7 Hz, 1H), 2.51 (d, $J = 11.3$ Hz, 1H), 2.70–2.83 (m, 3H), 2.89 (dd, $J = 12.8$, 5.7 Hz, 1H), 2.95 (d, $J = 11.7$ Hz, 1H), 4.01 (t, $J = 7.9$ Hz, 1H), 5.40–5.57 (m, 2H), 7.10–7.17 (m, 2H), 7.22–7.29 (m, 8H) ppm. ^{13}C NMR (101 MHz, MeOD) δ 25.79, 29.35, 39.65, 46.32, 52.56, 53.85, 57.87, 61.96, 127.17, 127.20, 128.71, 128.91, 129.07, 129.40, 129.42, 134.52, 145.87, 145.99, 182.88 ppm. HRMS (ESI): $[\text{M} + \text{H}]^+$ calcd. for $\text{C}_{23}\text{H}_{28}\text{O}_2\text{N}$, 350.2114; found 350.2114.

4.3.18. (*E*)-1-[4,4,4-Tri(benzofuran-5-yl)but-2-en-1-yl]piperidine-3-carboxylic acid, (*rac*-6a)

According to **GP2**: The ester *rac*-21a (59 mg, 0.10 mmol) with NaOH (0.5 mmol, 12 M in H_2O) was hydrolyzed to get the pure product. White solid (35 mg, 66%).

IR (KBr): $\tilde{\nu} = 3434$, 3114, 2935, 2859, 2794, 1713, 1590, 1535, 1506, 1463, 1393, 1330, 154, 1188, 1130, 1109, 1030, 991, 885, 812, 767, 738, 667 cm^{-1} . ^1H NMR (400 MHz, MeOD) δ 1.28–1.41 (m, 1H), 1.55 (qt, $J = 12.2$, 3.3 Hz, 1H), 1.65–1.73 (m, 1H), 1.89–2.01 (m, 2H), 2.07 (t, $J = 11.4$ Hz, 1H), 2.36 (tt, $J = 11.8$, 3.8 Hz, 1H), 2.88 (d, $J = 11.3$ Hz, 1H), 3.16 (d, $J = 11.4$ Hz, 1H), 3.22 (dd, $J = 6.7$, 2.2 Hz, 2H), 5.40 (dt, $J = 15.5$, 6.8 Hz, 1H), 6.72 (d, $J = 2.1$ Hz, 3H), 6.90 (d, $J = 15.6$ Hz, 1H), 7.11 (dd, $J = 8.8$, 2.0 Hz, 3H), 7.28 (d, $J = 2.0$ Hz, 3H), 7.40 (d, $J = 8.7$ Hz, 3H), 7.70 (d, $J = 2.3$ Hz, 3H) ppm. ^{13}C NMR (101 MHz, MeOD) δ 30.85, 34.39, 51.43, 59.85, 63.11, 66.85, 67.41, 112.91, 116.14, 128.71, 133.35, 133.93, 147.78, 148.99, 151.79, 159.92, 187.76 ppm. HRMS (ESI): $[\text{M} + \text{H}]^+$ calcd. for $\text{C}_{34}\text{H}_{30}\text{O}_5\text{N}$, 532.2118; found 532.2116.

4.3.19. (*E*)-1-[4,4,4-Tris(benzo[d][1,3]dioxol-5-yl)but-2-en-1-yl]piperidine-3-carboxylic acid, (*rac*-6b)

According to **GP2**: The ester *rac*-21b (44 mg, 0.080 mmol) with NaOH (0.38 mmol, 12 M in H_2O) was hydrolyzed to get the pure product. White solid (37 mg, 91%).

IR (KBr): $\tilde{\nu} = 3444$, 2892, 2777, 1715, 1609, 1503, 1483, 1435, 1398, 1348, 1234, 1124, 1094, 1039, 934, 895, 868, 799, 734, 700, 661 cm^{-1} . ^1H NMR (500 MHz, MeOD) δ 1.33 (qd, $J = 12.9$, 4.1 Hz, 1H), 1.55 (qt, $J = 13.0$, 3.9 Hz, 1H), 1.65–1.74 (m, 1H), 1.92 (td, $J = 11.8$, 2.8 Hz, 1H), 1.98 (d, $J = 13.0$ Hz, 1H), 2.05 (t, $J = 11.4$ Hz, 1H), 2.36 (tt, $J = 11.7$, 3.7 Hz, 1H), 2.86 (d, $J = 11.3$ Hz, 1H), 3.10 (d, $J = 11.1$ Hz, 1H), 3.12–3.22 (m, 2H), 5.37 (dt, $J = 15.5$, 6.8 Hz, 1H), 5.92 (s, 6H), 6.51 (d, $J = 1.9$ Hz, 3H), 6.54 (dd, $J = 8.2$, 2.0 Hz, 3H), 6.58 (d, $J = 15.5$ Hz, 1H), 6.72 (d, $J = 8.2$ Hz, 3H) ppm. ^{13}C NMR (126 MHz, MeOD) δ 25.85, 29.40, 46.37, 54.72, 58.18, 61.25, 62.30, 102.43, 108.15, 111.74, 124.33, 128.85, 141.44, 142.79, 147.48, 148.67, 182.77 ppm. HRMS (ESI): $[\text{M} + \text{H}]^+$ calcd. for $\text{C}_{31}\text{H}_{30}\text{O}_8\text{N}$, 544.1965; found 544.1964.

4.3.20. (*E*)-1-[4,4,4-Tris(benzo[b]thiophen-5-yl)but-2-en-1-yl]piperidine-3-carboxylic acid, (*rac*-6c)

According to **GP2**: The ester *rac*-21c (55 mg, 0.090 mmol) with NaOH (0.45 mmol, 12 M in H_2O) was hydrolyzed to get the pure product. White solid (43 mg, 87%).

IR (KBr): $\tilde{\nu} = 3429$, 3069, 2926, 2854, 2361, 1708, 1596, 1499, 1465, 1436, 1411, 1323, 1263, 1202, 1154, 1089, 1050, 977, 896, 816, 792, 754, 699, 534, 510, 479, 419 cm^{-1} . ^1H NMR (500 MHz, MeOD) δ 1.34 (qd, $J = 12.9$, 4.1 Hz, 1H), 1.55 (qt, $J = 13.0$, 3.9 Hz, 1H), 1.66–1.71 (m, 1H), 1.93–2.00 (m, 2H), 2.08 (t, $J = 11.4$ Hz, 1H), 2.36 (tt, $J = 11.9$, 3.8 Hz, 1H), 2.88 (d, $J = 11.3$ Hz, 1H), 3.19 (d, $J = 11.4$ Hz, 1H), 3.21–3.29 (m, 2H), 5.44 (dt, $J = 15.5$, 6.8 Hz, 1H), 6.94 (d, $J = 15.6$ Hz, 1H), 7.20 (dd, $J = 8.6$, 1.9 Hz, 3H), 7.23 (d, $J = 5.4$ Hz, 3H), 7.51 (d, $J = 5.4$ Hz, 3H), 7.55 (d, $J = 1.9$ Hz, 3H), 7.81 (d, $J = 8.6$ Hz, 3H) ppm. ^{13}C NMR (126 MHz, MeOD) δ 25.90, 29.42,

46.47, 54.95, 58.13, 61.98, 62.40, 122.53, 125.32, 125.95, 127.78, 128.45, 129.65, 139.32, 140.99, 143.20, 143.91, 182.67 ppm. HRMS (ESI): [M+H]⁺ calcd. for C₃₄H₃₀O₂NS₃, 580.1432; found 580.1433.

4.3.21. Ethyl (E)-1-[4,4,4-tris(4-methoxyphenyl)but-2-en-1-yl]piperidine-3-carboxylate, (rac-7a)

According to **GP1**: *N,O*-acetal *rac*-**10** (115 mg, 0.500 mmol), TMSCl (65 μL, 0.50 mmol), alkyne **11a** (0.37 g, 1.0 mmol) and Cp₂ZrHCl (0.27 g, 1.0 mmol). The crude product was purified by flash chromatography with DCM/ MeOH (97:3). Yellow oil (120 mg, 45%).

The characterization data are in agreement with previously published data.²⁵

4.3.22. Ethyl (E)-1-[4-(benzo[d][1,3]dioxol-5-yl)-4,4-bis(4-methoxyphenyl)but-2-en-1-yl]piperidine-3-carboxylate, (rac-7b)

According to **GP2**: *N,O*-acetal *rac*-**10** (113 mg, 0.500 mmol), TMSCl (56 mg, 0.50 mmol, 65 μL), alkyne **11b** (390 mg, 1.00 mmol), Cp₂ZrHCl (275 mg, 1.00 mmol). The crude product was purified by flash chromatography with Et₂O/ PE/ MeOH (50:50:2). Yellow oil (78 mg, 29%).

IR (Film): $\tilde{\nu}$ = 2939, 2905, 2835, 2048, 1729, 1607, 1580, 1505, 1484, 1464, 1441, 1392, 1367, 1296, 1249, 1180, 1152, 1134, 1096, 1037, 994, 936, 862, 830, 809, 737, 703, 639 cm⁻¹. ¹H NMR (500 MHz, CD₂Cl₂) δ 1.20 (t, *J* = 7.1 Hz, 3H), 1.36–1.47 (m, 1H), 1.47–1.58 (m, 1H), 1.66–1.73 (m, 1H), 1.87 (dd, *J* = 12.9, 4.2 Hz, 1H), 1.99 (td, *J* = 11.0, 2.9 Hz, 1H), 2.16 (t, *J* = 10.4 Hz, 1H), 2.49 (tt, *J* = 10.3, 3.8 Hz, 1H), 2.70 (d, *J* = 11.3 Hz, 1H), 2.87–2.95 (m, 1H), 3.04–3.15 (m, 2H), 3.78 (s, 6H), 4.08 (qd, *J* = 7.1, 2.5 Hz, 2H), 5.27 (dt, *J* = 15.4, 6.5 Hz, 1H), 5.92 (s, 2H), 6.52 (d, *J* = 1.7 Hz, 1H), 6.53–6.55 (m, 1H), 6.56 (d, *J* = 1.9 Hz, 1H), 6.69 (d, *J* = 8.2 Hz, 1H), 6.77–6.82 (m, 4H), 6.97–7.01 (m, 4H) ppm. ¹³C NMR (126 MHz, CD₂Cl₂) δ 14.59, 25.16, 27.43, 42.45, 54.25, 55.72, 56.09, 59.66, 60.69, 61.75, 101.72, 107.53, 111.34, 113.41, 123.64, 129.17, 131.56, 139.06, 140.93, 141.43, 146.38, 147.77, 158.52, 174.52 ppm. HRMS (EI): [M]⁺ calcd. for C₃₄H₃₇NO₅, 543.2621; found: 543.2615.

4.3.23. Ethyl (E)-1-[4,4-bis(4-methoxyphenyl)-4-(thiazol-2-yl)but-2-en-1-yl]piperidine-3-carboxylate, (rac-7c)

According to **GP1**: *N,O*-acetal *rac*-**10** (130 mg, 0.560 mmol), TMSCl (62 mg, 0.56 mmol, 73 μL), alkyne **11c** (400 mg, 1.12 mmol), Cp₂ZrHCl (304 mg, 1.12 mmol). The crude product was purified by flash chromatography with DCM/ MeOH (98:2). Yellow oil (145 mg, 51%).

IR (Film): $\tilde{\nu}$ = 2938, 2835, 2801, 2761, 1728, 1607, 1580, 1509, 1464, 1442, 1410, 1367, 1350, 1297, 1251, 1180, 1152, 1134, 1096, 1033, 991, 888, 863, 829, 727 cm⁻¹. ¹H NMR (400 MHz, CD₂Cl₂) δ 1.20 (t, *J* = 7.1 Hz, 3H), 1.36–1.57 (m, 2H), 1.64–1.75 (m, 1H), 1.83–1.91 (m, 1H), 2.00 (td, *J* = 10.6, 2.3 Hz, 1H), 2.16 (t, *J* = 10.5 Hz, 1H), 2.49 (tt, *J* = 10.2, 3.8 Hz, 1H), 2.71 (d, *J* = 11.3 Hz, 1H), 2.93 (d, *J* = 11.1 Hz, 1H), 3.05–3.16 (m, 2H), 3.78 (s, 6H), 4.08 (qd, *J* = 7.1, 1.5 Hz, 2H), 5.29 (dt, *J* = 15.6, 6.5, 6.4 Hz, 1H), 6.72 (dt, *J* = 15.5, 1.4 Hz, 1H), 6.78–6.83 (m, 4H), 7.02–7.08 (m, 4H), 7.29 (d, *J* = 3.3 Hz, 1H), 7.80 (d, *J* = 3.3 Hz, 1H) ppm. ¹³C NMR (101 MHz, CD₂Cl₂) δ 14.60, 25.17, 27.42, 42.47, 54.27, 55.75, 56.15, 59.80, 60.68, 61.41, 113.55, 119.59, 130.78, 131.24, 137.78, 139.20, 143.17, 159.07, 174.51, 178.64 ppm. HRMS (ESI): [M+H]⁺ calcd. for C₂₉H₃₅O₄N₂S, 507.2311; found: 507.2312.

4.3.24. Ethyl (E)-1-[4,4-bis(4-methoxyphenyl)-4-(1-methyl-1H-imidazol-2-yl)but-2-en-1-yl]piperidine-3-carboxylate, (rac-7d)

According to **GP1**: *N,O*-acetal *rac*-**10** (195 mg, 0.850 mmol), TMSCl (95 mg, 0.85 mmol, 0.11 mL), alkyne **11d** (580 mg, 1.70 mmol) and Cp₂ZrHCl (460 mg, 1.70 mmol). The crude product was purified by flash chromatography with DCM/ MeOH (97:3). Yellow oil (250 mg, 58%).

IR (Film): $\tilde{\nu}$ = 2938, 2836, 2802, 2362, 2342, 1728, 1608, 1582, 1508, 1465, 1397, 1368, 1349, 1299, 1279, 1251, 1180, 1151, 1135, 1095, 1033, 981, 831, 744, 684 cm⁻¹. ¹H NMR (500 MHz, CD₂Cl₂) δ

1.20 (t, *J* = 7.1 Hz, 3H), 1.42 (qd, *J* = 11.6, 3.7 Hz, 1H), 1.45–1.57 (m, 1H), 1.64–1.73 (m, 1H), 1.82–1.91 (m, 1H), 1.99 (t, *J* = 10.8 Hz, 1H), 2.14 (t, *J* = 10.5 Hz, 1H), 2.49 (tt, *J* = 10.1, 3.8 Hz, 1H), 2.70 (d, *J* = 11.2 Hz, 1H), 2.91 (d, *J* = 10.3 Hz, 1H), 3.00 (s, 3H), 3.07 (dt, *J* = 6.6, 1.5 Hz, 2H), 3.78 (s, 6H), 4.07 (qd, *J* = 7.1, 2.6 Hz, 2H), 5.13 (dt, *J* = 15.7, 6.6 Hz, 1H), 6.60 (dt, *J* = 15.7, 1.4 Hz, 1H), 6.79–6.85 (m, 4H), 6.87 (d, *J* = 1.2 Hz, 1H), 6.92 (d, *J* = 1.2 Hz, 1H), 6.95–7.00 (m, 4H) ppm. ¹³C NMR (126 MHz, CD₂Cl₂) δ 14.59, 25.14, 27.39, 35.37, 42.45, 54.31, 55.74, 56.07, 56.75, 60.69, 61.40, 113.72, 113.75, 123.13, 126.70, 127.68, 130.83, 130.87, 135.99, 136.02, 138.80, 151.19, 158.82, 174.46 ppm. HRMS (ESI): [M+H]⁺ calcd. for C₃₀H₃₈O₄N₃, 504.2856; found: 504.2856.

4.3.25. Ethyl (E)-1-[4,4-bis(4-methoxyphenyl)-4-(thiophen-3-yl)but-2-en-1-yl]piperidine-3-carboxylate, (rac-7e)

According to **GP1**: *N,O*-acetal *rac*-**10** (115 mg, 0.500 mmol), TMSCl (56 mg, 0.50 mmol, 65 μL), alkyne **11e** (340 mg, 1.00 mmol) and Cp₂ZrHCl (275 mg, 1.00 mmol). The crude product was purified by flash chromatography with DCM/ MeOH (98:2). Yellow oil (125 mg, 49%).

IR (Film): $\tilde{\nu}$ = 2937, 2834, 2799, 2758, 1728, 1607, 1579, 1508, 1464, 1440, 1366, 1349, 1296, 1249, 1179, 1151, 1112, 1096, 1034, 991, 829, 795, 776, 670, 650 cm⁻¹. ¹H NMR (400 MHz, CD₂Cl₂) δ 1.20 (t, *J* = 7.1 Hz, 3H), 1.36–1.57 (m, 2H), 1.69 (dt, *J* = 11.9, 3.8 Hz, 1H), 1.87 (dd, *J* = 12.6, 4.1 Hz, 1H), 1.99 (t, *J* = 11.2 Hz, 1H), 2.15 (t, *J* = 10.5 Hz, 1H), 2.49 (tt, *J* = 10.1, 3.8 Hz, 1H), 2.70 (d, *J* = 11.2 Hz, 1H), 2.91 (d, *J* = 11.1 Hz, 1H), 3.02–3.13 (m, 2H), 3.78 (s, 6H), 4.08 (qd, *J* = 7.1, 1.9 Hz, 2H), 5.26 (dt, *J* = 15.5, 6.5 Hz, 1H), 6.50 (dd, *J* = 15.5, 1.4 Hz, 1H), 6.68 (dd, *J* = 3.0, 1.4 Hz, 1H), 6.78–6.82 (m, 4H), 6.84 (dd, *J* = 5.0, 1.4 Hz, 1H), 6.97–7.03 (m, 4H), 7.28 (dd, *J* = 5.1, 3.0 Hz, 1H) ppm. ¹³C NMR (101 MHz, CD₂Cl₂) δ 14.61, 25.17, 27.42, 42.46, 54.40, 55.73, 56.09, 57.27, 60.68, 61.66, 113.48, 123.78, 125.22, 128.93, 130.27, 131.01, 138.94, 140.31, 148.93, 158.61, 174.52 ppm. HRMS (EI): [M]⁺ calcd. for C₃₀H₃₅NO₄S, 505.2287; found: 505.2266.

4.3.26. Ethyl (E)-1-[4-(benzo[b]thiophen-5-yl)-4,4-bis(4-methoxyphenyl)but-2-en-1-yl]piperidine-3-carboxylate, (rac-7f)

According to **GP1**: *N,O*-acetal *rac*-**10** (113 mg, 0.500 mmol), TMSCl (56 mg, 0.50 mmol, 65 μL), alkyne **11f** (405 mg, 1.00 mmol), Cp₂ZrHCl (280 mg, 1.00 mmol). The crude product was purified by MPLC with Et₂O/ PE/ MeOH (50:50:1). Yellow oil (65 mg, 23%).

IR (Film): $\tilde{\nu}$ = 2938, 2834, 2799, 2758, 1728, 1606, 1578, 1508, 1463, 1438, 1411, 1367, 1296, 1249, 1180, 1151, 1094, 1033, 994, 893, 864, 830, 808, 754, 736, 703 cm⁻¹. ¹H NMR (400 MHz, CD₂Cl₂) δ 1.19 (t, *J* = 7.1 Hz, 3H), 1.38–1.58 (m, 2H), 1.63–1.76 (m, 1H), 1.84–1.91 (m, 1H), 2.01 (td, *J* = 10.6, 2.7 Hz, 1H), 2.18 (t, *J* = 10.5 Hz, 1H), 2.50 (tt, *J* = 10.1, 3.8 Hz, 1H), 2.71 (d, *J* = 11.3 Hz, 1H), 2.94 (d, *J* = 11.1 Hz, 1H), 3.07–3.17 (m, 2H), 3.79 (s, 6H), 4.08 (qd, *J* = 7.2, 2.0 Hz, 2H), 5.30 (dt, *J* = 15.5, 6.9 Hz, 1H), 6.65 (dd, *J* = 15.6, 1.4 Hz, 1H), 6.78–6.85 (m, 4H), 6.99–7.06 (m, 4H), 7.14 (dd, *J* = 8.6, 1.9 Hz, 1H), 7.23 (d, *J* = 5.4 Hz, 1H), 7.43 (d, *J* = 5.4 Hz, 1H), 7.50 (d, *J* = 1.9 Hz, 1H), 7.77 (d, *J* = 8.6 Hz, 1H) ppm. ¹³C NMR (101 MHz, CD₂Cl₂) δ 14.58, 25.18, 27.45, 42.47, 54.27, 55.73, 56.08, 59.88, 60.69, 61.77, 113.46, 121.88, 124.75, 125.14, 126.98, 127.88, 129.40, 131.67, 138.13, 139.07, 139.96, 141.04, 143.83, 158.53, 174.53 ppm. HRMS (EI): [M]⁺ calcd. for C₃₄H₃₇O₄NS, 555.2443; found: 555.2440.

4.3.27. Ethyl (S,E)-1-[4-(benzo[b]thiophen-5-yl)-4,4-bis(4-methoxyphenyl)but-2-en-1-yl]piperidine-3-carboxylate, [(S)-7f]

According to **GP1**: *N,O*-acetal (*S*)-**10** (113 mg, 0.500 mmol), TMSCl (56 mg, 0.50 mmol, 65 μL), alkyne **11f** (405 mg, 1.00 mmol), Cp₂ZrHCl (280 mg, 1.00 mmol). The crude product was purified by MPLC with Et₂O/ PE/ MeOH (50:50:1). Yellow oil (42 mg, 16%).

Analytical data correspond to those of *rac*-**7f** except [α]_D²⁰ = +12.6 (c = 0.6, DCM).

4.3.28. Ethyl (E)-1-(4,4-bis(4-methoxyphenyl)-4-[(trimethylsilyloxy)but-2-en-1-yl]piperidine-3-carboxylate, (rac-7g)

According to **GP1**: *N,O*-Acetal **rac-10** (250 mg, 1.15 mmol), TMSCl (125 mg, 1.15 mmol, 150 μ L), alkyne **11g** (340 mg, 1.00 mmol), Cp_2ZrHCl (275 mg, 1.00 mmol). The crude product was purified by flash chromatography with DCM/MeOH (99:1). Yellow oil (300 mg, 59%).

IR (Film): $\tilde{\nu}$ = 2952, 2906, 2836, 2801, 2058, 1731, 1684, 1608, 1583, 1508, 1465, 1442, 1368, 1350, 1302, 1250, 1173, 1151, 1095, 1034, 1009, 984, 926, 894, 839, 755, 684 cm^{-1} . ^1H NMR (500 MHz, CD_2Cl_2) δ -0.04 (s, 9H), 1.22 (t, J = 7.2 Hz, 3H), 1.35–1.47 (m, 1H), 1.47–1.60 (m, 1H), 1.65–1.74 (m, 1H), 1.85–1.92 (m, 1H), 1.98 (td, J = 10.9, 2.8 Hz, 1H), 2.12 (t, J = 10.6 Hz, 1H), 2.50 (tt, J = 10.4, 3.8 Hz, 1H), 2.71 (d, J = 11.2 Hz, 1H), 2.94 (d, J = 10.9 Hz, 1H), 3.04 (dd, J = 6.5, 1.4 Hz, 2H), 3.78 (s, 6H), 4.03–4.14 (m, 2H), 5.47 (dt, J = 15.3, 6.5 Hz, 1H), 6.20 (dt, J = 15.3, 1.4 Hz, 1H), 6.76–6.84 (m, 4H), 7.18–7.25 (m, 4H) ppm. ^{13}C NMR (126 MHz, CD_2Cl_2) δ 2.34, 14.61, 25.19, 27.43, 42.50, 54.29, 55.72, 56.17, 60.68, 61.19, 81.62, 113.41, 128.30, 129.12, 129.16, 139.72, 139.74, 139.78, 159.06, 159.08, 174.52 ppm. HRMS (ESI): $[\text{M} + \text{H}]^+$ calcd. for $\text{C}_{29}\text{H}_{42}\text{O}_5\text{NSi}$, 512.2826; found 512.2837.

4.3.29. Ethyl (E)-1-[4,4-bis(4-methoxyphenyl)but-2-en-1-yl]piperidine-3-carboxylate, (rac-7h)

According to **GP1**: *N,O*-acetal **rac-10** (115 mg, 0.500 mmol), TMSCl (56 mg, 0.50 mmol, 65 μ L), alkyne **11h** (260 mg, 1.00 mmol) and Cp_2ZrHCl (275 mg, 1.00 mmol). The crude product was purified by flash chromatography with DCM/MeOH (97:3). Yellow oil (210 mg, 56%).

IR (Film): $\tilde{\nu}$ = 2936, 2834, 2802, 2762, 1728, 1608, 1582, 1509, 1465, 1441, 1367, 1351, 1300, 1247, 1151, 1135, 1108, 1091, 1034, 979, 854, 830, 806, 772, 737 cm^{-1} . ^1H NMR (400 MHz, CD_2Cl_2) δ 1.22 (t, J = 7.1 Hz, 3H), 1.33–1.59 (m, 2H), 1.63–1.75 (m, 1H), 1.83–1.92 (m, 1H), 1.97 (td, J = 10.9, 2.9 Hz, 1H, 1H), 2.13 (t, J = 10.5 Hz, 1H), 2.50 (tt, J = 10.3, 3.8 Hz, 1H), 2.71 (d, J = 11.3 Hz, 1H), 2.93 (d, J = 11.5 Hz, 1H), 3.00 (d, J = 6.4 Hz, 2H), 3.76 (s, 6H), 4.08 (q, J = 7.1 Hz, 2H), 4.63 (d, J = 7.5 Hz, 1H), 5.42 (dtd, J = 15.3, 6.6, 1.3 Hz, 1H), 6.03 (ddt, J = 15.3, 7.5, 1.3 Hz, 1H), 6.79–6.86 (m, 4H), 7.04–7.11 (m, 4H) ppm. ^{13}C NMR (101 MHz, CD_2Cl_2) δ 14.61, 25.19, 27.49, 42.50, 52.75, 54.16, 55.74, 56.03, 60.67, 61.42, 114.23, 128.98, 129.80, 136.71, 136.90, 158.66, 174.57 ppm. HRMS (EI): $[\text{M}]^+$ calcd. for $\text{C}_{26}\text{H}_{33}\text{O}_4\text{N}$, 423.2410; found: 423.2404.

4.3.30. Ethyl (E)-1-[4,4,5-tris(4-methoxyphenyl)pent-2-en-1-yl]piperidine-3-carboxylate, (rac-7i)

According to **GP1**: *N,O*-acetal **rac-10** (160 mg, 0.700 mmol), TMSCl (78 mg, 0.70 mmol, 91 μ L), alkyne **11i** (535 mg, 1.40 mmol), Cp_2ZrHCl (380 mg, 1.40 mmol). The crude product was purified by flash chromatography with DCM/MeOH (98:2). Yellow oil (320 mg, 84%).

IR (Film): $\tilde{\nu}$ = 2935, 2834, 1728, 1609, 1580, 1509, 1464, 1367, 1299, 1248, 1179, 1151, 1035, 996, 830, 779 cm^{-1} . ^1H NMR (500 MHz, CD_2Cl_2) δ 1.22 (t, J = 7.1 Hz, 3H), 1.35–1.44 (m, 1H), 1.45–1.54 (m, 1H), 1.65–1.71 (m, 1H), 1.85–1.97 (m, 2H), 2.08 (t, J = 10.7 Hz, 1H), 2.47 (tt, J = 10.4, 3.9 Hz, 1H), 2.67 (d, J = 11.3 Hz, 1H), 2.92 (d, J = 10.7 Hz, 1H), 2.97 (d, J = 6.5 Hz, 2H), 3.45 (s, 2H), 3.71 (s, 3H), 3.78 (s, 6H), 4.04–4.14 (m, 2H), 4.97 (dt, J = 15.6, 6.6 Hz, 1H), 6.08 (dt, J = 15.7, 1.3 Hz, 1H), 6.60–6.63 (m, 2H), 6.64–6.67 (m, 2H), 6.77–6.83 (m, 4H), 7.04–7.09 (m, 4H) ppm. ^{13}C NMR (126 MHz, CD_2Cl_2) δ 14.62, 25.21, 27.52, 42.47, 46.99, 53.27, 54.15, 55.54, 55.68, 56.04, 60.68, 61.78, 113.21, 113.47, 128.55, 130.42, 132.46, 139.63, 140.56, 158.32, 158.52, 174.56 ppm. HRMS (ESI): $[\text{M} + \text{H}]^+$ calcd. for $\text{C}_{34}\text{H}_{42}\text{O}_5\text{N}$, 544.3057; found: 544.3067.

4.3.31. Ethyl (E)-1-[4,4-bis(4-methoxyphenyl)-5-phenylpent-2-en-1-yl]piperidine-3-carboxylate, (rac-7j)

According to **GP1**: *N,O*-acetal **rac-10** (135 mg, 0.600 mmol), TMSCl (67 mg, 0.60 mmol, 78 μ L), alkyne **11j** (420 mg, 1.20 mmol), Cp_2ZrHCl

(330 mg, 1.20 mmol). The crude product was purified by flash chromatography with DCM/MeOH (99:1). Yellow oil (255 mg, 83%).

IR (Film): $\tilde{\nu}$ = 2935, 1729, 1678, 1608, 1579, 1509, 1462, 1452, 1437, 1366, 1346, 1289, 1249, 1180, 1151, 1094, 1034, 994, 830, 804, 755, 739, 701, 663 cm^{-1} . ^1H NMR (400 MHz, CD_2Cl_2) δ 1.21 (t, J = 7.1 Hz, 3H), 1.32–1.54 (m, 2H), 1.61–1.73 (m, 1H), 1.84–1.98 (m, 2H), 2.07 (t, J = 10.6 Hz, 1H), 2.46 (tt, J = 10.3, 3.8 Hz, 1H), 2.67 (d, J = 11.3 Hz, 1H), 2.91 (d, J = 9.4 Hz, 1H), 2.97 (d, J = 6.5 Hz, 2H), 3.51 (s, 2H), 3.78 (s, 6H), 4.10 (q, J = 6.9 Hz, 2H), 4.98 (dt, J = 15.6, 6.6 Hz, 1H), 6.08 (dt, J = 15.6, 1.4 Hz, 1H), 6.73–6.77 (m, 2H), 6.77–6.82 (m, 4H), 7.04–7.13 (m, 7H) ppm. ^{13}C NMR (101 MHz, CD_2Cl_2) δ 14.62, 25.20, 27.51, 42.48, 47.90, 53.21, 54.15, 55.69, 56.04, 60.68, 61.75, 113.49, 126.46, 127.84, 128.70, 130.40, 131.62, 138.60, 139.55, 139.57, 140.39, 158.36, 174.57 ppm. HRMS (ESI): $[\text{M} + \text{H}]^+$ calcd. for $\text{C}_{33}\text{H}_{40}\text{O}_4\text{N}$, 514.2951; found 514.2956.

4.3.32. Ethyl (E)-1-(4,4,4-triphenylbut-2-en-1-yl)piperidine-3-carboxylate, (rac-7k)

According to **GP1**: *N,O*-acetal **rac-10** (160 mg, 0.700 mmol), TMSCl (78 mg, 0.70 mmol, 91 μ L), alkyne **11k** (395 mg, 1.40 mmol), Cp_2ZrHCl (380 mg, 1.40 mmol). The crude product was purified by flash chromatography with DCM/MeOH (99:1). Yellow oil (170 mg, 55%).

IR (Film): $\tilde{\nu}$ = 3055, 2940, 2803, 1732, 1683, 1653, 1558, 1540, 1507, 1490, 1445, 1368, 1311, 1221, 1178, 1151, 1091, 1031, 991, 754, 700, 668 cm^{-1} . ^1H NMR (400 MHz, CD_2Cl_2) δ 1.20 (t, J = 7.1 Hz, 3H), 1.36–1.57 (m, 2H), 1.65–1.74 (m, 1H), 1.82–1.91 (m, 1H), 2.00 (td, J = 10.8, 2.8 Hz, 1H), 2.16 (t, J = 10.5 Hz, 1H), 2.49 (tt, J = 10.2, 3.8 Hz, 1H), 2.70 (d, J = 11.4 Hz, 1H), 2.92 (d, J = 10.8 Hz, 1H), 3.06–3.17 (m, 2H), 4.07 (qd, J = 7.1, 2.2 Hz, 2H), 5.28 (dt, J = 15.6, 6.6 Hz, 1H), 6.64 (dt, J = 15.6, 1.4 Hz, 1H), 7.07–7.13 (m, 6H), 7.20–7.30 (m, 9H) ppm. ^{13}C NMR (101 MHz, CD_2Cl_2) δ 14.60, 25.18, 27.43, 42.48, 54.27, 56.11, 60.68, 61.23, 61.77, 126.78, 128.20, 129.89, 130.71, 140.47, 146.79, 174.53 ppm. HRMS (ESI): $[\text{M} + \text{H}]^+$ calcd. for $\text{C}_{30}\text{H}_{34}\text{O}_2\text{N}$, 440.2583; found 440.2585.

4.3.33. Ethyl (E)-1-(4,4,4-tri-*p*-tolylbut-2-en-1-yl)piperidine-3-carboxylate, (rac-7l)

According to **GP1**: *N,O*-Acetal **rac-10** (115 mg, 0.500 mmol), TMSCl (56 mg, 0.50 mmol, 65 μ L), alkyne **11l** (320 mg, 1.00 mmol), Cp_2ZrHCl (280 mg, 1.00 mmol). The crude product was purified by flash chromatography with DCM/MeOH (99:1). Yellow oil (115 mg, 48%).

IR (Film): $\tilde{\nu}$ = 2939, 2859, 2800, 2755, 1731, 1508, 1450, 1363, 1348, 1305, 1244, 1217, 1179, 1151, 1132, 1092, 1022, 989, 810, 784, 730 668 cm^{-1} . ^1H NMR (400 MHz, CD_2Cl_2) δ 1.20 (t, J = 7.1 Hz, 3H), 1.35–1.56 (m, 2H), 1.63–1.74 (m, 1H), 1.83–1.90 (m, 1H), 1.98 (td, J = 10.6, 2.6 Hz, 1H), 2.14 (t, J = 10.5 Hz, 1H), 2.32 (s, 9H), 2.48 (tt, J = 10.1, 3.8 Hz, 1H), 2.69 (d, J = 11.4 Hz, 1H), 2.91 (d, J = 12.2 Hz, 1H), 3.03–3.13 (m, 2H), 4.07 (qd, J = 7.1, 2.2 Hz, 2H), 5.23 (dt, J = 15.5, 6.5 Hz, 1H), 6.57 (dt, J = 15.5, 1.4 Hz, 1H), 6.93–6.98 (m, 6H), 7.04–7.10 (m, 6H) ppm. ^{13}C NMR (126 MHz, CD_2Cl_2) δ 14.58, 21.15, 25.18, 27.45, 42.48, 56.09, 60.17, 60.67, 61.80, 128.79, 129.20, 130.48, 136.27, 140.86, 144.06, 174.55 ppm. HRMS (EI): $[\text{M}]^+$ calcd. for $\text{C}_{33}\text{H}_{39}\text{O}_2\text{N}$, 481.2981; found 481.2986.

4.3.34. Ethyl (E)-1-[5,5,5-tris(4-methoxyphenyl)pent-2-en-1-yl]piperidine-3-carboxylate, (rac-7m)

According to **GP1**: *N,O*-acetal **rac-10** (260 mg, 1.15 mmol), TMSCl (125 mg, 1.15 mmol, 145 μ L), alkyne **11m** (380 mg, 1.15 mmol), Cp_2ZrHCl (290 mg, 1.15 mmol). The crude product was purified by flash chromatography with DCM/MeOH (98:2). Yellow oil (310 mg, 57%)

IR (Film): $\tilde{\nu}$ = 3035, 2935, 2834, 2802, 1728, 1607, 1579, 1508, 1463, 1441, 1367, 1295, 1249, 1181, 1151, 1133, 1119, 1035, 983, 824 cm^{-1} . ^1H NMR (400 MHz, CD_2Cl_2) δ 1.21 (t, J = 7.1 Hz, 3H), 1.22–1.50 (m, 2H), 1.53–1.66 (m, 2H), 1.67–1.78 (m, 1H), 1.79–1.89 (m, 1H), 1.97 (t, J = 10.6 Hz, 1H), 2.36–2.49 (m, 2H), 2.69–2.86 (m,

2H), 3.20–3.39 (m, 2H), 3.76 (s, 9H), 4.08 (q, $J = 7.1$ Hz, 2H), 5.37–5.42 (m, 2H), 6.74–6.82 (m, 6H), 7.06–7.14 (m, 6H) ppm. ^{13}C NMR (101 MHz, CD_2Cl_2) δ 14.58, 25.14, 27.59, 42.51, 44.80, 54.40, 55.07, 55.67, 55.90, 60.66, 61.55, 113.44, 130.76, 131.26, 140.47, 158.14, 174.59 ppm. HRMS (EI): $[\text{M}]^+$ calcd. for $\text{C}_{34}\text{H}_{41}\text{O}_5\text{N}$, 543.2985; found: 543.2998.

4.3.35. Ethyl (E)-1-[5,5,5-triphenylpent-2-en-1-yl]piperidine-3-carboxylate, (rac-7n)

According to **GP1**: *N,O*-acetal *rac*-**10** (140 mg, 0.640 mmol), TMSCl (72 mg, 0.64 mmol, 84 μL), alkyne **11n** (165 mg, 0.560 mmol) and Cp_2ZrHCl (180 mg, 0.640 mmol). The crude product was purified by flash chromatography with DCM/ MeOH (99:1). Yellow oil (180 mg, 71%).

IR (Film): $\tilde{\nu} = 3056, 3031, 2979, 2938, 2862, 2801, 2758, 1730, 1596, 1559, 1541, 1492, 1466, 1446, 1367, 1307, 1217, 1179, 1150, 1094, 1033, 982, 908, 862, 758, 702, 886, 640\text{ cm}^{-1}$. ^1H NMR (500 MHz, CD_2Cl_2) δ 1.22 (t, $J = 7.2$ Hz, 3H), 1.28–1.46 (m, 2H), 1.55–1.63 (m, 1H), 1.70 (td, $J = 11.1, 2.9$ Hz, 1H), 1.80–1.87 (m, 1H), 1.92 (t, $J = 10.7$ Hz, 1H), 2.35–2.45 (m, 2H), 2.69–2.81 (m, 3H), 3.33–3.46 (m, 2H), 4.08 (q, $J = 7.1$ Hz, 2H), 5.33–5.45 (m, 2H), 7.14–7.22 (m, 3H), 7.20–7.30 (m, 12H) ppm. ^{13}C NMR (126 MHz, CD_2Cl_2) δ 14.60, 25.16, 27.62, 42.55, 44.32, 53.73, 55.81, 57.12, 60.64, 61.47, 126.43, 128.28, 129.90, 130.76, 130.97, 147.81, 174.60 ppm. HRMS (ESI): $[\text{M}+\text{H}]^+$ calcd. for $\text{C}_{31}\text{H}_{36}\text{O}_2\text{N}$, 454.2740; found: 454.2741.

4.3.36. Ethyl (E)-1-[5,5-bis(4-methoxyphenyl)pent-2-en-1-yl]piperidine-3-carboxylate, (rac-7o)

According to **GP1**: *N,O*-Acetal *rac*-**10** (115 mg, 0.500 mmol), TMSCl (56 mg, 0.50 mmol, 65 μL), alkyne **11o** (280 mg, 1.00 mmol), Cp_2ZrHCl (275 mg, 1.00 mmol). The crude product was purified by flash chromatography with $\text{Et}_2\text{O}/\text{PE}/\text{MeOH}$ (50:50:1). Yellow oil (170 mg, 78%).

IR (Film): $\tilde{\nu} = 2936, 2835, 2802, 2754, 1729, 1609, 1583, 1510, 1464, 1444, 1367, 1301, 1247, 1177, 1151, 1134, 1094, 1035, 973, 861, 827, 766, 744\text{ cm}^{-1}$. ^1H NMR (400 MHz, CD_2Cl_2) δ 1.23 (t, $J = 7.1$ Hz, 3H), 1.29–1.48 (m, 2H), 1.56–1.64 (m, 1H), 1.75 (td, $J = 11.0, 2.9$ Hz, 1H), 1.81–1.88 (m, 1H), 1.98 (t, $J = 10.6$ Hz, 1H), 2.37–2.51 (m, 2H), 2.69–2.87 (m, 5H), 3.75 (s, 6H), 3.90 (t, $J = 7.9$ Hz, 1H), 4.04–4.14 (m, 2H), 5.37–5.50 (m, 2H), 6.77–6.83 (m, 4H), 7.10–7.15 (m, 4H) ppm. ^{13}C NMR (101 MHz, CD_2Cl_2) δ 14.61, 25.19, 27.62, 39.39, 42.55, 50.28, 53.65, 55.69, 55.85, 60.65, 61.41, 114.20, 129.18, 129.25, 129.41, 132.49, 137.74, 137.80, 158.51, 174.62. HRMS (EI): $[\text{M}]^+$ calcd. for $\text{C}_{27}\text{H}_{35}\text{O}_4\text{N}$, 437.2566; found 437.2554.

4.3.37. Ethyl (E)-1-(5,5-diphenylpent-2-en-1-yl)piperidine-3-carboxylate, (rac-7p)

According to **GP1**: *N,O*-Acetal *rac*-**10** (250 mg, 1.15 mmol), TMSCl (125 mg, 1.15 mmol, 150 μL), alkyne **11p** (210 mg, 1.00 mmol), Cp_2ZrHCl (275 mg, 1.00 mmol). The crude product was purified by flash chromatography with DCM/ MeOH (99:1). Yellow oil (265 mg, 70%).

IR (Film): $\tilde{\nu} = 3446, 3026, 2971, 2938, 2865, 2801, 2758, 1730, 1654, 1600, 1559, 1541, 1507, 1494, 1450, 1368, 1309, 1218, 1179, 1151, 1133, 1095, 1031, 972, 905, 864, 828, 796, 761, 753, 737, 700, 640, 632\text{ cm}^{-1}$. ^1H NMR (500 MHz, CD_2Cl_2) δ 1.24 (t, $J = 7.1$ Hz, 3H), 1.28–1.39 (m, 1H), 1.39–1.48 (m, 1H), 1.55–1.65 (m, 1H), 1.75 (td, $J = 11.1, 3.0$ Hz, 1H), 1.81–1.88 (m, 1H), 1.96 (t, $J = 10.7$ Hz, 1H), 2.42 (tt, $J = 10.5, 3.8$ Hz, 1H), 2.45–2.52 (m, 1H), 2.74–2.86 (m, 5H), 4.00 (t, $J = 7.9$ Hz, 1H), 4.09 (q, $J = 7.1$ Hz, 2H), 5.38–5.53 (m, 2H), 7.13–7.19 (m, 2H), 7.22–7.31 (m, 8H) ppm. ^{13}C NMR (126 MHz, CD_2Cl_2) δ 14.61, 25.18, 27.62, 38.99, 42.52, 51.97, 53.66, 55.73, 60.66, 61.34, 126.66, 128.41, 128.45, 128.92, 129.56, 132.27, 145.26, 145.29, 174.60 ppm. HRMS (ESI): $[\text{M}+\text{H}]^+$ calcd. for $\text{C}_{25}\text{H}_{32}\text{O}_2\text{N}$, 378.2427; found 378.2429.

4.3.38. Ethyl (E)-1-(4,4-dimethylpent-2-en-1-yl)piperidine-3-carboxylate, (rac-7q)

According to **GP1**: *N,O*-Acetal *rac*-**10** (120 mg, 0.500 mmol), TMSCl (56 mg, 0.50 mmol, 65 μL), alkyne **11q** (84 mg, 1.0 mmol, 0.13 mL), Cp_2ZrHCl (280 mg, 1.00 mmol). The crude product was purified by flash chromatography with DCM/ MeOH (99:1). Yellow oil (110 mg, 87%).

IR (Film): $\tilde{\nu} = 2953, 2867, 2799, 2758, 1733, 1466, 1393, 1365, 1306, 1270, 1220, 1179, 1151, 1135, 1095, 1032, 975, 905, 863\text{ cm}^{-1}$. ^1H NMR (400 MHz, CD_2Cl_2) δ 1.01 (s, 9H), 1.22 (t, $J = 7.1$ Hz, 3H), 1.34–1.59 (m, 2H), 1.63–1.75 (m, 1H), 1.83–1.99 (m, 2H), 2.09 (t, $J = 10.6$ Hz, 1H), 2.49 (tt, $J = 10.3, 3.8$ Hz, 1H), 2.70 (d, $J = 11.1$ Hz, 1H), 2.83–2.98 (m, 2H), 4.08 (q, $J = 7.1$ Hz, 2H), 5.36 (dt, $J = 15.6, 6.6$ Hz, 1H), 5.59 (dt, $J = 15.6, 1.3$ Hz, 1H) ppm. ^{13}C NMR (101 MHz, CD_2Cl_2) δ 14.58, 25.20, 27.59, 29.93, 33.37, 42.53, 55.91, 60.65, 61.84, 121.95, 145.51, 174.66 ppm. HRMS (ESI): $[\text{M}+\text{H}]^+$ calcd. for $\text{C}_{15}\text{H}_{27}\text{O}_2\text{N}$, 253.2042; found 253.2035.

4.3.39. Ethyl 1-(ethoxymethyl)piperidine-3-carboxylate, (rac-10)

K_2CO_3 (4.2 g, 30 mmol) was added to a solution of ethyl nipecotate (4.9 mL, 30 mmol) in EtOH (7.0 mL, 0.12 mol) at 0 °C. After 15 min paraformaldehyde (PFA) (0.98 g, 30 mmol) was added, and the mixture was stirred at 25 °C for 6 h. The mixture was diluted with Et_2O and filtered. The filtrate was concentrated under reduced pressure. The crude product was purified by distillation (Kugelrohr distillation) at 130 °C (0.4 Torr) to obtain the product *N,O*-acetal (*rac*-**10**) as a colorless oil (5.7 g, 88%).

The characterization data are in agreement with previously published data.²⁷

4.3.40. Ethyl (S)-1-(ethoxymethyl)piperidine-3-carboxylate, (S)-10

K_2CO_3 (2.8 g, 20 mmol) was added to a solution of ethyl nipecotate (3.2 mL, 20 mmol) in EtOH (7.0 mL, 0.12 mol) at 0 °C. After 15 min paraformaldehyde (PFA) (0.63 g, 20 mmol) was added, and the mixture was stirred at 25 °C for 6 h. The mixture was diluted with Et_2O and filtered. The filtrate was concentrated under reduced pressure. The crude product was purified by distillation (Kugelrohr distillation) at 130 °C (0.4 Torr) to obtain the product *N,O*-acetal (*rac*-**10**) as a colorless oil (3.1 g, 71%).

Analytical data corresponds to those of *rac*-**10** except $[\alpha]_{\text{D}}^{20} = +13.3$ ($c = 2.0$, DCM).

4.3.41. {[1,1-Bis(4-methoxyphenyl)prop-2-yn-1-yl]oxy}trimethylsilane, (11g)

Analogously to a literature procedure³² TMSCl (0.30 mL, 2.4 mmol) was added to a solution of alkyne **11g**²⁷ (0.46 g, 1.7 mmol), DMAP (11 mg, 0.090 mmol) and TEA (0.38 mL, 2.7 mmol) in THF (3 mL) at 25 °C. After stirring for 4 h at 25 °C the mixture was quenched with H_2O , extracted with Et_2O , dried with Na_2SO_4 and evaporated to dryness. The crude product was purified by flash chromatography with PE/ EtOAc (97:3). Colorless oil (510 mg, 88%).

IR (Film): $\tilde{\nu} = 3283, 3000, 2956, 2903, 2836, 1607, 1585, 1507, 1464, 1441, 1415, 1303, 1249, 1195, 1172, 1119, 1079, 1035, 1024, 1006, 936, 916, 883, 842, 806, 782, 756, 636\text{ cm}^{-1}$. ^1H NMR (500 MHz, CD_2Cl_2) δ 0.11 (s, 9H), 2.93 (s, 1H), 3.77 (s, 6H), 6.79–6.84 (m, 4H), 7.41–7.46 (m, 4H) ppm. ^{13}C NMR (126 MHz, CD_2Cl_2) δ 1.75, 55.77, 75.35, 76.94, 87.31, 113.71, 127.71, 139.29, 159.44 ppm. HRMS (EI): $[\text{M}]^+$ calcd. for $\text{C}_{20}\text{H}_{24}\text{O}_3\text{Si}$, 340.1495; found 340.1486.

4.3.42. 1,1'-(But-3-yne-1,1-diyl)bis(4-methoxybenzene), (11o)

TMS alkyne **14o** (0.72 g, 2.0 mmol) was dissolved in MeOH (5 mL), K_2CO_3 (0.43 g, 3.0 mmol). The crude product was purified by flash chromatography with PE/ Et_2O (95:5). White solid (503 mg, 94%).

MP: 73–75 °C. IR (KBr): $\tilde{\nu} = 3289, 3033, 3000, 2955, 2933, 2909, 2835, 1610, 1583, 1510, 1463, 1441, 1302, 1248, 1177, 1112, 1035, 955, 862, 826, 808, 773, 742, 639, 586, 567, 547\text{ cm}^{-1}$. ^1H NMR

(400 MHz, CD₂Cl₂) δ 1.97 (t, J = 2.6 Hz, 1H), 2.86 (dd, J = 7.7, 2.6 Hz, 2H), 3.77 (s, 6H), 4.13 (t, J = 7.7 Hz, 1H), 6.81–6.86 (m, 4H), 7.14–7.19 (m, 4H) ppm. ¹³C NMR (101 MHz, CD₂Cl₂) δ 26.08, 48.98, 55.73, 70.06, 83.60, 114.26, 129.19, 136.51, 158.83 ppm. HRMS (EI): [M]⁺ calcd. for C₁₈H₁₈O₂, 266.1307; found 266.1305.

4.3.43. But-3-yne-1,1-diylidibenzene, (11p)

TMS alkyne **14p** (0.39 g, 1.2 mmol) was dissolved in MeOH (5 mL), K₂CO₃ (0.27 g, 1.9 mmol). The crude product was purified by flash chromatography with PE/DCM (90:10). White solid (210 mg, 82%).

The characterization data are in agreement with previously published data.³⁵

4.3.44. [4,4-Bis(4-methoxyphenyl)but-1-yn-1-yl]trimethylsilane, (14o)

Dibromoethane (35 μ L, 0.40 mmol) was added to magnesium turnings (0.260 g, 18.4 mmol) in Et₂O (2 mL) and stirred at 25 °C for 15 min. A solution of 3-(trimethylsilyl)propargyl bromide (1.6 mL, 9.2 mmol) in Et₂O (8 mL) was added dropwise at 25 °C. This mixture was stirred at 25 °C for 1 h to obtain the Grignard reagent. To a solution of diaryl bromide **13o** (2.5 g, 8.0 mmol) and CuBr (0.18 g, 1.2 mmol) in toluene (8 mL) was added the previously prepared Grignard reagent at 0 °C. After 2 h at 40 °C the mixture was quenched with saturated aqueous NH₄Cl. The aqueous layer was separated and extracted three times with Et₂O. The combined organic fractions were washed with brine, dried with Na₂SO₄ and concentrated under reduced pressure. The crude product was purified by flash chromatography with PE/EtOAc (98:2). Yellow oil **14o** (750 mg, 28%), and yellow oil **15o** (650 mg, 24%).

IR (Film): $\tilde{\nu}$ = 3000, 2956, 2934, 2905, 2360, 2342, 2175, 1609, 1583, 1510, 1464, 1441, 1301, 1249, 1177, 1111, 1037, 1003, 842, 807, 760, 699, 668, 643 cm⁻¹. ¹H NMR (500 MHz, CD₂Cl₂) δ 0.08 (s, 9H), 2.86 (d, J = 7.4 Hz, 2H), 3.77 (s, 6H), 4.12 (t, J = 7.5 Hz, 1H), 6.81–6.86 (m, 4H), 7.14–7.18 (m, 4H) ppm. ¹³C NMR (126 MHz, CD₂Cl₂) δ 0.22, 27.70, 48.98, 55.74, 87.04, 106.47, 114.11, 129.40, 136.68, 158.79 ppm. HRMS (EI): [M]⁺ calcd. for C₂₁H₂₆O₂Si, 338.1702; found 338.1686.

4.3.45. (4,4-Diphenylbut-1-yn-1-yl)trimethylsilane, (14p)

Dibromoethane (14 μ L, 0.15 mmol) was added to magnesium turnings (170 mg, 6.90 mmol) in Et₂O (2 mL) and stirred at 25 °C for 15 min. A solution of 3-(trimethylsilyl)propargyl bromide (0.580 mL, 3.45 mmol) in Et₂O (5 mL) was added dropwise at 25 °C. This mixture was stirred at 25 °C for 1 h to obtain the Grignard reagent. To a solution of diaryl bromide **13p** (0.78 g, 3.0 mmol) and CuBr (65 mg, 0.45 mmol) in toluene (7 mL) was added the previously prepared Grignard reagent at 0 °C. After 2 h at 40 °C the mixture was quenched with saturated aqueous NH₄Cl. The aqueous layer was separated and extracted three times with Et₂O. The combined organic fractions were washed with brine, dried with Na₂SO₄ and concentrated under reduced pressure. The crude product was purified by flash chromatography with PE/EtOAc (98:2). White oil **14p** (490 mg, 58%), and yellow oil **15p** (50 mg, 6%).

The characterization data are in agreement with previously published data.³⁵

4.3.46. [1,1-Bis(4-methoxyphenyl)buta-2,3-dien-2-yl]trimethylsilane, (15o)

Dibromoethane (35 μ L, 0.40 mmol) was added to magnesium turnings (0.260 g, 18.4 mmol) in Et₂O (2 mL) and stirred at 25 °C for 15 min. A solution of 3-(trimethylsilyl)propargyl bromide (1.6 mL, 9.2 mmol) in Et₂O (8 mL) was added dropwise at 25 °C. This mixture was stirred at 25 °C for 1 h to obtain the Grignard reagent. To a solution of diaryl bromide **13o** (2.5 g, 8.0 mmol) and CuBr (0.18 g, 1.2 mmol) in toluene (8 mL) was added the previously prepared Grignard reagent at 0 °C. After 2 h at 40 °C the mixture was quenched with saturated aqueous NH₄Cl. The aqueous layer was separated and extracted three times with Et₂O. The combined organic fractions were washed with brine, dried with Na₂SO₄ and concentrated under

reduced pressure. The crude product was purified by flash chromatography with PE/EtOAc (98:2). Yellow oil **14o** (750 mg, 28%), and yellow oil **15o** (650 mg, 24%).

IR (Film): $\tilde{\nu}$ = 2998, 2957, 2898, 2873, 2834, 1919, 1607, 1579, 1508, 1463, 1437, 1300, 1247, 1172, 1105, 1037, 999, 840, 809, 785, 761, 745, 699, 633 cm⁻¹. ¹H NMR (400 MHz, CD₂Cl₂) δ 0.02 (s, 9H), 3.76 (s, 6H), 4.32 (d, J = 2.5 Hz, 2H), 4.58 (t, J = 2.6 Hz, 1H), 6.77–6.83 (m, 4H), 7.10–7.14 (m, 4H) ppm. ¹³C NMR (101 MHz, CD₂Cl₂) δ -1.08, 50.48, 55.69, 71.21, 100.33, 113.81, 130.21, 136.66, 158.60, 210.79 ppm. HRMS (EI): [M]⁺ calcd. for C₂₁H₂₆O₂Si, 338.1702; found 338.1689.

4.3.47. (1,1-Diphenylbuta-2,3-dien-2-yl)trimethylsilane, (15p)

Dibromoethane (14 μ L, 0.15 mmol) was added to magnesium turnings (170 mg, 6.90 mmol) in Et₂O (2 mL) and stirred at 25 °C for 15 min. A solution of 3-(trimethylsilyl)propargyl bromide (0.580 mL, 3.45 mmol) in Et₂O (5 mL) was added dropwise at 25 °C. This mixture was stirred at 25 °C for 1 h to obtain the Grignard reagent. To a solution of diaryl bromide **13p** (0.78 g, 3.0 mmol) and CuBr (65 mg, 0.45 mmol) in toluene (7 mL) was added the previously prepared Grignard reagent at 0 °C. After 2 h at 40 °C the mixture was quenched with saturated aqueous NH₄Cl. The aqueous layer was separated and extracted three times with Et₂O. The combined organic fractions were washed with brine, dried with Na₂SO₄ and concentrated under reduced pressure. The crude product was purified by flash chromatography with PE/EtOAc (98:2). White oil **14p** (490 mg, 58%), and yellow oil **15p** (50 mg, 6%).

IR (Film): $\tilde{\nu}$ = 3085, 3061, 3026, 2956, 2896, 1928, 1599, 1494, 1450, 1405, 1248, 1077, 1030, 1007, 997, 915, 840, 812, 755, 723, 699, 642, 629 cm⁻¹. ¹H NMR (500 MHz, CD₂Cl₂) δ 0.03 (s, 9H), 4.33 (d, J = 2.5 Hz, 2H), 4.68 (t, J = 2.5 Hz, 1H), 7.16–7.30 (m, 10H) ppm. ¹³C NMR (126 MHz, CD₂Cl₂) δ -1.11, 52.10, 71.29, 99.75, 126.77, 128.55, 129.41, 144.16, 210.97 ppm. HRMS (EI): [M]⁺ calcd. for C₁₉H₂₂Si, 278.1491; found 278.1490.

4.3.48. Tri(benzofuran-5-yl)methanol, (17a)

According to **GP3**: Dibromoethane (77 mg, 0.40 mmol, 35 μ L), magnesium turnings (700 mg, 28.0 mmol), 5-bromobenzofuran **16a** (5.15 g, 25.6 mmol, 3.27 mL) and diethyl carbonate (0.96 g, 8.0 mmol, 0.99 mL). The crude product was purified by flash chromatography with PE /EtOAc (75:15). White solid (2.05 g, 67%).

MP: 130–132 °C. IR (KBr): $\tilde{\nu}$ = 3548, 3450, 4144, 3112, 3056, 2956, 1883, 1718, 1592, 1534, 1508, 1464, 1437, 1330, 1264, 1253, 1186, 1126, 1107, 1095, 1030, 958, 885, 848, 811, 767, 737, 666, 581, 560 cm⁻¹. ¹H NMR (400 MHz, CD₂Cl₂) δ 3.12 (s, 1H), 6.72 (dd, J = 2.2, 0.6 Hz, 3H), 7.31 (dd, J = 8.7, 2.0 Hz, 3H), 7.45 (d, J = 8.7 Hz, 3H), 7.51 (d, J = 2.0 Hz, 3H), 7.65 (d, J = 2.2 Hz, 3H) ppm. ¹³C NMR (101 MHz, CD₂Cl₂) δ 82.96, 107.44, 111.09, 121.37, 125.36, 127.45, 143.21, 146.19, 154.61 ppm. HRMS (EI): [M]⁺ calcd. for C₂₅H₁₆O₄, 380.1049; found 380.1044.

4.3.49. Tris(benzo[d][1,3]dioxol-5-yl)methanol, (17b)

According to **GP3**: Dibromoethane (96 mg, 0.50 mmol, 45 μ L), magnesium turnings (895 mg, 36.0 mmol), 1-bromo-3,4-(methylenedioxy)benzene **16b** (6.77 g, 33.0 mmol, 4.08 mL) and diethyl carbonate (1.20 g, 10.0 mmol, 1.24 mL). The crude product was purified by flash chromatography with PE /Et₂O (60:40). White solid (3.51 g, 90%).

MP: 62–64 °C. IR (KBr): $\tilde{\nu}$ = 3521, 3073, 2963, 2890, 2776, 1855, 1610, 1502, 1484, 1436, 1348, 1236, 1123, 1095, 1079, 1038, 933, 895, 869, 842, 798, 730, 717, 665 cm⁻¹. ¹H NMR (400 MHz, CD₂Cl₂) δ 2.76 (s, 1H), 5.94 (s, 6H), 6.69 (dd, J = 8.2, 1.8 Hz, 3H), 6.73 (d, J = 8.1 Hz, 3H), 6.77 (d, J = 1.7 Hz, 3H) ppm. ¹³C NMR (101 MHz, CD₂Cl₂) δ 82.07, 101.89, 107.77, 109.15, 121.81, 141.82, 147.31, 147.99 ppm. HRMS (ESI): [M–H]⁺ calcd. for C₂₂H₁₅O₇, 391.0823; found 391.0821.

4.3.50. *Tris(benzo[b]thiophen-5-yl)methanol, (17c)*

According to **GP3**: Dibromoethane (78 mg, 0.42 mmol, 37 μ L), magnesium turnings (713 mg, 29.1 mmol), 5-bromobenzo[b]thiophene **16c** (5.96 g, 27.4 mmol) and diethyl carbonate (1.01 g, 8.30 mmol, 1.03 mL). The crude product was purified by flash chromatography with PE/ Acetone (80:20), and recrystallized from PE/ DCM. White solid (1.7 g, 48%).

MP: 90–92 °C. IR (KBr): $\tilde{\nu}$ = 3595, 3102, 1757, 1595, 1433, 1411, 1325, 1285, 1257, 1220, 1203, 1161, 1118, 1086, 1047, 1023, 960, 894, 854, 811, 793, 754, 720, 698 cm^{-1} . ^1H NMR (400 MHz, CD_2Cl_2) δ 3.16 (s, 1H), 7.27 (d, J = 5.4 Hz, 3H), 7.39 (dd, J = 8.6, 1.9 Hz, 3H), 7.47 (d, J = 5.4 Hz, 3H), 7.76 (d, J = 1.8 Hz, 3H), 7.85 (d, J = 8.5 Hz, 3H) ppm. ^{13}C NMR (101 MHz, CD_2Cl_2) δ 82.88, 122.53, 123.51, 124.78, 125.29, 127.55, 139.28, 139.90, 144.21 ppm. HRMS (EI): $[\text{M}]^+$ calcd. for $\text{C}_{25}\text{H}_{16}\text{OS}_3$, 428.0363; found 428.0357.

4.3.51. *5,5',5''-(Chloromethanetriyl)tris(benzofuran), (18a)*

According to **GP4**: Alcohol **17a** (0.86 g, 2.2 mmol), AcCl (1.41 g, 17.6 mmol, 1.28 mL) in toluene (6 mL). The crude product was used without any further purification. Red oil (0.87 g, 99%).

IR (KBr): $\tilde{\nu}$ = 1606, 1536, 1508, 1464, 1438, 1331, 1266, 1186, 1127, 1109, 1030, 953, 886, 845, 811, 766, 738, 668, 554 cm^{-1} . ^1H NMR (400 MHz, CD_2Cl_2) δ 6.70 (dd, J = 2.3, 0.9 Hz, 3H), 7.36 (dd, J = 2.1, 0.7 Hz, 3H), 7.39 (dd, J = 8.7, 2.1 Hz, 3H), 7.47 (dt, J = 8.7, 0.9 Hz, 3H), 7.67 (d, J = 2.2 Hz, 3H) ppm. ^{13}C NMR (101 MHz, CD_2Cl_2) δ 83.71, 107.52, 111.06, 123.18, 127.20, 127.46, 141.46, 146.48, 154.76 ppm. HRMS (ESI): $[\text{M}-\text{Cl}]^+$ calcd. for $\text{C}_{25}\text{H}_{15}\text{O}_3$, 363.1021; found 363.1015.

4.3.52. *5,5',5''-(Chloromethanetriyl)tris(benzo[d][1,3]dioxole), (18b)*

According to **GP4**: Alcohol **17b** (1.24 g, 3.00 mmol), AcCl (0.75 g, 9.0 mmol, 0.68 mL) in toluene (6 mL). The crude product was used without any further purification. Red solid (1.2 g, 97%).

IR (KBr): $\tilde{\nu}$ = 2889, 2774, 1869, 1736, 1648, 1604, 1502, 1484, 1473, 1444, 1350, 1245, 1193, 1111, 1098, 1033, 928, 862, 823, 789, 730, 693, 629 cm^{-1} . ^1H NMR (500 MHz, CDCl_3) δ 5.99 (s, 6H), 6.59 (dd, J = 8.2, 2.1 Hz, 3H), 6.69 (d, J = 8.2 Hz, 3H), 6.89 (d, J = 2.0 Hz, 3H) ppm. ^{13}C NMR (126 MHz, CDCl_3) δ 83.05, 101.55, 106.96, 110.84, 123.60, 139.55, 147.45, 147.53 ppm. HRMS (EI): $[\text{M}-\text{HCl}]^+$ calcd. for $\text{C}_{22}\text{H}_{14}\text{O}_6$, 374.0796; found 374.0812.

4.3.53. *5,5',5''-(Chloromethanetriyl)tris(benzo[b]thiophene), (18c)*

According to **GP4**: Alcohol **17c** (0.44 g, 1.0 mmol), AcCl (0.66 g, 8.0 mmol, 0.60 mL) in toluene (3 mL). The crude product was used without any further purification. Red solid (440 mg, 98%).

IR (KBr): $\tilde{\nu}$ = 3102, 1898, 1793, 1755, 1632, 1595, 1499, 1457, 1436, 1409, 1325, 1260, 1221, 1203, 1166, 1154, 1087, 1048, 967, 928, 896, 845, 835, 815, 791, 773, 754, 730, 717, 699, 601, 542, 526, 482 cm^{-1} . ^1H NMR (500 MHz, CDCl_3) δ 7.24 (d, J = 5.4 Hz, 3H), 7.46 (d, J = 5.4 Hz, 3H), 7.50 (dd, J = 8.7, 2.0 Hz, 3H), 7.57 (d, J = 1.9 Hz, 3H), 7.86 (d, J = 8.5 Hz, 3H) ppm. ^{13}C NMR (126 MHz, CDCl_3) δ 82.67, 122.06, 124.51, 124.75, 126.84, 127.31, 139.05, 139.39, 142.00 ppm. HRMS (EI): $[\text{M}-\text{Cl}]^+$ calcd. for $\text{C}_{25}\text{H}_{15}\text{S}_3$, 411.0335; found 411.0331.

4.3.54. *Trimethyl[3,3,3-tri(benzofuran-5-yl)prop-1-yn-1-yl]silane, (19a)*

Chloride **18a** (0.88 g, 2.1 mmol) in toluene (6 mL), ethynyltrimethylsilane (245 mg, 2.42 mmol, 350 μ L), nBuLi (2.31 mmol, 2.5 M in hexanes) in Et₂O (3 mL). The crude product was purified by flash chromatography with PE/ Et₂O (90:10). White solid (335 mg, 35%).

MP: 197–199 °C. IR (KBr): $\tilde{\nu}$ = 3137, 3106, 3058, 2961, 2154, 1879, 1749, 1608, 1533, 1464, 1438, 1328, 167, 1250, 1185, 1137, 1111, 1062, 1029, 919, 884, 844, 809, 772, 742, 667, 627 cm^{-1} . ^1H NMR (400 MHz, CD_2Cl_2) δ 0.26 (s, 9H), 6.67–6.72 (m, 3H), 7.36 (dd, J = 8.7, 2.0 Hz, 3H), 7.39–7.45 (m, 6H), 7.64 (d, J = 2.2 Hz, 3H) ppm. ^{13}C NMR (101 MHz, CD_2Cl_2) δ 0.21, 56.77, 90.13, 107.42, 111.17, 113.53,

122.27, 126.62, 127.55, 141.21, 146.15, 154.39 ppm. HRMS (EI): $[\text{M}]^+$ calcd. for $\text{C}_{30}\text{H}_{24}\text{O}_3\text{Si}$, 460.1495; found 460.1502.

4.3.55. *Trimethyl[3,3,3-tris(benzo[d][1,3]dioxol-5-yl)prop-1-yn-1-yl]silane, (19b)*

Chloride **18b** (0.52 g, 1.2 mmol) in toluene (3 mL), ethynyltrimethylsilane (140 mg, 1.38 mmol, 200 μ L), nBuLi (1.38 mmol, 2.5 M in hexanes) in Et₂O (2 mL). The crude product was purified by flash chromatography with PE/Acetone (80:20). Yellow oil (160 mg, 28%).

IR (Film): $\tilde{\nu}$ = 3073, 3012, 2960, 2896, 2778, 2586, 2162, 1857, 1738, 1612, 1504, 1484, 1435, 1352, 1236, 1124, 1095, 1040, 936, 896, 842, 800, 760, 737, 703, 662 cm^{-1} . ^1H NMR (400 MHz, CDCl_3) δ 0.21 (s, 9H), 5.95 (s, 6H), 6.65 (dd, J = 8.2, 1.9 Hz, 3H), 6.70 (d, J = 8.2 Hz, 3H), 6.80 (d, J = 1.9 Hz, 3H) ppm. ^{13}C NMR (101 MHz, CDCl_3) δ 0.14, 55.66, 89.41, 101.27, 107.50, 110.04, 111.95, 122.44, 139.46, 146.54, 147.56 ppm. HRMS (EI): $[\text{M}]^+$ calcd. for $\text{C}_{27}\text{H}_{24}\text{O}_6\text{Si}$, 472.1342; found 472.1331.

4.3.56. *5,5',5''-(Prop-2-yne-1,1,1-triyl)tris(benzofuran), (20a)*

TMS alkyne **19a** (0.34 g, 0.70 mmol), K₂CO₃ (0.450 g, 3.15 mmol) in THF/MeOH (1 mL/ 2 mL). The crude product was purified by flash chromatography with PE/ EA (98:2). White solid (210 mg, 77%).

MP: 173–175 °C. IR (KBr): $\tilde{\nu}$ = 3306, 3143, 3109, 1626, 1531, 1461, 1437, 1328, 1265, 1186, 1136, 1108, 1026, 883, 847, 814, 769, 741, 668, 640, 627 571 cm^{-1} . ^1H NMR (400 MHz, CD_2Cl_2) δ 2.89 (s, 1H), 6.70 (dd, J = 2.2, 0.5 Hz, 3H), 7.37 (dd, J = 8.8, 2.0 Hz, 3H), 7.41–7.49 (m, 6H), 7.65 (d, J = 2.2 Hz, 3H) ppm. ^{13}C NMR (101 MHz, CD_2Cl_2) δ 55.90, 74.23, 91.34, 107.41, 111.22, 122.31, 126.55, 127.63, 140.91, 146.22, 154.44 ppm. HRMS (EI): $[\text{M}]^+$ calcd. for $\text{C}_{27}\text{H}_{16}\text{O}_3$, 388.1099; found 388.1096.

4.3.57. *5,5',5''-(Prop-2-yne-1,1,1-triyl)tris(benzo[d][1,3]dioxole), (20b)*

TMS alkyne **19b** (0.15 g, 0.30 mmol), K₂CO₃ (190 mg, 1.35 mmol) in THF/MeOH (1 mL/ 2 mL). The crude product was purified by flash chromatography with PE/ EA (90:10). White solid (105 mg, 87%).

MP: 104–105 °C. IR (KBr): $\tilde{\nu}$ = 3284, 2888, 2775, 1610, 1504, 1480, 1434, 1349, 1235, 1123, 1093, 1038, 933, 894, 866, 840, 797, 727, 717, 661 cm^{-1} . ^1H NMR (400 MHz, CD_2Cl_2) δ 2.76 (s, 1H), 5.95 (s, 6H), 6.69 (dd, J = 8.2, 1.7 Hz, 3H), 6.72 (dd, J = 8.2, 0.6 Hz, 3H), 6.79 (dd, J = 1.7, 0.7 Hz, 3H) ppm. ^{13}C NMR (101 MHz, CD_2Cl_2) δ 55.20, 74.06, 90.19, 101.98, 107.82, 110.24, 122.78, 139.45, 147.19, 148.15 ppm. HRMS (EI): $[\text{M}]^+$ calcd. for $\text{C}_{24}\text{H}_{16}\text{O}_6$, 400.0947; found 400.0941.

4.3.58. *5,5',5''-(Prop-2-yne-1,1,1-triyl)tris(benzo[b]thiophene), (20c)*

Chloride **18c** (0.24 g, 0.50 mmol) in toluene (6 mL), ethynylmagnesium bromide (1.0 mmol, 0.5 M in THF) auf 25 °C 3 h. The crude product was purified by flash chromatography with PE/EtOAc (96:4). White solid (108 mg, 50%).

MP: 238–240 °C. IR (KBr): $\tilde{\nu}$ = 3287, 3073, 1896, 1800, 1757, 1633, 1593, 1543, 1498, 1434, 1410, 1311, 1260, 1210, 1164, 1088, 1048, 963, 944, 898, 856, 810, 794, 755, 721, 699, 679, 654, 640, 551, 532, 487 cm^{-1} . ^1H NMR (400 MHz, CD_2Cl_2) δ 2.91 (s, 1H), 7.25 (d, J = 5.4 Hz, 3H), 7.44 (dd, J = 8.6, 1.9 Hz, 3H), 7.47 (d, J = 5.4 Hz, 3H), 7.70 (d, J = 1.9 Hz, 3H), 7.84 (d, J = 8.6 Hz, 3H) ppm. ^{13}C NMR (101 MHz, CD_2Cl_2) δ 56.02, 74.65, 90.55, 122.61, 124.51, 124.73, 126.54, 127.61, 139.07, 140.08, 141.96 ppm. HRMS (EI): $[\text{M}]^+$ calcd. for $\text{C}_{27}\text{H}_{16}\text{S}_3$, 436.0414; found 436.0408.

4.3.59. *Ethyl (E)-1-[4,4,4-tri(benzofuran-5-yl)but-2-en-1-yl]piperidine-3-carboxylate, (rac-21a)*

According to **GP1**: *N,O*-Acetal *rac-10* (500 mg, 2.20 mmol), TMSCl (245 mg, 2.20 mmol, 285 μ L), alkyne **20a** (865 mg, 2.00 mmol), Cp₂ZrHCl (600 mg, 2.20 mmol). The crude product was purified by MPLC with DCM/ MeOH (99:1). Yellow oil (315 mg, 28%).

IR (Film): $\tilde{\nu}$ = 3108, 2940, 2859, 2802, 1727, 1613, 1535, 1463, 1439, 1368, 1315, 1267, 1220, 1185, 1152, 1135, 1109, 1030, 995, 886,

858, 810, 768, 738, 701, 666 cm^{-1} . ^1H NMR (400 MHz, CD_2Cl_2) δ 1.17 (t, $J = 7.1$ Hz, 3H), 1.40–1.48 (m, 1H), 1.53 (ddt, $J = 12.8, 9.8, 3.3$ Hz, 1H), 1.66–1.73 (m, 1H), 1.84–1.92 (m, 1H), 2.03 (td, $J = 10.6, 2.7$ Hz, 1H), 2.20 (t, $J = 10.5$ Hz, 1H), 2.50 (tt, $J = 10.0, 3.8$ Hz, 1H), 2.73 (d, $J = 11.0$ Hz, 1H), 2.96 (d, $J = 11.0$ Hz, 1H), 3.16 (d, $J = 6.5$ Hz, 2H), 4.01–4.13 (m, 2H), 5.37 (dt, $J = 15.7, 6.6$ Hz, 1H), 6.69 (dd, $J = 2.3, 0.9$ Hz, 3H), 6.80 (d, $J = 15.6$ Hz, 1H), 7.15 (dd, $J = 8.8, 2.1$ Hz, 3H), 7.32 (d, $J = 2.0$ Hz, 3H), 7.41 (d, $J = 8.8$ Hz, 3H), 7.63 (d, $J = 2.2$ Hz, 3H) ppm. ^{13}C NMR (101 MHz, CD_2Cl_2) δ 14.55, 25.18, 27.45, 42.46, 54.34, 56.05, 60.70, 61.11, 61.78, 107.46, 110.75, 123.16, 127.42, 127.90, 129.66, 141.76, 142.22, 145.87, 154.05, 174.54 ppm. HRMS (ESI): $[\text{M} + \text{H}]^+$ calcd. for $\text{C}_{36}\text{H}_{34}\text{O}_5\text{N}$, 560.2431; found 560.2429.

4.3.60. Ethyl (E)-1-[4,4-tris(benzo[d][1,3]dioxol-5-yl)but-2-en-1-yl]piperidine-3-carboxylate, (rac-21b)

According to **GP1**: *N,O*-Acetal **rac-10** (250 mg, 1.10 mmol), TMSCl (125 mg, 1.10 mmol, 145 μL), alkyne **20b** (410 mg, 1.00 mmol), Cp_2ZrHCl (300 mg, 1.10 mmol). The crude product was purified by MPLC with DCM/ MeOH (98:2). Yellow oil (90 mg, 16%).

IR (Film): $\tilde{\nu} = 2940, 2898, 2801, 1728, 1503, 1483, 1435, 1350, 134, 1182, 1152, 1130, 1094, 1039, 995, 935, 895, 869, 799, 736, 701, 660$ cm^{-1} . ^1H NMR (500 MHz, CD_2Cl_2) δ 1.20 (t, $J = 7.1$ Hz, 3H), 1.37–1.46 (m, 1H), 1.46–1.56 (m, 1H), 1.66–1.73 (m, 1H), 1.83–1.91 (m, 1H), 1.96–2.03 (m, 1H), 2.16 (t, $J = 10.5$ Hz, 1H), 2.49 (tt, $J = 10.2, 3.9$ Hz, 1H), 2.69 (d, $J = 11.6$ Hz, 1H), 2.91 (d, $J = 9.9$ Hz, 1H), 3.03–3.15 (m, 2H), 4.04–4.11 (m, 2H), 5.31 (dt, $J = 15.5, 6.5$ Hz, 1H), 5.93 (s, 6H), 6.48 (d, $J = 15.5$ Hz, 1H), 6.55 (dd, $J = 8.2, 1.9$ Hz, 3H), 6.58 (d, $J = 1.9$ Hz, 3H), 6.70 (d, $J = 8.2$ Hz, 3H) ppm. ^{13}C NMR (126 MHz, CD_2Cl_2) δ 14.56, 25.15, 27.42, 42.44, 54.29, 56.11, 60.49, 60.69, 61.72, 101.77, 107.59, 111.35, 123.70, 129.66, 140.48, 140.90, 146.54, 147.81, 174.52 ppm. HRMS (EI): $[\text{M}]^+$ calcd. for $\text{C}_{33}\text{H}_{33}\text{O}_8\text{N}$, 571.2206; found 571.2198.

4.3.61. Ethyl (E)-1-[4,4-tris(benzo[b]thiophen-5-yl)but-2-en-1-yl]piperidine-3-carboxylate, (rac-21c)

According to **GP1**: *N,O*-Acetal **rac-10** (330 mg, 1.49 mmol), TMSCl (165 mg, 1.49 mmol, 195 μL), alkyne **20c** (620 mg, 1.35 mmol), Cp_2ZrHCl (405 mg, 1.49 mmol). The crude product was purified by MPLC with DCM/ MeOH (99:1). Yellow oil (160 mg, 20%).

IR (Film): $\tilde{\nu} = 3102, 3073, 2977, 2939, 2865, 2801, 2758, 1726, 1598, 1499, 1465, 1437, 1413, 1367, 1346, 1309, 1263, 1216, 1180, 1152, 1091, 1049, 994, 953, 897, 817, 793, 755, 710, 699$ cm^{-1} . ^1H NMR (500 MHz, CD_2Cl_2) δ 1.16 (t, $J = 7.1$ Hz, 3H), 1.39–1.56 (m, 2H), 1.65–1.74 (m, 1H), 1.84–1.91 (m, 1H), 2.04 (td, $J = 10.7, 2.8$ Hz, 1H), 2.21 (t, $J = 10.5$ Hz, 1H), 2.50 (tt, $J = 10.1, 3.8$ Hz, 1H), 2.73 (d, $J = 11.1$ Hz, 1H), 2.96 (d, $J = 9.8$ Hz, 1H), 3.17 (d, $J = 6.5$ Hz, 2H), 4.03–4.10 (m, 2H), 5.40 (dt, $J = 15.6, 6.5$ Hz, 1H), 6.81 (d, $J = 15.6$ Hz, 1H), 7.21–7.25 (m, 6H), 7.44 (d, $J = 5.4$ Hz, 3H), 7.59 (d, $J = 1.9$ Hz, 3H), 7.80 (d, $J = 8.6$ Hz, 3H) ppm. ^{13}C NMR (126 MHz, CD_2Cl_2) δ 14.55, 25.20, 27.45, 42.48, 54.35, 56.07, 60.70, 61.20, 61.77, 122.07, 124.82, 125.41, 127.11, 128.03, 130.31, 138.35, 140.05, 140.89, 143.33, 174.54 ppm. HRMS (EI): $[\text{M}]^+$ calcd. for $\text{C}_{36}\text{H}_{33}\text{O}_2\text{NS}_3$, 607.1673; found 607.1663.

4.4. Biological evaluation

4.4.1. MS binding assays

The MS Binding Assays were performed with mGAT1 membrane preparations obtained from a stable HEK293 cell line and NO711 as non-labeled marker in competitive binding experiments as described previously.⁴⁸

4.4.2. GABA uptake assay

The [^3H]GABA uptake assays were performed in a 96-well plate format with intact HEK293 cells stably expressing mGAT1, mGAT2, mGAT3, mGAT4 as described earlier.⁴⁷

Funding

This research did not receive any specific grant from funding agencies in the public, commercial, or not-for-profit sectors

Appendix A. Supplementary data

Supplementary data to this article can be found online at <https://doi.org/10.1016/j.bmc.2018.11.002>.

References

- Krogsgaard-Larsen P. GABA synaptic mechanisms: stereochemical and conformational requirements. *Med Res Rev.* 1988;8:27–56. <https://doi.org/10.1002/med.2610080103>.
- Lancot KL, Herrmann N, Mazzotta P, Khan LR, Ingber N. GABAergic function in Alzheimer's disease: evidence for dysfunction and potential as a therapeutic target for the treatment of behavioural and psychological symptoms of dementia. *Can J Psychiatr.* 2004;49:439–453. <https://doi.org/10.1177/070674370404900704>.
- Kalueff AV, Nutt DJ. Role of GABA in anxiety and depression. *Depr Anx.* 2007;24:495–517. <https://doi.org/10.1002/da.20262>.
- Treiman DM. GABAergic mechanisms in epilepsy. *Epilepsia.* 2001;42(Suppl 3):8–12. <https://doi.org/10.1046/j.1528-1157.2001.042suppl.3008.x>.
- Dalby NO. Inhibition of gamma-aminobutyric acid uptake: anatomy, physiology and effects against epileptic seizures. *Eur J Pharmacol.* 2003;479:127–137. <https://doi.org/10.1016/j.ejphar.2003.08.063>.
- Cherubini E. Generating diversity at GABAergic synapses. *Trends Neurosci.* 2001;24:155–162. [https://doi.org/10.1016/S0166-2236\(00\)01724-0](https://doi.org/10.1016/S0166-2236(00)01724-0).
- Borden LA. GABA transporter heterogeneity: pharmacology and cellular localization. *Neurochem Int.* 1996;29:335–356. [https://doi.org/10.1016/0197-0186\(95\)00158-1](https://doi.org/10.1016/0197-0186(95)00158-1).
- Conti F, Minelli A, Melone M. GABA transporters in the mammalian cerebral cortex: localization, development and pathological implications. *Brain Res Rev.* 2004;45:196–212. <https://doi.org/10.1016/j.brainresrev.2004.03.003>.
- Masson J, Sagne C, Hamon M, El Mestikawy S. Neurotransmitter transporters in the central nervous system. *Pharmacol Rev.* 1999;51:439–464.
- Kristensen AS, Andersen J, Jorgensen TN, Sorensen L, Eriksen J, Loland CJ, Stromgaard K, Gether U. SLC6 neurotransmitter transporters: structure, function, and regulation. *Pharmacol Rev.* 2011;63:585–640. <https://doi.org/10.1124/pr.108.000869>.
- Madsen KK, Clausen RP, Larsson OM, Krogsgaard-Larsen P, Schousboe A, White HS. Synaptic and extrasynaptic GABA transporters as targets for anti-epileptic drugs. *J Neurochem.* 2009;109(Suppl 1):139–144. <https://doi.org/10.1111/j.1471-4159.2009.05982.x>.
- Palacin M, Estevez R, Bertran J, Zorzano A. Molecular biology of mammalian plasma membrane amino acid transporters. *Physiol Rev.* 1998;78:969–1054. <https://doi.org/10.1152/physrev.1998.78.4.969>.
- Minelli A, DeBiasi S, Brecha NC, Zuccarello LV, Conti F. GAT-3, a high-affinity GABA plasma membrane transporter, is localized to astrocytic processes, and it is not confined to the vicinity of GABAergic synapses in the cerebral cortex. *J Neurosci.* 1996;16:6255–6264. <https://doi.org/10.1523/JNEUROSCI.16-19-06255.1996>.
- Jin XT, Galvan A, Wichmann T, Smith Y. Localization and Function of GABA Transporters GAT-1 and GAT-3 in the Basal Ganglia. *Front Syst Neurosci.* 2011;5:63. <https://doi.org/10.3389/fnsys.2011.00063>.
- Zhou Y, Holmseth S, Hua R, et al. The betaine-GABA transporter (BGT1, slc6a12) is predominantly expressed in the liver and at lower levels in the kidneys and at the brain surface. *Am J Physiol Renal Physiol.* 2012;302:F316–328. <https://doi.org/10.1152/ajprenal.00464.2011>.
- Kempson SA, Zhou Y, Danbolt NC. The betaine/GABA transporter and betaine: roles in brain, kidney, and liver. *Front Physiol.* 2014;5:159. <https://doi.org/10.3389/fphys.2014.00159>.
- Leppik IE. Tiagabine: the safety landscape. *Epilepsia.* 1995;36(Suppl 6):S10–S13. <https://doi.org/10.1111/j.1528-1157.1995.tb06009.x>.
- Nielsen EB, Suzdak PD, Andersen KE, Knutsen LJ, Sonnewald U, Braestrup C. Characterization of tiagabine (NO-328), a new potent and selective GABA uptake inhibitor. *Eur J Pharmacol.* 1991;196:257–266. [https://doi.org/10.1016/0014-2999\(91\)90438-V](https://doi.org/10.1016/0014-2999(91)90438-V).
- Andersen KE, Braestrup C, Groenwald FC, Joergensen AS, Nielsen EB, Sonnewald U, Soerensen PO, Suzdak PD, Knutsen LJS. The synthesis of novel GABA uptake inhibitors. 1. Elucidation of the structure-activity studies leading to the choice of (R)-1-[4,4-bis(3-methyl-2-thienyl)-3-butenyl]-3-piperidinecarboxylic acid (Tiagabine) as an anticonvulsant drug candidate. *J Med Chem.* 1993;36:1716–1725. <https://doi.org/10.1021/jm00064a005>.
- Steffan T, Renukappa-Gutke T, Höfner G, Wanner KT. Design, synthesis and SAR studies of GABA uptake inhibitors derived from 2-substituted pyrrolidine-2-yl-acetic acids. *Bioorg Med Chem.* 2015;23:1284–1306. <https://doi.org/10.1016/j.bmc.2015.01.035>.
- Hellenbrand T, Höfner G, Wein T, Wanner KT. Synthesis of 4-substituted piperonic acid derivatives and their evaluation as potential GABA uptake inhibitors. *Bioorg Med Chem.* 2016;24:2072–2096. <https://doi.org/10.1016/j.bmc.2016.03.038>.
- Vogensen SB, Jorgensen L, Madsen KK, et al. Structure activity relationship of selective GABA uptake inhibitors. *Bioorg Med Chem.* 2015;23:2480–2488. <https://doi.org/10.1016/j.bmc.2015.03.060>.

23. Vogensen SB, Jorgensen L, Madsen KK, et al. Selective mGAT2 (BGT-1) GABA uptake inhibitors: design, synthesis, and pharmacological characterization. *J Med Chem.* 2013;56:2160–2164. <https://doi.org/10.1021/jm301872x>.
24. Kersch-Hack S, Renukappa-Gutke T, Höfner G, Wanner KT. Synthesis and biological evaluation of a series of N-alkylated imidazole alkanolic acids as mGAT3 selective GABA uptake inhibitors. *Eur J Med Chem.* 2016;124:852–880. <https://doi.org/10.1016/j.ejmech.2016.09.012>.
25. Pabel J, Faust M, Prehn C, Wörlein B, Allmendinger L, Höfner G, Wanner KT. Development of an (S)-1-([2-(tris(4-methoxyphenyl)methoxy)ethyl]piperidine-3-carboxylic acid [(S)-SNAP-5114] carba analogue inhibitor for murine gamma-aminobutyric acid transporter type 4. *ChemMedChem.* 2012;7:1245–1255. <https://doi.org/10.1002/cmdc.201200126>.
26. Dhar TGM, Borden LA, Tyagarajan S, et al. Design, synthesis and evaluation of substituted triarylnepepotic acid derivatives as GABA uptake inhibitors: identification of a ligand with moderate affinity and selectivity for the cloned human GABA transporter GAT-3. *J Med Chem.* 1994;37:2334–2342. <https://doi.org/10.1021/jm00041a012>.
27. Toth K, Höfner G, Wanner KT. Synthesis and biological evaluation of novel N-substituted nipecotic acid derivatives with an alkyne spacer as GABA uptake inhibitors. *Bioorg Med Chem.* 2018;26:3668–3687. <https://doi.org/10.1016/j.bmc.2018.05.049>.
28. Damgaard M, Al-Khawaja A, Vogensen SB, et al. Identification of the first highly subtype-selective inhibitor of human GABA transporter GAT3. *ACS Chem Neurosci.* 2015;6:1591–1599. <https://doi.org/10.1021/acschemneuro.5b0015>.
29. Schwartz J, Labinger JA. Hydrozirconation: a new transition metal reagent for organic synthesis. *Angew Chem Int Ed.* 1976;15:333–340. <https://doi.org/10.1002/ange.197603211>.
30. Hansmann MM, Melaimi M, Bertrand G. Crystalline monomeric allenyl/propargyl radical. *J Am Chem Soc.* 2017;139:15620–15623. <https://doi.org/10.1021/jacs.7b09622>.
31. Nösel P, Moghimi S, Hendrich C, et al. Oxidative gold catalysis meets photochemistry – synthesis of benzo[a]fluorenones from diynes. *Adv Synth Catal.* 2014;356:3755–3760. <https://doi.org/10.1002/adsc.201400969>.
32. Arai S, Sato T, Koike Y, Hayashi M, Nishida A. Palladium-catalyzed cyanation of carbon-carbon triple bonds under aerobic conditions. *Angew Chem Int Ed.* 2009;48:4528–4531. <https://doi.org/10.1002/anie.200900030>.
33. Eckenberg P, Groth U, Köhler T. Stereoselective synthesis of steroids and related compounds, IV. Addition of cerium reagents derived from (Trimethylsilyl)propargyl bromide to aldehydes. *Liebigs An Chem.* 1994;1994:673–677. <https://doi.org/10.1002/jlac.199419940707>.
34. Yu T, Ma S. Allenes in catalytic asymmetric synthesis and natural product syntheses. *Angew Chem Int Ed.* 2012;51:3074–3112. <https://doi.org/10.1002/anie.201101460>.
35. Schaarschmidt M, Wanner KT. Synthesis of allene substituted nipecotic acids by allenylation of terminal alkynes. *J Org Chem.* 2017;82:8371–8388. <https://doi.org/10.1021/acs.joc.7b00630>.
36. Millot N, Piazza C, Avolio S, Knochel P. Aminomethylation of functionalized organozinc reagents and grignard reagents using immonium trifluoroacetates. *Synthesis.* 2000:941–948. <https://doi.org/10.1055/s-2000-6307>.
37. Barl NM, Sansiaume-Dagoussset E, Monzón G, Wagner AJ, Knochel P. Preparation and reactions of heteroarylmethylzinc reagents. *Org Lett.* 2014;16:2422–2425. <https://doi.org/10.1021/ol500790p>.
38. Cooper MS, Heaney H. Mannich reactions of aryl-trialkylstannanes using preformed dialkyl-methyleneiminium salts. *Tetrahedron Lett.* 1986;27:5011–5014. [https://doi.org/10.1016/S0040-4039\(00\)85120-5](https://doi.org/10.1016/S0040-4039(00)85120-5).
39. Suga S, Okajima M, Yoshida J-I. Reaction of an electrogenerated 'iminium cation pool' with organometallic reagents. Direct oxidative α -alkylation and -arylation of amine derivatives. *Tetrahedron Lett.* 2001;42:2173–2176. [https://doi.org/10.1016/S0040-4039\(01\)00128-9](https://doi.org/10.1016/S0040-4039(01)00128-9).
40. Werner V, Ellwart M, Wagner AJ, Knochel P. Preparation of tertiary amines by the reaction of iminium ions derived from unsymmetrical aminals with zinc and magnesium organometallics. *Org Lett.* 2015;17:2026–2029. <https://doi.org/10.1021/acs.orglett.5b00801>.
41. Saito A, Imura K, Hayashi M, Hanzawa Y. Catalytic addition of alkenylzirconocene chloride to 3,4-dihydroisoquinoline and its enantioselective reaction. *Tetrahedron Lett.* 2009;50:587–589. <https://doi.org/10.1016/j.tetlet.2008.11.078>.
42. Karlsson S, Hallberg A, Gronowitz S. Hydrozirconation of (E)-3-methoxy-1-phenyl-1-propene and (E)-3-phenyl-2-propenol. *J Organomet Chem.* 1991;403:133–144. [https://doi.org/10.1016/0022-328X\(91\)83094-K](https://doi.org/10.1016/0022-328X(91)83094-K).
43. Wang G, Huang Z, Negishi E-i. Highly stereoselective and efficient synthesis of ω -heterofunctional di- and trienoic esters for Horner–Wadsworth–Emmons reaction via alkyne hydrozirconation and Pd-catalyzed alkenylation. *Tetrahedron Lett.* 2009;50:3220–3223. <https://doi.org/10.1016/j.tetlet.2009.02.023>.
44. Liu X, Ready JM. Directed hydrozirconation of homopropargylic alcohols. *Tetrahedron.* 2008;64:6955–6960. <https://doi.org/10.1016/j.tet.2008.03.052>.
45. Carr DB, Schwartz J. Preparation of organoaluminum compounds by hydrozirconation-transmetalation. *J Am Chem Soc.* 1979;101:3521–3531. <https://doi.org/10.1021/ja00507a017>.
46. Iwai T, Okochi H, Ito H, Sawamura M. Construction of eight-membered carbocycles through gold catalysis with acetylene-tethered silyl enol ethers. *Angew Chem Int Ed.* 2013;52:4239–4242. <https://doi.org/10.1002/anie.201300265>.
47. Kragler A, Höfner G, Wanner KT. Synthesis and biological evaluation of amino-methylphenol derivatives as inhibitors of the murine GABA transporters mGAT1-mGAT4. *Eur J Med Chem.* 2008;43:2404–2411. <https://doi.org/10.1016/j.ejmech.2008.01.005>.
48. Zepperitz C, Höfner G, Wanner KT. MS-binding assays: kinetic, saturation, and competitive experiments based on quantitation of bound marker as exemplified by the GABA transporter mGAT1. *ChemMedChem.* 2006;1:208–217. <https://doi.org/10.1002/cmdc.200500038>.
49. Petrerá M, Wein T, Allmendinger L, et al. Development of highly potent GAT1 inhibitors: synthesis of nipecotic acid derivatives by suzuki-miyaura cross-coupling reactions. *ChemMedChem.* 2016;11:519–538. <https://doi.org/10.1002/cmdc.201500490>.
50. Schmitt S, Höfner G, Wanner KT. Application of MS transport assays to the four human gamma-aminobutyric acid transporters. *ChemMedChem.* 2015;10:1498–1510. <https://doi.org/10.1002/cmdc.201500254>.
51. Madsen KK, Ebert B, Clausen RP, Krogsgaard-Larsen P, Schousboe A, White HS. Selective GABA transporter inhibitors tiagabine and EF1502 exhibit mechanistic differences in their ability to modulate the ataxia and anticonvulsant action of the extrasynaptic GABA(A) receptor agonist gaboxadol. *J Pharmacol Exp Ther.* 2011;338:214–219. <https://doi.org/10.1124/jpet.111.179671>.
52. Madsen KK, White HS, Schousboe A. Neuronal and non-neuronal GABA transporters as targets for antiepileptic drugs. *Pharmacol Ther.* 2010;125:394–401. <https://doi.org/10.1016/j.pharmthera.2009.11.007>.

Supporting Information

Synthesis and biological evaluation of novel N-substituted nipecotic acid derivatives with a *trans*-alkene spacer as potent GABA uptake inhibitors

Krisztián Tóth, Georg Höfner, Klaus T. Wanner*

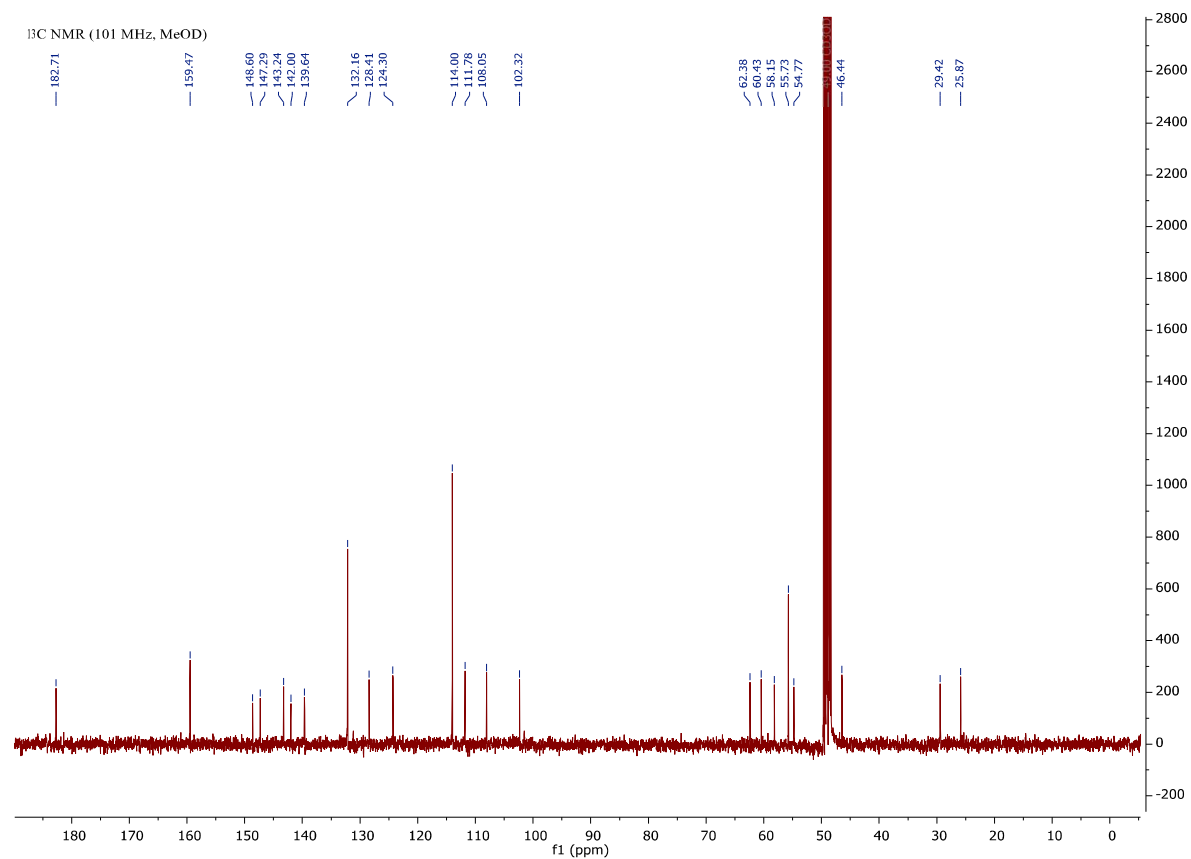
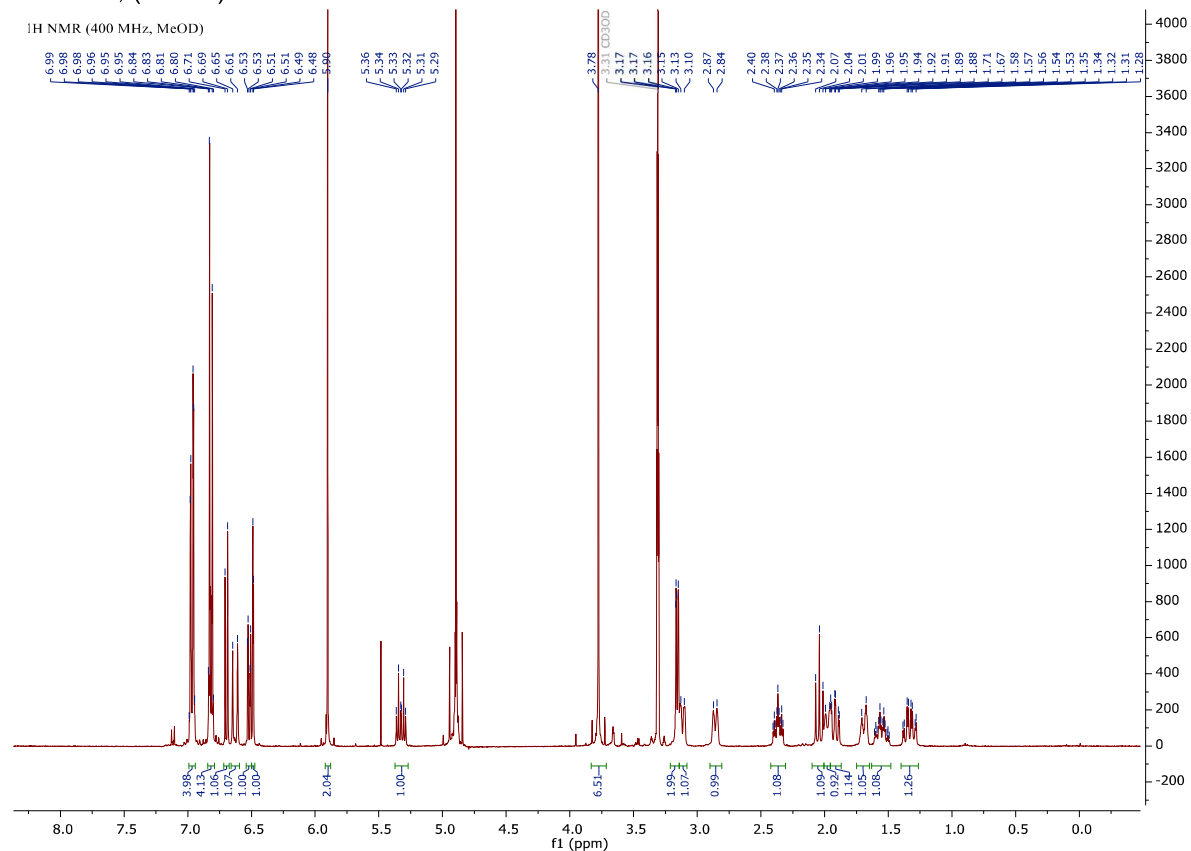
Department of Pharmacy – Center for Drug Research, Ludwig-Maximilians-Universität München, Butenandtstr. 5–13, 81377 Munich, Germany

Table of contents:

1. List of the ¹H NMR, ¹³C NMR, and HRMS data of synthesized compounds *rac*-2b–p. 2
2. List of the ¹H NMR, ¹³C NMR, and HRMS data of synthesized compounds *rac*-6a–b..... 32

1. List of the ¹H NMR, ¹³C NMR, and HRMS data of synthesized compounds *rac*-2b-p.

1.1. (E)-1-[4-(Benzo[d][1,3]dioxol-5-yl)-4,4-bis(4-methoxyphenyl)but-2-en-1-yl]piperidine-3-carboxylic acid, (*rac*-2b)

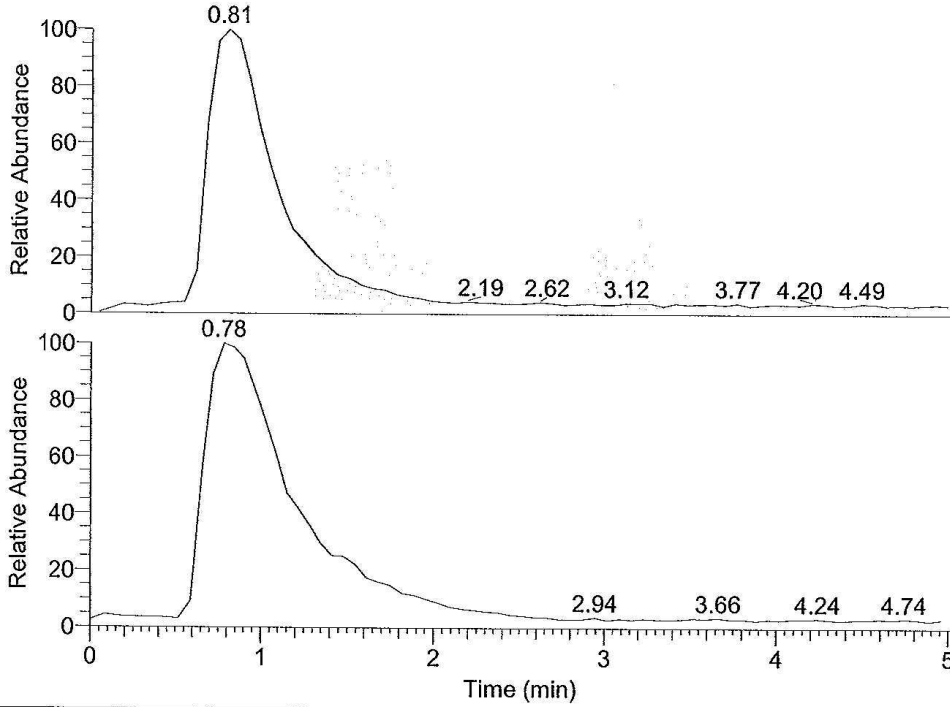


Probennamen: C:\Data\03-krtoph-607KT
Auftraggeber: Toth, Wanner

Probe: 515, c31h33no6, fest, Aceton
Methode: 100 ul/min Acetonitril/Wasser, FIA/ESI, LTQ FT, Spahl

Inj Vol: 1.000000
Zeit:

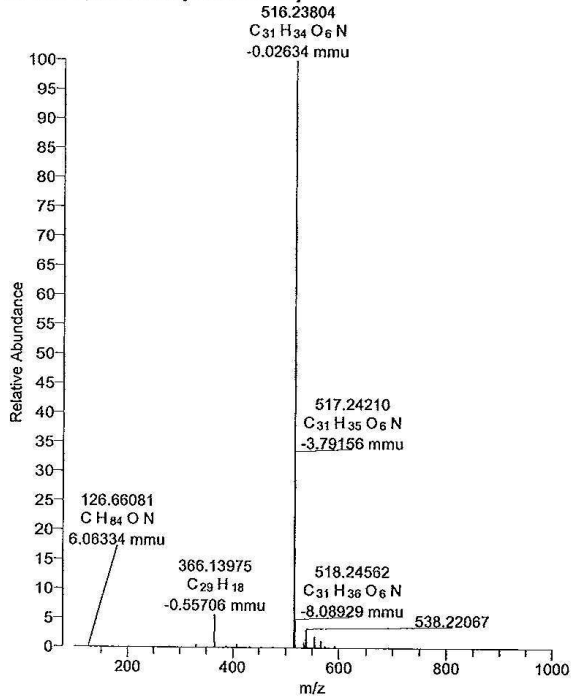
RT: 0.00 - 5.02



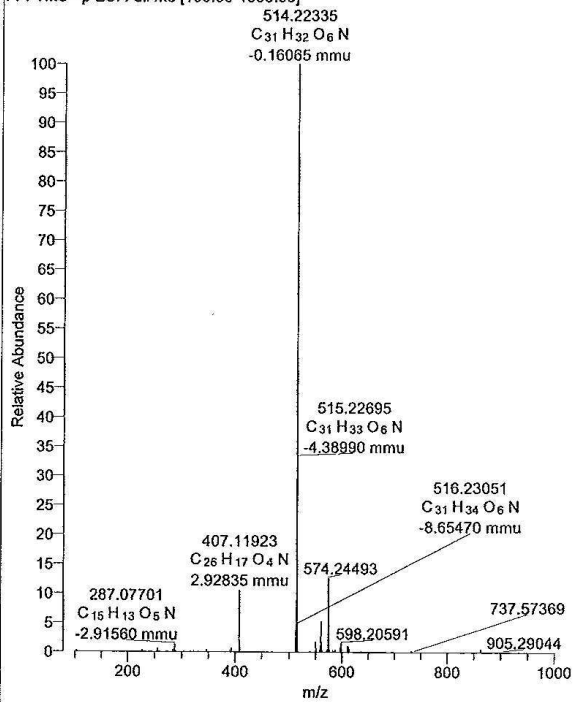
NL: 1.94E6
Base Peak F: FTMS
- p ESI Full ms
[100.00-1000.00]
MS 03-krtoph-607KT

NL: 3.60E6
Base Peak F: FTMS
+ p ESI Full ms
[100.00-1000.00]
MS 03-krtoph-607KT

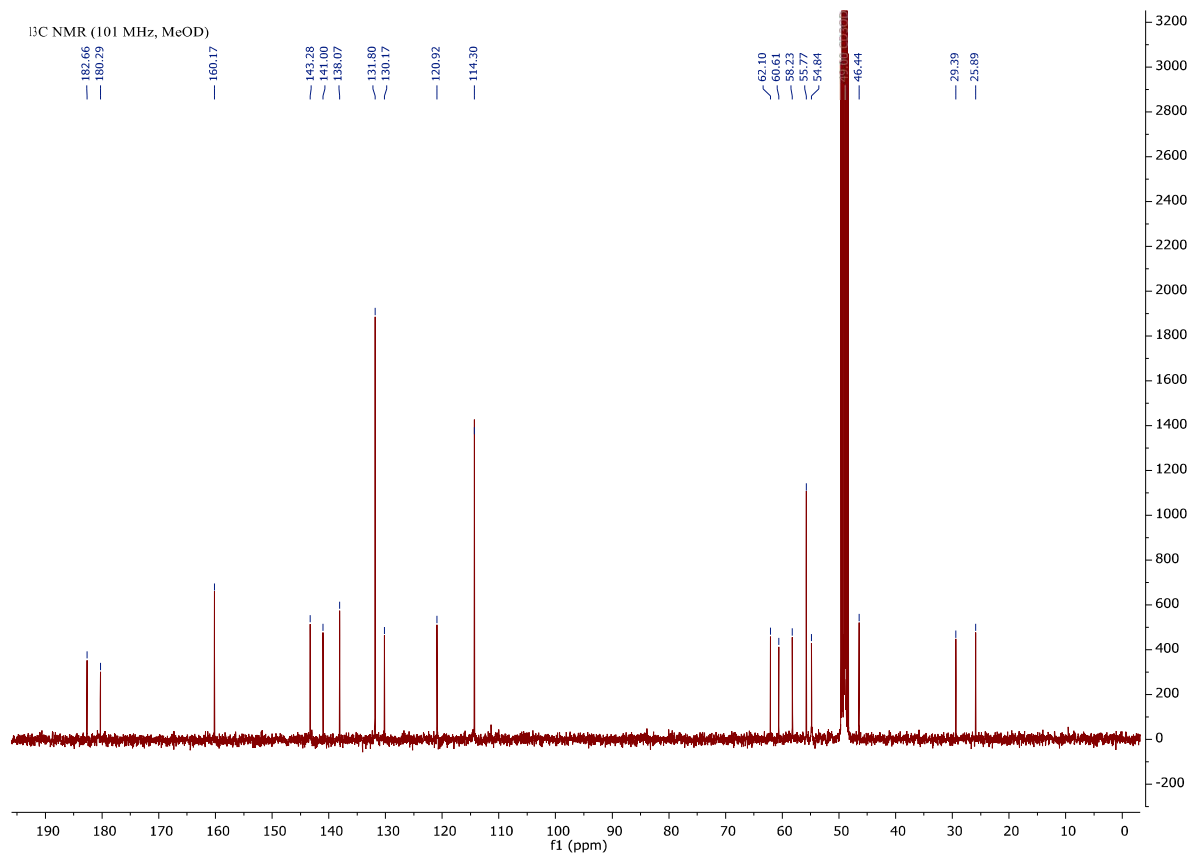
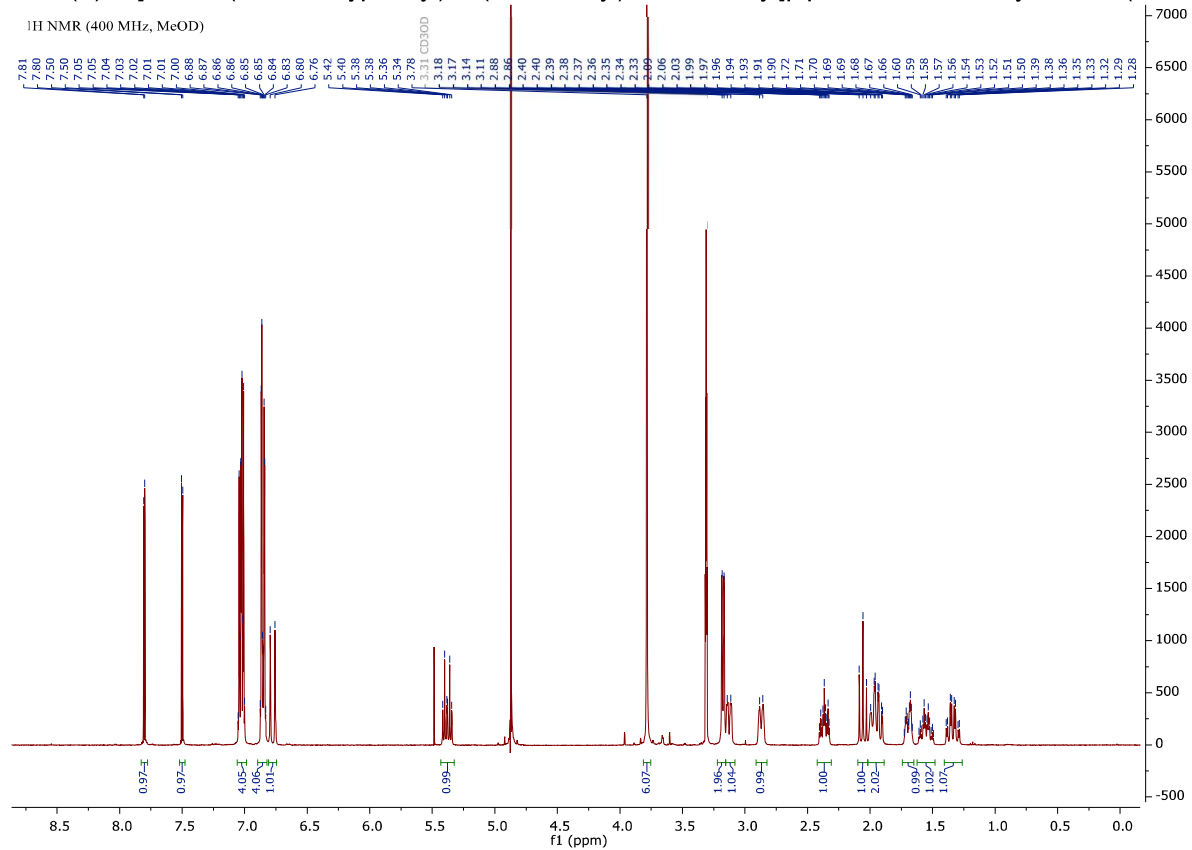
03-krtoph-607KT #55-180 RT: 0.52-1.48 AV: 16 NL: 1.94E6
F: FTMS + p ESI Full ms [100.00-1000.00]



03-krtoph-607KT #55-174 RT: 0.55-1.44 AV: 15 NL: 8.76E5
F: FTMS - p ESI Full ms [100.00-1000.00]



1.2. (E)-1-[4,4-Bis(4-methoxyphenyl)-4-(thiazol-2-yl)but-2-en-1-yl]piperidine-3-carboxylic acid, (*rac*-**2c**)

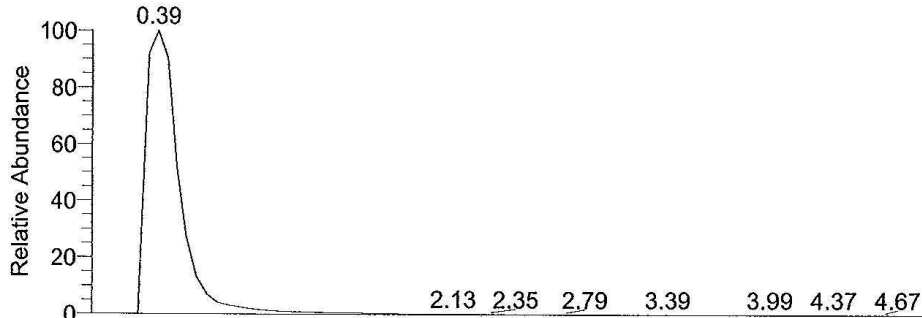


Probenname: C:\Data\04-krtoph-617KT
Auftraggeber:

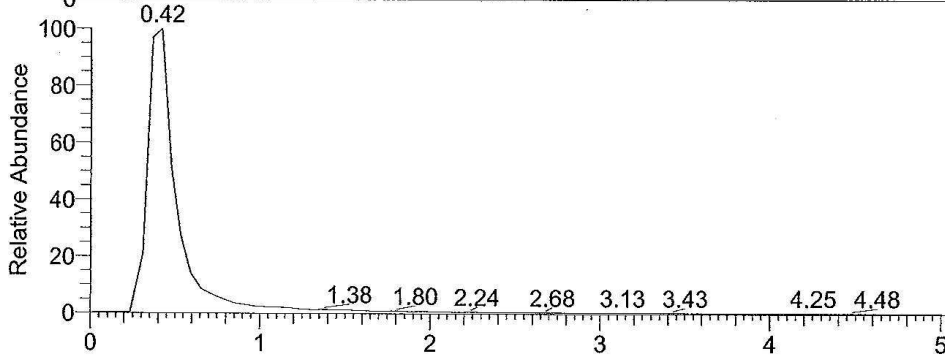
Probe: 478, c27h30n2o4s, fest, Aceton
Methode: Toth, Wanner

Inj Vol: 0.000000
Zeit:

RT: 0.00 - 5.07



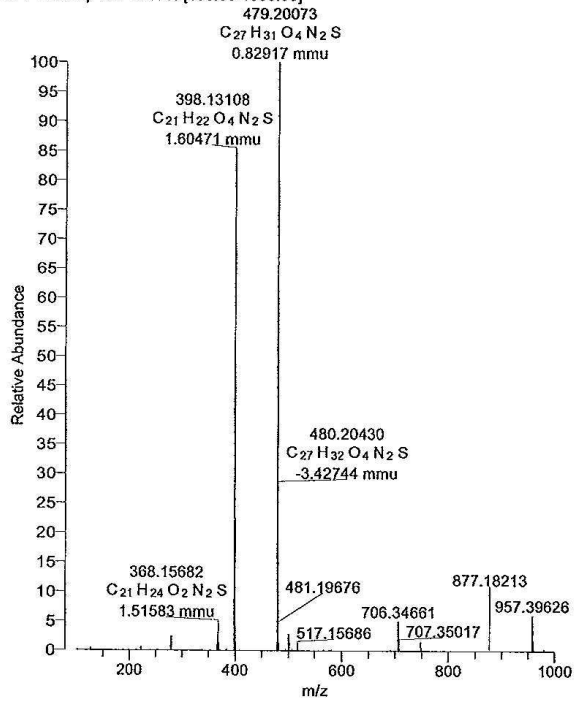
NL: 4.38E6
Base Peak F: FTMS
- p ESI Full ms
[100.00-1000.00]
MS 04-krtoph-617KT



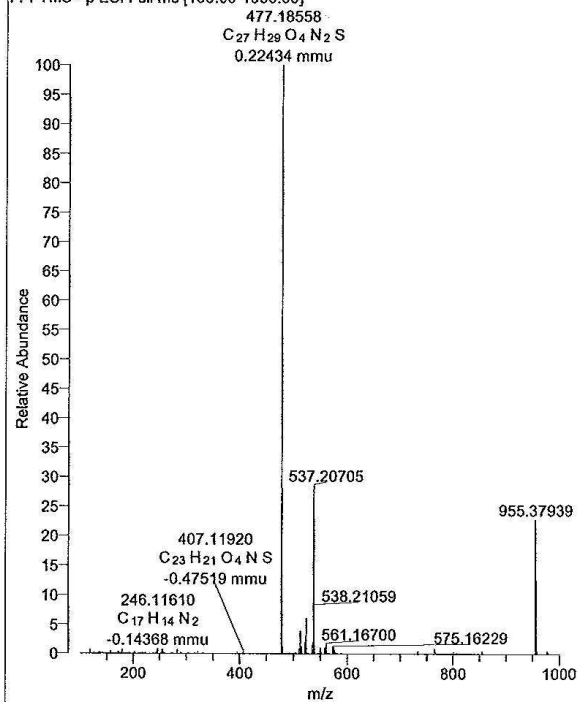
NL: 1.62E7
Base Peak F: FTMS
+ p ESI Full ms
[100.00-1000.00]
MS 04-krtoph-617KT

Time (min)

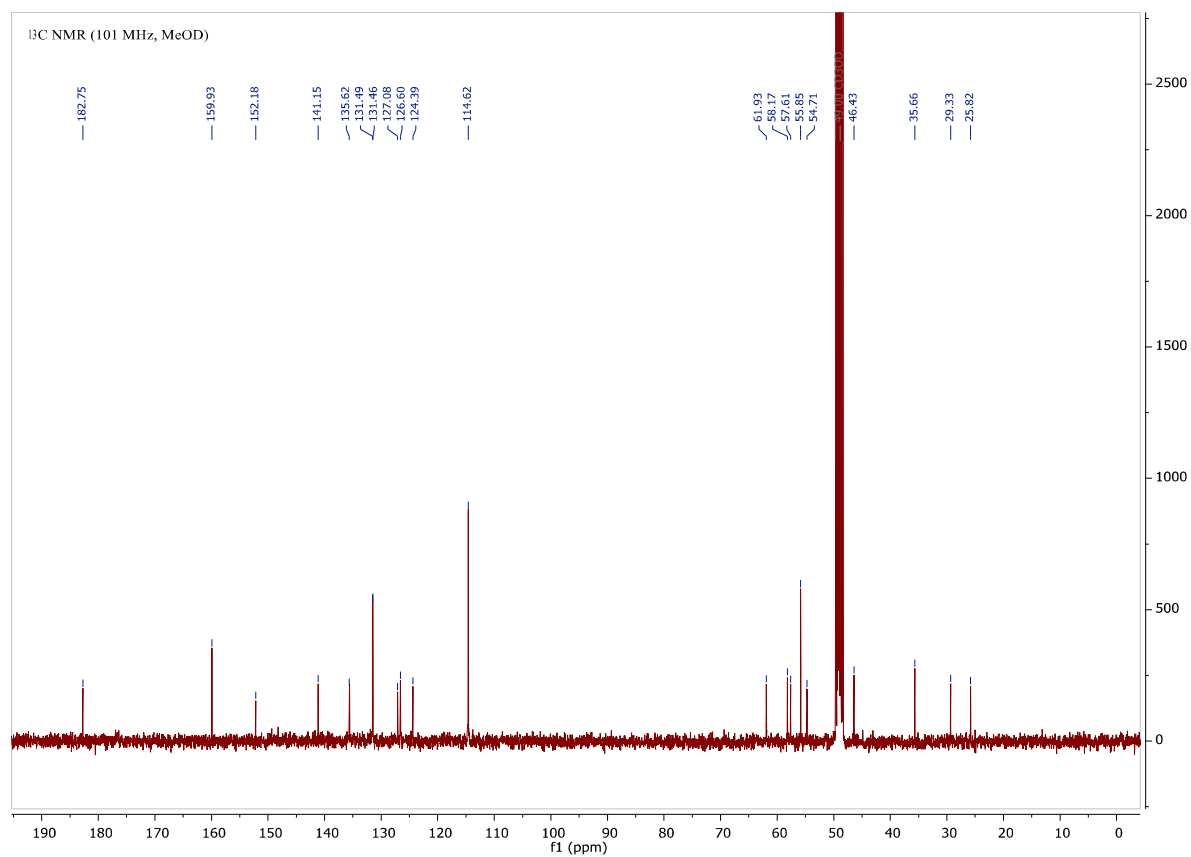
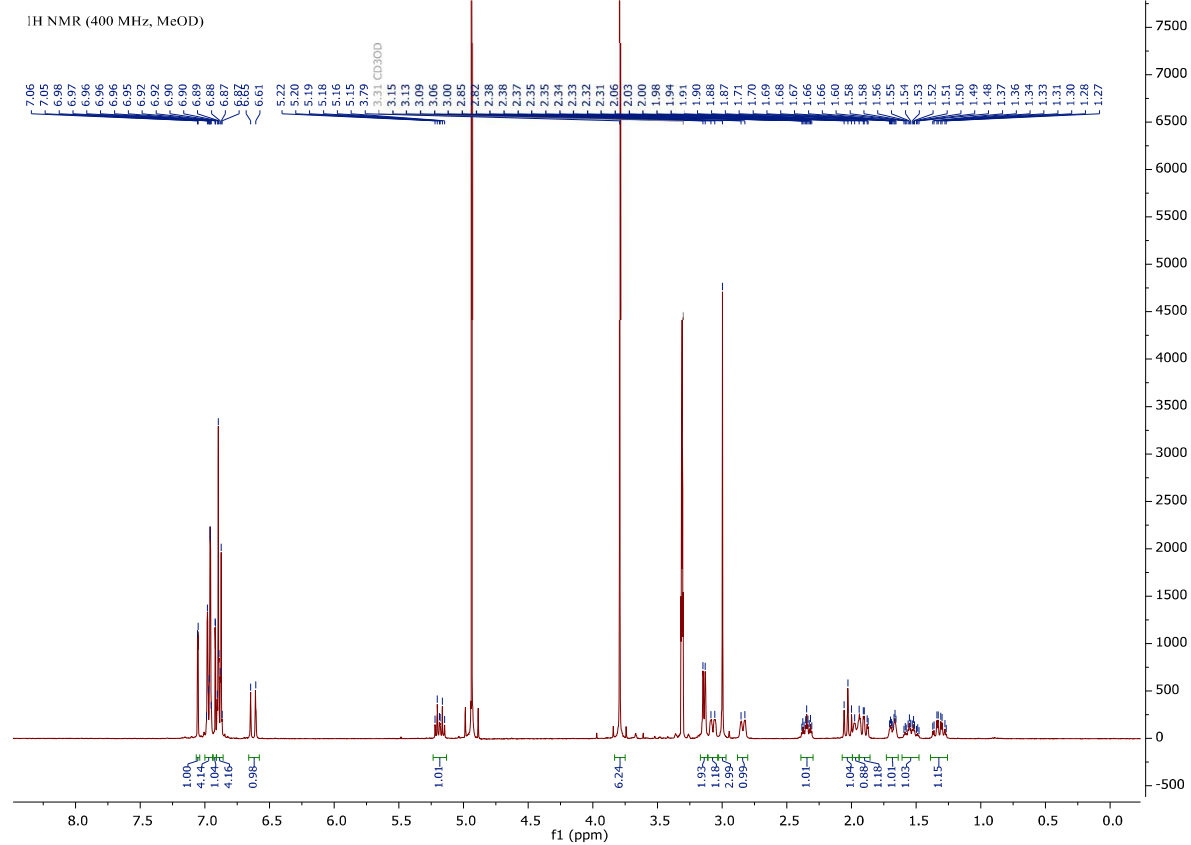
04-krtoph-617KT #61-182 RT: 0.53-1.45 AV: 15 NL: 8.61E5
F: FTMS + p ESI Full ms [100.00-1000.00]



04-krtoph-617KT #61-177 RT: 0.50-1.41 AV: 15 NL: 3.21E5
F: FTMS - p ESI Full ms [100.00-1000.00]



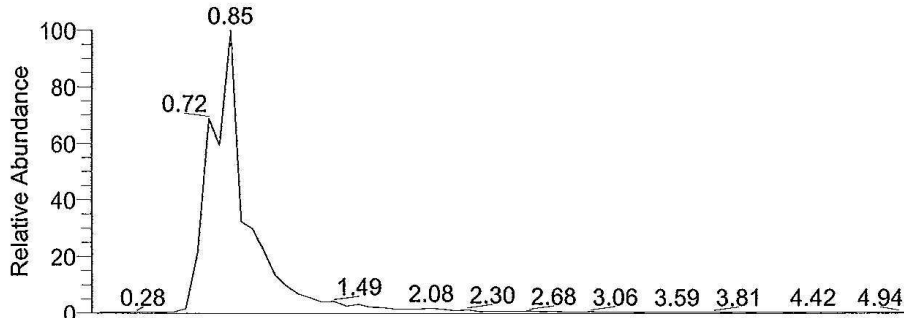
1.3. (E)-1-[4,4-Bis(4-methoxyphenyl)-4-(1-methyl-1H-imidazol-2-yl)but-2-en-1-yl]piperidine-3-carboxylic acid, (*rac*-2d)



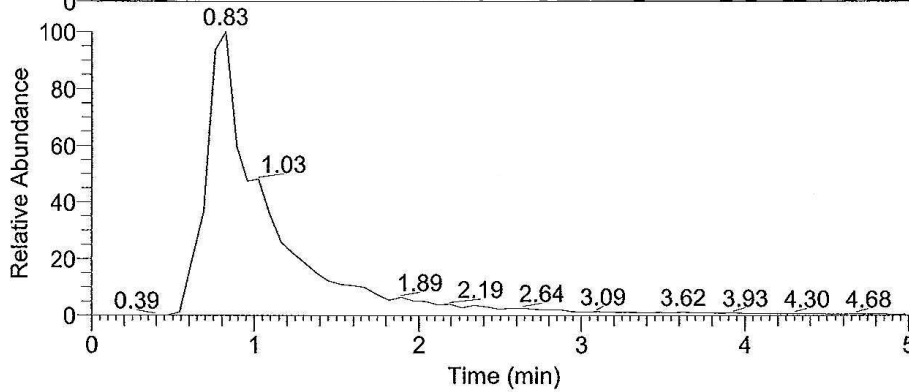
Probenbezeichnung: C:\Data\01-krtoph-567KT_170116095227
Auftraggeber: Toth, Wanner
RT: 0.00 - 5.04

Probe: 475, c28h33n3o4, fest, Aceton
Methode: 100 ul/min Acetonitril/Wasser, FIA/ESI, LTQ FT, Spahl

Inj Vol: 1.000000
Zeit:

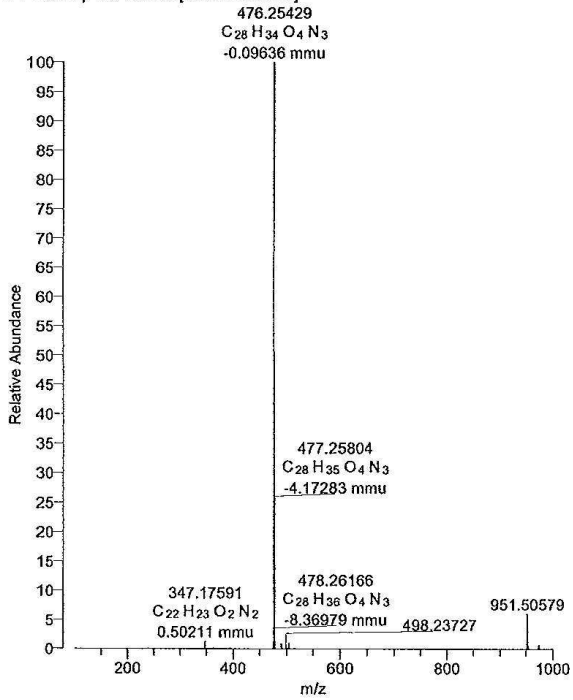


NL: 3.21E5
Base Peak F: FTMS -
p ESI Full ms
[100.00-1000.00] MS
01-krtoph-
567KT_17011609522
7

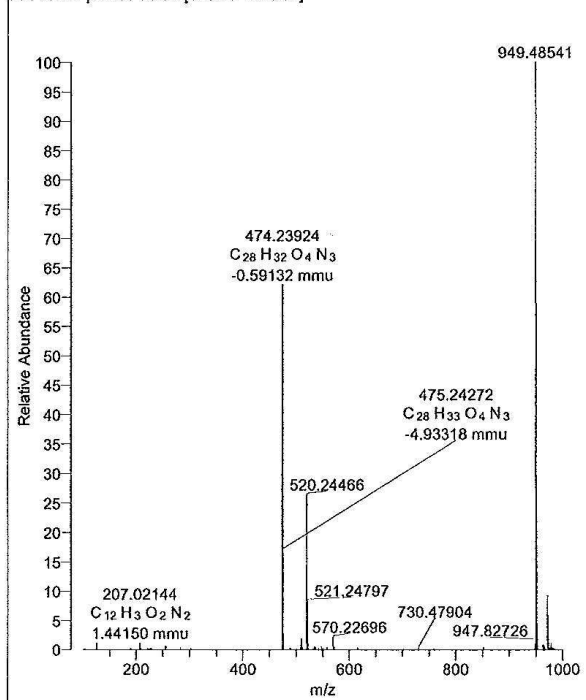


NL: 1.33E7
Base Peak F: FTMS
+ p ESI Full ms
[100.00-1000.00] MS
01-krtoph-
567KT_17011609522
7

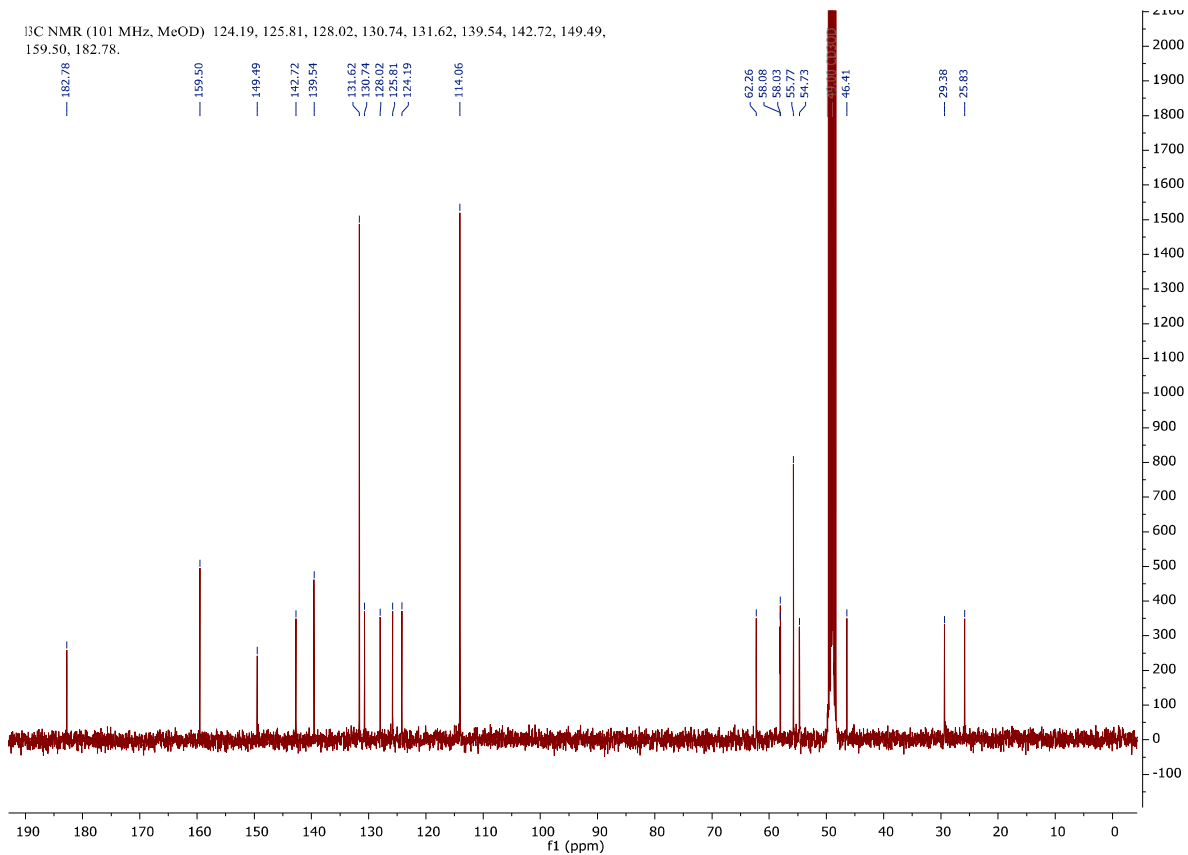
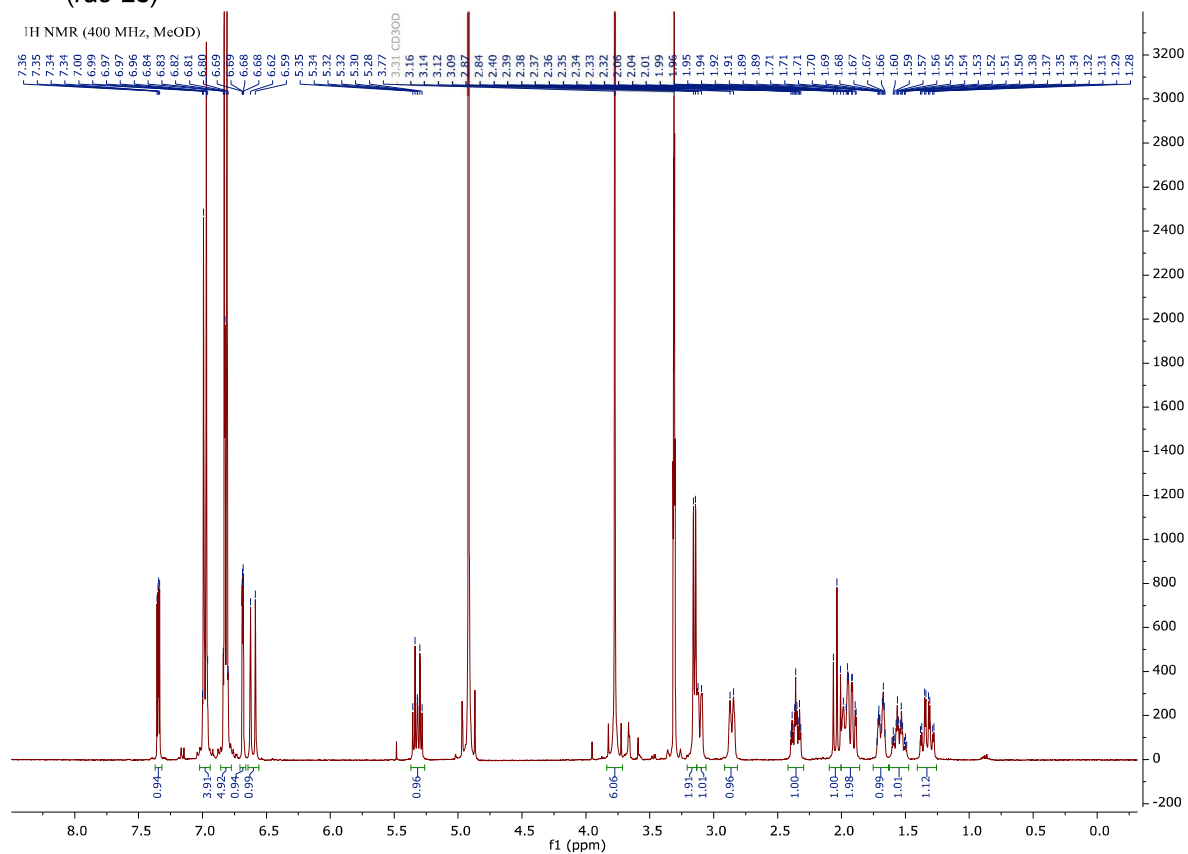
01-krtoph-567KT_170116095227 #52-166 RT: 0.54-1.45 AV: 14 NL: 4.77E6
F: FTMS + p ESI Full ms [100.00-1000.00]



01-krtoph-567KT_170116095227 #52-161 RT: 0.50-1.41 AV: 14 NL: 8.48E4
F: FTMS - p ESI Full ms [100.00-1000.00]



1.4. (E)-1-[4,4-Bis(4-methoxyphenyl)-4-(thiophen-3-yl)but-2-en-1-yl]piperidine-3-carboxylic acid, (rac-2e)

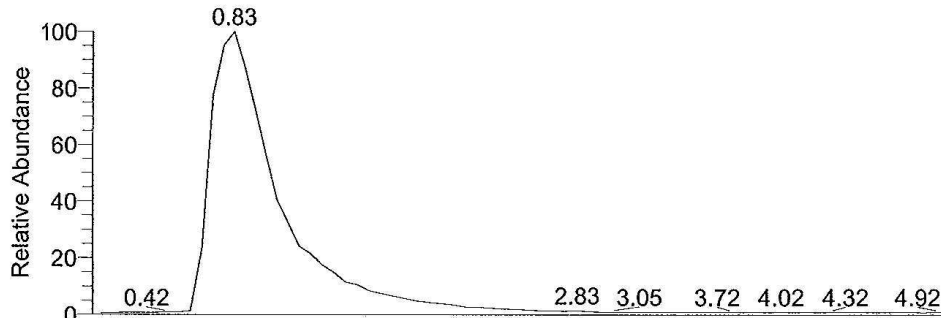


Probenname: C:\Data\04-krtoph-610KT
 Auftraggeber: Toth, Wanner

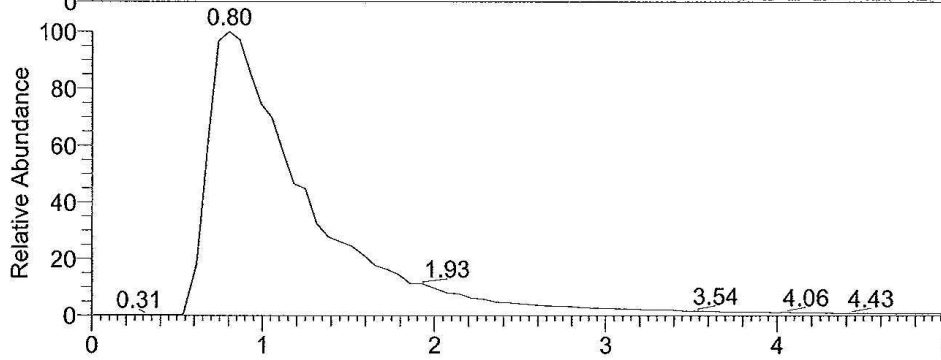
Probe: 477, c28h31no4s, fest, Aceton
 Methode: 100 ul/min Acetonitril/Wasser, FIA/ESI, LTQ FT, Spahl

Inj Vol: 1.000000
 Zeit:

RT: 0.00 - 5.02



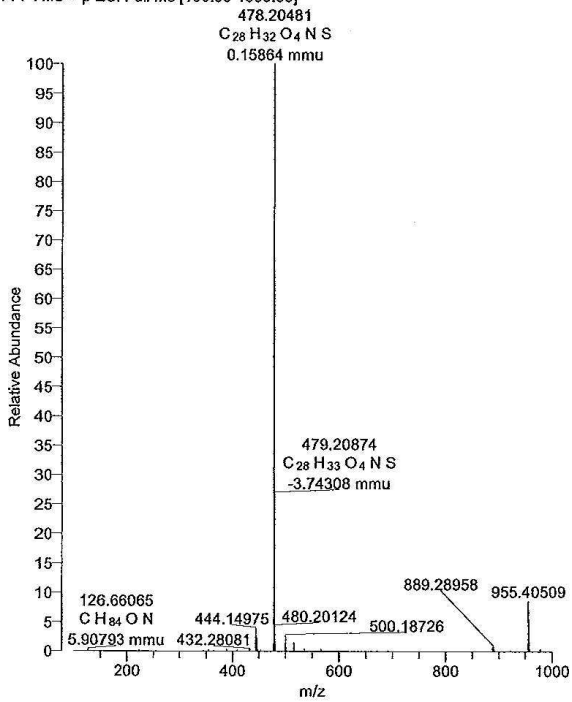
NL: 1.37E6
 Base Peak F: FTMS
 - p ESI Full ms
 [100.00-1000.00]
 MS 04-krtoph-610KT



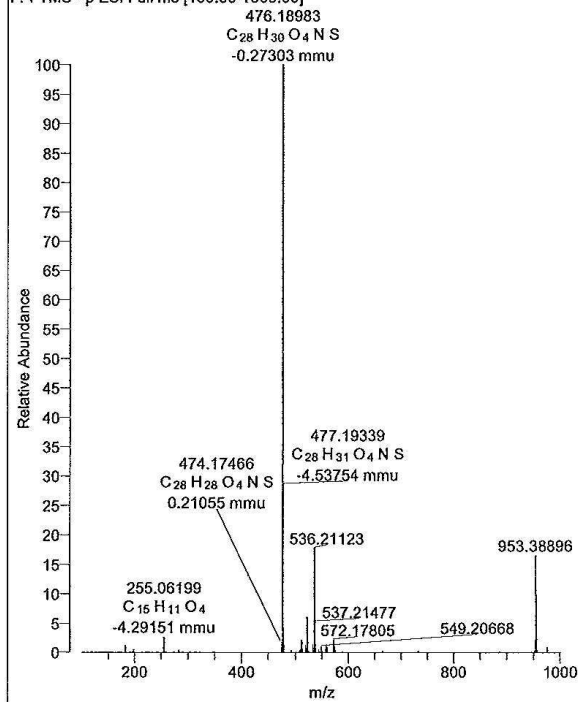
NL: 3.26E6
 Base Peak F: FTMS
 + p ESI Full ms
 [100.00-1000.00]
 MS 04-krtoph-610KT

Time (min)

04-krtoph-610KT #53-174 RT: 0.54-1.45 AV: 15 NL: 1.82E6
 F: FTMS + p ESI Full ms [100.00-1000.00]

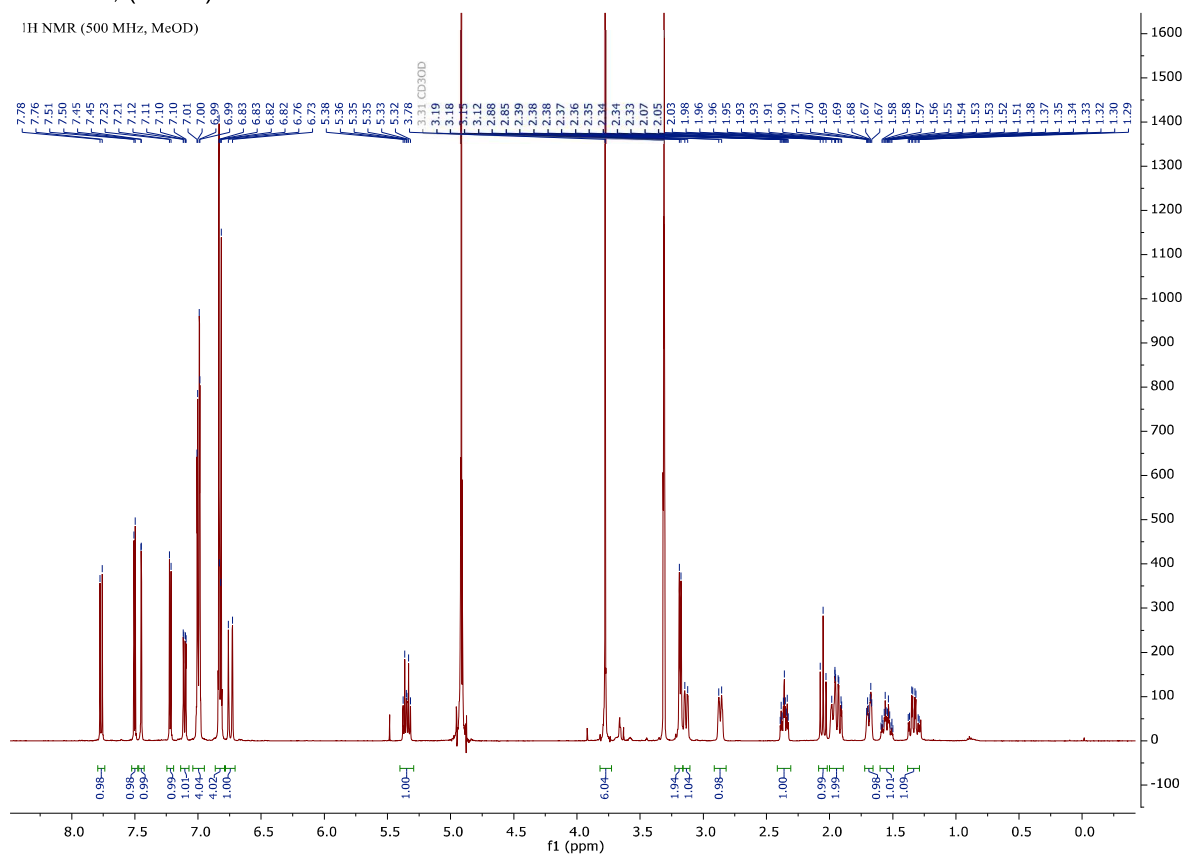


04-krtoph-610KT #53-169 RT: 0.50-1.41 AV: 15 NL: 5.69E5
 F: FTMS - p ESI Full ms [100.00-1000.00]

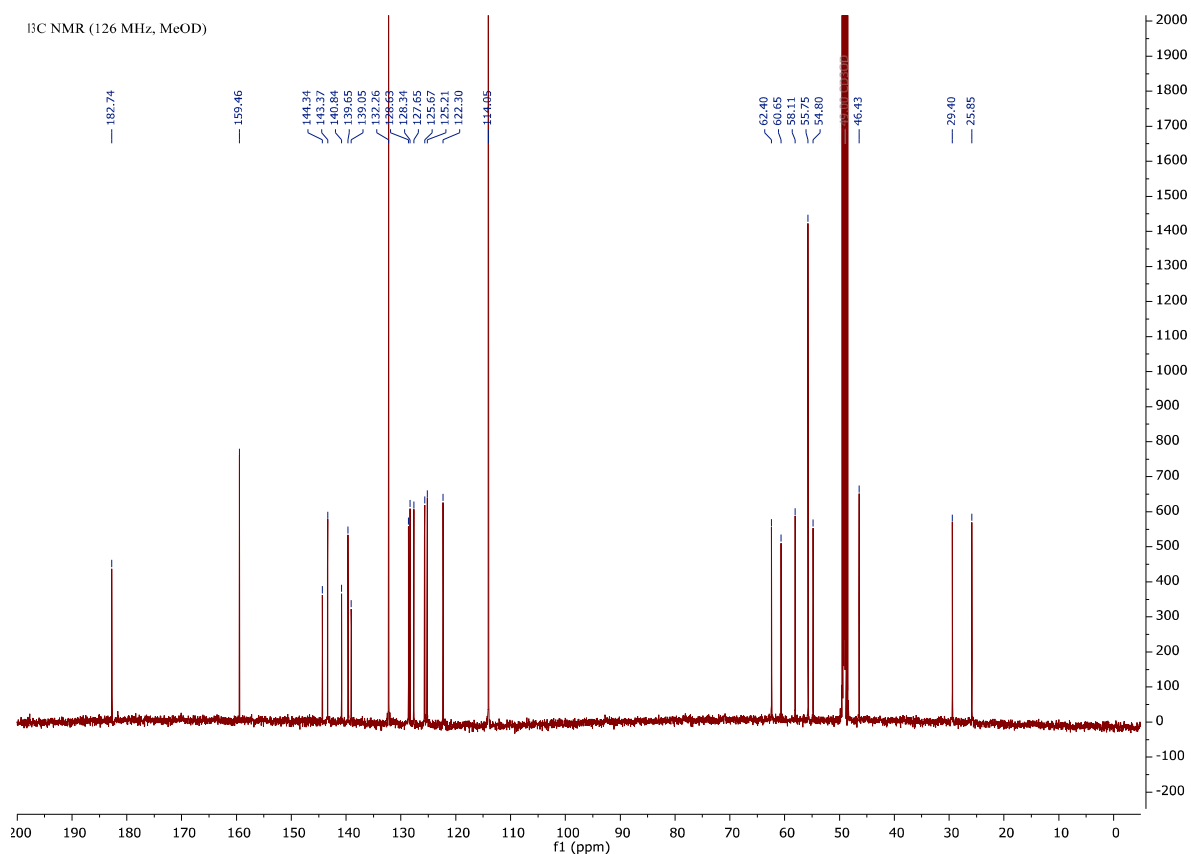


1.5. (E)-1-[4-(Benzo[b]thiophen-5-yl)-4,4-bis(4-methoxyphenyl)but-2-en-1-yl]piperidine-3-carboxylic acid, (rac-2f)

¹H NMR (500 MHz, MeOD)



¹³C NMR (126 MHz, MeOD)

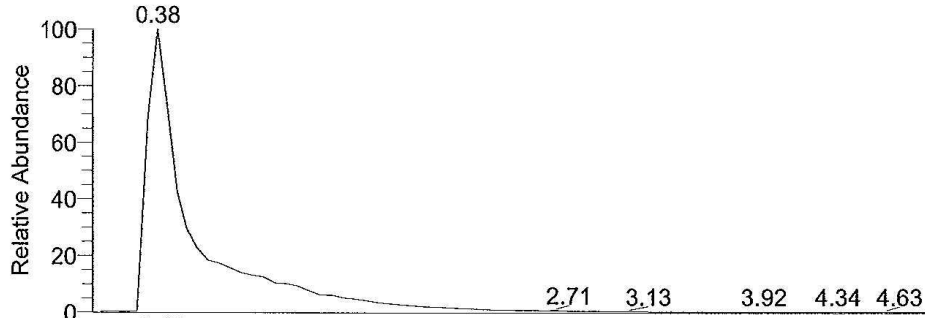


Probename: C:\Data\04-krtoph-612KT
Auftraggeber:

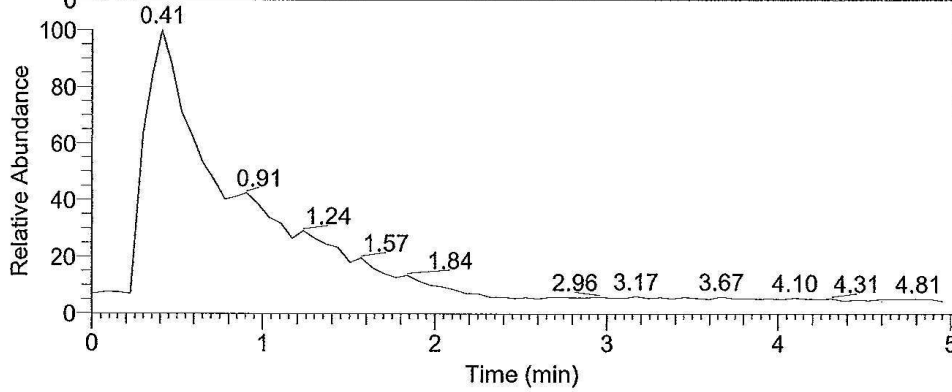
Probe: 527, c32h33no4s, fest, Aceton
Methode: Toth, Wanner

Inj Vol: 0.000000
Zeit:

RT: 0.00 - 5.01

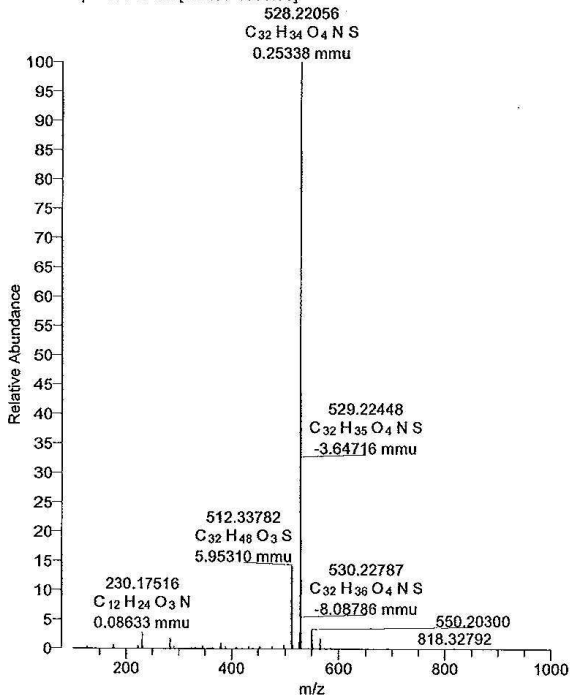


NL: 4.97E6
Base Peak F: FTMS
- p ESI Full ms
[100.00-1000.00]
MS 04-krtoph-612KT

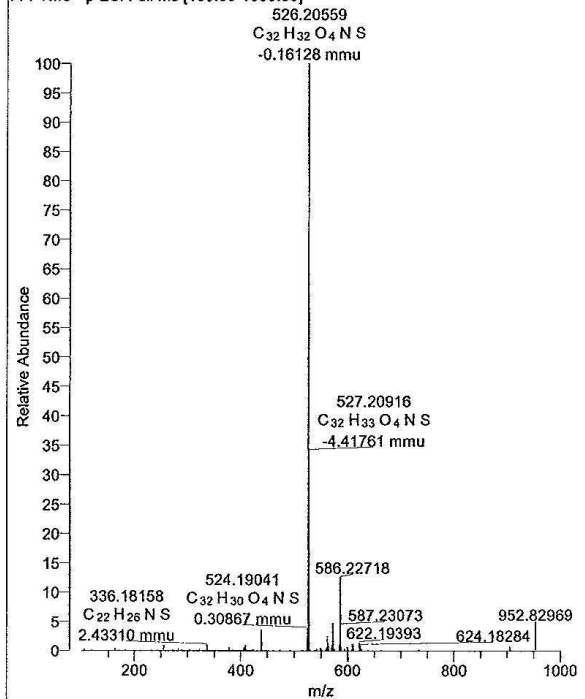


NL: 4.66E6
Base Peak F: FTMS
+ p ESI Full ms
[100.00-1000.00]
MS 04-krtoph-612KT

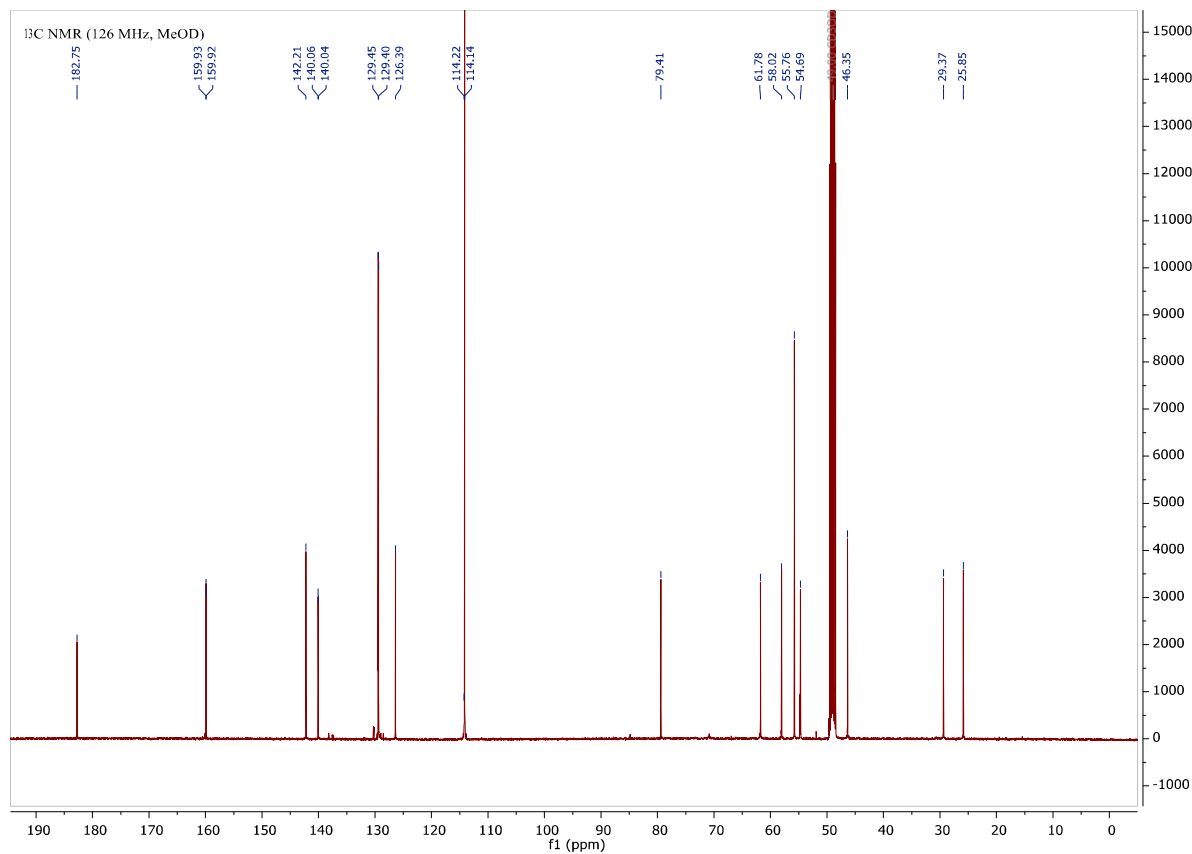
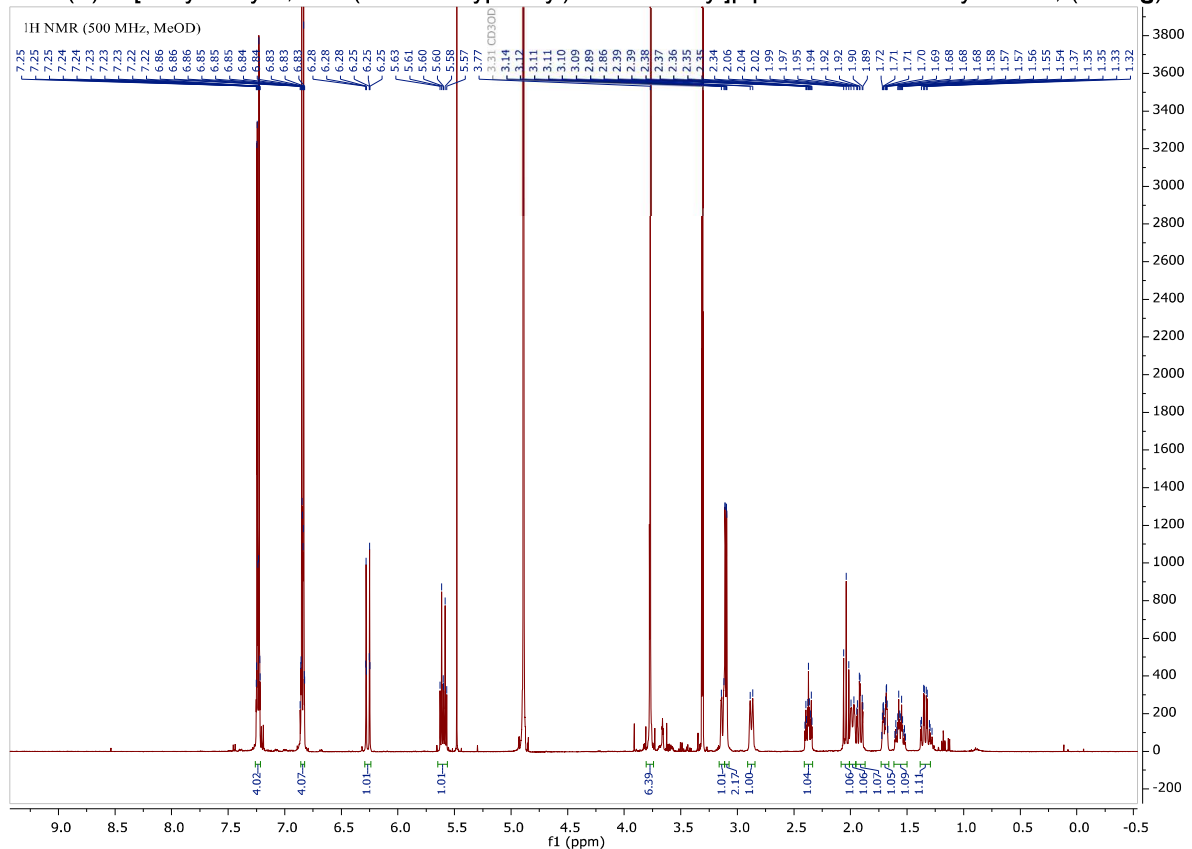
04-krtoph-612KT #61-184 RT: 0.53-1.44 AV: 15 NL: 1.83E6
F: FTMS + p ESI Full ms [100.00-1000.00]



04-krtoph-612KT #61-180 RT: 0.49-1.40 AV: 15 NL: 7.21E5
F: FTMS - p ESI Full ms [100.00-1000.00]



1.6. (E)-1-[4-Hydroxy-4,4-bis(4-methoxyphenyl)but-2-en-1-yl]piperidine-3-carboxylic acid, (*rac*-**2g**)

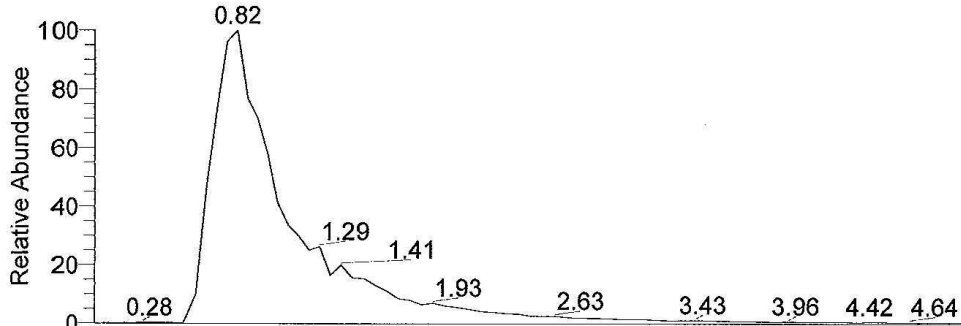


Probenbezeichnung: C:\Data\03-krtoph-422KT
 Auftraggeber: Tolh, Wanner

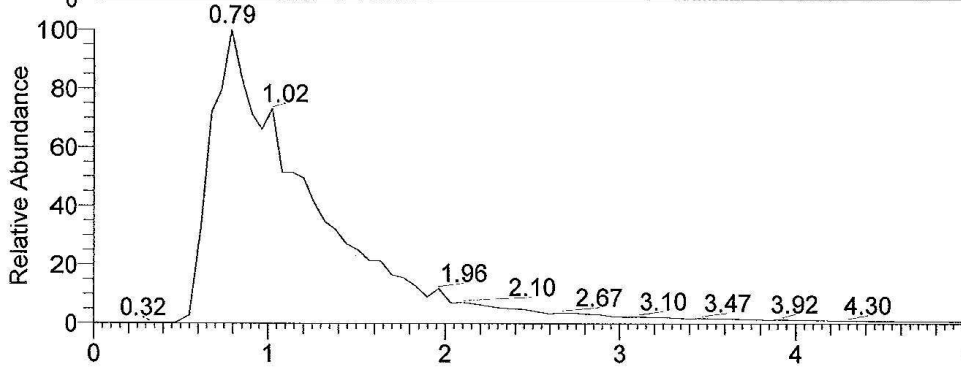
Probe: 411, c24h29no5, fest, Aceton
 Methode: 100 ul/min Acetonitril/Wasser, FIA/ESI, LTQ FT, Spahl

Inj Vol: 1.000000
 Zeit:

RT: 0.00 - 5.05

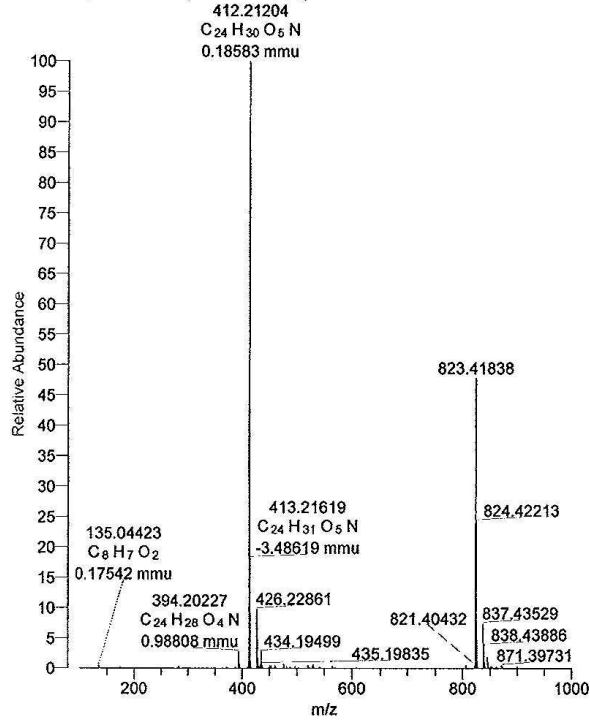


NL: 2.09E6
 Base Peak F: FTMS
 - p ESI Full ms
 [100.00-1000.00]
 MS 03-krtoph-422KT

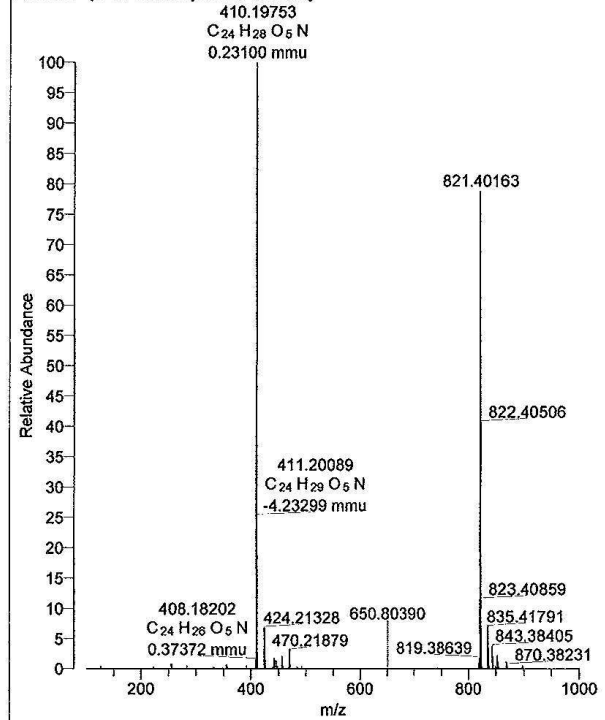


NL: 1.68E7
 Base Peak F: FTMS
 + p ESI Full ms
 [100.00-1000.00]
 MS 03-krtoph-422KT

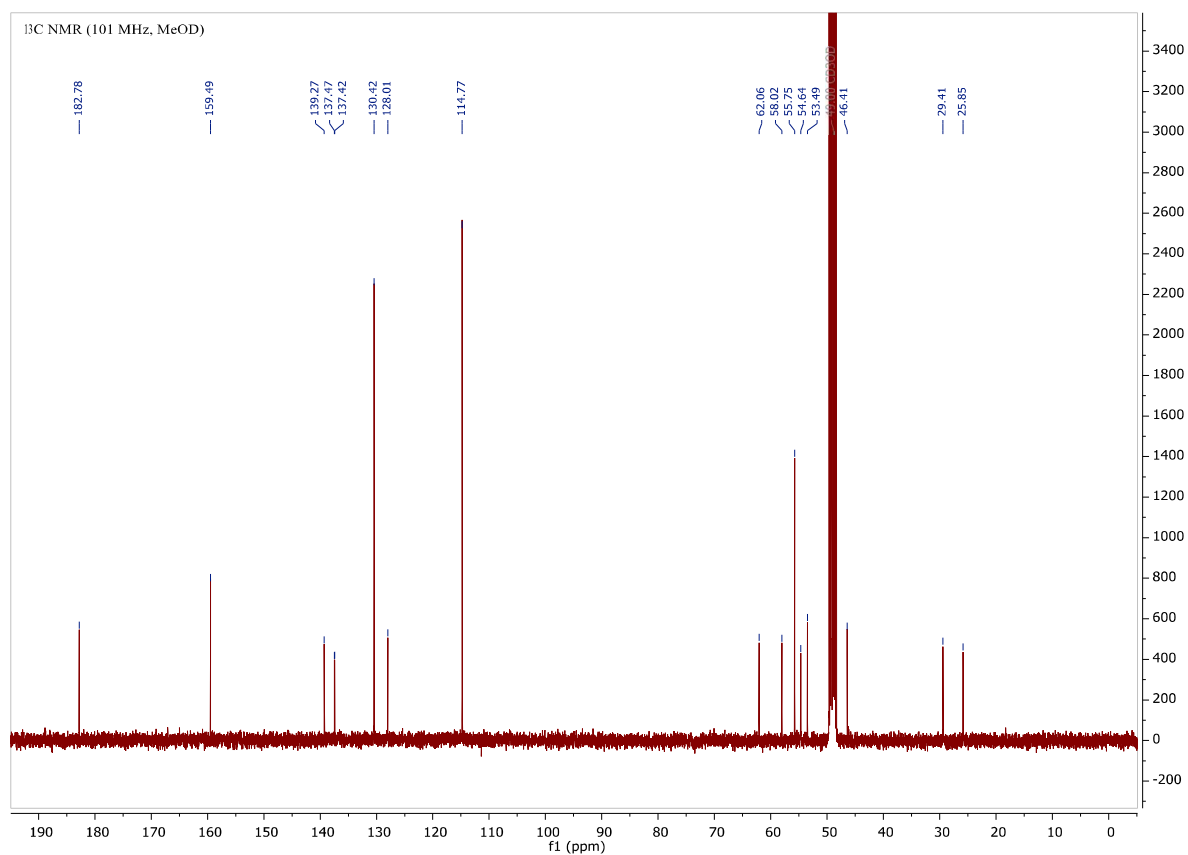
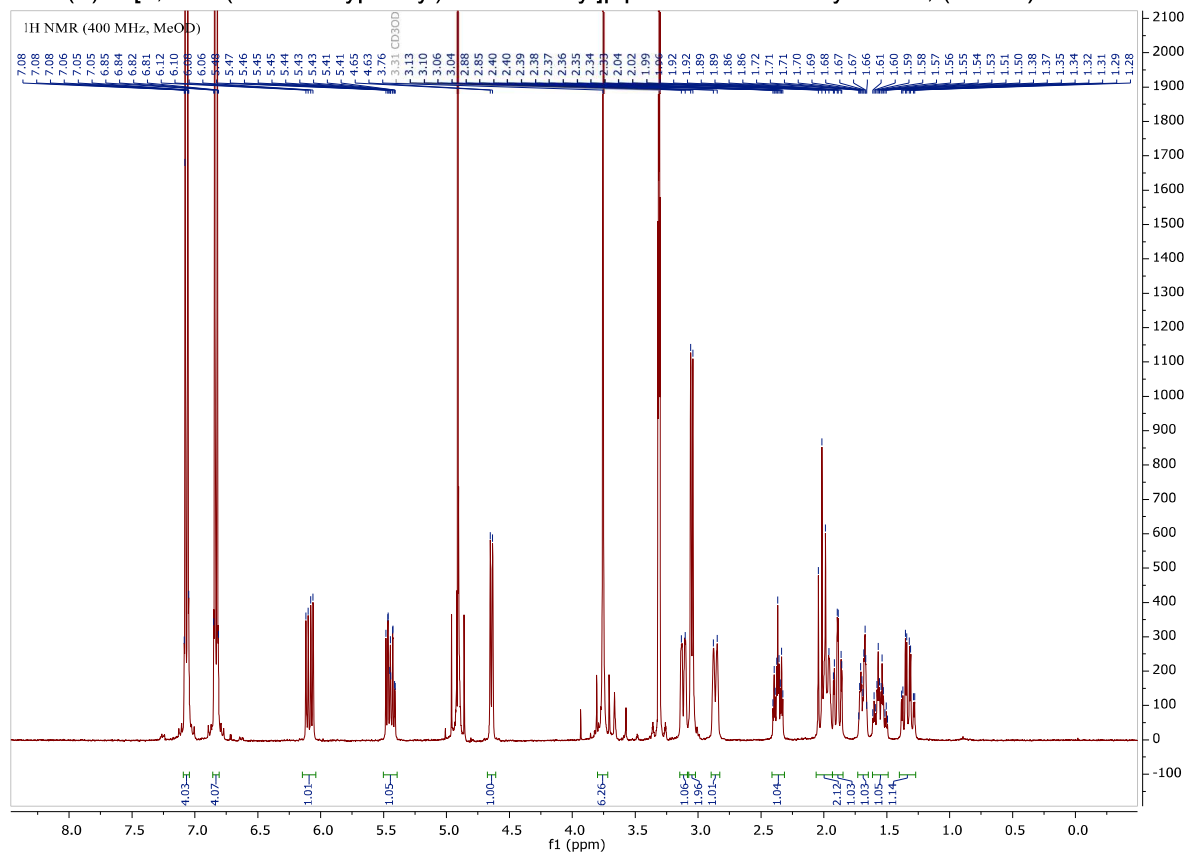
03-krtoph-422KT #52-184 RT: 0.55-1.44 AV: 16 NL: 9.07E6
 F: FTMS + p ESI Full ms [100.00-1000.00]



03-krtoph-422KT #52-179 RT: 0.51-1.41 AV: 16 NL: 9.04E5
 F: FTMS - p ESI Full ms [100.00-1000.00]



1.7. (E)-1-[4,4-Bis(4-methoxyphenyl)but-2-en-1-yl]piperidine-3-carboxylic acid, (*rac*-2h)

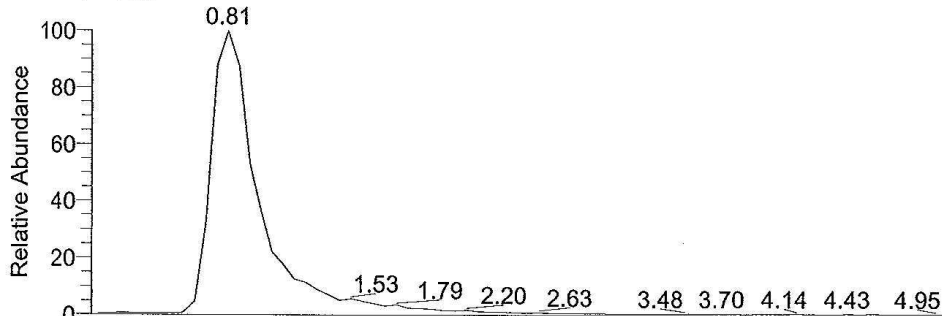


Probenname: C:\Data\02-krtoph-576KT
 Auftraggeber: Toth, Wanner

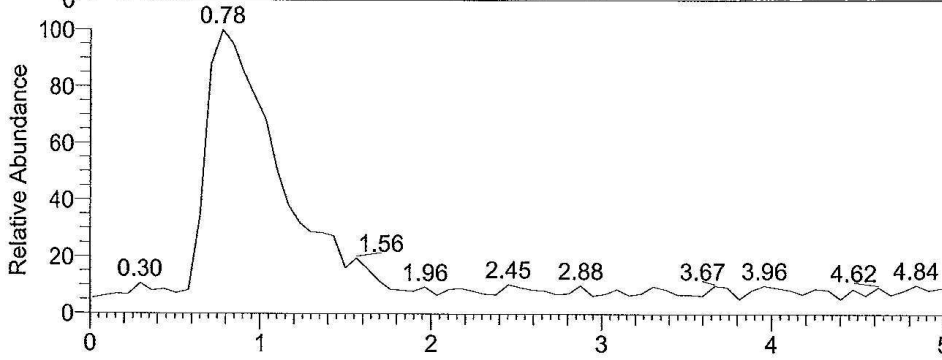
Probe: 395, c24h29no4, fest, Aceton
 Methode: 100 ul/min Aceton/Tril/Wasser, FIA/ESI, LTQ FT, Spahl

Inj Vol: 1.000000
 Zeit:

RT: 0.00 - 5.05



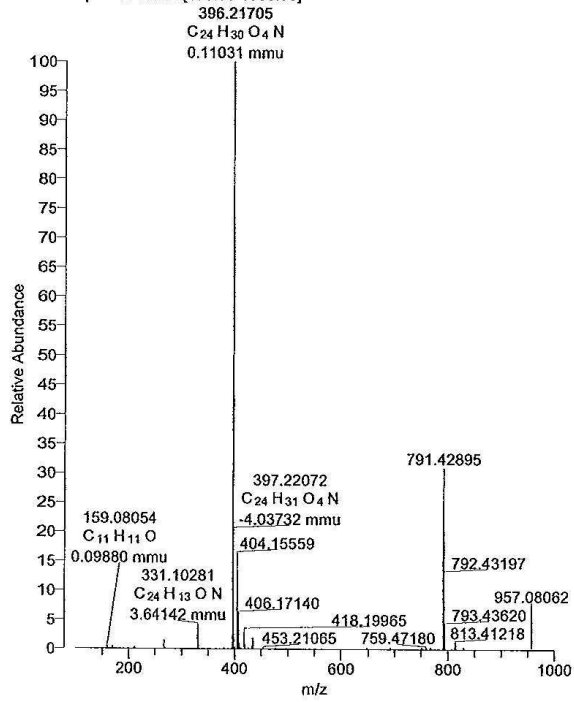
NL: 1.31E6
 Base Peak F: FTMS
 - p ESI Full ms
 [100.00-1000.00]
 MS 02-krtoph-576KT



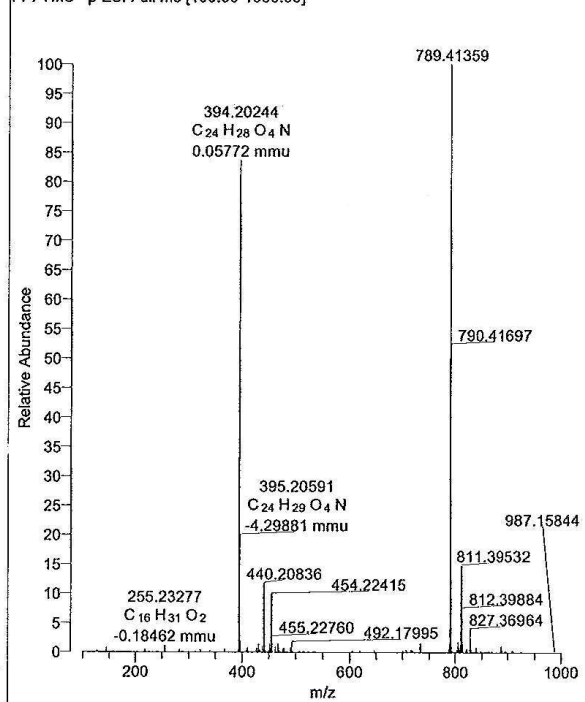
NL: 1.56E7
 Base Peak F: FTMS
 + p ESI Full ms
 [100.00-1000.00]
 MS 02-krtoph-576KT

Time (min)

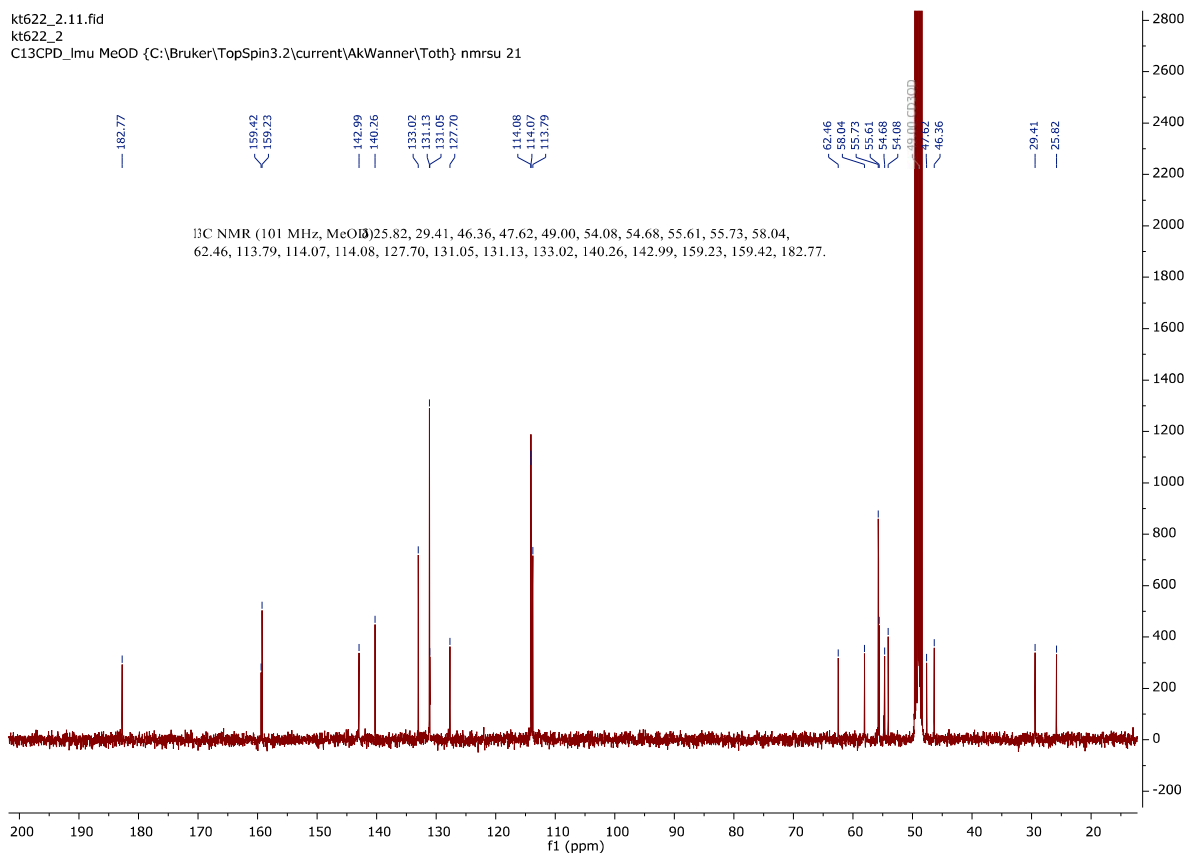
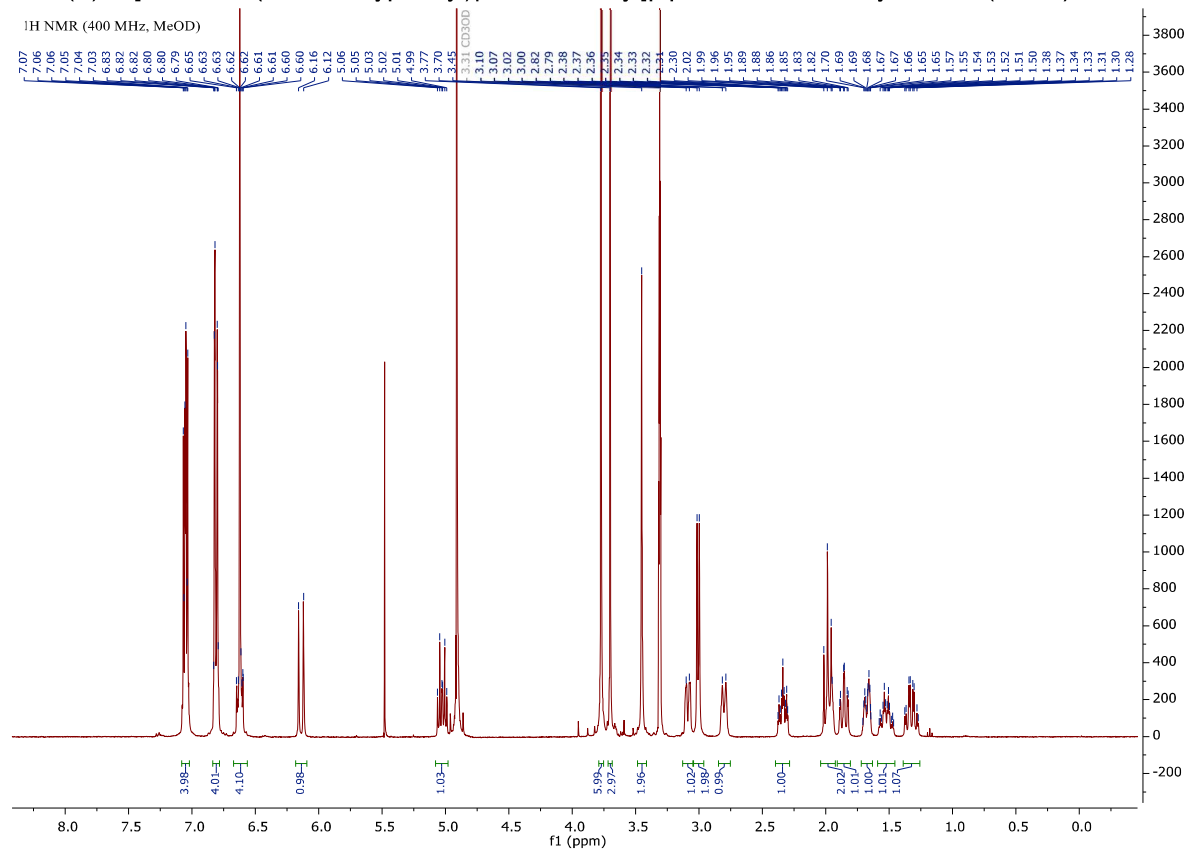
02-krtoph-576KT #56-177 RT: 0.51-1.50 AV: 16 NL: 7.22E6
 F: FTMS + p ESI Full ms [100.00-1000.00]



02-krtoph-576KT #56-173 RT: 0.54-1.46 AV: 15 NL: 3.82E5
 F: FTMS - p ESI Full ms [100.00-1000.00]



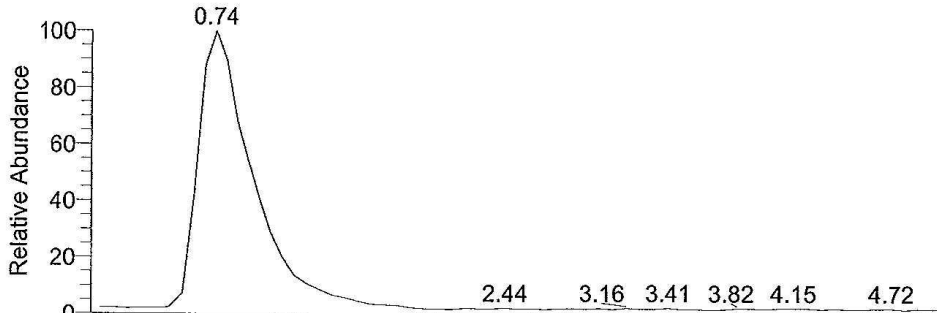
1.8. (E)-1-[4,4,5-Tris(4-methoxyphenyl)pent-2-en-1-yl]piperidine-3-carboxylic acid, (rac-2i)



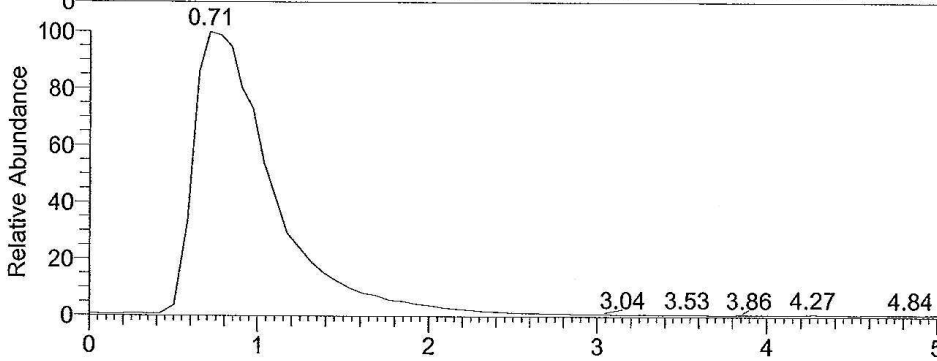
Probenname: C:\Data\05-krtoph-622KT
Auftraggeber: Toth, Wannier
RT: 0.00 - 5.07

Probe: 515, c32h37no5, fest, Aceton
Methode: 100 ul/min Acetonitril/Wasser, FIA/ESI, LTQ FT, Spahl

Inj Vol: 1.000000
Zeit:

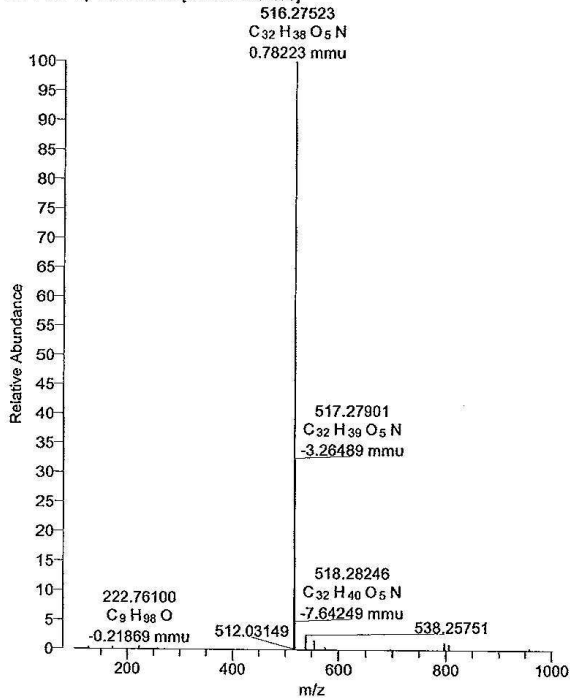


NL: 5.55E5
Base Peak F: FTMS
- p ESI Full ms
[100.00-1000.00]
MS 05-krtoph-622KT

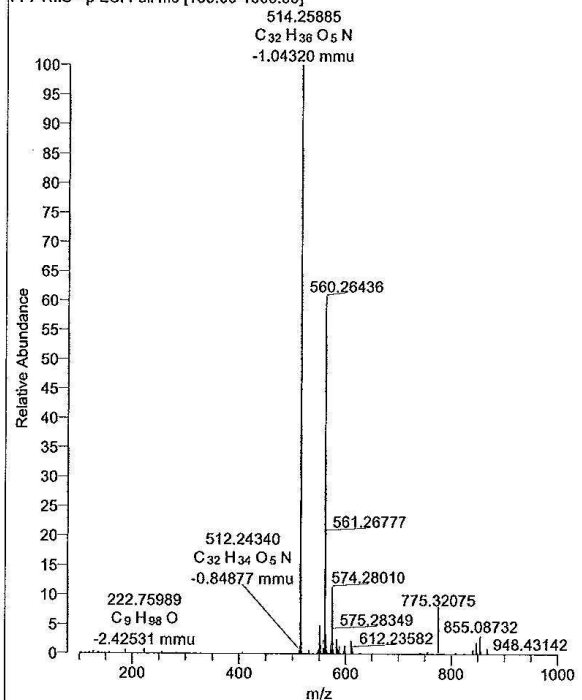


NL: 1.68E6
Base Peak F: FTMS
+ p ESI Full ms
[100.00-1000.00]
MS 05-krtoph-622KT

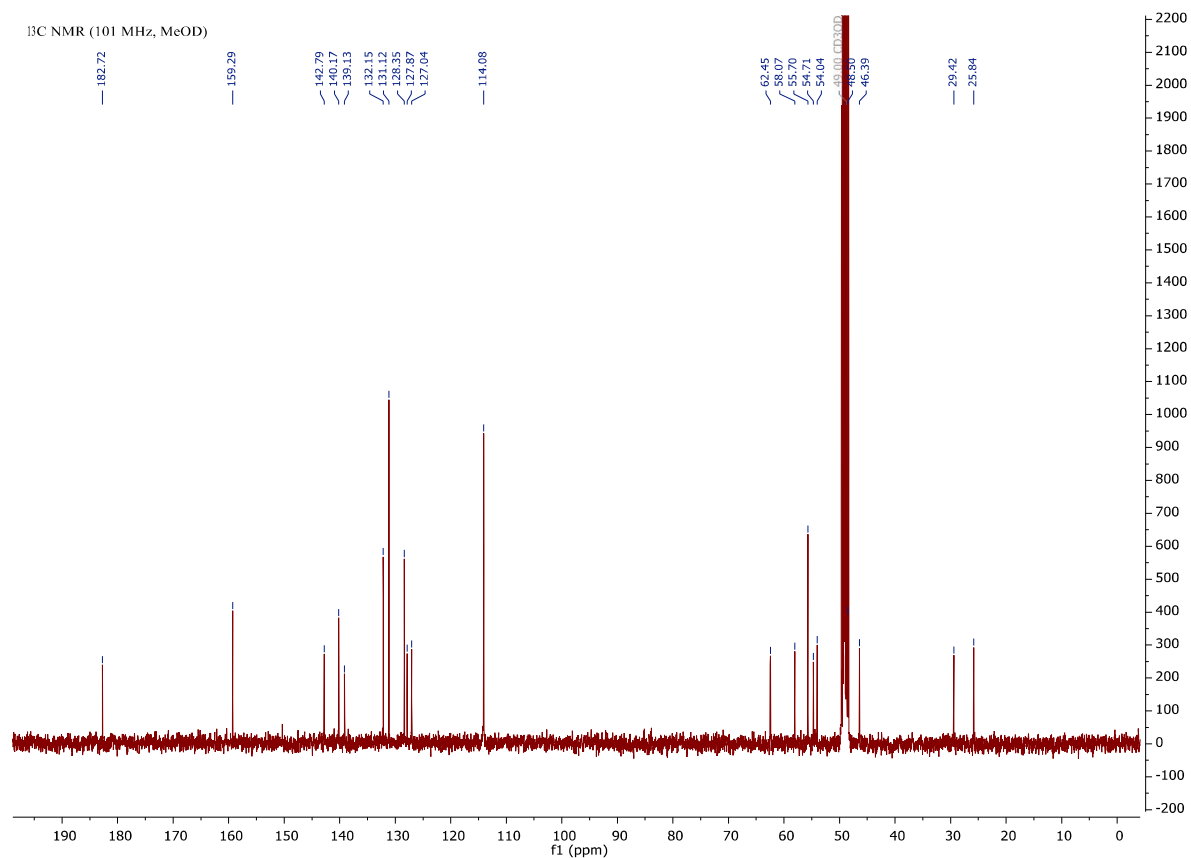
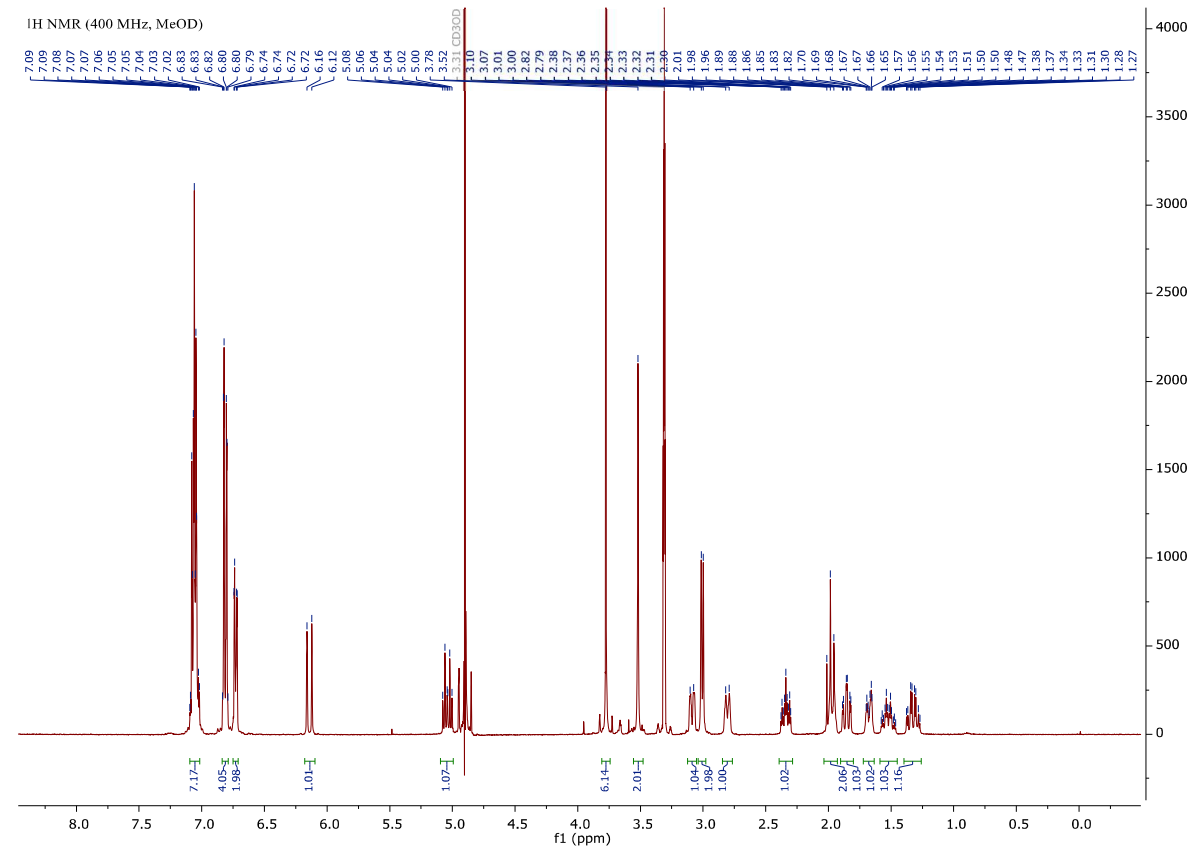
05-krtoph-622KT #49-165 RT: 0.50-1.46 AV: 15 NL: 8.54E5
F: FTMS + p ESI Full ms [100.00-1000.00]



05-krtoph-622KT #49-161 RT: 0.54-1.42 AV: 14 NL: 2.18E5
F: FTMS - p ESI Full ms [100.00-1000.00]



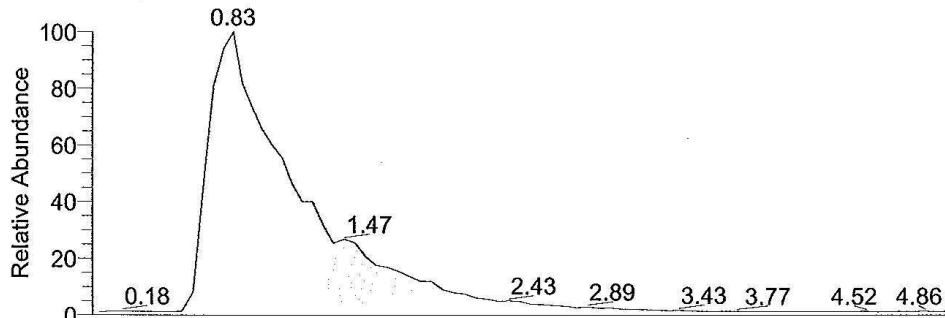
1.9. (E)-1-[4,4-Bis(4-methoxyphenyl)-5-phenylpent-2-en-1-yl]piperidine-3-carboxylic acid, (*rac*-2j)



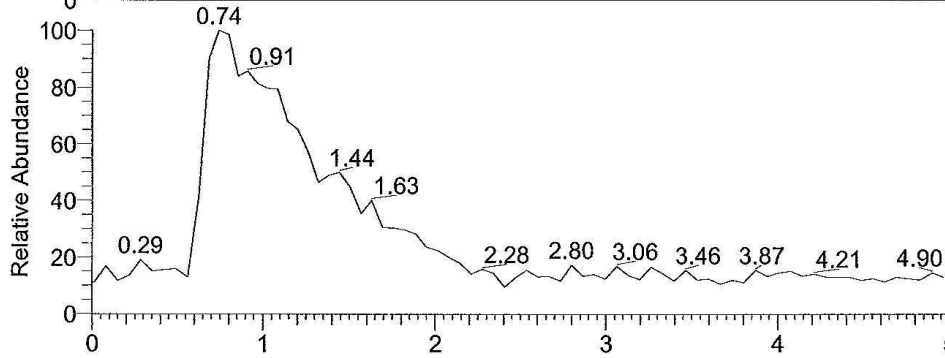
Probennamen: C:\Data\03-krtoph-599KT
Auftraggeber: Toth, Wanner
RT: 0.00 - 5.02

Probe: 485, c31h35no4, fest, Aceton
Methode: 100 u/min Acetonitril/Wasser, FIA/ESI, LTQ FT, Spahl

Inj Vol: 1.000000
Zeit:

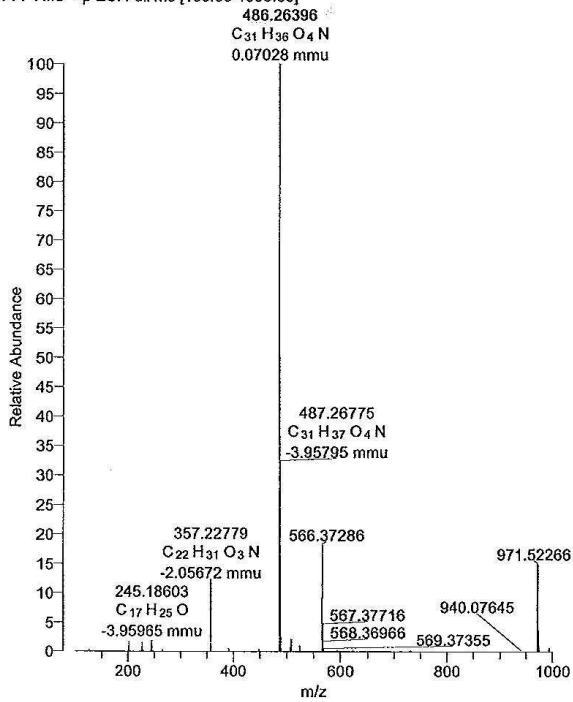


NL: 4.00E6
Base Peak F: FTMS
- p ESI Full ms
[100.00-1000.00]
MS 03-krtoph-599KT

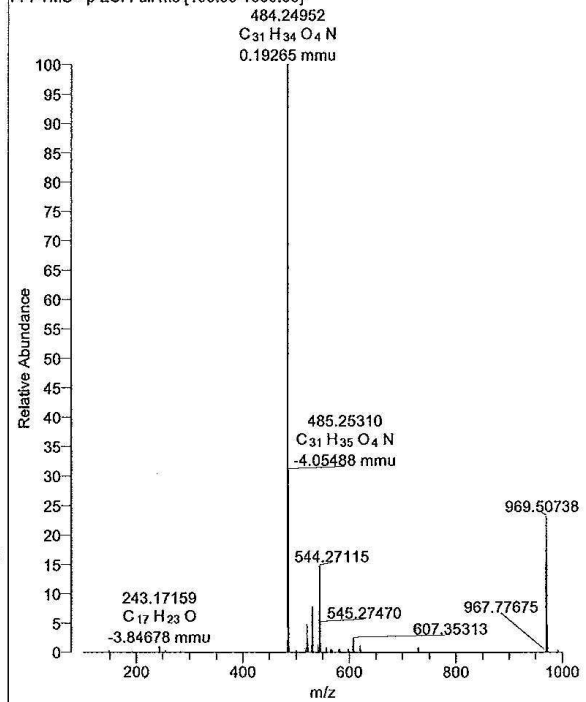


NL: 9.60E6
Base Peak F: FTMS
+ p ESI Full ms
[100.00-1000.00]
MS 03-krtoph-599KT

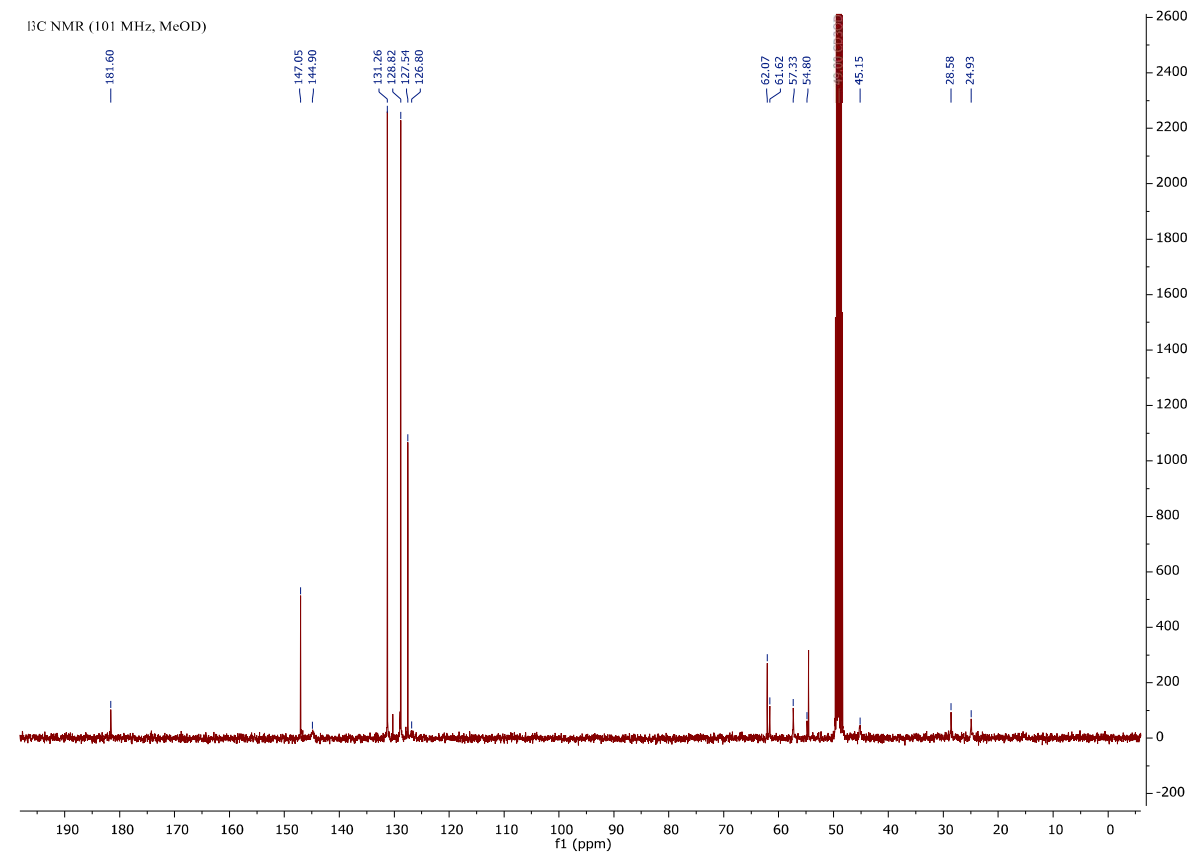
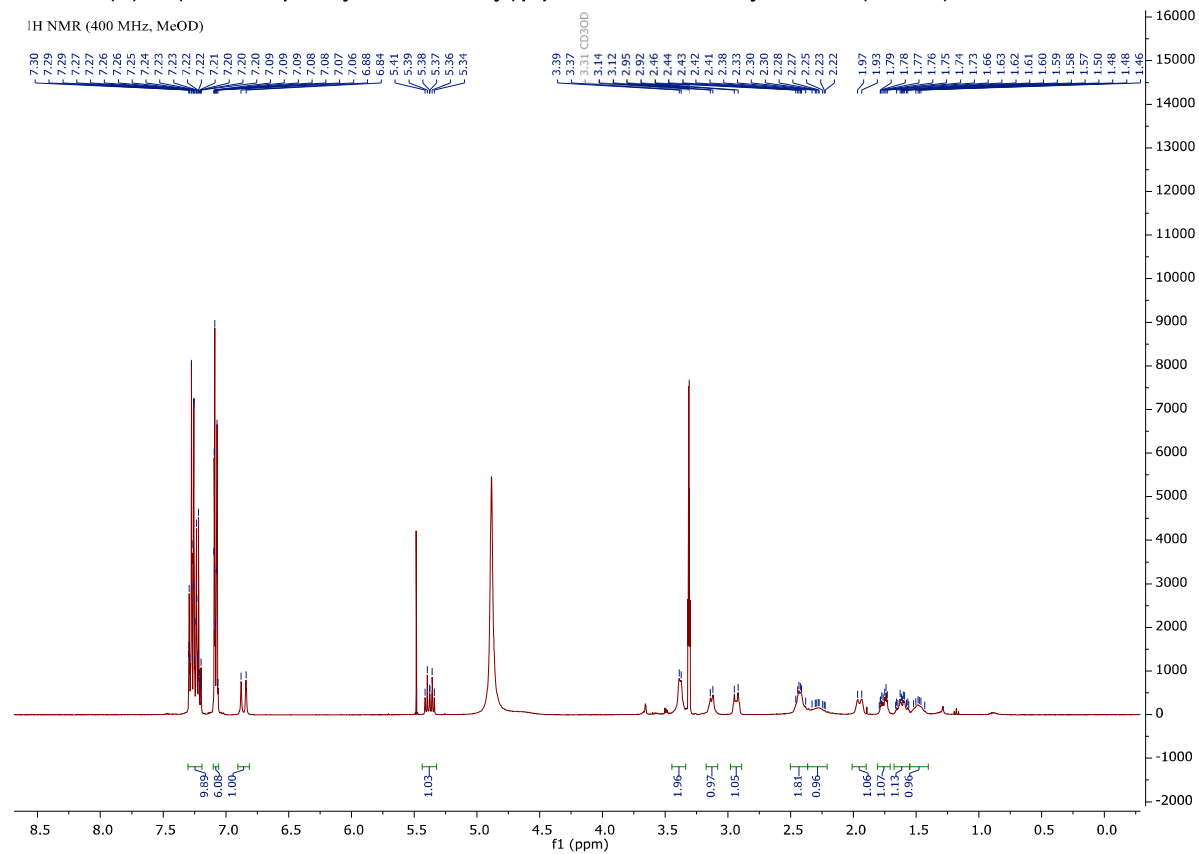
03-krtoph-599KT #57-192 RT: 0.49-1.44 AV: 17 NL: 6.09E6
F: FTMS + p ESI Full ms [100.00-1000.00]



03-krtoph-599KT #57-187 RT: 0.52-1.41 AV: 16 NL: 2.12E6
F: FTMS - p ESI Full ms [100.00-1000.00]



1.10. (E)-1-(4,4-Triphenylbut-2-en-1-yl)piperidine-3-carboxylic acid, (*rac*-**2k**)

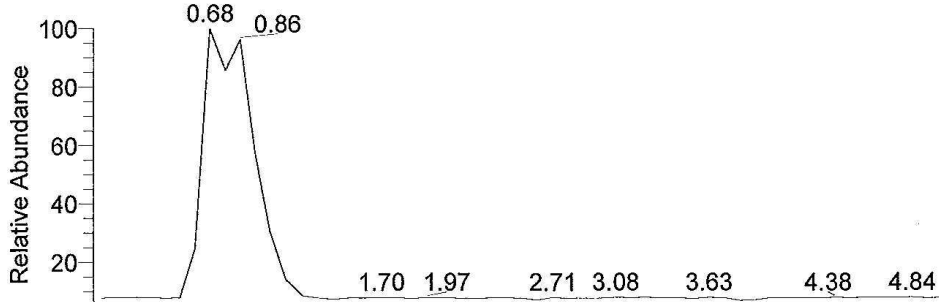


Probenbezeichnung: C:\Data\06-krtoph-297KT
 Auftraggeber: Tolth, Wanner

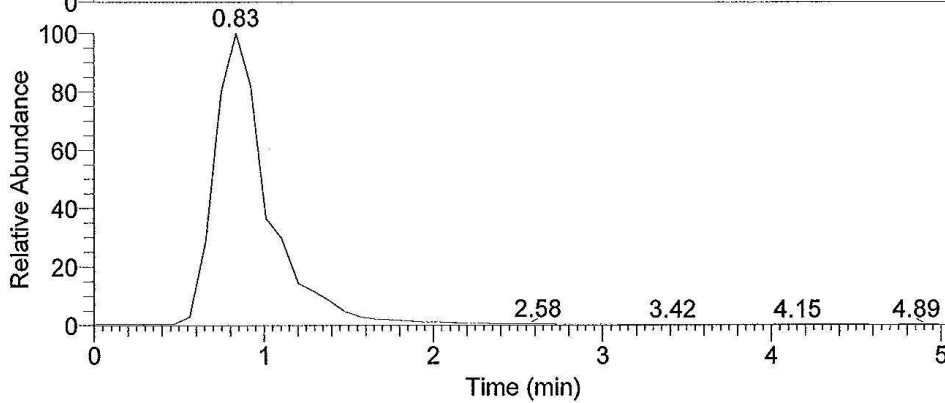
Probe: 411, c28h29no2, fest, Aceton
 Methode: 100 ul/min Acetonitril/Wasser, FIA/ESI, LTQ FT, Spahl

Inj Vol: 1.000000
 Zeit:

RT: 0.00 - 5.07

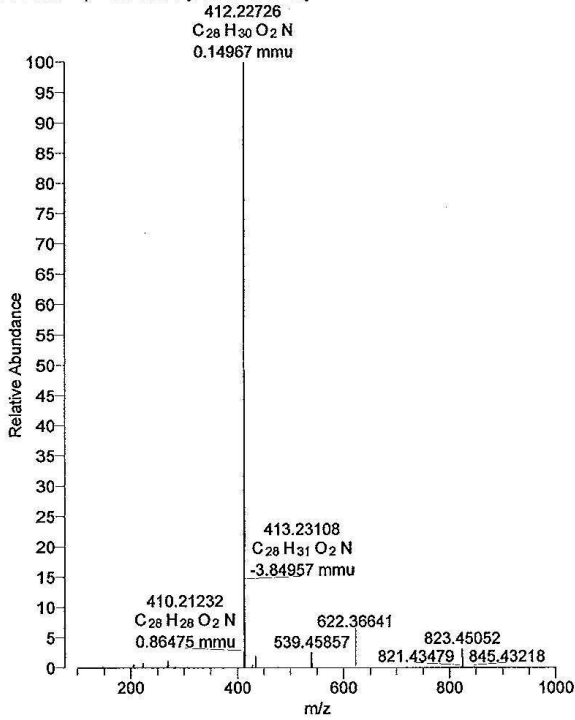


NL: 2.64E5
 Base Peak F: FTMS
 - p ESI Full ms
 [100.00-1000.00]
 MS 06-krtoph-297KT

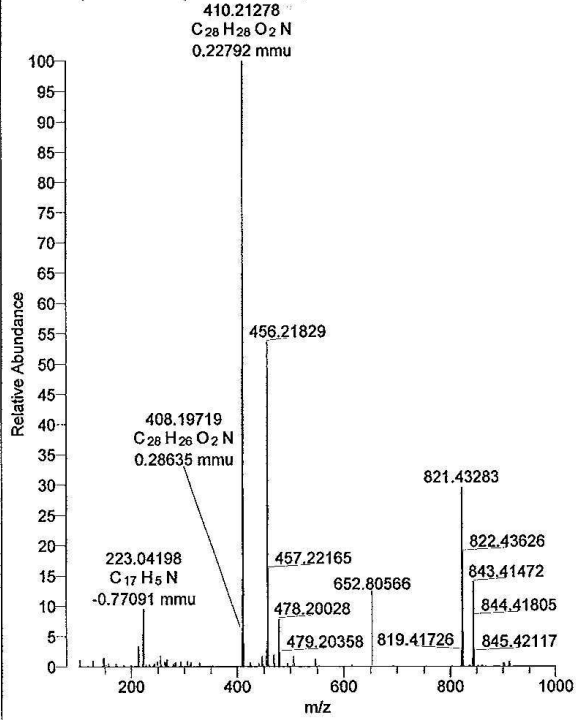


NL: 9.29E6
 Base Peak F: FTMS
 + p ESI Full ms
 [100.00-1000.00]
 MS 06-krtoph-297KT

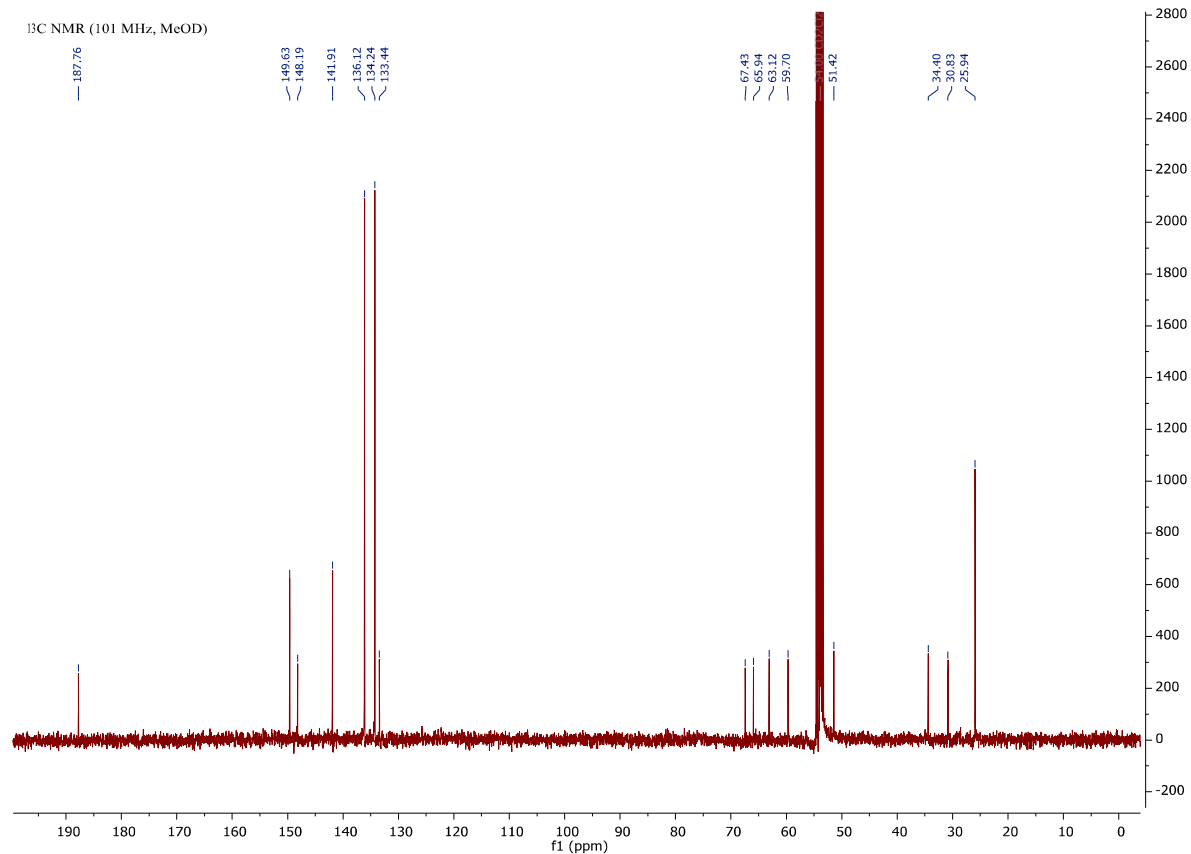
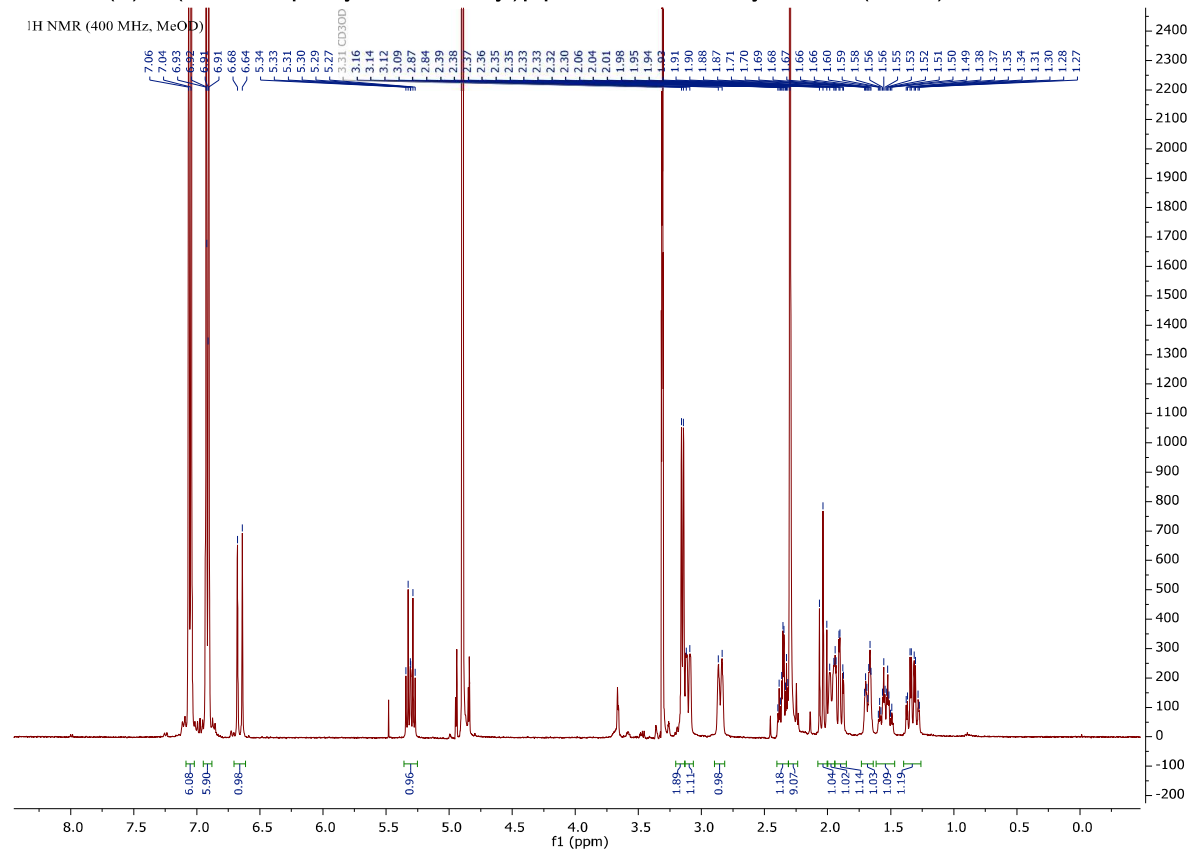
06-krtoph-297KT #39-123 RT: 0.56-1.48 AV: 11 NL: 3.29E6
 F: FTMS + p ESI Full ms [100.00-1000.00]



06-krtoph-297KT #39-119 RT: 0.51-1.42 AV: 11 NL: 1.01E5
 F: FTMS - p ESI Full ms [100.00-1000.00]



1.11. (E)-1-(4,4,4-Tri-p-tolylbut-2-en-1-yl)piperidine-3-carboxylic acid, (*rac*-**21**)

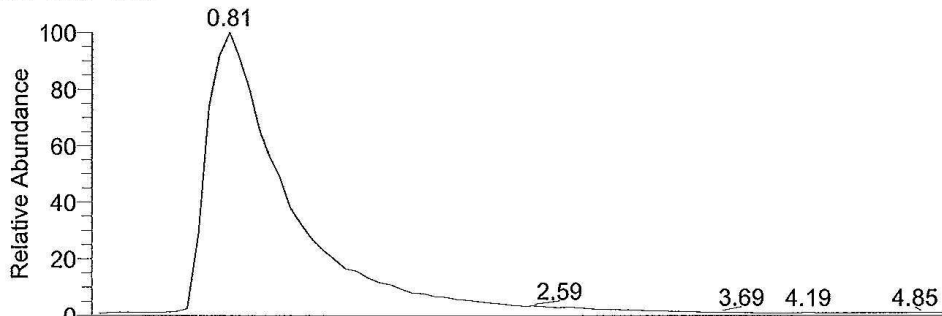


Probenname: C:\Data\03-krthoph-596KT
Auftraggeber: Toth, Wanner

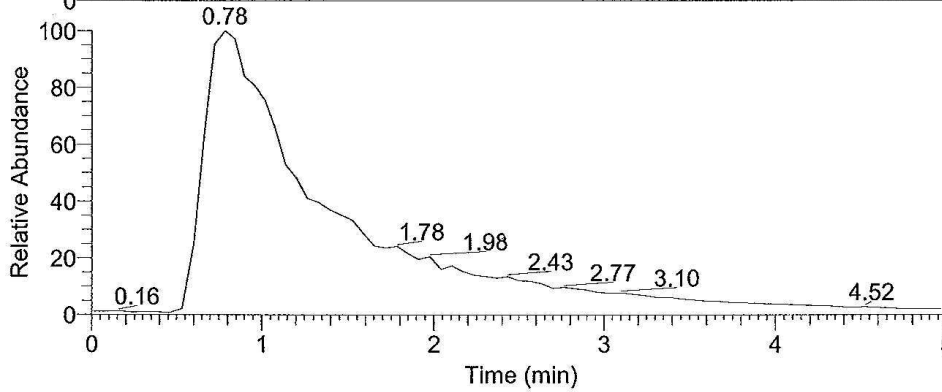
Probe: 453, c31h35no2, fest, Aceton
Methode: 100 ul/min Acetonitril/Wasser, FIA/ESI, LTQ FT, Spahl

Inj Vol: 1.000000
Zeit:

RT: 0.00 - 5.02

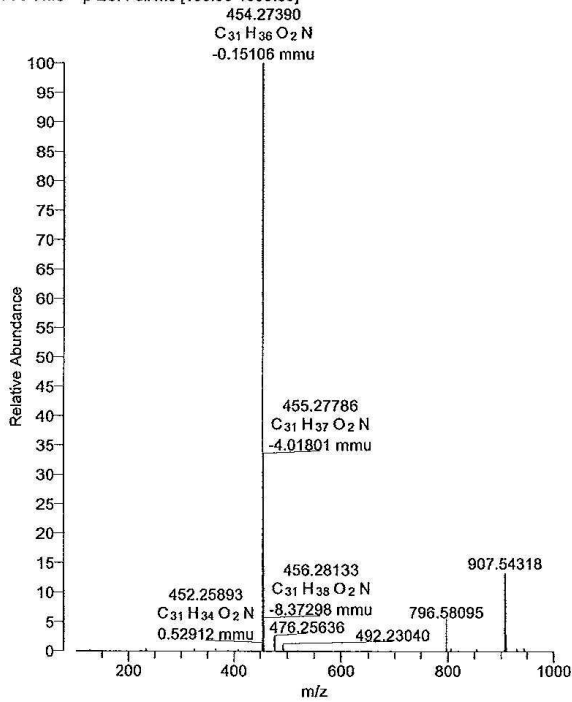


NL: 2.37E6
Base Peak F:
FTMS - p ESI Full
ms
[100.00-1000.00]
MS
03-krthoph-596KT

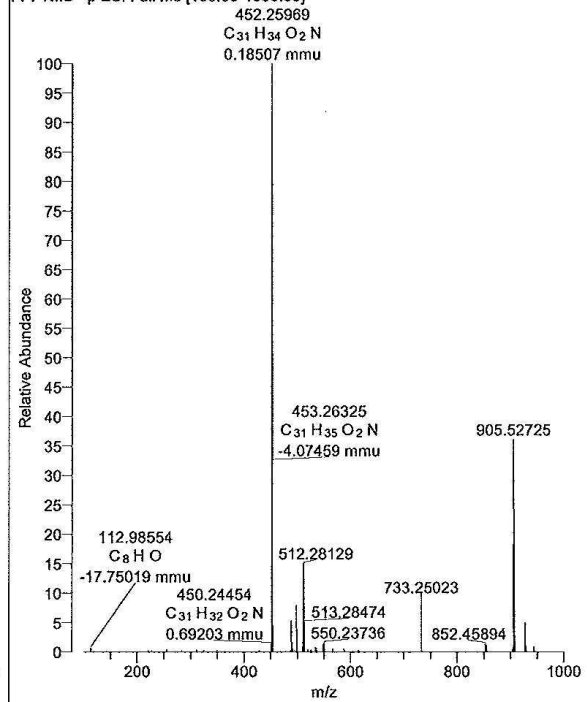


NL: 7.12E6
Base Peak F:
FTMS + p ESI Full
ms
[100.00-1000.00]
MS
03-krthoph-596KT

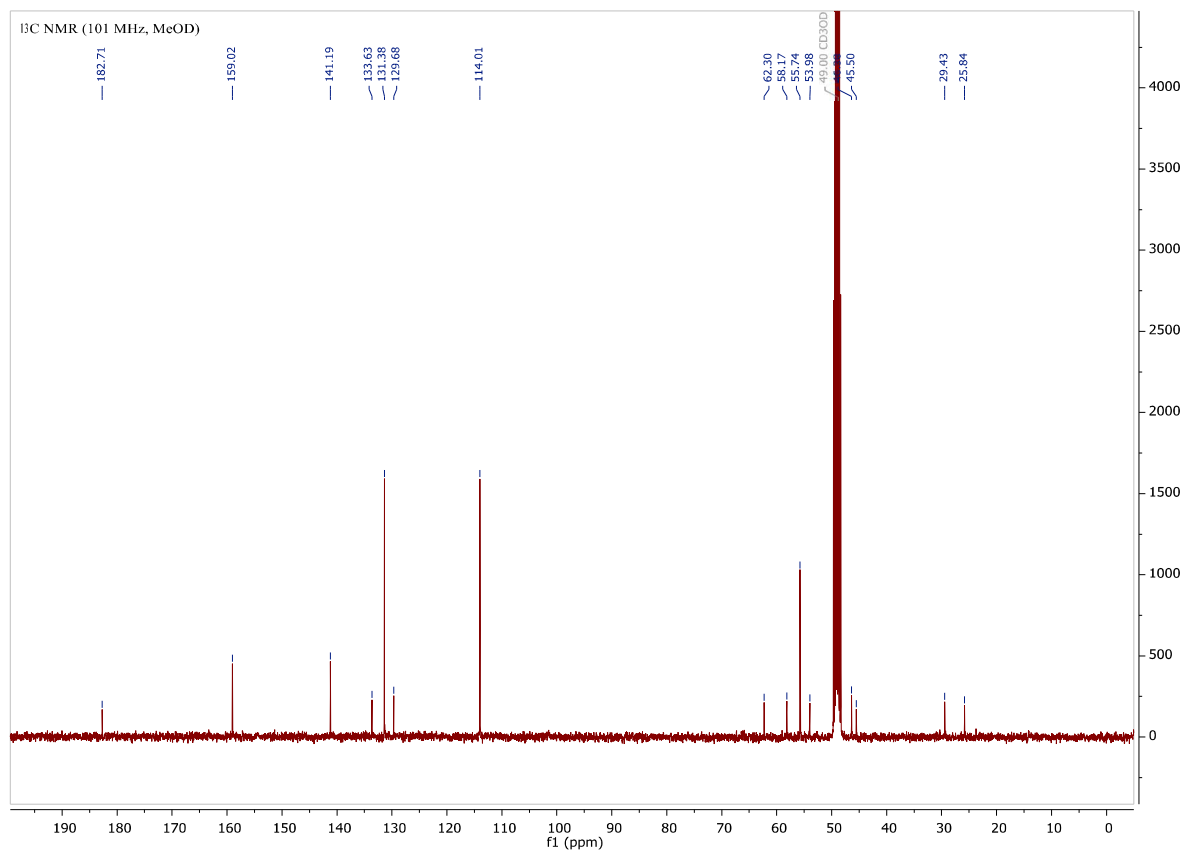
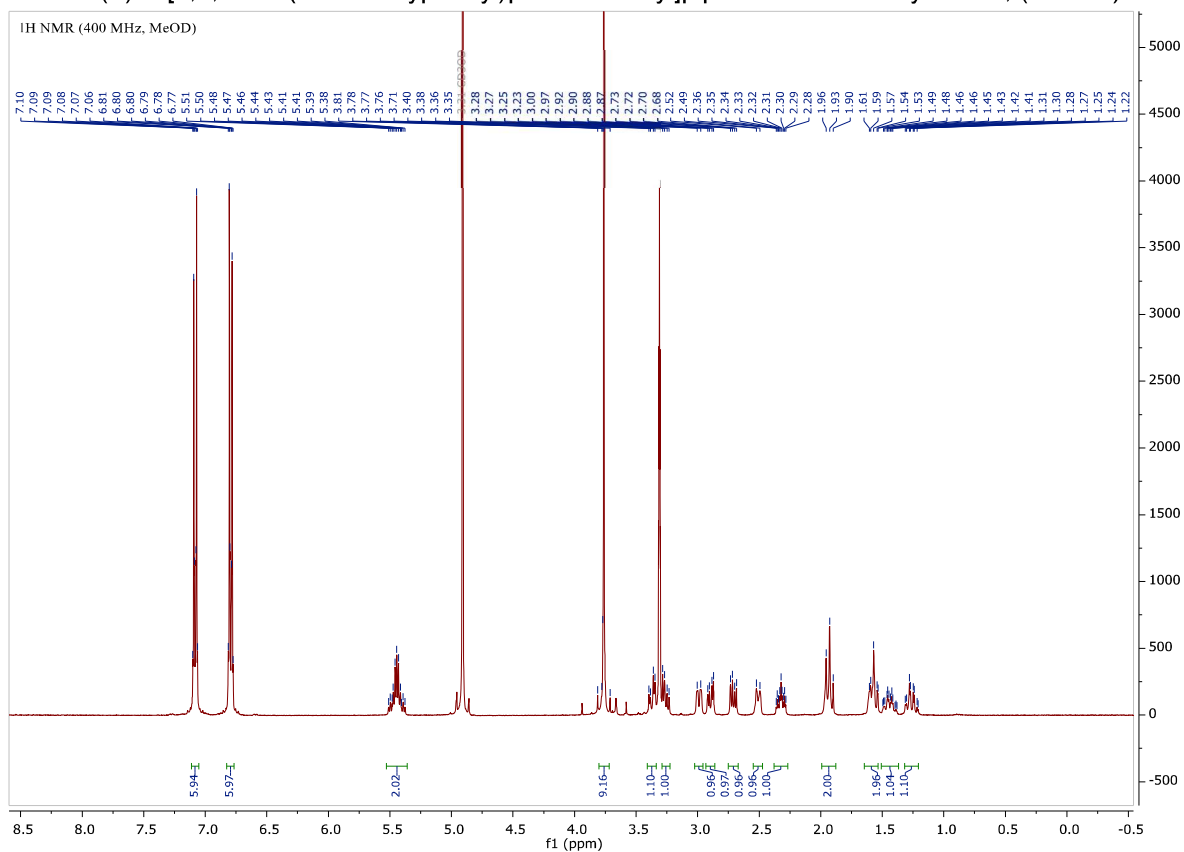
03-krthoph-596KT #53-182 RT: 0.53-1.46 AV: 16 NL: 4.17E6
F: FTMS + p ESI Full ms [100.00-1000.00]



03-krthoph-596KT #53-177 RT: 0.49-1.42 AV: 16 NL: 1.09E6
F: FTMS - p ESI Full ms [100.00-1000.00]



1.12. (E)-1-[5,5,5-Tris(4-methoxyphenyl)pent-2-en-1-yl]piperidine-3-carboxylic acid, (*rac*-2m)

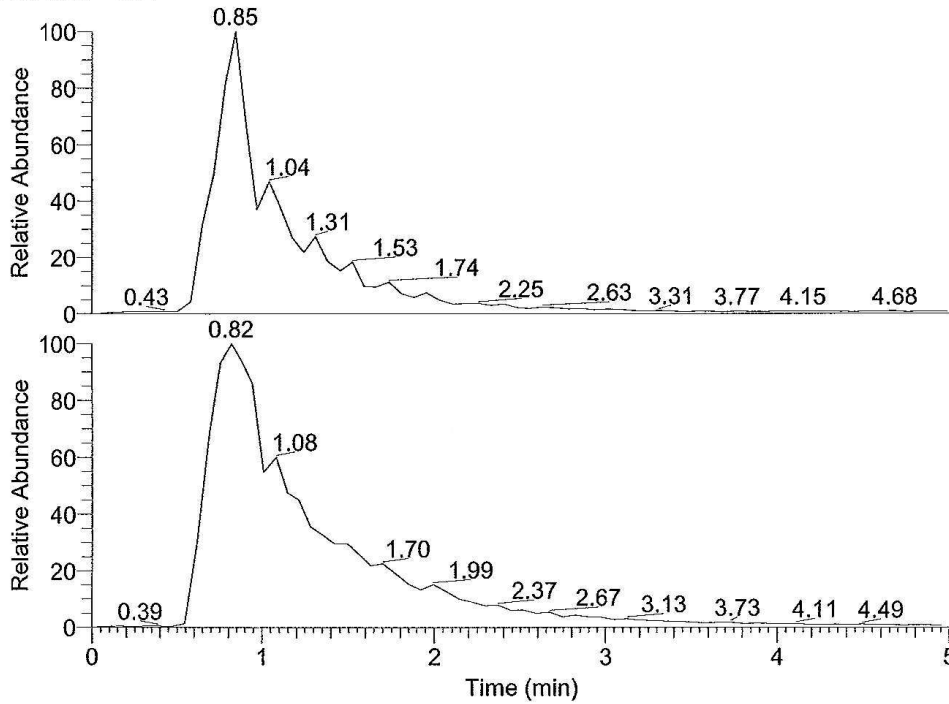


Probenbezeichnung: C:\Data\10-krtoph-536KT
Auftraggeber: Toth, Wanner

Probe: 515, c32h37no5, fest, Aceton
Methode: 100 ul/min Acetonitril/Wasser, FIA/ESI, LTQ FT, Spahl

Inj Vol: 1.000000
Zeit:

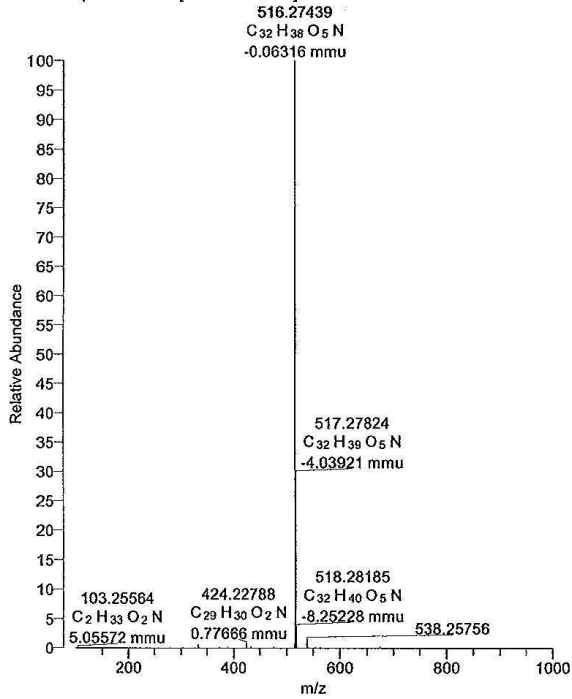
RT: 0.00 - 5.01



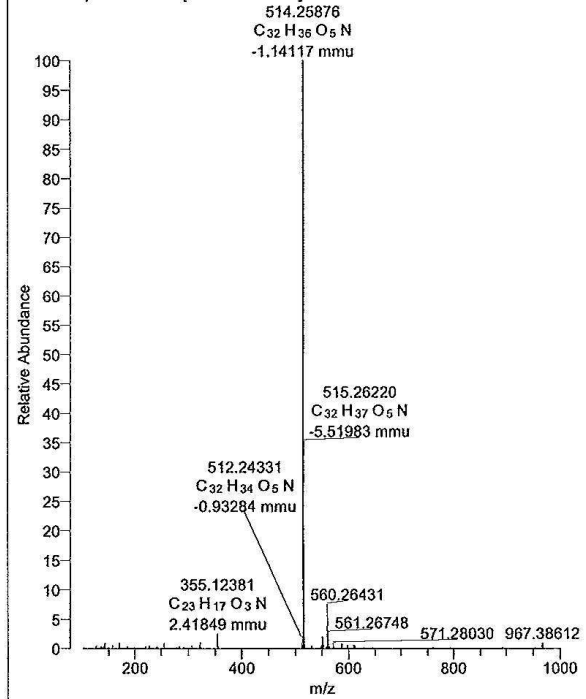
NL: 5.12E5
Base Peak F: FTMS
- p ESI Full ms
[100.00-1000.00]
MS 10-krtoph-536KT

NL: 7.40E6
Base Peak F: FTMS
+ p ESI Full ms
[100.00-1000.00]
MS 10-krtoph-536KT

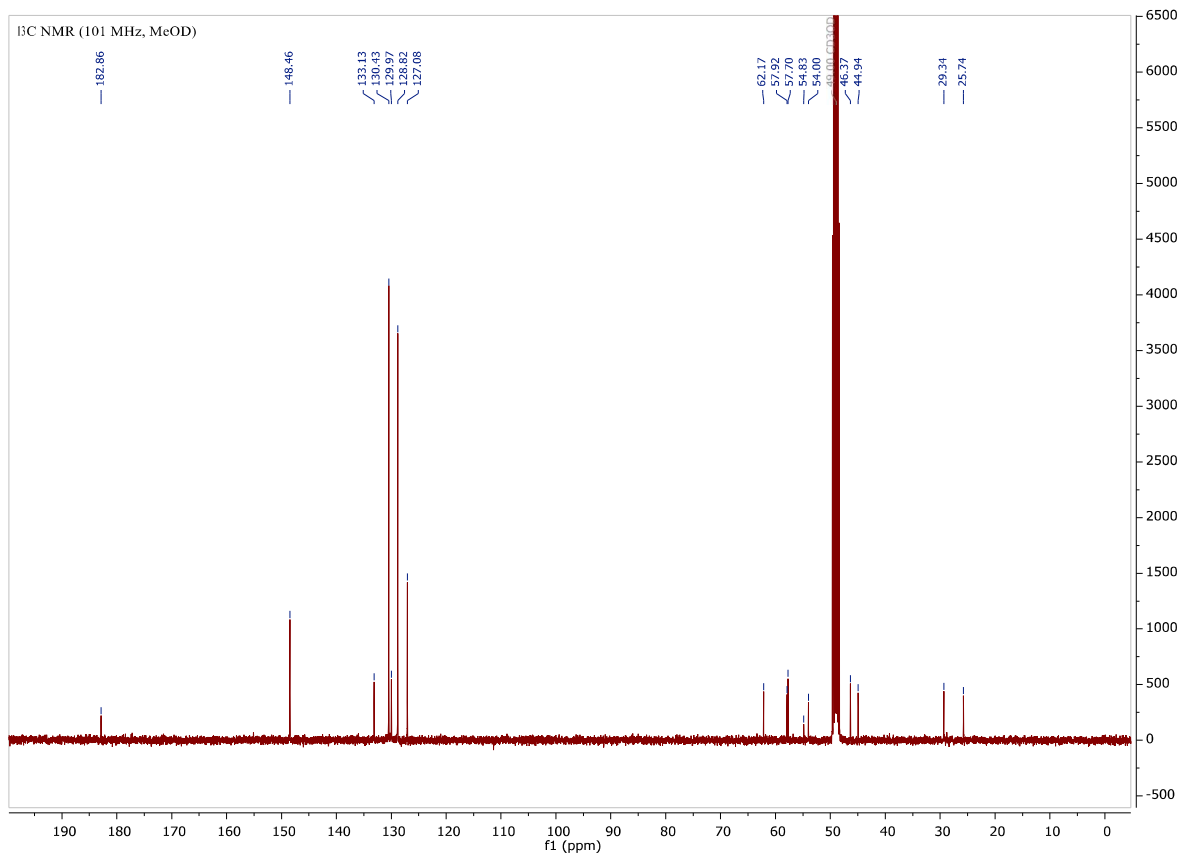
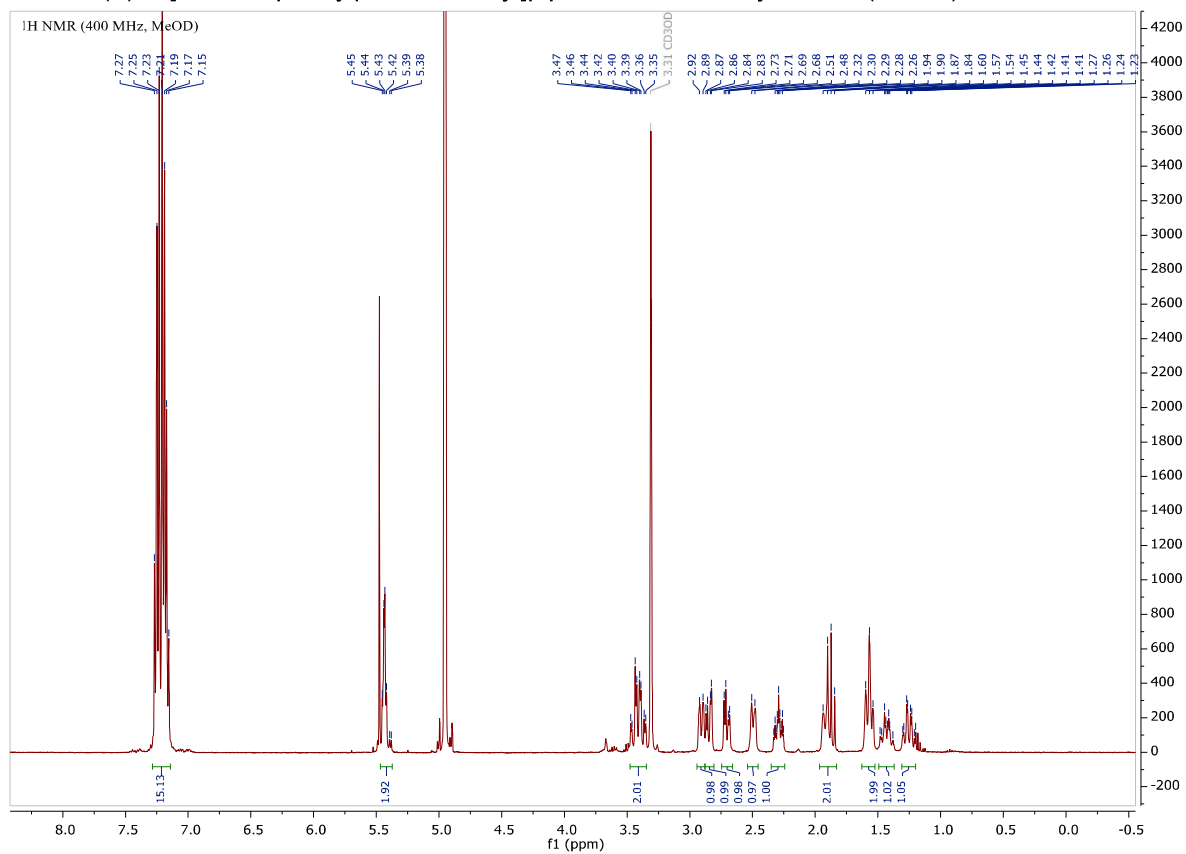
10-krtoph-536KT #52-169 RT: 0.54-1.49 AV: 15 NL: 3.90E6
F: FTMS + p ESI Full ms [100.00-1000.00]



10-krtoph-536KT #52-165 RT: 0.50-1.46 AV: 15 NL: 1.84E5
F: FTMS - p ESI Full ms [100.00-1000.00]



1.13. (E)-1-[5,5,5-Triphenylpent-2-en-1-yl]piperidine-3-carboxylic acid, (*rac*-**2n**)

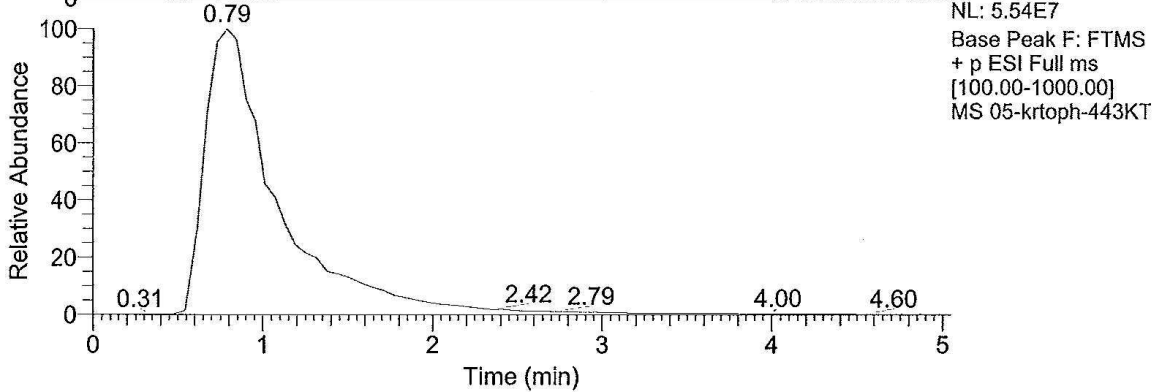
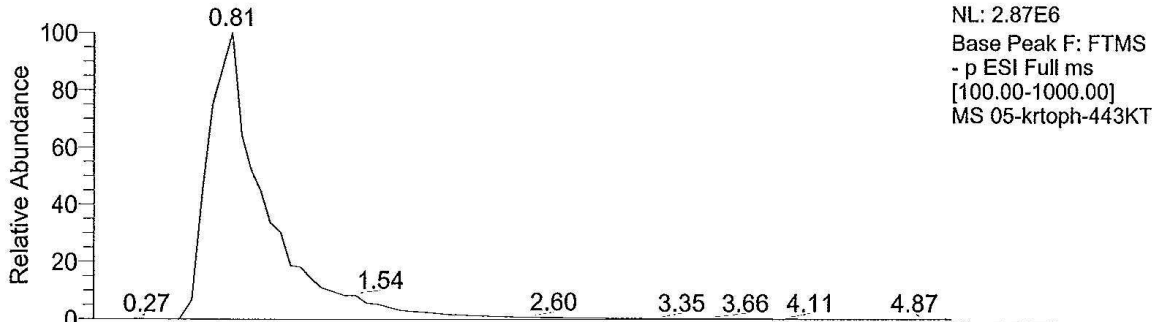


Probenbezeichnung: C:\Data\05-krtoph-443KT
Auftraggeber: Toth, Wanner

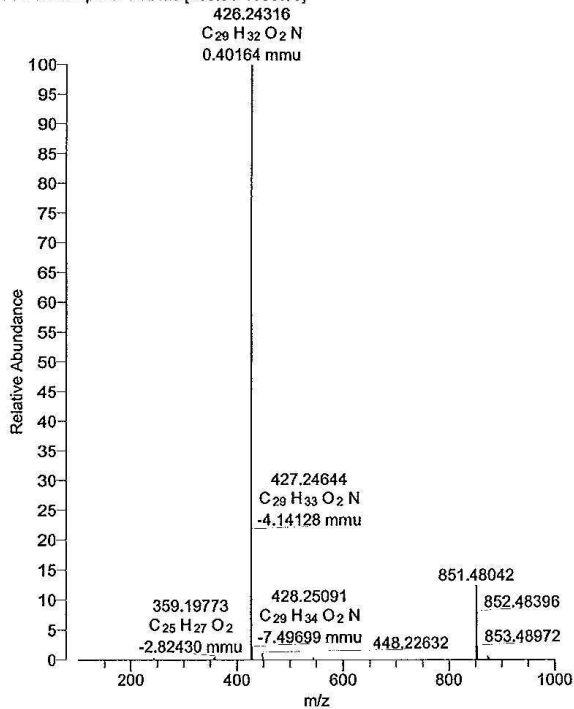
Probe: 425, c29h31no2, fest, Aceton
Methode: 100 ul/min Acetonitril/Wasser, FIA/ESI, LTQ FT, Spahl

Inj Vol: 1.000000
Zeit:

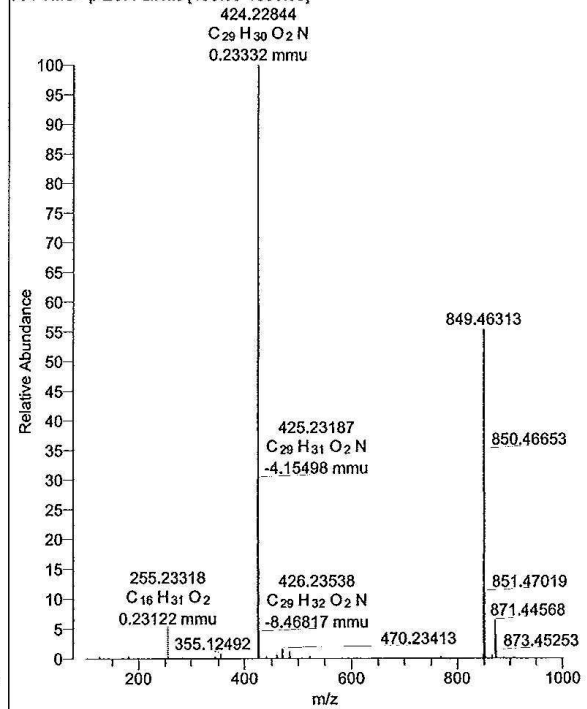
RT: 0.00 - 5.05



05-krtoph-443KT #52-184 RT: 0.54-1.44 AV: 16 NL: 2.50E7
F: FTMS + p ESI Full ms [100.00-1000.00]

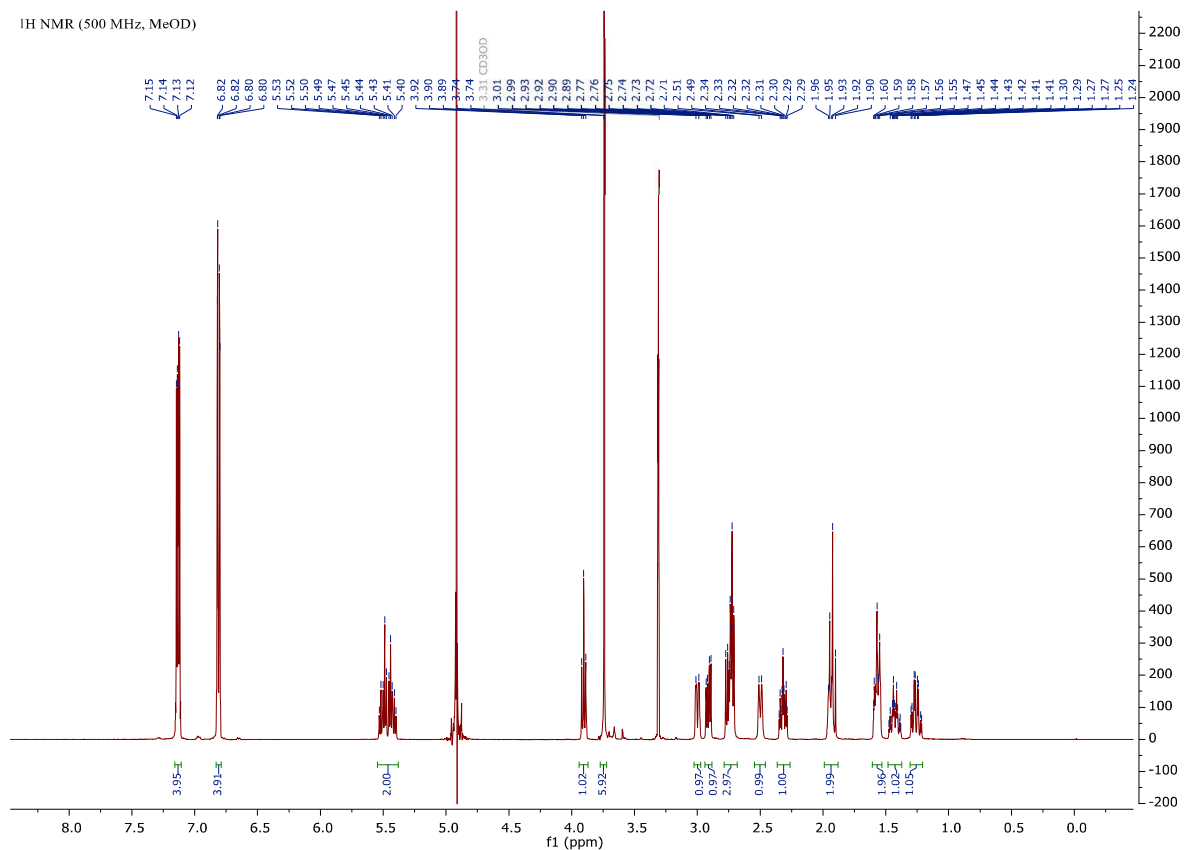


05-krtoph-443KT #52-179 RT: 0.50-1.41 AV: 16 NL: 1.08E6
F: FTMS - p ESI Full ms [100.00-1000.00]

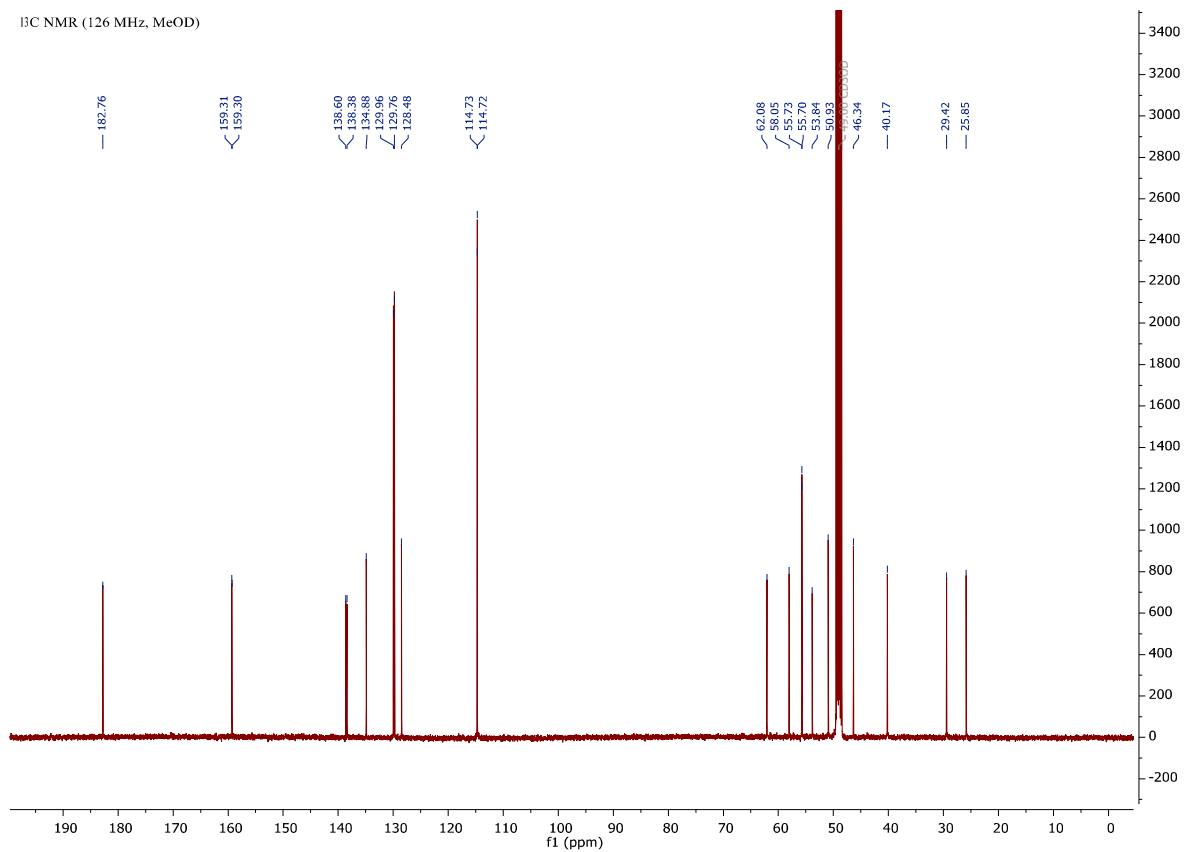


1.14. (E)-1-[5,5-Bis(4-methoxyphenyl)pent-2-en-1-yl]piperidine-3-carboxylic acid, (*rac*-**2o**)

¹H NMR (500 MHz, MeOD)



¹³C NMR (126 MHz, MeOD)



- Second publication -

Probenname: C:\Data\07-krtoph-655KT

Probe: 409. c25h31no4, fest, Aceton

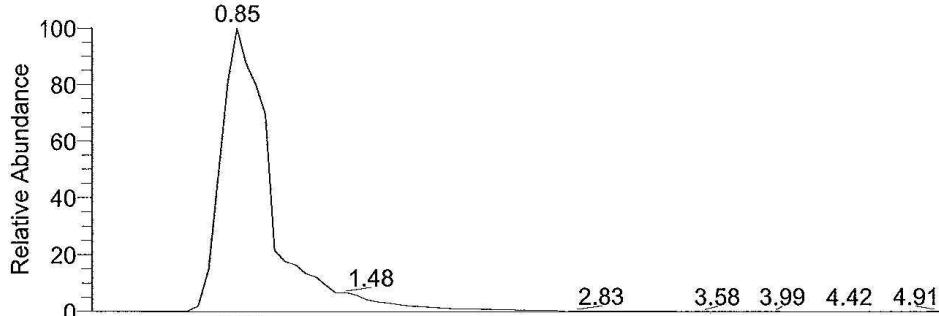
Inj Vol: 1.000000

Auftragegeber: Toth, Wanner

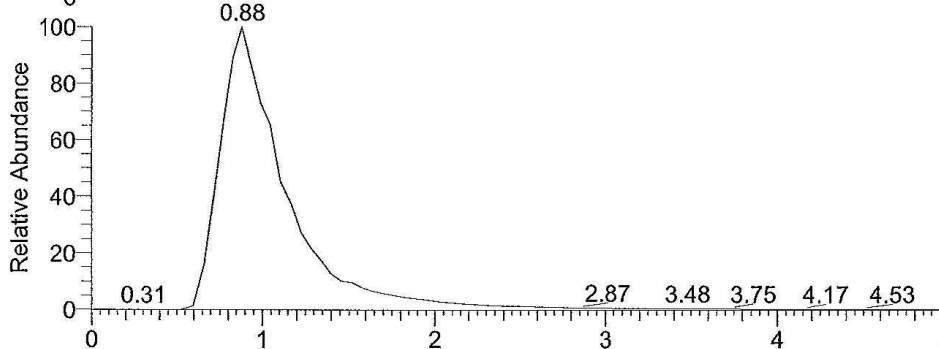
Methode: 100 ul/min Acetonitril/Wasser, FIA/ESI, LTQ FT, Spahl

Zelt:

RT: 0.00 - 5.01



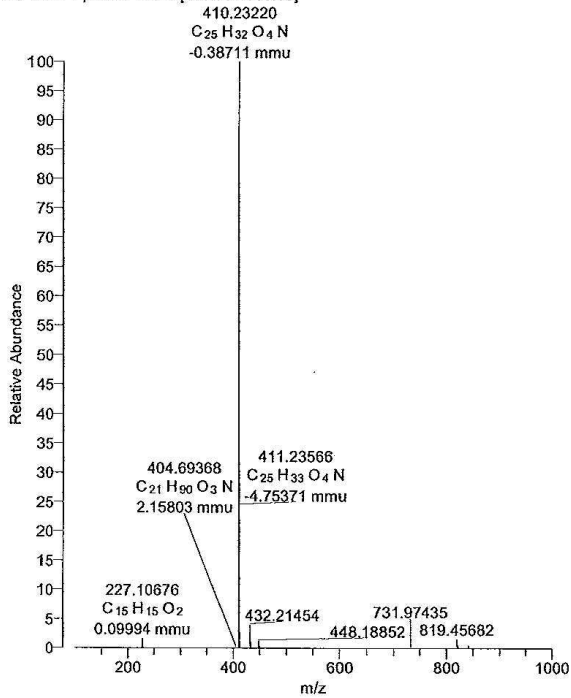
NL: 1.42E7
Base Peak F: FTMS
- p ESI Full ms
[100.00-1000.00]
MS 07-krtoph-655KT



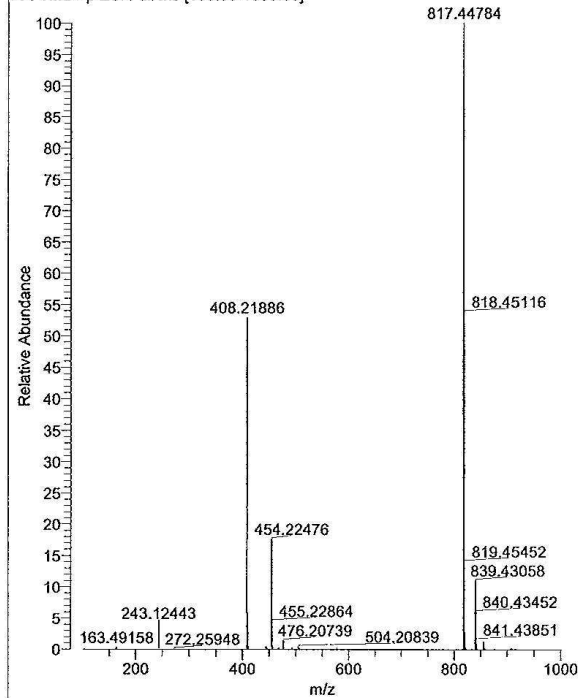
NL: 6.32E7
Base Peak F: FTMS
+ p ESI Full ms
[100.00-1000.00]
MS 07-krtoph-655KT

Time (min)

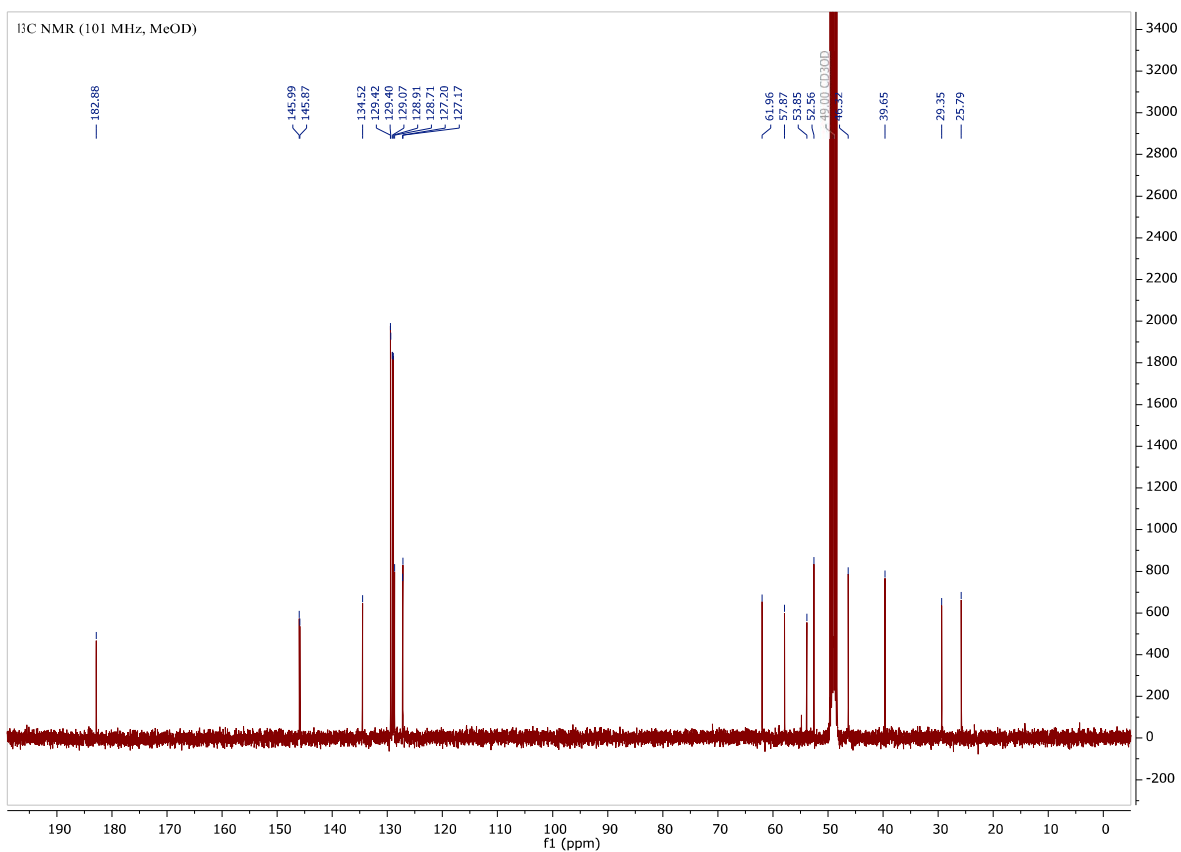
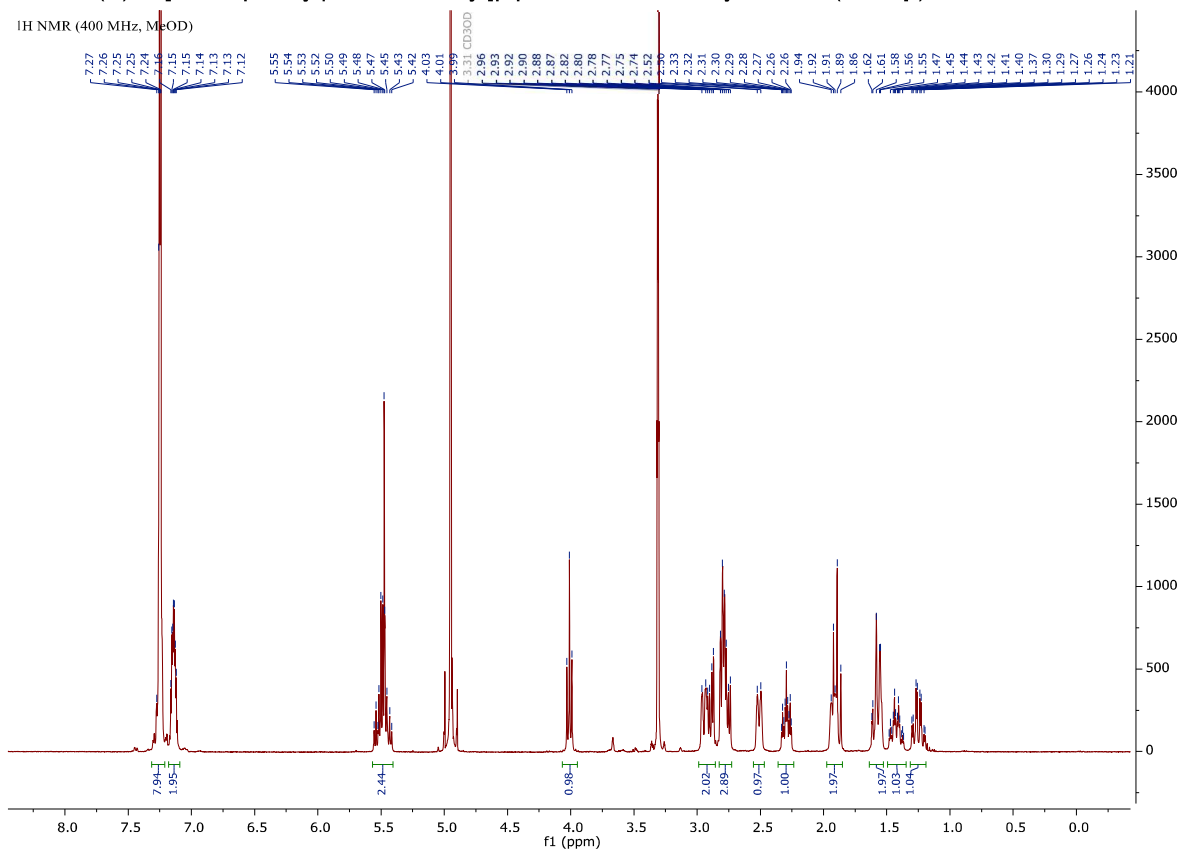
07-krtoph-655KT #54-190 RT: 0.52-1.46 AV: 17 NL: 2.62E7
F: FTMS + p ESI Full ms [100.00-1000.00]



07-krtoph-655KT #54-185 RT: 0.56-1.43 AV: 16 NL: 4.69E6
F: FTMS - p ESI Full ms [100.00-1000.00]



1.15. (E)-1-[5,5-Diphenylpent-2-en-1-yl]piperidine-3-carboxylic acid, (rac-2p)

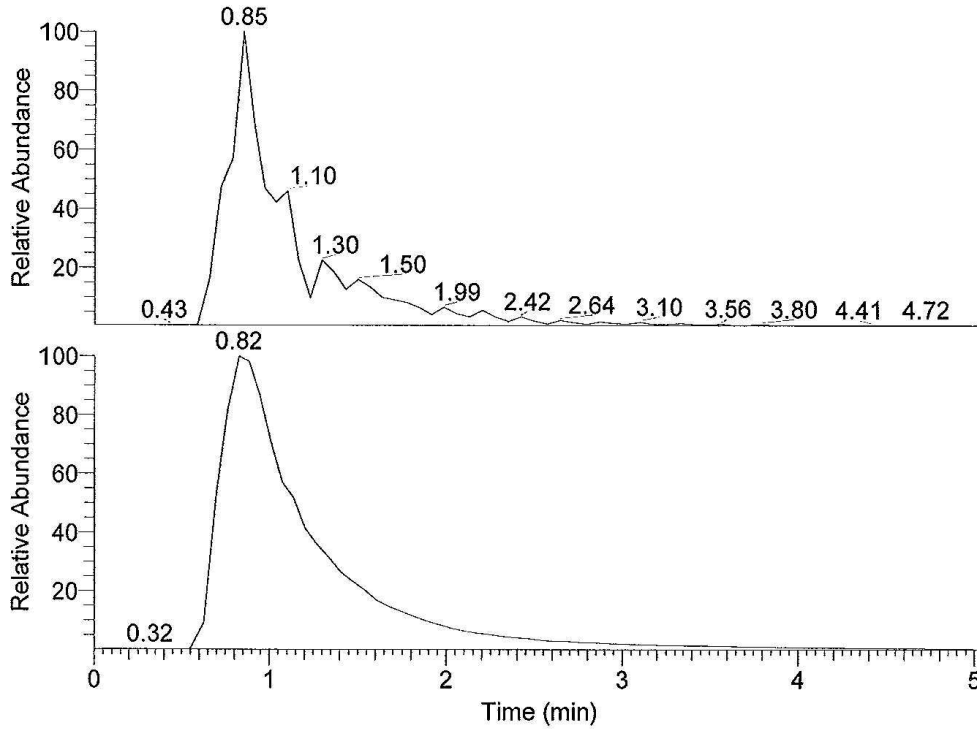


Probenbezeichnung: C:\Data\02-krtoph-404KT
 Auftraggeber: Toth, Wanner

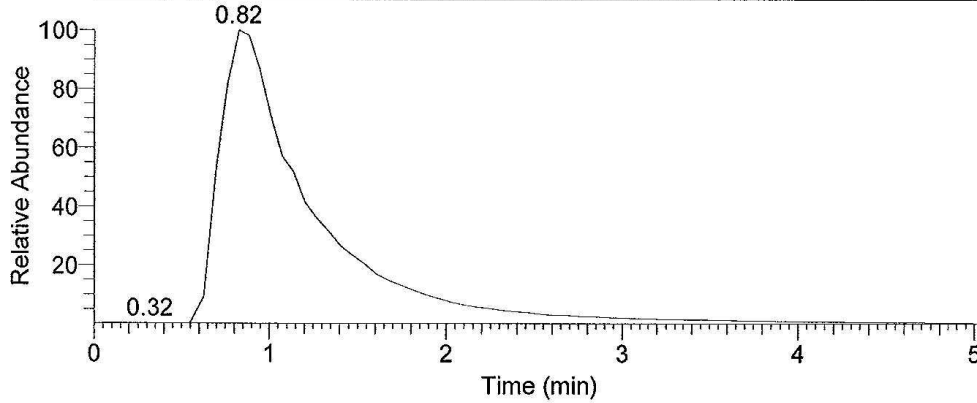
Probe: 349, c23h27no2, fest, Aceton
 Methode: 100 ul/min Acetonitril/Wasser, FIA/ESI, LTQ FT, Spahl

Inj Vol: 1.000000
 Zeit:

RT: 0.00 - 5.06

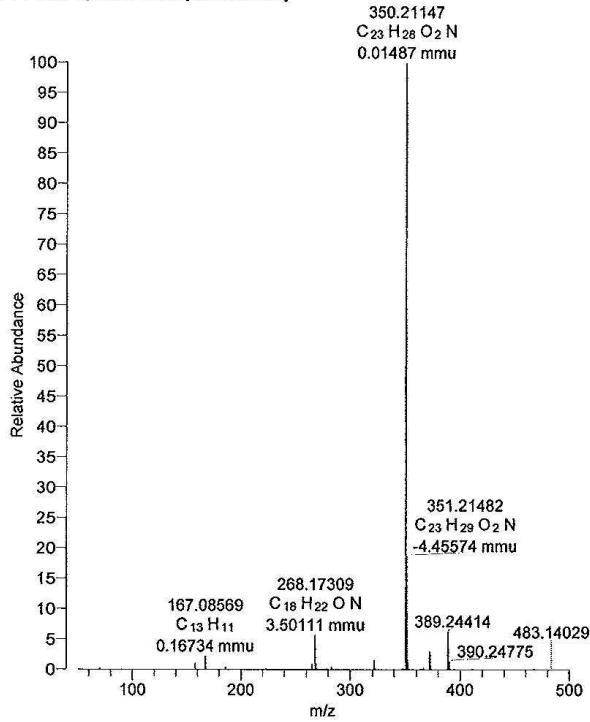


NL: 2.74E6
 Base Peak F:
 FTMS - p ESI Full
 ms [50.00-500.00]
 MS
 02-krtoph-404KT

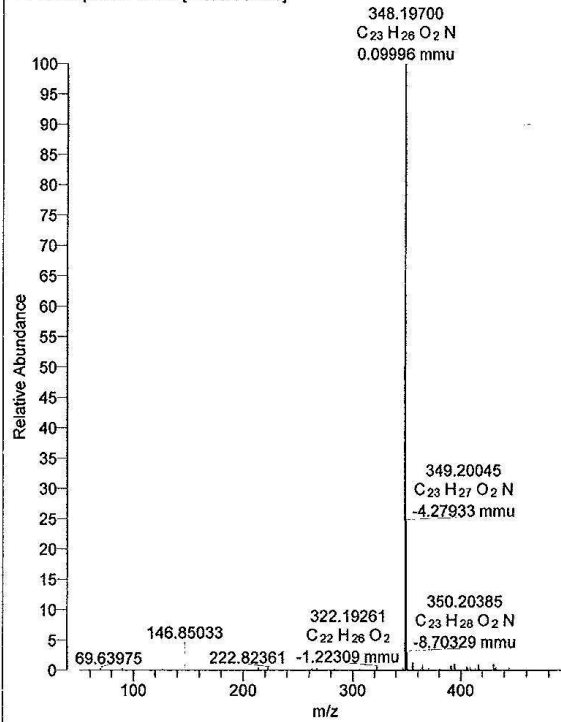


NL: 3.06E7
 Base Peak F:
 FTMS + p ESI Full
 ms [50.00-500.00]
 MS
 02-krtoph-404KT

02-krtoph-404KT #50-232 RT: 0.55-1.95 AV: 22 NL: 1.17E7
 F: FTMS + p ESI Full ms [50.00-500.00]

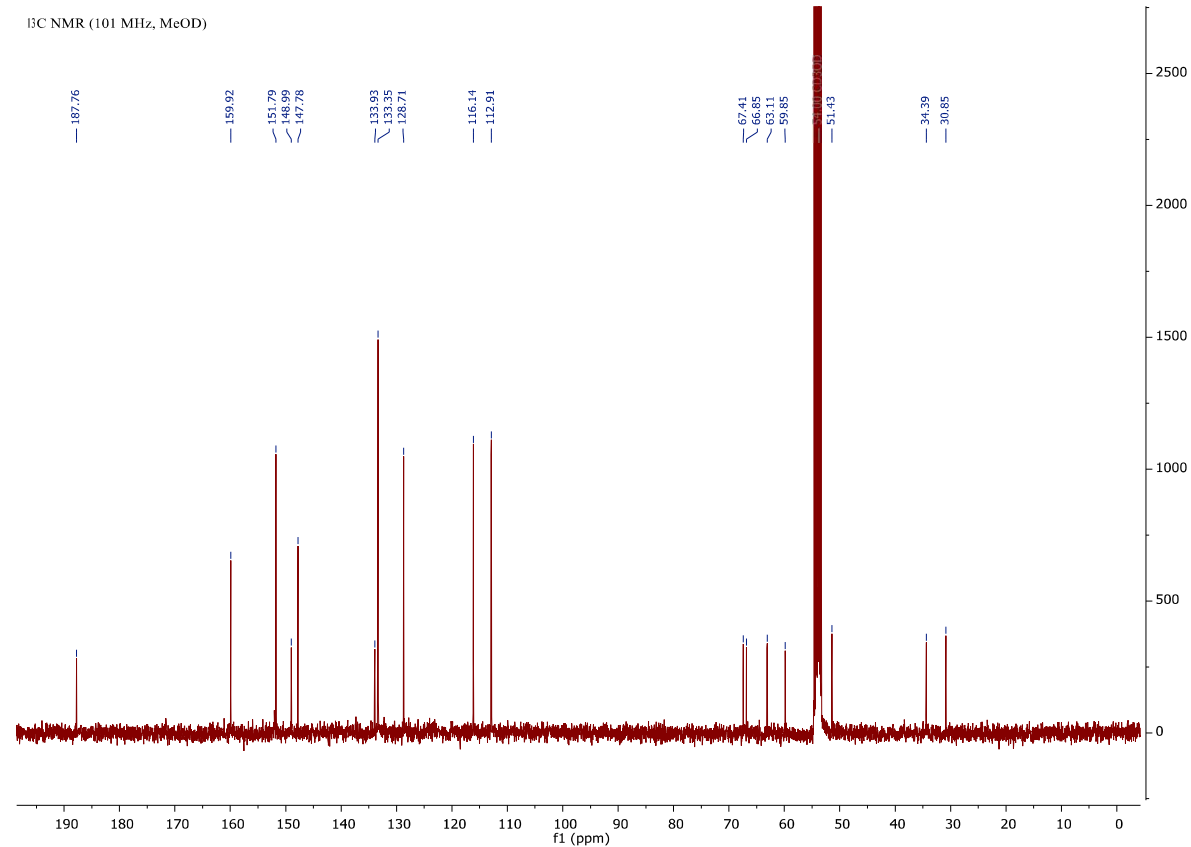
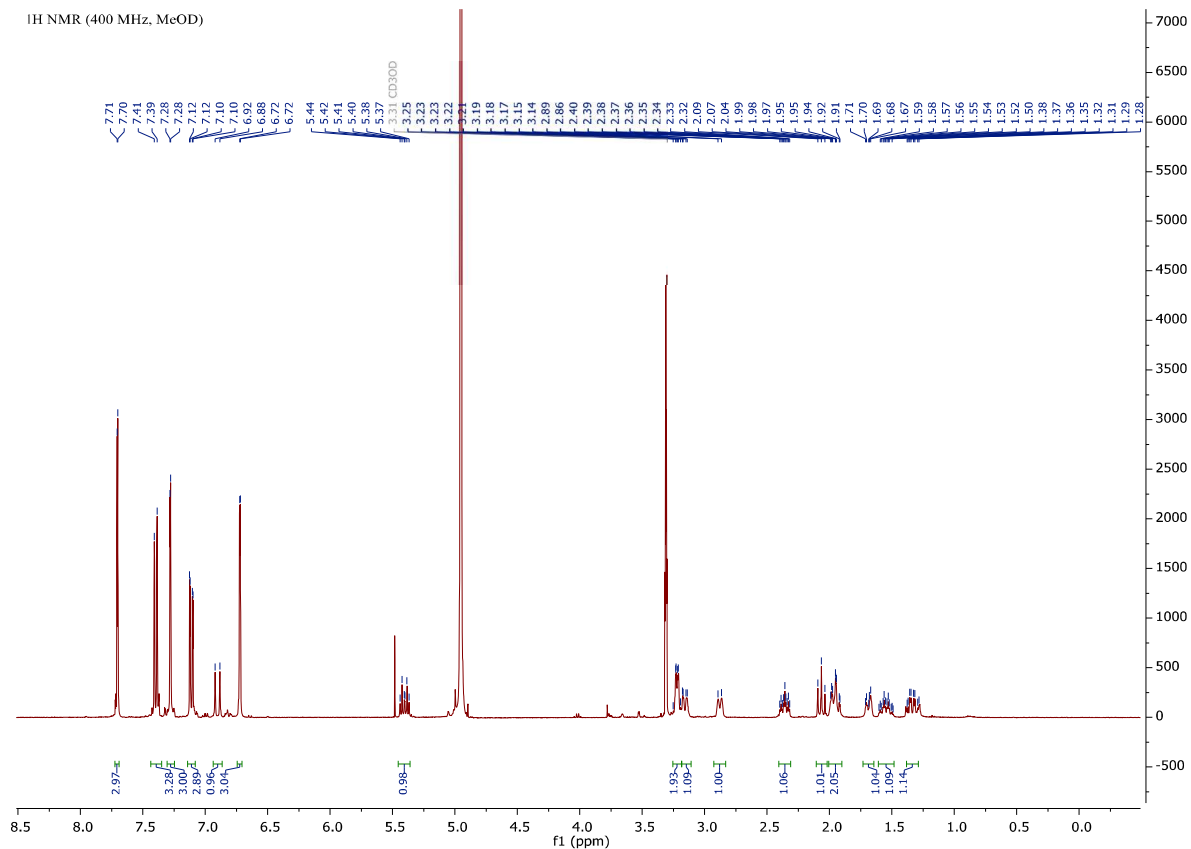


02-krtoph-404KT #50-221 RT: 0.51-1.91 AV: 22 NL: 6.99E5
 F: FTMS - p ESI Full ms [50.00-500.00]



2. List of the ¹H NMR, ¹³C NMR, and HRMS data of synthesized compounds *rac*-6a–b.

2.1. (E)-1-[4,4,4-Tri(benzofuran-5-yl)but-2-en-1-yl]piperidine-3-carboxylic acid, (*rac*-6a)

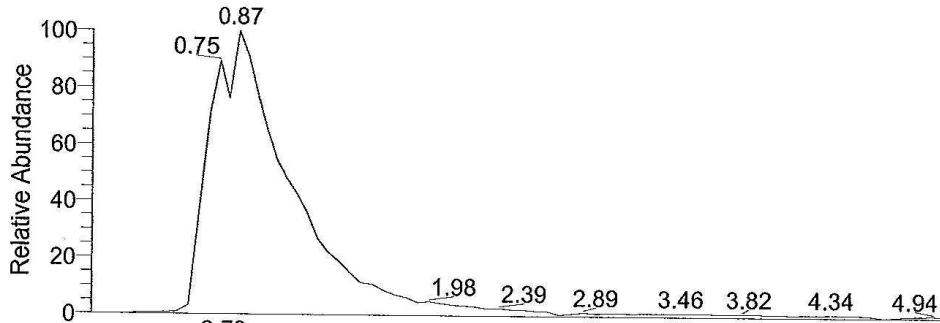


Probenname: C:\Data\01-krtoph-723KT
 Auftraggeber: Toth, Wanner

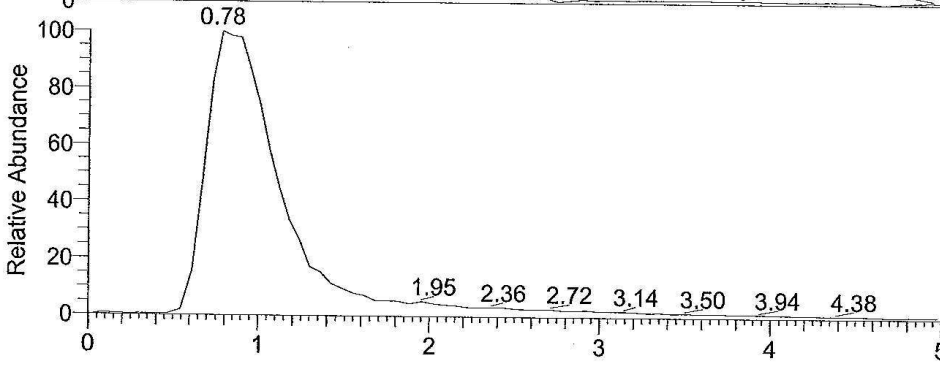
Probe: 531, c34h29no5, fest, Aceton
 Methode: 100 ul/min Acetonitril/Wasser, FIA/ESI, LTQ FT, Spahl

Inj Vol: 1.000000
 Zeit:

RT: 0.00 - 5.04



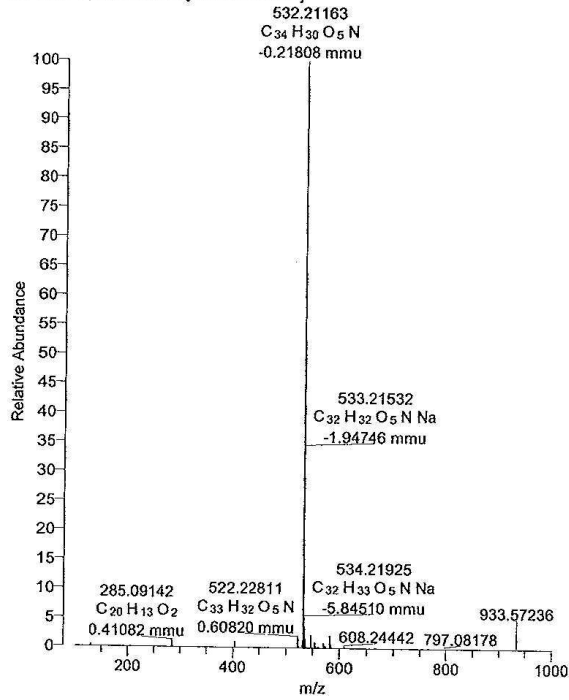
NL: 4.31E6
 Base Peak F: FTMS
 - p ESI Full ms
 [100.00-1000.00]
 MS 01-krtoph-723KT



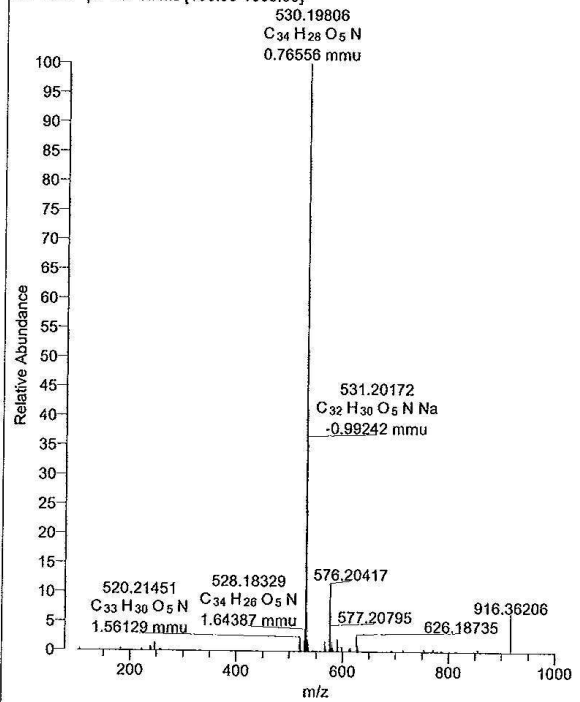
NL: 3.35E7
 Base Peak F: FTMS
 + p ESI Full ms
 [100.00-1000.00]
 MS 01-krtoph-723KT

Time (min)

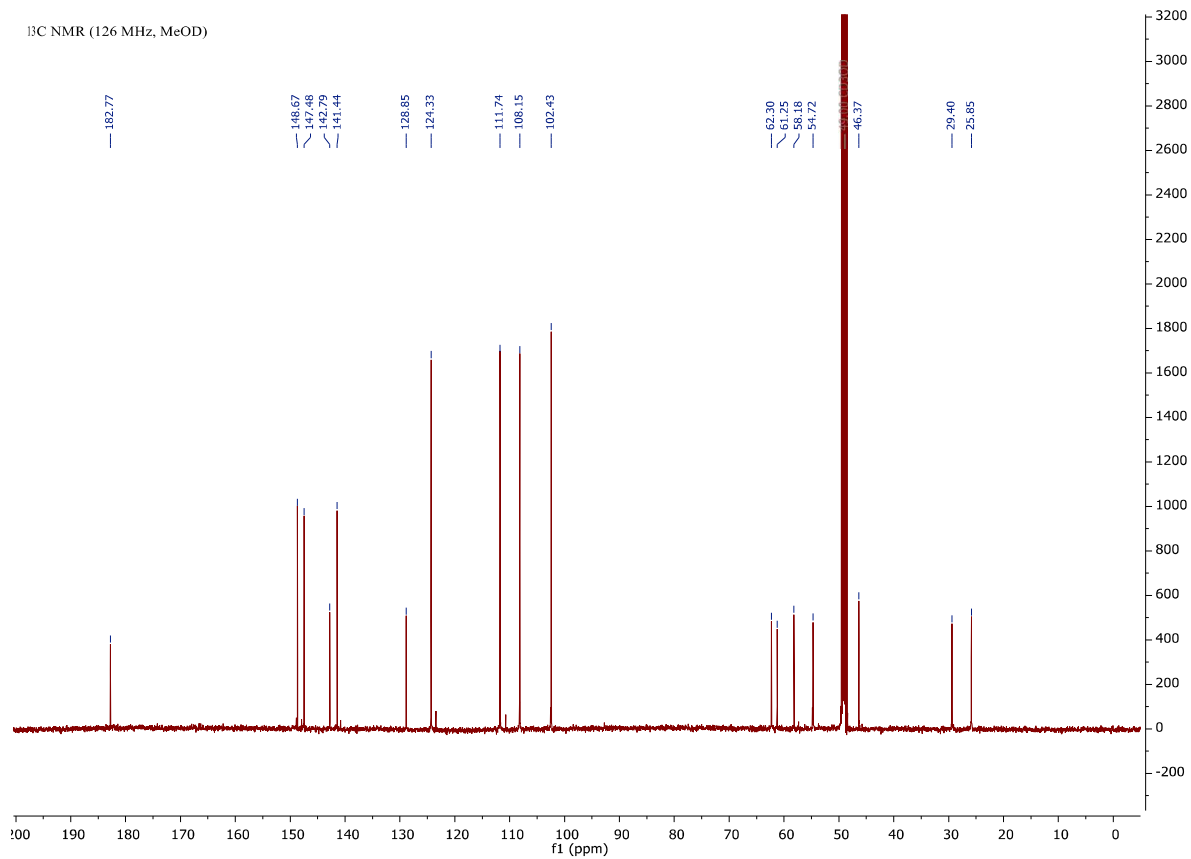
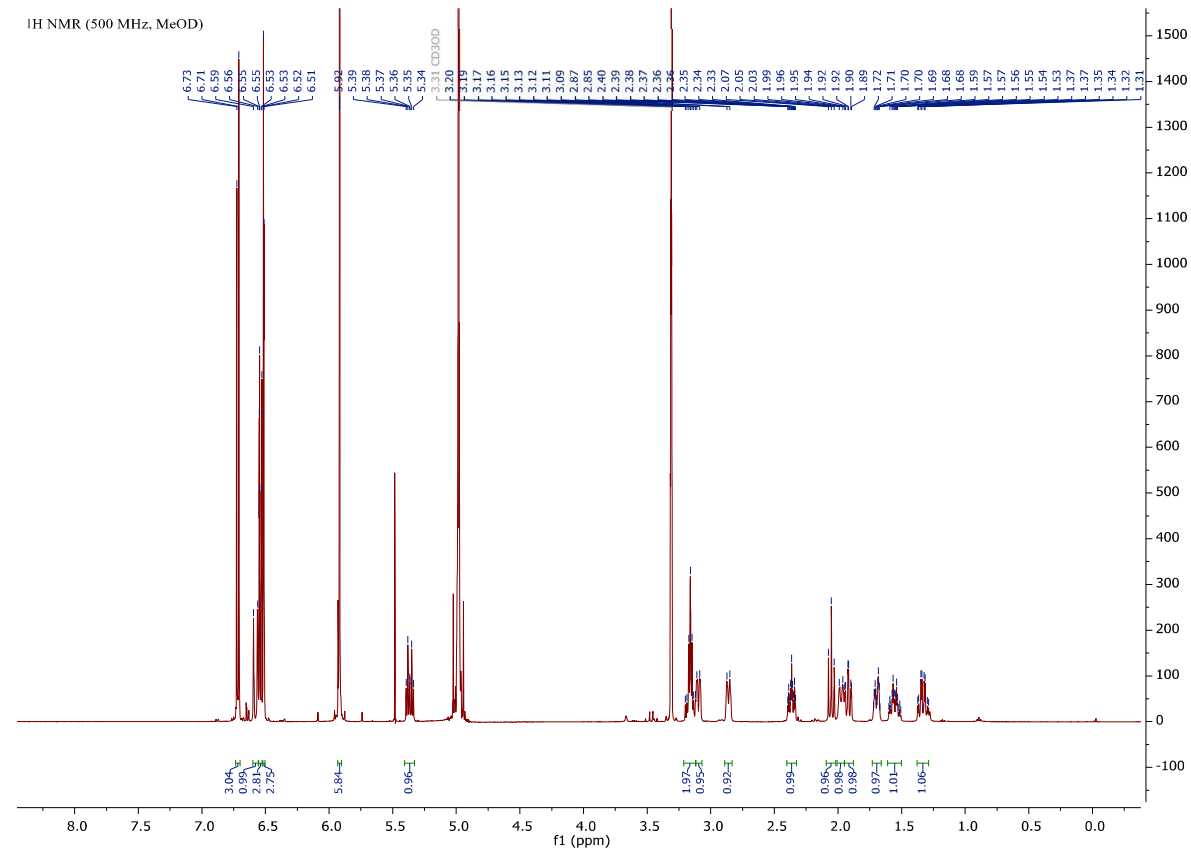
01-krtoph-723KT #53-186 RT: 0.54-1.49 AV: 17 NL: 1.61E7
 F: FTMS + p ESI Full ms [100.00-1000.00]



01-krtoph-723KT #53-181 RT: 0.50-1.45 AV: 17 NL: 2.10E8
 F: FTMS - p ESI Full ms [100.00-1000.00]



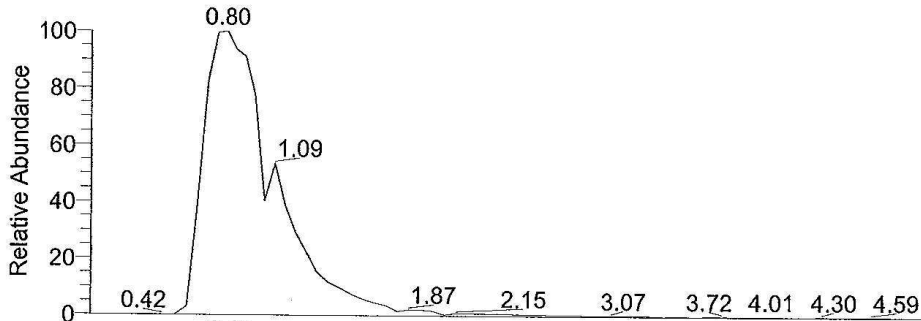
2.2. (E)-1-[4,4,4-Tris(benzo[d][1,3]dioxol-5-yl)but-2-en-1-yl]piperidine-3-carboxylic acid, (*rac*-6b)



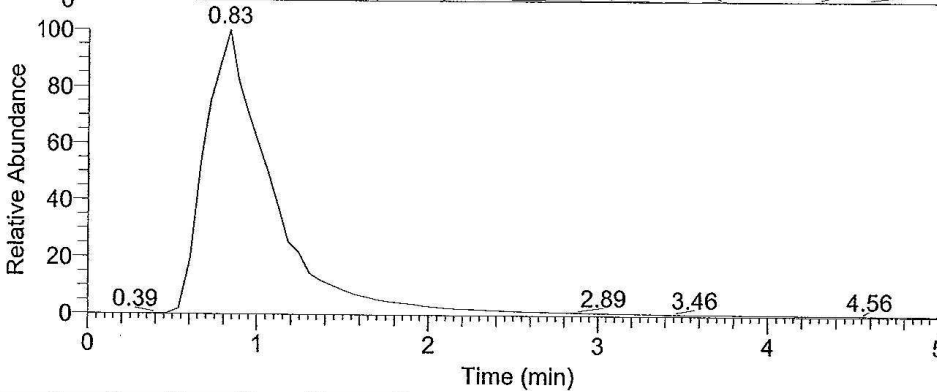
Probenname: C:\Data\02-krtoph-734KT
 Auftraggeber: Toth, Wannier
 RT: 0.00 - 5.06

Probe: 543 c31h29no8, fest, Aceton
 Methode: 100 ul/min Acetonitril/Wasser, FIA/ESI, LTQ FT, Spahl

Inj Vol: 1.000000
 Zeit:

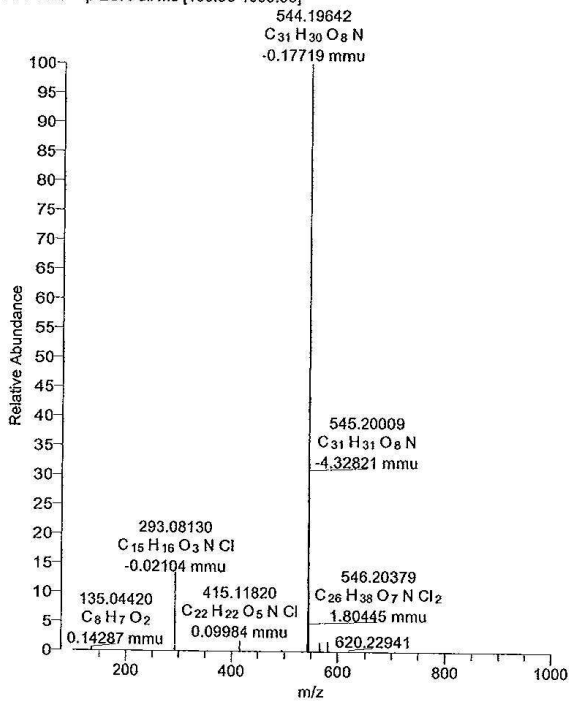


NL: 4.86E6
 Base Peak F: FTMS
 - p ESI Full ms
 [100.00-1000.00]
 MS 02-krtoph-734KT

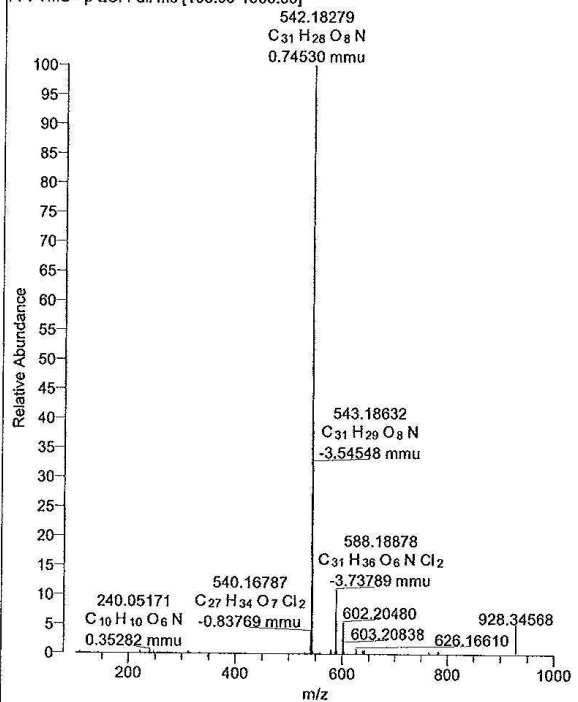


NL: 3.13E7
 Base Peak F: FTMS
 + p ESI Full ms
 [100.00-1000.00]
 MS 02-krtoph-734KT

02-krtoph-734KT #53-184 RT: 0.54-1.44 AV: 16 NL: 1.40E7
 F: FTMS + p ESI Full ms [100.00-1000.00]

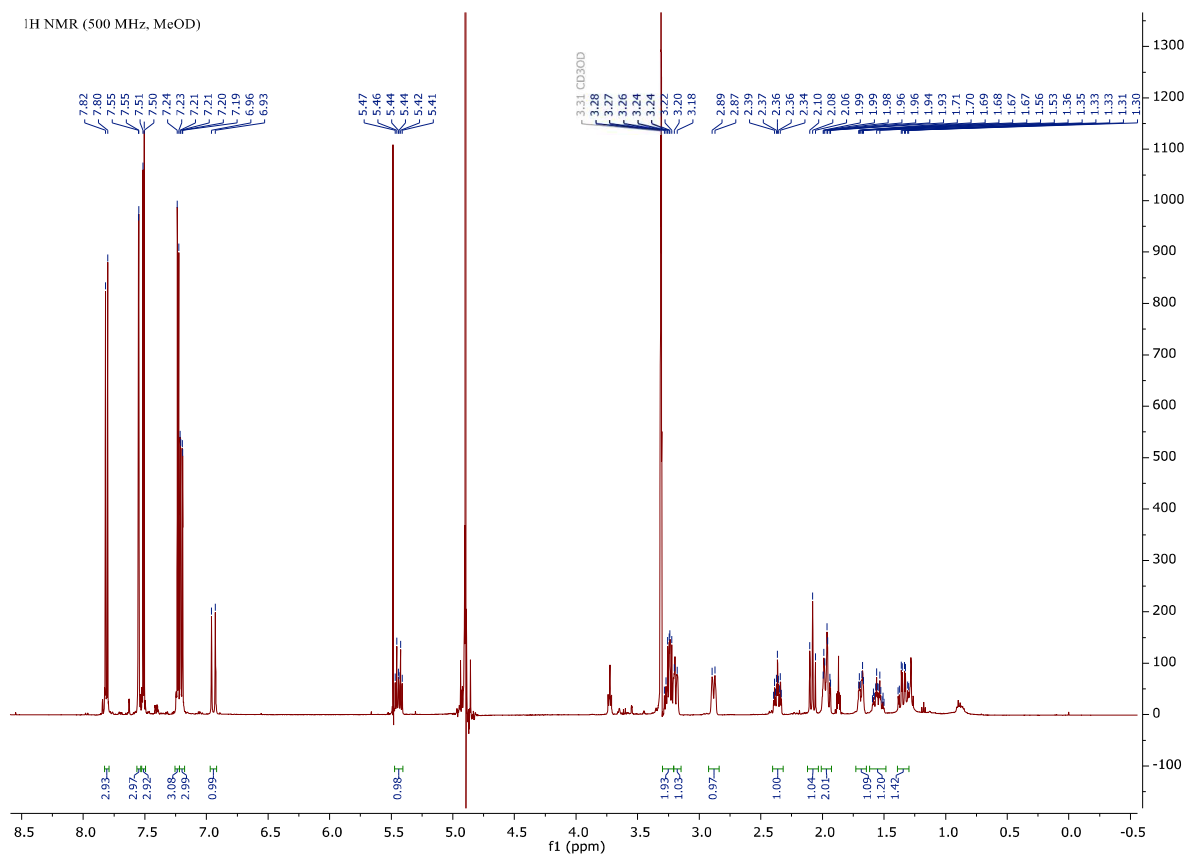


02-krtoph-734KT #53-180 RT: 0.50-1.40 AV: 16 NL: 2.34E6
 F: FTMS - p ESI Full ms [100.00-1000.00]

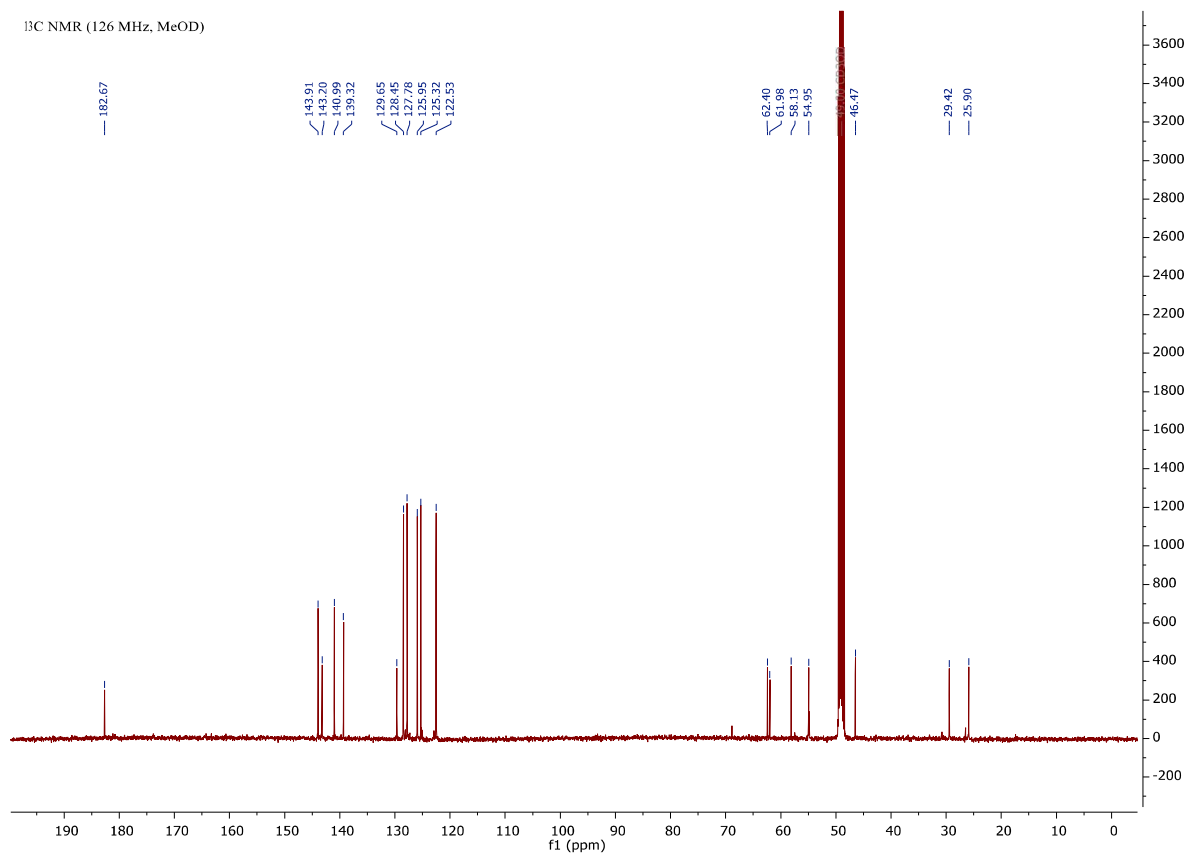


2.3. (E)-1-[4,4,4-Tris(benzo[b]thiophen-5-yl)but-2-en-1-yl]piperidine-3-carboxylic acid, (*rac*-6c)

¹H NMR (500 MHz, MeOD)



¹³C NMR (126 MHz, MeOD)

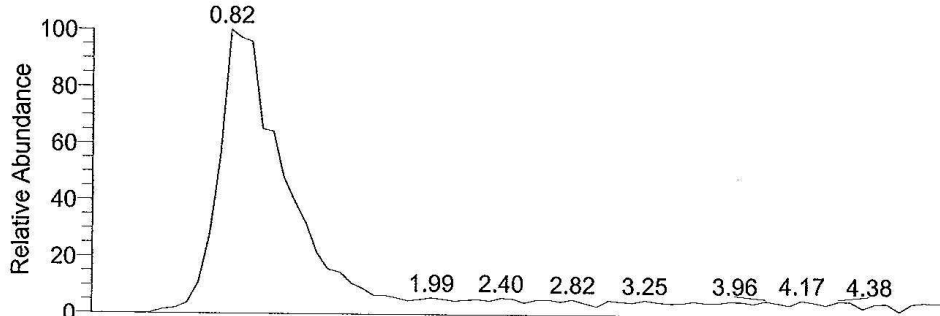


Probenname: C:\Data\03-krtoph-753KT
 Auftraggeber: Toth, Wanner

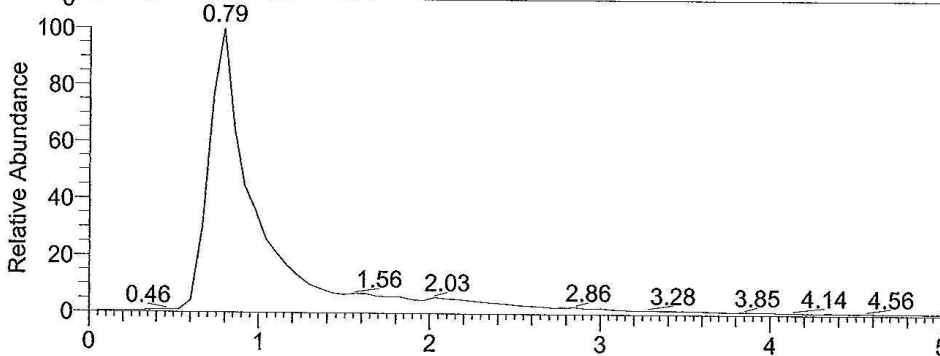
Probe: 579_c34h29no2s3, fest, Aceton
 Methode: 100 ul/min Acetonitril/Wasser, FIA/ESI, LTQ FT, Spahl

Inj Vol: 1.000000
 Zeit:

RT: 0.00 - 5.05



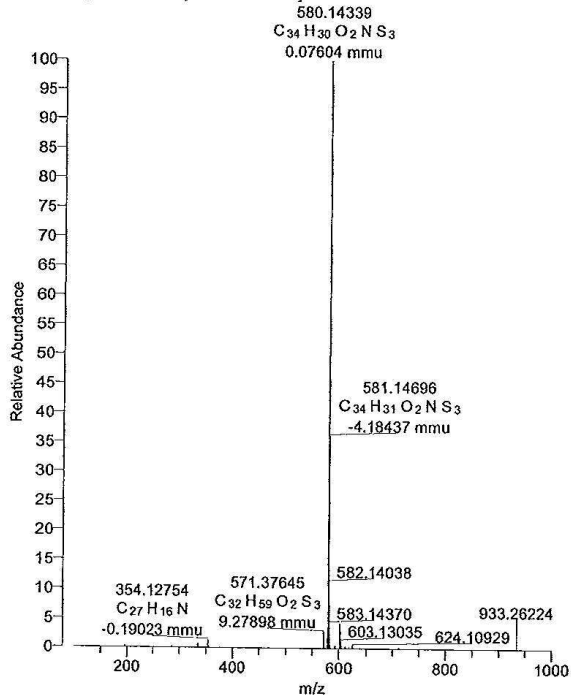
NL: 1.46E6
 Base Peak F: FTMS
 - p ESI Full ms
 [100.00-1000.00]
 MS 03-krtoph-753KT



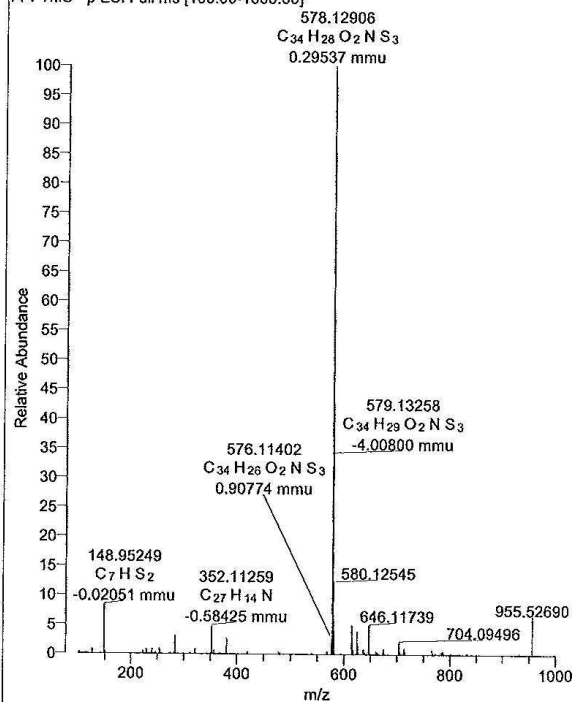
NL: 2.81E7
 Base Peak F: FTMS
 + p ESI Full ms
 [100.00-1000.00]
 MS 03-krtoph-753KT

Time (min)

03-krtoph-753KT #53-177 RT: 0.53-1.49 AV: 16 NL: 7.86E6
 F: FTMS + p ESI Full ms [100.00-1000.00]



03-krtoph-753KT #53-173 RT: 0.49-1.46 AV: 16 NL: 5.93E5
 F: FTMS - p ESI Full ms [100.00-1000.00]



Synthesis and biological evaluation of novel N-substituted nipecotic acid derivatives with a *cis*-alkene spacer as GABA uptake inhibitors

Krisztián Tóth, Georg Höfner, Klaus T. Wanner*

Department of Pharmacy–Center for Drug Research, Ludwig-Maximilians-Universität München, Butenandtstr. 5–13, 81377 Munich, Germany; klaus.wanner@cup.uni-muenchen.de

Abstract:

To discover new, potent, and selective inhibitors for the murine gamma-aminobutyric acid transporter 4 (mGAT4), the structure-activity relationship (SAR) study of a new *cis*-alkene analog family based on DDPM-1457 [(*S*)-**2**], which previously showed promising inhibitory potency at and subtype selectivity for mGAT4, was conducted. To uncover the importance of the differences between the *trans*- and the *cis*-alkene moiety in the spacer, this present publication describes the synthesis of the new compounds via catalytic hydrogenation with Lindlar's catalyst and their biological results collected by the SAR study in our group.

1. Introduction

Disorders in the GABAergic neurotransmission can cause severe neurological illnesses like Alzheimer's disease,¹ depression,² epilepsy,^{3,4} and neuropathic pain.⁵ These conditions are closely related to the levels of gamma-aminobutyric acid (GABA), the major inhibitory neurotransmitter in the central nervous system (CNS).⁶ GABA concentration in the synaptic cleft, amongst other factors, is regulated by the GABA transporter proteins (GATs).⁷ Four different subtypes of these membrane-bound proteins exist,^{8,9} which belong to the solute carrier 6 (SLC6) family.^{10,11} Depending on the species they are cloned from, different nomenclatures can be applied for these transporters. The Human Genome Organization (HUGO) denotes them as GAT1, BGT-1, GAT2, and GAT3. Alternatively, if the transporters are originating from mice, they are termed as mGAT1 (\equiv GAT1), mGAT2 (\equiv BGT-1), mGAT3 (\equiv GAT2), and mGAT4 (\equiv GAT3).¹² mGAT1 and mGAT4 have been found to be clearly predominating in the CNS,¹³ from which mGAT1 is mainly accountable for the neuronal uptake of GABA in presynaptic cells and mGAT4, in particular, mediates GABA transport from the synaptic cleft into the adjacent glial cells.^{14,15} The next two subtypes (mGAT2–mGAT3) are mainly observed in the kidneys and liver¹⁶ and are playing no significant role in the termination of the GABAergic neurotransmission in the brain.¹⁷

The inhibition of mGAT1 and mGAT4 leads to elevated GABA concentrations in the synaptic cleft, which can be used as a treatment option in the above mentioned diverse neurological diseases. The highly potent and selective mGAT1 inhibitor tiagabine (**5**) is already in medical use, but its main drawbacks are the commonly observed side effects (asthenia, depression, diarrhea, dizziness, nervousness, and tremor).^{18, 19, 20} Additionally to mGAT1 selective reuptake inhibitors, a large selection of ligands for mGAT2–mGAT4 were identified over the last years. However, these compounds in general display only mediocre affinities and selectivities for their target.^{21, 22, 23, 24, 25} Hence, there is a need for more potent and subtype-selective GAT inhibitors on the one hand for mGAT2–mGAT4, but also for mGAT1. This would allow a more in-depth study of the physiological role of these proteins, that could serve as alternative treatment options for tiagabine (**5**), which might give rise to fewer side effects. (S)-SNAP-5114 [(S)-**1**] was the first prototypic mGAT4 inhibitor with reasonable potency at and selectivity for this target.²⁶ Based on the structure of (S)-**1**, carba-analogs such as DDPM-1457 [(S)-**2**]²⁷ were developed, the latter of which displays a similar potency and subtype selectivity for mGAT4 as (S)-SNAP-5114 [(S)-**1**], and, in addition, a significantly enhanced chemical stability. Later on, a series of substances including compound **3** (Figure 1) which is similar to (S)-**2**, but with an alkyne spacer instead of a *trans*-alkene moiety were also synthesized. These compounds, however, showed significantly lower potencies at the mGATs as compared to (S)-**2**.²⁸ More recently, the compound family represented by a *trans*-alkene spacer (S)-**2** was expanded with analogs (**4**, Figure 1) by a variation of the triaryl moiety, i.e. by substituting one of the three aryl rings by a variety of different substituents (Table 1).²⁹ Finally, as a representative of a new class of hGAT3 (≡mGAT4) inhibitors isatin derivative **6** is to be mentioned which represents the most potent compound of this set of inhibitors.³⁰

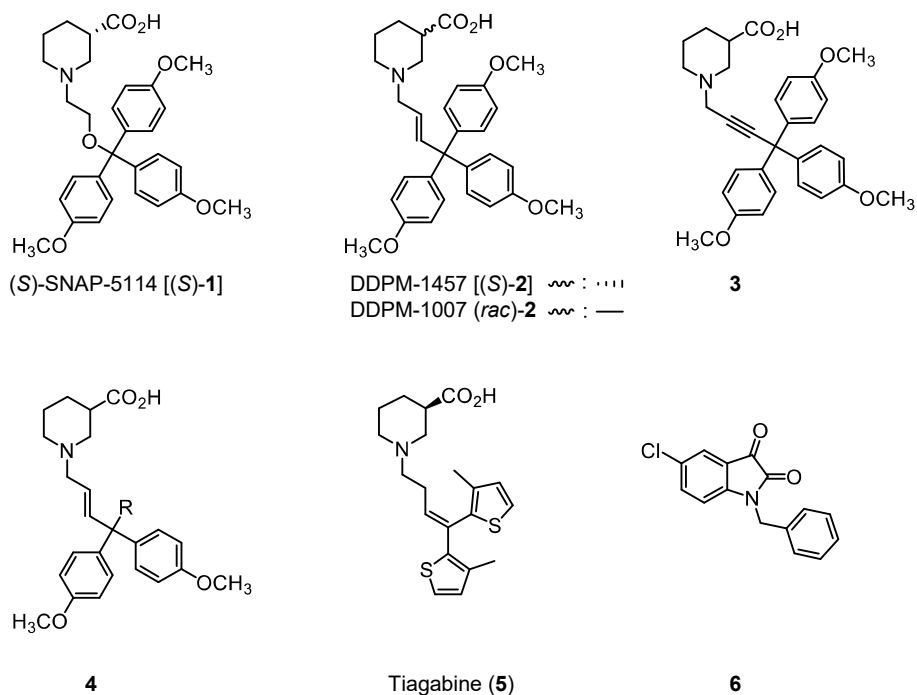


Figure 1. Selected GABA uptake inhibitors. For the structure of residue R see Table 1 (R = R¹: a–h).

In this study, we aimed at the development of an additional carba-analog family of (S)-SNAP-5114 [(S)-1] with a *cis*-configured alkene spacer to supplement the already published results regarding structure-activity relationship (SAR) of the alkyne (**3**, Figure 1) and the *trans*-alkene analogs ((S)-2 and **4**, Figure 1) and to possibly identify more potent and selective inhibitors for mGAT4. The structure of this new *cis*-alkene analog family is related to DDPM-1007 (*rac*-2), the racemic form of DDPM-1457 [(S)-2], and the applied modifications are shown in Figure 2. On the one hand, the spacer between the nipecotic acid and the aromatic lipophilic residue should be modified by replacing the *trans*-alkene moiety by a *cis*-alkene unit. In addition, as a major modification, one of the aromatic moieties of the lipophilic triarylmethane unit should be replaced with a series of different residues, such as aromatic and heteroaromatic rings, benzylic residues or sterically less demanding groups (*rac*-7a–h, Table 1). Finally, we intended to increase the spacer length by one methylene group either by insertion of this unit between the *cis*-alkene group and the lipophilic residue (*rac*-7i–j, Table 1) or between the nipecotic acid and the *cis*-alkene moiety (*rac*-7k–l, Table 1). This should uncover which linker length would be most beneficial regarding biological activity.

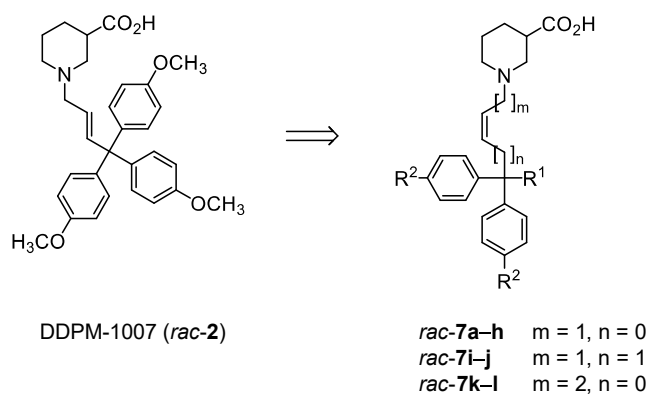


Figure 2. General structures of targeted N-substituted nipecotic acid derivatives *rac-7a-l*. For structures of residues R¹ and R² see Table 1.

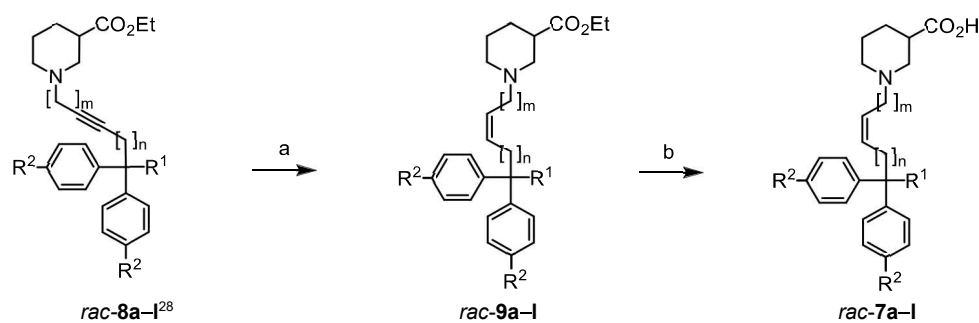
2. Results and Discussion

2.1. Chemistry

As previously reported, the nipecotic acid derivatives *rac-8a-l* displaying an alkyne unit as spacer (see Table 1) are easily accessible by trapping of a nipecotic acid derived iminium ion with an appropriate organomagnesium species.²⁸ In the present study, the thus obtained alkyne unit comprising nipecotic acid derivatives *rac-8a-l* were intended to serve as starting material for the synthesis of the desired target compounds *rac-7a-l* exhibiting an alkene-based spacer with a *cis*-configured double bond. The transformation of these compounds should be accomplished by partial hydrogenation employing Lindlar's catalyst which is well known to effect stereoselective reduction of alkynes to *cis*-alkenes.^{31, 32, 33} The conditions for the hydrogenation were briefly optimized to keep the amount of side products at a minimum and hence to avoid a tedious separation of the desired *cis*-alkenes from starting material and from alkanes resulting from overreduction. Two different sets of reaction conditions were found to serve best this purpose. In any case, first mild reaction conditions (atmospheric pressure, 30 °C) were applied and in a separate experiment more harsh ones (30 bar, 50 °C) when the compound appeared to be reluctant to hydrogenation. The yields for the hydrogenation reaction ranging between 49% – 73% are listed in Table 1.

Lastly, the carboxylic acid esters *rac-9a-l* were subjected to hydrolysis under conditions previously reported for analogous compounds (12 M NaOH, MeOH) that gave the free acids *rac-7a-l* with good to excellent yields (82% – 98%, Table 1).²⁸

Table 1. Formation of the N-substituted nipecotic acid esters *rac-9a-l*, and their hydrolysis to the corresponding free acids *rac-7a-l*.



Entry	Alkyne <i>rac-8</i>	<i>R</i> ¹	<i>R</i> ²	<i>m</i>	<i>n</i>	Ester <i>rac-9</i>	Conditions ^a	Yield % ^c	Acid <i>rac-7</i>	Yield % ^d
1	<i>rac-8a</i>		OCH ₃	1	0	<i>rac-9a</i>	A	71	<i>rac-7a</i>	82
2	<i>rac-8b</i>		OCH ₃	1	0	<i>rac-9b</i>	A	54	<i>rac-7b</i>	88
3	<i>rac-8c</i>		OCH ₃	1	0	<i>rac-9c</i>	B	57	<i>rac-7c</i>	97
4	<i>rac-8d</i>		OCH ₃	1	0	<i>rac-9d</i>	B	59	<i>rac-7d</i>	93
5	<i>rac-8e</i>	OH	OCH ₃	1	0	<i>rac-9e</i>	A	73	<i>rac-7e</i>	83
6	<i>rac-8f</i>	H	OCH ₃	1	0	<i>rac-9f</i>	A	57	<i>rac-7f</i>	98
7	<i>rac-8g</i>		OCH ₃	1	0	<i>rac-9g</i>	B	55	<i>rac-7g</i>	90
8	<i>rac-8h</i>		OCH ₃	1	0	<i>rac-9h</i>	B	64	<i>rac-7h</i>	88
9	<i>rac-8i</i>		OCH ₃	1	1	<i>rac-9i</i>	A	49	<i>rac-7i</i>	89
10	<i>rac-8j</i>		H	1	1	<i>rac-9j</i>	A	68	<i>rac-7j</i>	98
11	<i>rac-8k</i>		OCH ₃	2	0	<i>rac-9k</i>	A	61	<i>rac-7k</i>	90
12	<i>rac-8l</i>		H	2	0	<i>rac-9l</i>	A	53	<i>rac-7l</i>	98

Reagents and conditions: (a) Lindlar's catalyst, Quinoline, H₂, EtOH, Conditions A: atmospheric pressure, 30 °C, Conditions B: 30 bar, 50 °C; (b) 12 M NaOH, MeOH; ^cIsolated yield after chromatography; ^dIsolated yield after extraction.

2.2. Biological evaluation

The synthesized N-substituted nipecotic acid derivatives with a *cis*-alkene spacer *rac-7a-l* were evaluated for their inhibitory potencies at mGAT4 and additionally for the other murine GABA transporter subtypes (mGAT1–mGAT3) in a standardized [³H]GABA uptake assay based on HEK cells developed in our group.³⁴ Binding affinities of these compounds towards mGAT1 (expressed in HEK cells) were also determined using a standardized MS Binding Assay.³⁵ The measurements were done in triplicates and wherever possible, the potencies of the tested compounds in the uptake assays are given as pIC₅₀ values. In cases where test compounds at a concentration of 100 μM were not able to reduce [³H]GABA uptake to a value of below 50%, which equals pIC₅₀ values ≤ 4.00, only the percent values of the remaining [³H]GABA uptake are given.

The comparison of (S)-SNAP-5114 [(S)-1] with its chemically more stable carba-analog DDPM-1457 [(S)-2] shows that replacing the ether moiety of the spacer with a *trans*-alkene unit causes only minor differences in their binding affinity and inhibitory potencies (Table 2). As the *cis*-alkene analogs of the present study are all racemic compounds, we also included DDPM-1007 (*rac-2*),²⁷ the racemic analog of (S)-2, in Table 2 as it appears to be the more suitable reference compound in this case. Compound 3,²⁸ a representative of analogs of DDPM-1007 (*rac-2*), with an alkyne spacer shows that the transition from a *trans*-alkene spacer to an alkyne spacer causes a significant decrease in the inhibitory potencies and binding affinities. Furthermore, tiagabine (5) is listed in Table 2 as a reference compound for potent mGAT1 inhibitors with high selectivity for this target (Table 2, entry 6).³⁶

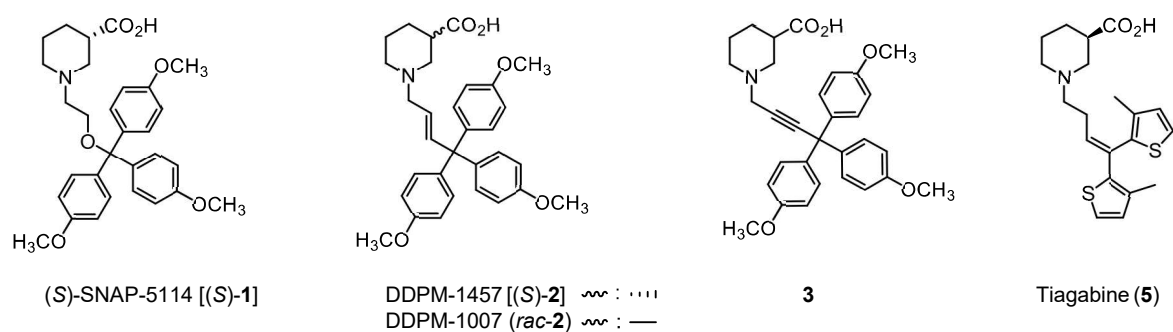
Compound *rac-7a* presents the structural closest analog of DDPM-1007 (*rac-2*) in this study (Table 3, entry 1) possessing a *cis*- instead of a *trans*-configured alkene spacer. Remarkably, this relatively small change of the structure results in a significant reduction of the inhibitory potencies at all mGAT proteins, but without loss of the selectivity in favor of mGAT4. However, compared to the alkyne-analog 3, the so obtained results for *rac-7a* shows a significant selectivity for and slightly higher potency at mGAT4. Similarly to *rac-7a*, the *cis*-alkene analogs *rac-7b*, *rac-7d*, and *rac-7f*, where one 4-methoxyphenyl ring was replaced by a 1,3-benzodioxole, thiophene, or H substituent, respectively, showed, as compared to *rac-2*, lower potencies at all mGAT proteins combined with a slight subtype selectivity in favor of mGAT4. Analogs *rac-7c* having a thiazole ring, and *rac-7e*, an OH substituent replacing one methoxyphenyl unit of the lipophilic residue, were more or less devoid of any reasonable potency at all mGAT proteins. Derivatives with a benzylic residue *rac-7g* and *rac-7h* instead of one of

the three 4-methoxyphenyl moieties in *rac-7a* had greatly reduced inhibitory potencies at mGAT4, compared to *rac-2*, partly also at other mGAT proteins, the potencies at all mGATs getting very close in a range from about 4.0 to 4.5.

Compounds *rac-7i-l* gave insight on the influence of the spacer length on the inhibitory potencies at the different mGAT proteins. An additional methylene group between the lipophilic residue and the *cis*-alkene group resulted in a significantly lower inhibitory potency at mGAT4 for analog *rac-7i* having three 4-methoxyphenyl residues compared to *rac-7a* all pIC₅₀ values being now close to 4. Surprisingly, compound *rac-7j* as an analog of *rac-7i*, but devoid of the three methoxy substituents, displayed a significantly increased potency at mGAT1 by almost 2 log units to a value of pIC₅₀ = 6.00 ± 0.04 (Table 3, entry 10). Also the potency at mGAT4 rose (from pIC₅₀ = 4.21 for *rac-7i* to 4.82) being now almost as high as that of *rac-7a* (pIC₅₀ = 4.99 ± 0.06, Table 3 entry 1). Hence, though the potency at mGAT1 of *rac-7i* still lays somewhat behind that of tiagabine (**5**) with pIC₅₀ = 6.88 ± 0.12 (Table 2, entry 5), it possesses at the same time a reasonable potency at mGAT4 (pIC₅₀ = 4.82, Table 3, entry 10). Compounds *rac-7k* and *rac-7l* represent analogs of *rac-7i* and *rac-7j*, respectively, the spacer extension being now a result of the insertion of a CH₂ group adjacent to the amino function. Both compounds have slightly lower potencies at mGAT4 and somewhat higher potencies at mGAT1, as compared to *rac-7a*, the pIC₅₀ values for mGAT1–mGAT3 being now in a similar range, around 4.0 – 4.5 and only for mGAT4 somewhat higher (~ 4.8, Table 3, entries 11-12). Remarkably, for *rac-7l*, a significantly increased inhibitory potency could not be observed at mGAT1, as it was the case for *rac-7j* with the same trityl residue and spacer length, but the additional methylene group being in a different position.

The binding affinities of *rac-7a-l* determined in binding assays for mGAT1 and given as pK_i values were in the same range as the potencies found in the uptake assays (pIC₅₀ values) for this same transporter. As a general phenomenon already well known from the literature, also here the pK_i values turned out to be about half a log unit higher than the corresponding pIC₅₀ values.^{21,28,29,35}

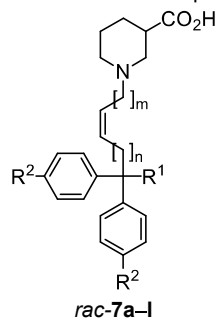
Table 2. Binding affinities and inhibitory potencies of reference compounds (S)-1, (S)-2, (rac)-2, 3, and 5 from the literature.



Entry	Compound	Conf.	pK_i^a	pIC_{50}^b			
				mGAT1	mGAT2	mGAT3	mGAT4
1	(S)-SNAP-5114 [(S)-1] ^c	S	4.56 ^d ± 0.02	4.07 ± 0.09	56%	5.29 ± 0.04	5.71 ± 0.07
2	DDPM-1457 [(S)-2] ^c	S	4.33 ^d ± 0.06	4.40 ± 0.05	4.42 ± 0.11	5.47 ± 0.02	5.87 ± 0.08
3	DDPM-1007 rac-2 ^c	rac	4.83 ^d ± 0.04	4.32 ± 0.05	4.68 ± 0.09	5.19 ± 0.06	5.67 ± 0.06
4	3 ^d	rac	5.36 ± 0.02	4.84	4.36	4.61	4.53
6	Tiagabine (5) ^e	R	7.43 ± 0.11	6.88 ± 0.12	50%	64%	73%

^aResults of the MS Binding Assays are given as $pK_i \pm SEM$; ^bResults of the [³H]GABA uptake assays are given as $pIC_{50} \pm SEM$. Percentages represent remaining [³H]GABA uptake in presence of 100 μM test compound; ^cReference literature,²⁷ ^dReference literature,²⁸ ^eReference literature.³⁶

Table 3. Binding affinities and inhibitory potencies of the N-substituted nipecotic acids with a *cis*-alkene spacer *rac-7a-l*.



Entry	Compound (<i>rac-7</i>)	R ¹	R ²	m	n	pK _i ^a	pIC ₅₀ ^b			
							mGAT1	mGAT2	mGAT3	mGAT4
1	<i>rac-7a</i>		OCH ₃	1	0	4.75	4.14	65%	4.14	4.99 ± 0.06
2	<i>rac-7b</i>		OCH ₃	1	0	4.27	4.02	4.21	4.34	5.00 ± 0.20
3	<i>rac-7c</i>		OCH ₃	1	0	78%	69%	67%	78%	83%
4	<i>rac-7d</i>		OCH ₃	1	0	62%	4.10	4.05	49%	4.48
5	<i>rac-7e</i>	OH	OCH ₃	1	0	53%	81%	85%	97%	80%
6	<i>rac-7f</i>	H	OCH ₃	1	0	4.58	62%	68%	72%	4.31
7	<i>rac-7g</i>		OCH ₃	1	0	4.59	4.13	65%	4.01	4.24
8	<i>rac-7h</i>		OCH ₃	1	0	4.38	4.42	4.52	57%	4.20
9	<i>rac-7i</i>		OCH ₃	1	1	4.62	4.38	52%	4.07	4.21
10	<i>rac-7j</i>		H	1	1	6.29 ± 0.08	6.00 ± 0.04	70%	56%	4.82
11	<i>rac-7k</i>		OCH ₃	2	0	4.63	4.51	63%	4.34	4.79
12	<i>rac-7l</i>		H	2	0	5.13 ± 0.11	4.39	4.26	4.10	4.76

^aResults of the MS Binding Assays are given as pK_i ± SEM. For low pK_i values, only one measurement was performed in triplicate, therefore no SEM could be calculated. Percentages represent remaining specific NO711 binding in presence of 100 μM test compound; ^bResults of the [³H]GABA uptake assays are given as pIC₅₀ ± SEM. For low pIC₅₀ values, only one measurement was performed in triplicate, therefore no SEM could be calculated. Percentages represent remaining [³H]GABA uptake in presence of 100 μM test compound.

3. Conclusion

The design and synthesis of a new *cis*-alkene analog family of (*S*)-SNAP-5114 [(*S*)-**1**] was continued using DDPM-1007 (*rac*-**2**) as the starting point with the aim to identify more potent and selective inhibitors of mGAT4.

The synthesis of the desired *cis*-alkene derivatives *rac*-**9a–l** was accomplished by heterogenic, catalytic reduction of the known alkyne-analogs *rac*-**8a–l** employing Lindlar's catalyst. The new *cis*-alkene analogs *rac*-**7a–l**, as compared to the *trans*-alkene isomer DDPM-1007 (*rac*-**2**), generally show slightly lower potencies at mGAT1–mGAT3 and significantly decreased potency at mGAT4.

Analogs with an increased spacer length and three aromatic rings showed diverse results at mGAT1. Compound *rac*-**7j** having an additional methylene group between the trityl moiety and the *cis*-alkene unit exhibited surprisingly high inhibitory potency at mGAT1 ($pIC_{50} = 6.00 \pm 0.04$) which was not present if the additional methylene group was placed between the nipecotic acid and the *cis*-alkene moiety (*rac*-**7l**, $pIC_{50} = 4.39$).

This research revealed that by changing only the stereochemistry of the potent *trans*-alkene analog DDPM-1007 (*rac*-**2**) into a *cis*-alkene isomer (*rac*-**7a**) results in significantly lowered potency at mGAT4 suggesting that the *trans*-double bond in the spacer plays a significant role for the biological activity of these analogs.

4. Experimental section

4.1. Chemistry

Reactions were carried out in vacuum dried glassware under argon atmosphere. All commercially available starting materials were used without further purification and solvents were distilled before use. As petroleum ether (PE) the fraction 40–60 °C was used. Flash chromatography was performed on silica gel (Merck 60 F-254, 0.040–0.063 mm). Medium pressure liquid chromatography (MPLC) was performed using a Büchi instrument (C-605 binary pump system, C-630 UV detector at 254 nm, and C-660 fraction collector) and a Sepacore glass column B-685 (26*230 mm) equipped with silica gel (YMC Gel SIL-HG, 12 nm, S-20 µm). HRMS data were obtained with JMS-GCmate II (EI, Jeol) or Thermo Finnigan LTQ FT Ultra (ESI, Thermo Finnigan). NMR spectra were recorded with a JNMR-GX (JEOL 400 or 500 MHz) or Bruker BioSpin Avance III HD (400 or 500 MHz). As an internal standard, the known chemical shift of solvent traces was used to reference the spectra. Spectra were processed using the software MestReNova. For IR spectroscopy, a Perkin Elmer FT-IR Spectrometer 1600 was used.

4.2. General procedures

4.2.1. Hydrogenation of the *N*-substituted nipecotic acid esters with an alkyne spacer to the corresponding *N*-substituted nipecotic acid esters with a *cis*-alkene spacer under standard reaction conditions (GP 1)

For mild reaction conditions, Lindlar's catalyst (0.25 equiv.) was added to the solution of the ester with an alkyne spacer (1 equiv.) and quinoline (0.1 equiv.) in ethanol (20 mL/mmol). The flask was evacuated and purged with hydrogen three times and a balloon filled with hydrogen was attached to the sealed flask (atmospheric pressure). The mixture was stirred at 30 °C until most of the starting material was converted to the corresponding ester with a *cis*-alkene spacer, which was followed by thin layer chromatography (TLC) and NMR experiments. Finally, the mixture was filtered through celite, rinsed with Et₂O, and concentrated in vacuum. The crude product was purified by flash chromatography or MPLC on silica gel with DCM/MeOH (99:1) or with Et₂O/PE/MeOH (50:50:1).

4.2.2. Hydrogenation of the *N*-substituted nipecotic acid esters with an alkyne spacer to the corresponding *N*-substituted nipecotic acid esters with a *cis*-alkene spacer under enhanced reaction conditions (GP 2)

For the harsher reaction conditions, Lindlar's catalyst (0.35 equiv.) was added to the solution of the ester with an alkyne spacer (1 equiv.) and quinoline (0.05 equiv.) in ethanol (20 mL/mmol). The pressure vessel was evacuated and purged with hydrogen three times and finally filled with hydrogen (30 bar). The mixture was stirred at 50 °C until most of the starting material was converted to the corresponding ester with a *cis*-alkene spacer which was followed by thin layer chromatography (TLC) and NMR experiments. Finally, the mixture was filtered through celite, rinsed with Et₂O, and concentrated in vacuum. The crude product was purified by flash chromatography or MPLC on silica gel with DCM/MeOH (99:1) or with Et₂O/PE/MeOH (50:50:1).

4.2.3. Hydrolysis of the *N*-substituted nipecotic acid esters (GP 3)

The ester (1 equiv.) was dissolved in MeOH (1 mL/mmol), then an excess of NaOH (5 equiv., 12 M in H₂O) was added dropwise at 0 °C. The mixture was stirred at 25 °C for 3–6 h until the hydrolysis was complete (TLC). The mixture was diluted with H₂O, stirred for 1 h at 25 °C and extracted with Et₂O. The water phase was collected and pH= 6.0 was set by adding HCl (5 equiv., 6 M in H₂O) and phosphate buffer (pH= 6.0, 1.0 M). This solution was extracted with DCM. The combined organic layers were dried over Na₂SO₄ and concentrated under reduced pressure to get the pure product as a thick oil. To get the *N*-substituted nipecotic acid as a solid, the oil was dissolved in DCM (0.1 mL), H₂O (2 mL) was added and an emulsion was prepared by sonication. This emulsion was freeze-dried to obtain a white, amorphous solid.

4.3. Synthesized compounds

4.3.1. (Z)-1-[4,4,4-Tris(4-methoxyphenyl)but-2-en-1-yl]piperidine-3-carboxylic acid, (rac-7a)

According to **GP3**: Ester *rac-9a* (40 mg, 0.070 mmol) with NaOH (0.37 mmol, 12 M in H₂O) was hydrolyzed to get the pure product. White solid (30 mg, 82%).

IR (KBr): $\tilde{\nu}$ = 3428, 3032, 2998, 2934, 2834, 1717, 1700, 1606, 1580, 1507, 1464, 1396, 1295, 1250, 1179, 1117, 1034, 915, 826, 700, 669, 638, 573 cm⁻¹. ¹H NMR (400 MHz, MeOD) δ 1.15 – 1.31 (m, 1H), 1.42 – 1.65 (m, 3H), 1.73 (t, *J* = 11.4 Hz, 1H), 1.91 (d, *J* = 13.0 Hz, 1H), 2.28 – 2.34 (m, 3H), 2.63 (d, *J* = 9.1 Hz, 1H), 2.92 (d, *J* = 11.3 Hz, 1H), 3.78 (s, 9H), 5.79 (dt, *J* = 11.9, 5.8 Hz, 1H), 6.54 (d, *J* = 12.2 Hz, 1H), 6.78 – 6.84 (m, 6H), 6.97 – 7.04 (m, 6H) ppm. ¹³C NMR (101 MHz, MeOD) δ 25.79, 29.12, 46.30, 54.68, 55.83, 58.24, 58.36, 59.68, 114.12, 130.55, 131.98, 140.91, 141.80, 159.28, 182.65 ppm. HRMS (ESI): [M+H]⁺ calcd. for C₃₁H₃₆O₅N, 502.2587; found 502.2586.

4.3.2. (Z)-1-[4-(Benzo[d][1,3]dioxol-5-yl)-4,4-bis(4-methoxyphenyl)but-2-en-1-yl]piperidine-3-carboxylic acid, (rac-7b)

According to **GP3**: Ester *rac-9b* (42 mg, 0.080 mmol), NaOH (0.38 mmol, 12 M in H₂O) was hydrolyzed to get the pure product. White solid (34 mg, 88%).

IR (KBr): $\tilde{\nu}$ = 3425, 2935, 2835, 1717, 1607, 1580, 1506, 1483, 1440, 1396, 1333, 1296, 1248, 1180, 1119, 1097, 1036, 932, 862, 826, 811, 731, 678, 638, 569 cm⁻¹. ¹H NMR (500 MHz, MeOD) δ 1.23 (qd, *J* = 12.5, 4.0 Hz, 1H), 1.43 – 1.58 (m, 2H), 1.58 – 1.64 (m, 1H), 1.74 (t, *J* = 11.4 Hz, 1H), 1.91 (d, *J* = 13.3 Hz, 1H), 2.26 – 2.40 (m, 3H), 2.65 (d, *J* = 9.7 Hz, 1H), 2.92 (d, *J* = 10.9 Hz, 1H), 3.78 (s, 6H), 5.80 (dt, *J* = 11.9, 5.8 Hz, 1H), 5.90 (s, 2H), 6.52 (d, *J* = 12.3 Hz, 1H), 6.52 (d, *J* = 2.0 Hz, 1H), 6.58 (dd, *J* = 8.2, 1.9 Hz, 1H), 6.69 (d, *J* = 8.1 Hz, 1H), 6.80 – 6.84 (m, 4H), 7.00 – 7.04 (m, 4H) ppm. ¹³C NMR (126 MHz, MeOD) δ 25.80, 29.11, 46.32, 54.68, 55.83, 58.28, 58.34, 60.10, 102.37, 108.10, 111.66, 114.17, 123.96, 130.76, 131.98, 132.00, 140.59, 140.63, 141.64, 143.01, 147.21, 148.80, 159.36, 182.61 ppm. HRMS (ESI): [M+H]⁺ calcd. for C₃₁H₃₄O₆N, 516.2380; found: 516.2375.

4.3.3. (Z)-1-[4,4-Bis(4-methoxyphenyl)-4-(thiazol-2-yl)but-2-en-1-yl]piperidine-3-carboxylic acid, (rac-7c)

According to **GP3**: Ester *rac-9c* (32 mg, 0.060 mmol) NaOH (0.3 mmol, 12 M in H₂O) was hydrolyzed to get the pure product. White solid (28 mg, 97%).

IR (KBr): $\tilde{\nu}$ = 3423, 2934, 2835, 1717, 1606, 1580, 1508, 1463, 1389, 1297, 1252, 1180, 1131, 1032, 887, 865, 826, 757, 728, 669, 591, 562, 538 cm⁻¹. ¹H NMR (400 MHz, MeOD) δ 1.17 – 1.31 (m, 1H), 1.42 – 1.65 (m, 3H), 1.74 (t, *J* = 11.4 Hz, 1H), 1.91 (d, *J* = 12.1 Hz, 1H), 2.26 – 2.34 (m, 1H), 2.34 – 2.42 (m, 2H), 2.67 (d, *J* = 9.1 Hz, 1H), 2.93 (d, *J* = 10.9 Hz, 1H), 3.79 (s, 6H), 5.89 (dt, *J* = 11.9, 5.9 Hz, 1H), 6.66 (d, *J* = 12.1 Hz, 1H), 6.84 – 6.89 (m, 4H), 7.06 – 7.12 (m, 4H), 7.49 (d, *J* = 3.4 Hz, 1H), 7.79 (d, *J* = 3.3 Hz, 1H) ppm. ¹³C NMR (101 MHz, MeOD) δ 25.77, 29.08, 46.30, 54.76, 55.90, 58.12, 58.27, 60.03, 114.51, 121.14, 131.63, 131.74, 138.50, 138.55, 138.95, 143.54, 160.16, 181.49, 182.62 ppm. HRMS (ESI): [M+H]⁺ calcd. for C₂₇H₃₁O₄N₂S, 479.1998; found: 479.1999.

4.3.4. (Z)-1-[4,4-Bis(4-methoxyphenyl)-4-(thiophen-3-yl)but-2-en-1-yl]piperidine-3-carboxylic acid, (rac-7d)

According to **GP3**: Ester *rac-9d* (23 mg, 0.050 mmol) and NaOH (0.23 mmol, 12 M in H₂O) was hydrolyzed to get the pure product. White solid (20 mg, 93%).

IR (KBr): $\tilde{\nu}$ = 2423, 2934, 2834, 1717, 1606, 1579, 1508, 1463, 1389, 1361, 1296, 1250, 1179, 1116, 1033, 828, 795, 779, 729, 670, 652, 572 cm⁻¹. ¹H NMR (500 MHz, MeOD) δ 1.23 (qd, *J* = 12.5, 4.0 Hz, 1H), 1.43 – 1.57 (m, 2H), 1.58 – 1.63 (m, 1H), 1.73 (t, *J* = 11.4 Hz, 1H), 1.91 (d, *J* = 11.6 Hz, 1H), 2.30 (tt, *J* = 11.8, 3.8 Hz, 1H), 2.34 – 2.41 (m, 2H), 2.64 (d, *J* = 10.0 Hz, 1H), 2.93 (d, *J* = 11.8 Hz, 1H), 3.77 (s, 6H), 5.78 (dt, *J* = 12.0, 5.9 Hz, 1H), 6.48 (d, *J* = 12.1 Hz, 1H), 6.78 (d, *J* = 3.2 Hz, 2H), 6.80 – 6.84 (m, 4H), 7.00 – 7.07 (m, 4H), 7.33 – 7.35 (m, 1H) ppm. ¹³C NMR (126 MHz, MeOD) δ 25.79, 29.12, 46.32, 54.72, 55.82, 57.47, 57.93, 58.21, 114.23, 123.93, 126.32, 130.47, 130.91, 131.42, 140.40,

140.44, 140.69, 150.25, 159.46, 182.63 ppm. HRMS (ESI): $[M+H]^+$ calcd. for $C_{28}H_{32}O_4NS$, 478.2046; found: 478.2043.

4.3.5. (Z)-1-[4-Hydroxy-4,4-bis(4-methoxyphenyl)but-2-en-1-yl]piperidine-3-carboxylic acid, (rac-7e)

According to **GP3**: The ester *rac-9e* (45 mg, 0.10 mmol) with NaOH (0.5 mmol, 12 M in H_2O) was hydrolyzed to get the pure product. White solid (34 mg, 83%).

IR (KBr): $\tilde{\nu}$ = 3201, 3000, 2931, 2832, 1607, 1583, 1507, 1454, 1389, 1342, 1304, 1247, 1174, 1102, 1063, 1036, 983, 911, 830, 803, 766, 751, 709, 676, 636, 616, 592, 553 cm^{-1} . 1H NMR (500 MHz, MeOD) δ 1.27 (qd, J = 12.8, 3.9 Hz, 1H), 1.41 (qt, J = 12.8, 3.9 Hz, 1H), 1.55 – 1.62 (m, 1H), 1.79 (td, J = 11.8, 2.8 Hz, 1H), 1.93 – 1.99 (m, 2H), 2.28 (tt, J = 11.8, 3.8 Hz, 1H), 2.81 (d, J = 11.4 Hz, 1H), 2.87 (dd, J = 14.2, 6.3 Hz, 1H), 2.92 (ddd, J = 13.8, 5.7, 1.3 Hz, 1H), 3.06 (d, J = 11.3 Hz, 1H), 3.77 (s, 3H), 3.77 (s, 3H), 5.72 (dt, J = 11.9, 5.9 Hz, 1H), 6.32 (d, J = 12.1 Hz, 1H), 6.81 – 6.86 (m, 4H), 7.27 – 7.33 (m, 4H) ppm. ^{13}C NMR (126 MHz, MeOD) δ 25.93, 29.37, 46.28, 54.25, 55.77, 56.28, 57.66, 79.21, 114.21, 114.26, 126.72, 128.87, 128.94, 141.45, 141.50, 142.81, 159.81, 159.85, 182.55 ppm. HRMS (ESI): $[M+H]^+$ calcd. for $C_{24}H_{30}NO_5$, 412.2118; found 412.2117.

4.3.6. (Z)-1-[4,4-Bis(4-methoxyphenyl)but-2-en-1-yl]piperidine-3-carboxylic acid, (rac-7f)

According to **GP3**: Ester *rac-9f* (43 mg, 0.10 mmol) with NaOH (0.5 mmol, 12 M in H_2O) was hydrolyzed to get the pure product. White solid (39 mg, 99%).

IR (KBr): $\tilde{\nu}$ = 3424, 2998, 2935, 2835, 1708, 1608, 1583, 1509, 1464, 1442, 1368, 1302, 1248, 1176, 1113, 1033, 828, 815, 719, 590, 542 cm^{-1} . 1H NMR (400 MHz, MeOD) δ 1.34 (qd, J = 13.0, 4.6 Hz, 1H), 1.54 (qt, J = 12.8, 3.8 Hz, 1H), 1.62 – 1.70 (m, 1H), 1.86 (td, J = 11.8, 2.9 Hz, 1H), 1.96 (d, J = 12.9 Hz, 1H), 2.06 (t, J = 11.4 Hz, 1H), 2.38 (tt, J = 11.8, 3.7 Hz, 1H), 2.85 (d, J = 11.4 Hz, 1H), 3.09 – 3.17 (m, 3H), 3.75 (s, 3H), 3.76 (s, 3H), 4.91 – 4.93 (m, 1H), 5.65 (dt, J = 11.2, 6.7 Hz, 1H), 6.02 (t, J = 10.4 Hz, 1H), 6.80 – 6.85 (m, 4H), 7.05 – 7.11 (m, 4H) ppm. ^{13}C NMR (101 MHz, MeOD) δ 25.86, 29.29, 46.48, 54.69, 55.77, 56.56, 58.37, 114.86, 126.32, 130.07, 130.10, 137.37, 138.07, 138.13, 159.43, 182.72 ppm. HRMS (ESI): $[M+H]^+$ calcd. for $C_{24}H_{30}O_4N$, 396.2169; found: 396.2165.

4.3.7. (Z)-1-[4,4,5-Tris(4-methoxyphenyl)pent-2-en-1-yl]piperidine-3-carboxylic acid, (rac-7g)

According to **GP3**: Ester *rac-9g* (34 mg, 0.060 mmol) with NaOH (0.3 mmol, 12 M in H_2O) was hydrolyzed to get the pure product. White solid (28 mg, 90%).

IR (KBr): $\tilde{\nu}$ = 3424, 3033, 2998, 2938, 2934, 2834, 1716, 1609, 1580, 1510, 1464, 1442, 1392, 1299, 1249, 1179, 1151, 1119, 1035, 784, 759, 745, 702, 669, 592, 550 cm^{-1} . 1H NMR (500 MHz, MeOD) δ 1.21 (qd, J = 12.4, 4.6 Hz, 1H), 1.40 – 1.50 (m, 2H), 1.53 – 1.61 (m, 1H), 1.71 (t, J = 11.4 Hz, 1H), 1.90 (d, J = 13.0 Hz, 1H), 2.29 (tt, J = 11.8, 3.8 Hz, 1H), 2.33 – 2.39 (m, 2H), 2.58 (d, J = 6.4 Hz, 1H), 2.90 (d, J = 9.9 Hz, 1H), 3.44 (s, 2H), 3.70 (s, 3H), 3.78 (s, 3H), 3.78 (s, 3H), 5.61 (dt, J = 12.1, 6.0 Hz, 1H), 6.12 (dt, J = 12.2, 2.2 Hz, 1H), 6.58 – 6.65 (m, 4H), 6.79 – 6.85 (m, 4H), 7.12 – 7.18 (m, 4H) ppm. ^{13}C NMR (126 MHz, MeOD) δ 25.76, 29.16, 46.31, 48.41, 53.37, 54.53, 55.58, 55.76, 57.49, 58.20, 113.72, 114.20, 129.43, 131.00, 131.05, 131.23, 133.01, 138.86, 140.53, 140.62, 159.27, 159.29, 159.47, 182.58 ppm. HRMS (ESI): $[M+H]^+$ calcd. for $C_{32}H_{38}NO_5$, 516.2744; found: 516.2736.

4.3.8. (Z)-1-[4,4-Bis(4-methoxyphenyl)-5-phenylpent-2-en-1-yl]piperidine-3-carboxylic acid, (rac-7h)

According to **GP3**: Ester *rac-9h* (21 mg, 0.040 mmol) with NaOH (0.2 mmol, 12 M in H_2O) was hydrolyzed to get the pure product. White solid (17 mg, 88%).

IR (KBr): $\tilde{\nu}$ = 3429, 3025, 2995, 2934, 2835, 1715, 1607, 1579, 1509, 1454, 1396, 1290, 1250, 1181, 1151, 1118, 1034, 830, 767, 734, 702, 668, 600, 565 cm^{-1} . 1H NMR (400 MHz, MeOD) δ 1.21 (qd, J = 12.2, 4.3 Hz, 1H), 1.41 – 1.50 (m, 2H), 1.53 – 1.61 (m, 1H), 1.71 (t, J = 11.5 Hz, 1H), 1.90 (d, J = 13.3 Hz, 1H), 2.29 (tt, J = 11.8, 3.7 Hz, 1H), 2.36 (d, J = 5.7 Hz, 3H), 2.58 (d, J = 7.1 Hz, 1H), 2.90 (d, J = 11.0 Hz, 1H), 3.50 (s, 2H), 3.78 (s, 3H), 3.78 (s, 3H), 5.61 (dt, J = 12.2, 6.0 Hz, 1H), 6.12 (dt, J = 12.2, 2.2 Hz, 1H), 6.70 – 6.74 (m, 2H), 6.79 – 6.85 (m, 4H), 7.00 – 7.10 (m, 3H), 7.12 – 7.19 (m, 4H) ppm. ^{13}C NMR (101 MHz, MeOD) δ 25.75, 29.15, 46.31, 49.19, 53.30, 54.53, 55.78, 57.46, 58.20, 114.22, 127.06,

128.28, 129.53, 130.97, 131.01, 132.12, 138.71, 139.26, 140.49, 140.59, 159.29, 182.59 ppm. HRMS (ESI): $[M+H]^+$ calcd. for $C_{31}H_{36}O_4N$ 486.2638; found 486.2635.

4.3.9. (Z)-1-[5,5,5-Tris(4-methoxyphenyl)pent-2-en-1-yl]piperidine-3-carboxylic acid, (rac-7i)

According to **GP3**: Ester *rac-9i* (29 mg, 0.050 mmol) with NaOH (0.25 mmol, 12 M in H_2O) was hydrolyzed to get the pure product. White solid (23 mg, 89%).

IR (KBr): $\tilde{\nu}$ = 3424, 3034, 2998, 2934, 2834, 1717, 1607, 1580, 1508, 1463, 1441, 1387, 1295, 1249, 1182, 1119, 1035, 823, 577 cm^{-1} . 1H NMR (400 MHz, MeOD) δ 1.31 (qd, J = 12.6, 4.1 Hz, 1H), 1.42 – 1.58 (m, 1H), 1.59 – 1.69 (m, 1H), 1.73 (td, J = 11.9, 2.7 Hz, 1H), 1.89 – 1.97 (m, 1H), 1.98 (t, J = 11.4 Hz, 1H), 2.34 (tt, J = 11.7, 3.7 Hz, 1H), 2.68 (d, J = 11.2 Hz, 1H), 2.79 – 2.94 (m, 2H), 3.05 (d, J = 11.5 Hz, 1H), 3.23 – 3.29 (m, 1H), 3.32 – 3.39 (m, 1H), 3.76 (s, 9H), 5.39 (dt, J = 12.0, 6.6 Hz, 1H), 5.49 (dt, J = 12.3, 6.3 Hz, 1H), 6.75 – 6.84 (m, 6H), 7.03 – 7.12 (m, 6H). ^{13}C NMR (101 MHz, MeOD) δ 25.83, 29.30, 40.40, 46.45, 54.59, 55.70, 55.78, 56.71, 58.26, 114.05, 127.72, 131.31, 131.97, 141.18, 159.04, 182.76. HRMS (ESI): $[M+H]^+$ calcd. for $C_{32}H_{38}O_5N$, 516.2744; found: 516.2742.

4.3.10. (Z)-1-[5,5,5-Triphenylpent-2-en-1-yl]piperidine-3-carboxylic acid, (rac-7j)

According to **GP3**: The ester *rac-9j* (56 mg, 0.12 mmol) with NaOH (0.6 mmol, 12 M in H_2O) was hydrolyzed to get the pure product. White solid (50 mg, 98%).

IR (KBr): $\tilde{\nu}$ = 3054, 3027, 2937, 2859, 2788, 1952, 1887, 1709, 1595, 1492, 1467, 1445, 1388, 1338, 1304, 1269, 1188, 1135, 1103, 1035, 1001, 961, 866, 760, 749, 700, 625, 613, 521 cm^{-1} . 1H NMR (500 MHz, MeOD) δ 1.31 (qd, J = 12.8, 4.2 Hz, 1H), 1.50 (qt, J = 13.0, 3.9 Hz, 1H), 1.61 – 1.67 (m, 1H), 1.76 (td, J = 11.9, 2.9 Hz, 1H), 1.92 – 2.00 (m, 2H), 2.35 (tt, J = 11.8, 3.7 Hz, 1H), 2.70 (d, J = 11.4 Hz, 1H), 2.79 – 2.91 (m, 2H), 3.04 (d, J = 11.3 Hz, 1H), 3.43 (qd, J = 15.4, 6.5 Hz, 2H), 5.36 – 5.43 (m, 1H), 5.45 – 5.52 (m, 1H), 7.15 – 7.28 (m, 15H) ppm. ^{13}C NMR (126 MHz, MeOD) δ 30.88, 34.31, 44.97, 51.50, 59.70, 61.69, 62.71, 63.26, 132.10, 133.08, 133.84, 135.45, 136.56, 153.52, 187.68 ppm. HRMS (ESI): $[M+H]^+$ calcd. for $C_{29}H_{32}O_2N$, 426.2427; found 426.2437.

4.3.11. (Z)-1-[5,5,5-Tris(4-methoxyphenyl)pent-3-en-1-yl]piperidine-3-carboxylic acid, (rac-7k)

According to **GP3**: Ester *rac-9k* (40 mg, 0.070 mmol) with NaOH (0.36 mmol, 12 M in H_2O) was hydrolyzed to get the pure product. White solid (23 mg, 89%).

IR (KBr): $\tilde{\nu}$ = 3448, 2998, 2934, 2834, 1717, 1606, 1579, 1507, 1463, 1442, 1399, 1294, 1249, 1178, 1117, 1034, 915, 826, 79, 707, 669, 637, 609, 571 cm^{-1} . 1H NMR (400 MHz, MeOD) δ 1.23 (qd, J = 12.6, 3.8 Hz, 1H), 1.43 (qt, J = 12.5, 3.5 Hz, 1H), 1.52 – 1.63 (m, 2H), 1.68 – 1.76 (m, 2H), 1.83 (t, J = 11.4 Hz, 1H), 1.89 (d, J = 13.0 Hz, 1H), 1.97 – 2.07 (m, 1H), 2.07 – 2.17 (m, 1H), 2.27 (tt, J = 11.8, 3.7 Hz, 1H), 2.44 (d, J = 11.1 Hz, 1H), 2.81 (d, J = 11.0 Hz, 1H), 3.77 (s, 9H), 5.59 (dt, J = 11.7, 7.4 Hz, 1H), 6.46 (d, J = 11.7 Hz, 1H), 6.76 – 6.82 (m, 6H), 6.96 – 7.03 (m, 6H) ppm. ^{13}C NMR (101 MHz, MeOD) δ 25.71, 27.67, 29.36, 46.28, 54.32, 55.79, 58.17, 58.63, 59.63, 114.07, 131.72, 131.96, 141.56, 141.65, 159.19, 182.71 ppm. HRMS (ESI): $[M+H]^+$ calcd. for $C_{32}H_{38}O_5N$, 516.2744; found: 516.2739.

4.3.12. (Z)-1-[5,5,5-Triphenylpent-3-en-1-yl]piperidine-3-carboxylic acid, (rac-7l)

According to **GP3**: The ester *rac-9l* (51 mg, 0.11 mmol) with NaOH (0.55 mmol, 12 M in H_2O) was hydrolyzed to get the pure product. White solid (46 mg, 98%).

IR (KBr): $\tilde{\nu}$ = 3427, 3055, 3019, 2938, 2858, 2804, 1711, 1594, 1490, 1445, 1395, 1301, 1186, 1154, 1103, 1088, 1033, 1001, 930, 901, 871, 757, 701, 667, 600, 526 cm^{-1} . 1H NMR (400 MHz, MeOD) δ 1.22 (qd, J = 12.8, 4.2 Hz, 1H), 1.42 (qt, J = 12.9, 3.8 Hz, 1H), 1.52 – 1.62 (m, 2H), 1.68 – 1.74 (m, 2H), 1.78 (t, J = 11.4 Hz, 1H), 1.88 (d, J = 12.8 Hz, 1H), 2.04 (qt, J = 12.3, 7.0 Hz, 2H), 2.25 (tt, J = 11.8, 3.7 Hz, 1H), 2.44 (d, J = 11.1 Hz, 1H), 2.76 (d, J = 11.1 Hz, 1H), 5.67 (dt, J = 11.7, 7.4 Hz, 1H), 6.54 (dt, J = 11.6, 1.8 Hz, 1H), 7.11 – 7.29 (m, 15H) ppm. ^{13}C NMR (101 MHz, MeOD) δ 25.71, 27.91, 29.32, 46.31, 54.38, 58.10, 58.43, 61.62, 127.19, 128.84, 131.10, 132.59, 141.10, 148.97, 182.71 ppm. HRMS (ESI): $[M+H]^+$ calcd. for $C_{29}H_{32}O_2N$, 426.2427; found 426.2424.

4.3.13. *Ethyl (Z)-1-[4,4,4-tris(4-methoxyphenyl)but-2-en-1-yl]piperidine-3-carboxylate, (rac-9a)*

According to **GP1**: Ester *rac-8a* (211 mg, 0.400 mmol), quinoline (5 mg, 0.04 mmol), Lindlar's catalyst (85 mg, 0.040 mmol) in ethanol (10 mL). The crude product was purified by flash chromatography with DCM/MeOH (99:1). Yellow oil (150 mg, 71%).

IR (Film): $\tilde{\nu}$ = 2937, 2833, 2794, 1728, 1606, 1580, 1506, 1463, 1294, 1248, 1178, 1151, 1134, 1098, 1035, 826 cm^{-1} . ^1H NMR (500 MHz, CD_2Cl_2) δ 1.23 (t, J = 7.1 Hz, 3H), 1.27 – 1.37 (m, 1H), 1.39 – 1.49 (m, 1H), 1.57 – 1.64 (m, 1H), 1.69 (td, J = 11.2, 2.8 Hz, 1H), 1.76 – 1.90 (m, 2H), 2.29 (dd, J = 6.1, 2.2 Hz, 2H), 2.41 (tt, J = 10.3, 3.8 Hz, 1H), 2.46 (d, J = 10.4 Hz, 1H), 2.65 (d, J = 11.1 Hz, 1H), 3.77 (s, 9H), 4.08 (q, J = 7.1 Hz, 2H), 5.74 (dt, J = 12.1, 6.0 Hz, 1H), 6.48 (dt, J = 12.1, 2.2 Hz, 1H), 6.75 – 6.80 (m, 6H), 7.01 – 7.06 (m, 6H) ppm. ^{13}C NMR (126 MHz, CD_2Cl_2) δ 14.60, 25.16, 27.29, 42.49, 54.09, 55.73, 55.97, 57.44, 58.87, 60.66, 113.49, 131.34, 131.81, 140.40, 158.32, 174.48 ppm. HRMS (EI): $[\text{M}]^+$ calcd. for $\text{C}_{33}\text{H}_{39}\text{O}_5\text{N}$, 529.2828; found: 529.2817.

4.3.14. *Ethyl (Z)-1-[4-(benzo[d][1,3]dioxol-5-yl)-4,4-bis(4-methoxyphenyl)but-2-en-1-yl]piperidine-3-carboxylate, (rac-9b)*

According to **GP2**: Ester *rac-8b* (42 mg, 0.080 mmol), quinoline (1 mg, 0.01 mmol), and Lindlar's catalyst (40 mg, 0.019 mmol) in ethanol (4 mL). The crude product was purified by MPLC with DCM/MeOH (98:2). Yellow oil (22 mg, 54%).

IR (Film): $\tilde{\nu}$ = 2939, 2900, 2835, 2782, 1729, 1607, 1579, 1506, 1483, 1465, 1440, 1299, 1248, 1180, 1151, 1134, 1098, 1037, 935, 862, 826, 810, 732, 699, 677 cm^{-1} . ^1H NMR (500 MHz, CD_2Cl_2) δ 1.23 (t, J = 7.1 Hz, 3H), 1.27 – 1.37 (m, 1H), 1.40 – 1.49 (m, 1H), 1.57 – 1.64 (m, 1H), 1.66 – 1.74 (m, 1H), 1.77 – 1.89 (m, 2H), 2.31 (d, J = 3.9 Hz, 2H), 2.42 (tt, J = 10.3, 3.9 Hz, 1H), 2.48 (d, J = 10.8 Hz, 1H), 2.66 (d, J = 11.2 Hz, 1H), 3.77 (s, 6H), 4.08 (q, J = 7.1 Hz, 2H), 5.75 (dt, J = 12.1, 6.0 Hz, 1H), 5.92 (s, 2H), 6.46 (dt, J = 12.1, 2.2 Hz, 1H), 6.59 – 6.62 (m, 2H), 6.68 (d, J = 8.9 Hz, 1H), 6.76 – 6.80 (m, 4H), 7.02 – 7.07 (m, 4H) ppm. ^{13}C NMR (126 MHz, CD_2Cl_2) δ 14.59, 25.14, 27.27, 42.48, 54.11, 55.74, 55.99, 57.42, 59.32, 60.68, 101.72, 107.54, 111.21, 113.53, 123.32, 131.36, 131.94, 140.09, 140.16, 140.34, 142.49, 146.26, 147.94, 158.40, 174.49 ppm. HRMS (ESI): $[\text{M}+\text{H}]^+$ calcd. for $\text{C}_{33}\text{H}_{38}\text{NO}_6$, 544.2693; found: 544.2689.

4.3.15. *Ethyl (Z)-1-[4,4-bis(4-methoxyphenyl)-4-(thiazol-2-yl)but-2-en-1-yl]piperidine-3-carboxylate, (rac-9c)*

According to **GP2**: Ester *rac-8c* (67 mg, 0.13 mmol), quinoline (2 mg, 0.01 mmol), and Lindlar's catalyst (70 mg, 0.033 mmol) in ethanol (4 mL). The crude product was purified by MPLC with DCM/MeOH (97:3). Yellow oil (38 mg, 58%).

IR (Film): $\tilde{\nu}$ = 2936, 2829, 1727, 1606, 1579, 1508, 1461, 1440, 1384, 1298, 1251, 1180, 1148, 1130, 1097, 1032, 890, 861, 825, 719, 668 cm^{-1} . ^1H NMR (500 MHz, CD_2Cl_2) δ 1.23 (t, J = 7.2 Hz, 3H), 1.29 – 1.37 (m, 1H), 1.40 – 1.50 (m, 1H), 1.56 – 1.67 (m, 1H), 1.68 – 1.76 (m, 1H), 1.77 – 1.84 (m, 1H), 1.84 – 1.92 (m, 1H), 2.30 – 2.39 (m, 2H), 2.40 – 2.46 (m, 1H), 2.49 (d, J = 10.2 Hz, 1H), 2.68 (d, J = 10.0 Hz, 1H), 3.79 (s, 6H), 4.08 (q, J = 7.1 Hz, 2H), 5.83 (dt, J = 12.0, 6.0 Hz, 1H), 6.65 (d, J = 12.1 Hz, 1H), 6.79 – 6.83 (m, 4H), 7.10 – 7.15 (m, 4H), 7.27 (d, J = 3.3 Hz, 1H), 7.77 (d, J = 3.3 Hz, 1H) ppm. ^{13}C NMR (101 MHz, CD_2Cl_2) δ 14.60, 25.11, 27.26, 42.43, 54.13, 55.78, 56.00, 57.25, 59.23, 60.68, 113.74, 119.84, 131.05, 132.71, 138.01, 138.28, 138.35, 143.25, 159.08, 174.47, 179.78 ppm. HRMS (ESI): $[\text{M}+\text{H}]^+$ calcd. for $\text{C}_{29}\text{H}_{35}\text{O}_4\text{N}_2\text{S}$ 507.2312; found: 507.2313.

4.3.16. *Ethyl (Z)-1-[4,4-bis(4-methoxyphenyl)-4-(thiophen-3-yl)but-2-en-1-yl]piperidine-3-carboxylate, (rac-9d)*

According to **GP2**: Ester *rac-8d* (26 mg, 0.050 mmol), quinoline (1 mg, 0.01 mmol), and Lindlar's catalyst (32 mg, 0.015 mmol) in ethanol (3 mL). The crude product was purified by MPLC with DCM/MeOH (98:2). Yellow oil (15 mg, 59%).

IR (Film): $\tilde{\nu}$ = 2927, 2853, 1729, 1607, 1578, 1508, 1459, 1375, 1297, 1249, 1180, 1151, 1116, 1099, 1034, 828, 793, 782, 669, 654 cm^{-1} . ^1H NMR (500 MHz, CD_2Cl_2) δ 1.23 (t, J = 7.1 Hz, 3H), 1.27 – 1.38

(m, 1H), 1.39 – 1.50 (m, 1H), 1.57 – 1.64 (m, 1H), 1.65 – 1.74 (m, 1H), 1.76 – 1.91 (m, 2H), 2.33 (d, $J = 4.8$ Hz, 2H), 2.42 (tt, $J = 10.2, 3.8$ Hz, 1H), 2.47 (d, $J = 10.6$ Hz, 1H), 2.67 (d, $J = 10.1$ Hz, 1H), 3.77 (s, 6H), 4.08 (q, $J = 7.1$ Hz, 2H), 5.74 (dt, $J = 12.1, 6.0$ Hz, 1H), 6.42 (dt, $J = 12.1, 2.2$ Hz, 1H), 6.77 – 6.81 (m, 6H), 7.04 – 7.08 (m, 4H), 7.26 (dd, $J = 5.1, 3.0$ Hz, 1H) ppm. ^{13}C NMR (126 MHz, CD_2Cl_2) δ 14.60, 25.12, 27.26, 42.45, 54.11, 55.74, 55.97, 56.69, 57.03, 60.67, 113.61, 123.50, 125.61, 130.45, 130.78, 131.75, 139.33, 139.86, 139.92, 149.63, 158.52, 174.48 ppm. HRMS (ESI): $[\text{M}+\text{H}]^+$ calcd. for $\text{C}_{30}\text{H}_{36}\text{NO}_4\text{S}$, 506.2359; found: 506.2354.

4.3.17. Ethyl (Z)-1-[4-hydroxy-4,4-bis(4-methoxyphenyl)but-2-en-1-yl]piperidine-3-carboxylate, (rac-9e)

According to **GP1**: Ester *rac-8e* (63 mg, 0.14 mmol), quinoline (2 mg, 0.01 mmol), and Lindlar's catalyst (45 mg, 0.021 mmol) in ethanol (2 mL). The reaction time was 20 min. The crude product was purified by flash chromatography with $\text{Et}_2\text{O}/\text{PE}/\text{MeOH}$ (50:50:2). Yellow oil (45 mg, 73%).

IR (Film): $\tilde{\nu} = 2938, 2833, 1729, 1607, 1583, 1506, 1465, 1440, 1301, 1246, 1171, 1151, 1131, 1086, 1034, 1000, 914, 829, 692, 668$ cm^{-1} . ^1H NMR (500 MHz, CDCl_3) δ 1.23 (t, $J = 7.1$ Hz, 3H), 1.23 – 1.35 (m, 1H), 1.36 – 1.46 (m, 1H), 1.56 – 1.65 (m, 1H), 1.83 – 2.02 (m, 3H), 2.29 (tt, $J = 11.3, 3.8$ Hz, 1H), 2.83 (d, $J = 11.1$ Hz, 1H), 2.89 (ddd, $J = 13.7, 6.0, 1.1$ Hz, 1H), 2.99 (ddd, $J = 13.7, 5.5, 1.4$ Hz, 1H), 3.07 (d, $J = 11.1$ Hz, 1H), 3.77 (s, 3H), 3.78 (s, 3H), 4.08 (qd, $J = 7.1, 1.8$ Hz, 2H), 5.65 (dt, $J = 11.8, 5.7$ Hz, 1H), 6.38 (d, $J = 12.2$ Hz, 1H), 6.78 – 6.83 (m, 4H), 7.32 – 7.38 (m, 4H), 8.71 (s, 1H) ppm. ^{13}C NMR (126 MHz, CDCl_3) δ 14.30, 24.35, 27.04, 41.38, 53.16, 54.70, 55.06, 55.32, 55.36, 60.50, 77.76, 113.35, 113.39, 123.68, 127.63, 127.69, 140.96, 141.00, 143.12, 158.27, 158.32, 173.82 ppm. HRMS (EI): $[\text{M}]^+$ calcd. for $\text{C}_{26}\text{H}_{33}\text{O}_5\text{N}$ 439.2359; found 439.2361.

4.3.18. Ethyl (Z)-1-[4,4-bis(4-methoxyphenyl)but-2-en-1-yl]piperidine-3-carboxylate, (rac-9f)

According to **GP1**: Ester *rac-8f* (108 mg, 0.250 mmol), quinoline (4 mg, 0.03 mmol), and Lindlar's catalyst (54 mg, 0.025 mmol) in ethanol (3 mL). The crude product was purified by flash chromatography with DCM/MeOH (99:1). Yellow oil (60 mg, 57%).

IR (Film): $\tilde{\nu} = 2936, 1728, 1674, 1609, 1577, 1508, 1465, 1437, 1301, 1247, 1176, 1148, 1097, 1034, 908, 826, 728$ cm^{-1} . ^1H NMR (400 MHz, CDCl_3) δ 1.23 (t, $J = 7.1$ Hz, 3H), 1.42 (qd, $J = 12.0, 4.0$ Hz, 1H), 1.51 – 1.63 (m, 1H), 1.65 – 1.75 (m, 1H), 1.89 – 2.01 (m, 2H), 2.13 (t, $J = 10.7$ Hz, 1H), 2.50 – 2.60 (m, 1H), 2.78 (d, $J = 11.2$ Hz, 1H), 3.01 (d, $J = 11.3$ Hz, 1H), 3.13 (dd, $J = 6.8, 1.7$ Hz, 2H), 3.77 (s, 3H), 3.78 (s, 3H), 4.11 (q, $J = 7.1$ Hz, 2H), 4.92 (d, $J = 9.9$ Hz, 1H), 5.65 (dt, $J = 10.9, 6.7$ Hz, 1H), 5.98 (t, $J = 10.4$ Hz, 1H), 6.79 – 6.85 (m, 4H), 7.05 – 7.11 (m, 4H) ppm. ^{13}C NMR (101 MHz, CDCl_3) δ 14.36, 24.73, 27.03, 42.08, 47.08, 53.89, 55.38, 55.67, 55.70, 60.44, 113.97, 126.49, 129.21, 135.74, 136.76, 158.11, 174.24 ppm. HRMS (ESI): $[\text{M}+\text{H}]^+$ calcd. for $\text{C}_{26}\text{H}_{34}\text{O}_4\text{N}$, 424.2482; found: 424.2477.

4.3.19. Ethyl (Z)-1-[4,4,5-tris(4-methoxyphenyl)pent-2-en-1-yl]piperidine-3-carboxylate, (rac-9g)

According to **GP2**: Ester *rac-8g* (56 mg, 0.10 mmol), quinoline (1 mg, 0.01 mmol), and Lindlar's catalyst (53 mg, 0.025 mmol) in ethanol (3 mL). The crude product was purified by MPLC with DCM/MeOH (98:2). Yellow oil (30 mg, 55%).

IR (Film): $\tilde{\nu} = 2935, 2829, 1729, 1609, 1579, 1511, 1467, 1440, 1372, 1301, 1249, 1179, 1151, 1109, 1035, 828, 775, 668$ cm^{-1} . ^1H NMR (500 MHz, CD_2Cl_2) δ 1.22 (t, $J = 7.1$ Hz, 3H), 1.25 – 1.36 (m, 1H), 1.38 – 1.47 (m, 1H), 1.55 – 1.68 (m, 2H), 1.75 – 1.83 (m, 2H), 2.32 (dd, $J = 6.1, 2.1$ Hz, 2H), 2.37 – 2.47 (m, 2H), 2.64 (d, $J = 11.3$ Hz, 1H), 3.44 (s, 2H), 3.71 (s, 3H), 3.78 (s, 6H), 4.07 (q, $J = 7.1$ Hz, 2H), 5.59 (dt, $J = 12.3, 6.2$ Hz, 1H), 6.07 (dt, $J = 12.1, 2.1$ Hz, 1H), 6.58 – 6.62 (m, 2H), 6.63 – 6.67 (m, 2H), 6.76 – 6.81 (m, 4H), 7.13 – 7.17 (m, 4H) ppm. ^{13}C NMR (126 MHz, CD_2Cl_2) δ 14.59, 25.08, 27.26, 42.42, 47.59, 52.55, 54.04, 55.55, 55.72, 55.91, 56.64, 60.66, 113.16, 113.59, 130.22, 130.57, 130.74, 132.46, 137.44, 140.02, 140.08, 158.29, 158.58, 174.49 ppm. HRMS (EI): $[\text{M}+\text{H}]^+$ calcd. for $\text{C}_{34}\text{H}_{42}\text{O}_5\text{N}$, 544.3058; found: 544.3059.

4.3.20. Ethyl (Z)-1-[4,4-bis(4-methoxyphenyl)-5-phenylpent-2-en-1-yl]piperidine-3-carboxylate, (*rac-9h*)

According to **GP2**: Ester *rac-8h* (32 mg, 0.060 mmol), quinoline (1 mg, 0.01 mmol), and Lindlar's catalyst (32 mg, 0.015 mmol) in ethanol (3 mL). The crude product was purified by MPLC with DCM/MeOH (98:2). Yellow oil (20 mg, 64%).

IR (Film): $\tilde{\nu}$ = 2938, 2835, 1730, 1677, 1607, 1579, 1509, 1454, 1372, 1290, 1249, 1181, 1150, 1097, 1034, 858, 829, 804, 757, 733, 702, 668 cm^{-1} . ^1H NMR (500 MHz, CD_2Cl_2) δ 1.22 (t, J = 7.1 Hz, 3H), 1.26 – 1.36 (m, 1H), 1.38 – 1.48 (m, 1H), 1.56 – 1.62 (m, 1H), 1.66 (t, J = 10.8 Hz, 1H), 1.76 – 1.84 (m, 2H), 2.33 (dd, J = 6.2, 2.2 Hz, 2H), 2.37 – 2.47 (m, 2H), 2.65 (d, J = 10.6 Hz, 1H), 3.51 (s, 2H), 3.78 (s, 6H), 4.07 (q, J = 7.1 Hz, 2H), 5.60 (dt, J = 12.2, 6.1 Hz, 1H), 6.09 (dt, J = 12.2, 2.2 Hz, 1H), 6.74 – 6.77 (m, 2H), 6.77 – 6.81 (m, 4H), 7.04 – 7.12 (m, 3H), 7.14 – 7.18 (m, 4H) ppm. ^{13}C NMR (126 MHz, CD_2Cl_2) δ 14.60, 25.10, 27.27, 42.44, 48.38, 52.47, 54.07, 55.72, 55.94, 56.64, 60.66, 113.61, 126.50, 127.79, 130.18, 130.89, 131.61, 137.27, 138.73, 140.01, 140.07, 158.32, 174.50 ppm. HRMS (EI): $[\text{M}]^+$ calcd. for $\text{C}_{33}\text{H}_{39}\text{O}_4\text{N}$, 513.2879; found 513.2880.

4.3.21. Ethyl (Z)-1-[5,5,5-tris(4-methoxyphenyl)pent-2-en-1-yl]piperidine-3-carboxylate, (*rac-9i*)

According to **GP1**: Ester *rac-8i* (83 mg, 0.15 mmol), quinoline (10 mg, 0.080 mmol), and Lindlar's catalyst (64 mg, 0.030 mmol) in ethanol (2 mL). The crude product was purified by flash chromatography with DCM/MeOH (98:2). Yellow oil (40 mg, 49%).

IR (Film): $\tilde{\nu}$ = 2937, 2835, 1728, 1676, 1607, 1579, 1509, 1464, 1441, 195, 1250, 1182, 1152, 1035, 826, 734 cm^{-1} . ^1H NMR (400 MHz, CD_2Cl_2) δ 1.23 (t, J = 7.1 Hz, 3H), 1.34 – 1.57 (m, 2H), 1.62 – 1.72 (m, 1H), 1.81 – 1.95 (m, 2H), 2.09 (t, J = 10.5 Hz, 1H), 2.49 (tt, J = 10.2, 3.8 Hz, 1H), 2.60 (d, J = 11.3 Hz, 1H), 2.82 – 2.89 (m, 1H), 2.89 (d, J = 5.1 Hz, 2H), 3.23 – 3.40 (m, 2H), 3.77 (s, 9H), 4.09 (q, J = 7.1 Hz, 2H), 5.33 – 5.45 (m, 2H), 6.75 – 6.82 (m, 6H), 7.06 – 7.13 (m, 6H) ppm. ^{13}C NMR (101 MHz, CD_2Cl_2) δ 14.60, 25.20, 27.49, 39.88, 42.53, 54.25, 54.99, 55.69, 56.16, 56.31, 60.69, 113.51, 128.73, 130.26, 130.71, 140.51, 158.20, 174.55 ppm. HRMS (EI): $[\text{M}]^+$ calcd. for $\text{C}_{34}\text{H}_{41}\text{O}_5\text{N}$, 543.2985; found: 543.2964.

4.3.22. Ethyl (Z)-1-[5,5,5-triphenylpent-2-en-1-yl]piperidine-3-carboxylate, (*rac-9j*)

According to **GP1**: Ester *rac-8j* (56 mg, 0.12 mmol), quinoline (2 mg, 0.01 mmol), and Lindlar's catalyst (51 mg, 0.024 mmol) in ethanol (2 mL). The crude product was purified by flash chromatography with $\text{Et}_2\text{O}/\text{PE}/\text{MeOH}$ (50:50:0.5). Yellow oil (37 mg, 68%).

IR (Film): $\tilde{\nu}$ = 3056, 3021, 2937, 2853, 2788, 1730, 1595, 1492, 1445, 1374, 1306, 1217, 1179, 1150, 1133, 1100, 1032, 855, 801, 759, 700, 669 cm^{-1} . ^1H NMR (400 MHz, CD_2Cl_2) δ 1.24 (t, J = 7.1 Hz, 3H), 1.36 – 1.56 (m, 2H), 1.64 – 1.71 (m, 1H), 1.84 – 1.94 (m, 2H), 2.08 (t, J = 10.5 Hz, 1H), 2.49 (tt, J = 10.3, 3.8 Hz, 1H), 2.60 (d, J = 11.8 Hz, 1H), 2.82 – 2.89 (m, 3H), 3.37 – 3.48 (m, 2H), 4.10 (q, J = 7.1 Hz, 2H), 5.35 – 5.45 (m, 2H), 7.18 – 7.30 (m, 15H) ppm. ^{13}C NMR (101 MHz, CD_2Cl_2) δ 14.61, 25.20, 27.48, 39.45, 42.56, 54.27, 56.17, 56.25, 57.03, 60.69, 126.52, 128.36, 129.13, 129.80, 129.88, 147.88, 174.56 ppm. HRMS (EI): $[\text{M}]^+$ calcd. for $\text{C}_{31}\text{H}_{35}\text{O}_2\text{N}$, 453.2668; found: 453.2650.

4.3.23. Ethyl (Z)-1-[5,5,5-tris(4-methoxyphenyl)pent-3-en-1-yl]piperidine-3-carboxylate, (*rac-9k*)

According to **GP1**: Ester *rac-8k* (83 mg, 0.15 mmol), quinoline (1 mg, 0.01 mmol), and Lindlar's catalyst (64 mg, 0.030 mmol) in ethanol (3 mL). The crude product was purified by flash chromatography with DCM/MeOH (99:1). Yellow oil (50 mg, 61%).

IR (Film): $\tilde{\nu}$ = 2938, 2834, 2807, 1729, 1606, 1579, 1506, 1464, 1442, 1370, 1297, 1249, 1178, 1151, 1116, 1035, 914, 826, 703, 668, 572 cm^{-1} . ^1H NMR (400 MHz, CD_2Cl_2) δ 1.22 (t, J = 7.1 Hz, 3H), 1.29 – 1.49 (m, 2H), 1.56 – 1.65 (m, 3H), 1.75 (td, J = 10.9, 2.9 Hz, 1H), 1.79 – 1.86 (m, 1H), 1.92 (t, J = 10.6 Hz, 1H), 2.01 – 2.13 (m, 2H), 2.37 – 2.46 (m, 2H), 2.66 (d, J = 10.9 Hz, 1H), 3.77 (s, 9H), 4.08 (q, J = 7.2 Hz, 2H), 5.64 (dt, J = 11.7, 7.3 Hz, 1H), 6.42 (dt, J = 11.8, 1.9 Hz, 1H), 6.76 – 6.81 (m, 6H), 7.02 – 7.07 (m, 6H) ppm. ^{13}C NMR (101 MHz, CD_2Cl_2) δ 14.59, 25.16, 27.53, 27.56, 42.51, 54.04, 54.40, 55.70, 56.07, 58.16, 58.91, 113.47, 131.34, 132.11, 139.94, 140.86, 158.26, 174.57 ppm. HRMS (EI): $[\text{M}-\text{H}]^+$ calcd. for $\text{C}_{34}\text{H}_{40}\text{O}_5\text{N}$, 542.2912; found: 542.2900.

4.3.24. Ethyl (Z)-1-[5,5-triphenylpent-3-en-1-yl]piperidine-3-carboxylate, (rac-9I)

According to **GP1**: Ester *rac-8I* (78 mg, 0.17 mmol), quinoline (2 mg, 0.02 mmol), and Lindlar's catalyst (73 mg, 0.034 mmol) in ethanol (4 mL). The crude product was purified by flash chromatography with DCM/MeOH (99:1). Yellow oil (41 mg, 53%).

IR (Film): $\tilde{\nu}$ = 3057, 3019, 2978, 2940, 2853, 2806, 1731, 1594, 1490, 1467, 1445, 1370, 1311, 1271, 114, 1179, 1151, 1134, 1103, 1033, 1001, 964, 931, 901, 862, 752, 701, 667 cm^{-1} . ^1H NMR (500 MHz, CD_2Cl_2) δ 1.22 (t, J = 7.1 Hz, 3H), 1.28 – 1.37 (m, 1H), 1.37 – 1.46 (m, 1H), 1.55 – 1.63 (m, 3H), 1.73 (td, J = 10.9, 3.0 Hz, 1H), 1.78 – 1.84 (m, 1H), 1.88 (t, J = 10.6 Hz, 1H), 1.98 – 2.07 (m, 2H), 2.36 – 2.43 (m, 2H), 2.62 (d, J = 11.1 Hz, 1H), 4.07 (q, J = 7.1 Hz, 2H), 5.70 (dt, J = 11.7, 7.3 Hz, 1H), 6.49 (dt, J = 11.7, 2.0 Hz, 1H), 7.16 – 7.21 (m, 9H), 7.24 – 7.28 (m, 6H) ppm. ^{13}C NMR (126 MHz, CD_2Cl_2) δ 14.60, 25.13, 27.49, 27.70, 42.47, 53.99, 55.99, 57.91, 60.63, 60.92, 126.48, 128.29, 130.50, 132.94, 139.48, 148.28, 174.57 ppm. HRMS (EI): $[\text{M}-\text{H}]^+$ calcd. for $\text{C}_{31}\text{H}_{34}\text{O}_2\text{N}$, 452.2595; found: 452.2573.

4.4. Biological evaluation

4.4.1. MS Binding Assays

The MS Binding Assays were performed with mGAT1 membrane preparations obtained from a stable HEK293 cell line and NO711 as non labeled marker in competitive binding experiments as described previously.³⁵

4.4.2. GABA uptake assay

The [^3H]GABA uptake assays were performed in a 96-well plate format with intact HEK293 cells stably expressing mGAT1, mGAT2, mGAT3, mGAT4 as described earlier.³⁴

Funding:

This research did not receive any specific grant from funding agencies in the public, commercial, or not-for-profit sectors.

Appendix A. Supplementary data:

Supplementary data to this article can be found online at: <https://doi.org/XXXX>

5. References and notes

1. Lanctot KL, Herrmann N, Mazzotta P, Khan LR, Ingber N. GABAergic function in Alzheimer's disease: evidence for dysfunction and potential as a therapeutic target for the treatment of behavioural and psychological symptoms of dementia. *Can J Psychiatry*. 2004;49:439-453. <https://doi.org/10.1177/070674370404900705>
2. Kalueff AV, Nutt DJ. Role of GABA in anxiety and depression. *Depress Anxiety*. 2007;24:495-517. <https://doi.org/10.1002/da.20262>
3. Treiman DM. GABAergic mechanisms in epilepsy. *Epilepsia*. 2001;42 Suppl 3:8-12. <https://doi.org/10.1046/j.1528-1157.2001.042suppl.3008.x>
4. Dalby NO. Inhibition of gamma-aminobutyric acid uptake: anatomy, physiology and effects against epileptic seizures. *Eur. J. Pharmacol.* 2003;479:127-137. <https://doi.org/10.1016/j.ejphar.2003.08.063>
5. Daemen MA, Hoogland G, Cijntje JM, Spincemaille GH. Upregulation of the GABA-transporter GAT-1 in the spinal cord contributes to pain behaviour in experimental neuropathy. *Neurosci. Lett.* 2008;444:112-115. <https://doi.org/10.1016/j.neulet.2008.08.001>
6. Bowery NG, Smart TG. GABA and glycine as neurotransmitters: a brief history. *Br. J. Pharmacol.* 2006;147 Suppl 1:S109-119. <https://doi.org/10.1038/sj.bjp.0706443>
7. Cherubini E. Generating diversity at GABAergic synapses. *Trends Neurosci.* 2001;24:155-162. [https://doi.org/10.1016/S0166-2236\(00\)01724-0](https://doi.org/10.1016/S0166-2236(00)01724-0)
8. Borden LA. GABA transporter heterogeneity: pharmacology and cellular localization. *Neurochem. Int.* 1996;29:335-356. [https://doi.org/10.1016/0197-0186\(95\)00158-1](https://doi.org/10.1016/0197-0186(95)00158-1)
9. Conti F, Minelli A, Melone M. GABA transporters in the mammalian cerebral cortex: localization, development and pathological implications. *Brain Res. Brain Res. Rev.* 2004;45:196-212. <https://doi.org/10.1016/j.brainresrev.2004.03.003>
10. Masson J, Sagne C, Hamon M, El Mestikawy S. Neurotransmitter transporters in the central nervous system. *Pharmacol. Rev.* 1999;51:439-464.
11. Kristensen AS, Andersen J, Jorgensen TN, Sorensen L, Eriksen J, Loland CJ, Stromgaard K, Gether U. SLC6 neurotransmitter transporters: structure, function, and regulation. *Pharmacol. Rev.* 2011;63:585-640. <https://doi.org/10.1124/pr.108.000869>
12. Madsen KK, Clausen RP, Larsson OM, Krogsgaard-Larsen P, Schousboe A, White HS. Synaptic and extrasynaptic GABA transporters as targets for anti-epileptic drugs. *J. Neurochem.* 2009;109 Suppl 1:139-144. <https://doi.org/10.1111/j.1471-4159.2009.05982.x>
13. Palacin M, Estevez R, Bertran J, Zorzano A. Molecular biology of mammalian plasma membrane amino acid transporters. *Physiol. Rev.* 1998;78:969-1054. <https://doi.org/10.1152/physrev.1998.78.4.969>
14. Minelli A, DeBiasi S, Brecha NC, Zuccarello LV, Conti F. GAT-3, a high-affinity GABA plasma membrane transporter, is localized to astrocytic processes, and it is not confined to the vicinity of GABAergic synapses in the cerebral cortex. *J. Neurosci.* 1996;16:6255-6264. <https://doi.org/10.1523/JNEUROSCI.16-19-06255.1996>

15. Jin XT, Galvan A, Wichmann T, Smith Y. Localization and Function of GABA Transporters GAT-1 and GAT-3 in the Basal Ganglia. *Front. Syst. Neurosci.* 2011;5:63. <https://doi.org/10.3389/fnsys.2011.00063>
16. Zhou Y, Holmseth S, Hua R, Lehre AC, Olofsson AM, Poblete-Naredo I, Kempson SA, Danbolt NC. The betaine-GABA transporter (BGT1, slc6a12) is predominantly expressed in the liver and at lower levels in the kidneys and at the brain surface. *Am. J. Physiol. Renal. Physiol.* 2012;302:316-328. <https://doi.org/10.1152/ajprenal.00464.2011>
17. Kempson SA, Zhou Y, Danbolt NC. The betaine/GABA transporter and betaine: roles in brain, kidney, and liver. *Front Physiol.* 2014;5:159. <https://doi.org/10.3389/fphys.2014.00159>
18. Leppik IE, Gram L, Deaton R, Sommerville KW. Safety of tiagabine: summary of 53 trials. *Epilepsy Res.* 1999;33:235-246. [https://doi.org/10.1016/S0920-1211\(98\)00094-1](https://doi.org/10.1016/S0920-1211(98)00094-1)
19. Nielsen EB, Suzdak PD, Andersen KE, Knutsen LJ, Sonnewald U, Braestrup C. Characterization of tiagabine (NO-328), a new potent and selective GABA uptake inhibitor. *Eur. J. Pharmacol.* 1991;196:257-266. [https://doi.org/10.1016/0014-2999\(91\)90438-V](https://doi.org/10.1016/0014-2999(91)90438-V)
20. Andersen KE, Braestrup C, Groenwald FC, Joergensen AS, Nielsen EB, Sonnewald U, Soerensen PO, Suzdak PD, Knutsen LJS. The synthesis of novel GABA uptake inhibitors. 1. Elucidation of the structure-activity studies leading to the choice of (R)-1-[4,4-bis(3-methyl-2-thienyl)-3-butenyl]-3-piperidinecarboxylic acid (Tiagabine) as an anticonvulsant drug candidate. *J. Med. Chem.* 1993;36:1716-1725. <https://doi.org/10.1021/jm00064a005>
21. Steffan T, Renukappa-Gutke T, Hofner G, Wanner KT. Design, synthesis and SAR studies of GABA uptake inhibitors derived from 2-substituted pyrrolidine-2-yl-acetic acids. *Bioorg. Med. Chem.* 2015;23:1284-1306. <https://doi.org/10.1016/j.bmc.2015.01.035>
22. Hellenbrand T, Hofner G, Wein T, Wanner KT. Synthesis of 4-substituted nipecotic acid derivatives and their evaluation as potential GABA uptake inhibitors. *Bioorg. Med. Chem.* 2016;24:2072-2096. <https://doi.org/10.1016/j.bmc.2016.03.038>
23. Vogensen SB, Jorgensen L, Madsen KK, Jurik A, Borkar N, Rosatelli E, Nielsen B, Ecker GF, Schousboe A, Clausen RP. Structure activity relationship of selective GABA uptake inhibitors. *Bioorg. Med. Chem.* 2015;23:2480-2488. <https://doi.org/10.1016/j.bmc.2015.03.060>
24. Vogensen SB, Jorgensen L, Madsen KK, Borkar N, Wellendorph P, Skovgaard-Petersen J, Schousboe A, White HS, Krogsgaard-Larsen P, Clausen RP. Selective mGAT2 (BGT-1) GABA uptake inhibitors: design, synthesis, and pharmacological characterization. *J. Med. Chem.* 2013;56:2160-2164. <https://doi.org/10.1021/jm301872x>
25. Kerscher-Hack S, Renukappa-Gutke T, Hofner G, Wanner KT. Synthesis and biological evaluation of a series of N-alkylated imidazole alcanoic acids as mGAT3 selective GABA uptake inhibitors. *Eur. J. Med. Chem.* 2016;124:852-880. <https://doi.org/10.1016/j.ejmech.2016.09.012>
26. Dhar TGM, Borden LA, Tyagarajan S, Smith KE, Branchek TA, Weinshank RL, Gluchowski C. Design, Synthesis and Evaluation of Substituted TriarylNipecotic Acid Derivatives as GABA Uptake Inhibitors: Identification of a Ligand with Moderate Affinity and Selectivity for the Cloned Human GABA Transporter GAT-3. *J. Med. Chem.* 1994;37:2334-2342. <https://doi.org/10.1021/jm00041a012>

27. Pabel J, Faust M, Prehn C, Worlein B, Allmendinger L, Hofner G, Wanner KT. Development of an (S)-1-{2-[tris(4-methoxyphenyl)methoxy]ethyl}piperidine-3-carboxylic acid [(S)-SNAP-5114] carba analogue inhibitor for murine gamma-aminobutyric acid transporter type 4. *ChemMedChem*. 2012;7:1245-1255. <https://doi.org/10.1002/cmdc.201200126>
28. Tóth K, Höfner G, Wanner KT. Synthesis and biological evaluation of novel N-substituted nipecotic acid derivatives with an alkyne spacer as GABA uptake inhibitors. *Bioorg. Med. Chem.* 2018;26:3668-3687. <https://doi.org/10.1016/j.bmc.2018.05.049>
29. Toth K, Hofner G, Wanner KT. Synthesis and biological evaluation of novel N-substituted nipecotic acid derivatives with a trans-alkene spacer as potent GABA uptake inhibitors. *Bioorg Med Chem*. 2018;26:5944-5961. <https://doi.org/10.1016/j.bmc.2018.11.002>
30. Damgaard M, Al-Khawaja A, Vogensen SB, Jurik A, Sijm M, Lie ME, Baek MI, Rosenthal E, Jensen AA, Ecker GF, Frolund B, Wellendorph P, Clausen RP. Identification of the First Highly Subtype-Selective Inhibitor of Human GABA Transporter GAT3. *ACS Chem Neurosci*. 2015;6:1591-1599. <https://doi.org/10.1021/acschemneuro.5b00150>
31. Kuemmerle J, Jiang S, Tseng B, Kasibhatla S, Drewe J, Cai SX. Synthesis of caged 2,3,3a,7a-tetrahydro-3,6-methanobenzofuran-7(6H)-ones: Evaluating the minimum structure for apoptosis induction by gambogic acid. *Bioorg. Med. Chem.* 2008;16:4233-4241. <https://doi.org/10.1016/j.bmc.2008.02.084>
32. Albert BJ, Sivaramakrishnan A, Naka T, Koide K. Total Synthesis of FR901464, an Antitumor Agent that Regulates the Transcription of Oncogenes and Tumor Suppressor Genes. *J. Am. Chem. Soc.* 2006;128:2792-2793. <https://doi.org/10.1021/ja058216u>
33. Srikrishna A, Satyanarayana G. Total synthesis of (±)-herbertenediol. *Tetrahedron*. 2006;62:2892-2900. <https://doi.org/10.1016/j.tet.2006.01.021>
34. Kragler A, Hofner G, Wanner KT. Synthesis and biological evaluation of aminomethylphenol derivatives as inhibitors of the murine GABA transporters mGAT1-mGAT4. *Eur. J. Med Chem*. 2008;43:2404-2411. <https://doi.org/10.1016/j.ejmech.2008.01.005>
35. Zepperitz C, Hofner G, Wanner KT. MS-binding assays: kinetic, saturation, and competitive experiments based on quantitation of bound marker as exemplified by the GABA transporter mGAT1. *ChemMedChem*. 2006;1:208-217. <https://doi.org/10.1002/cmdc.200500038>
36. Petrera M, Wein T, Allmendinger L, Sindelar M, Pabel J, Hofner G, Wanner KT. Development of Highly Potent GAT1 Inhibitors: Synthesis of Nipecotic Acid Derivatives by Suzuki-Miyaura Cross-Coupling Reactions. *ChemMedChem*. 2016;11:519-538. <https://doi.org/10.1002/cmdc.201500490>

Supporting Information

Synthesis and biological evaluation of novel N-substituted nipecotic acid derivatives with a *cis*-alkene spacer as potent GABA uptake inhibitors

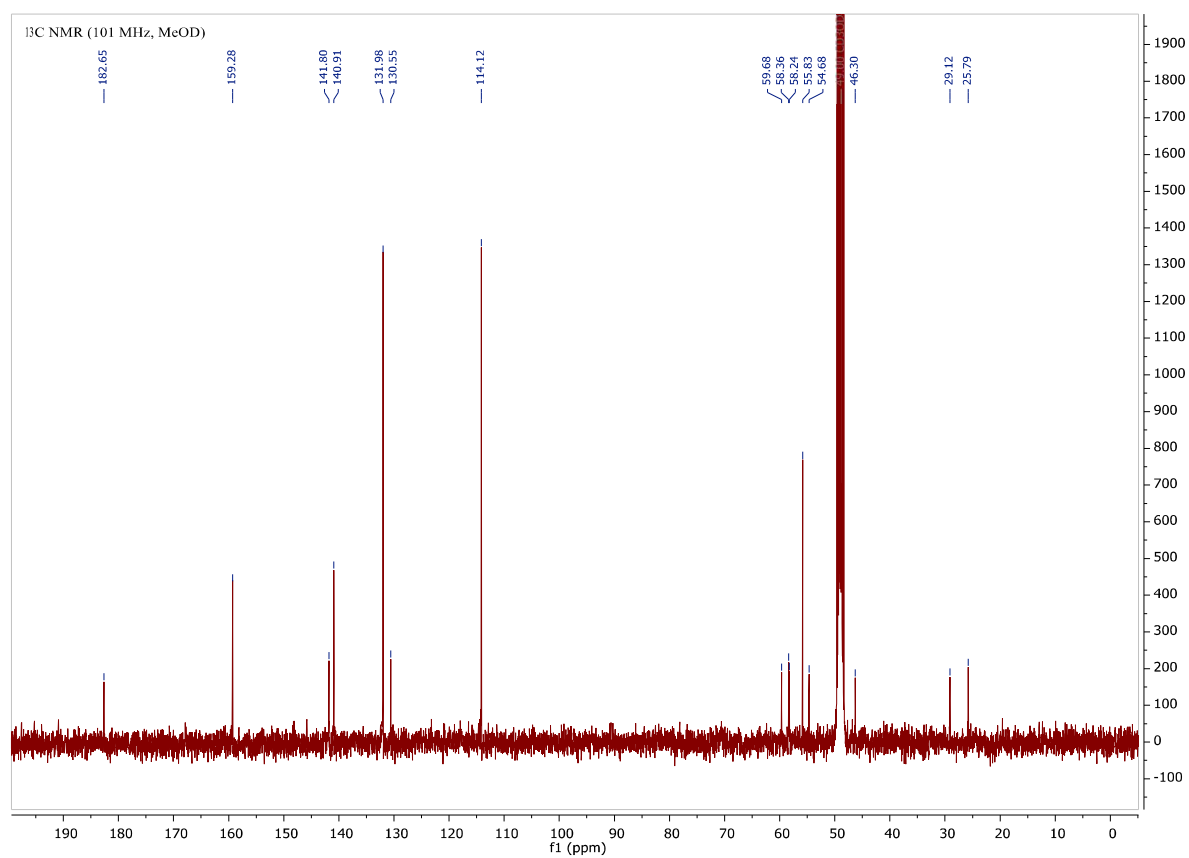
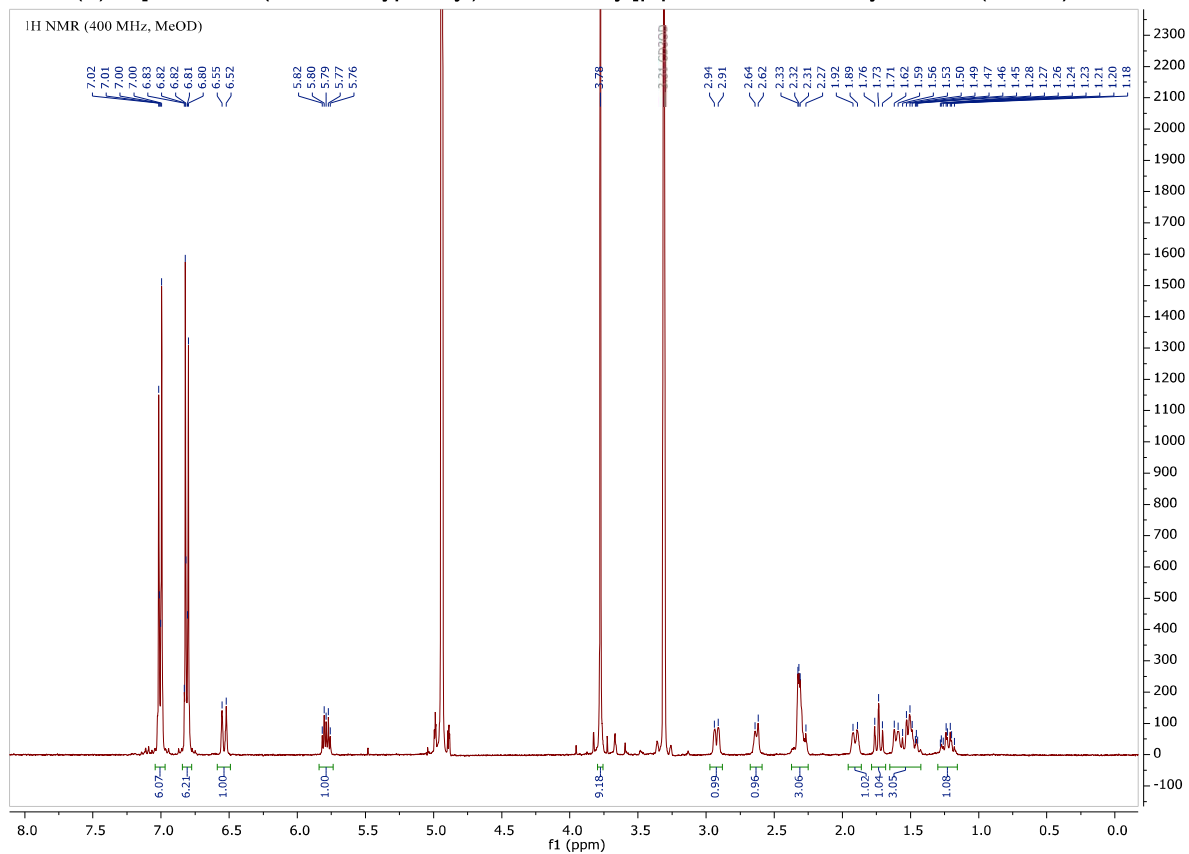
Krisztián Tóth, Georg Höfner, Klaus T. Wanner*

Department of Pharmacy – Center for Drug Research, Ludwig-Maximilians-Universität München, Butenandtstr. 5–13, 81377 Munich, Germany

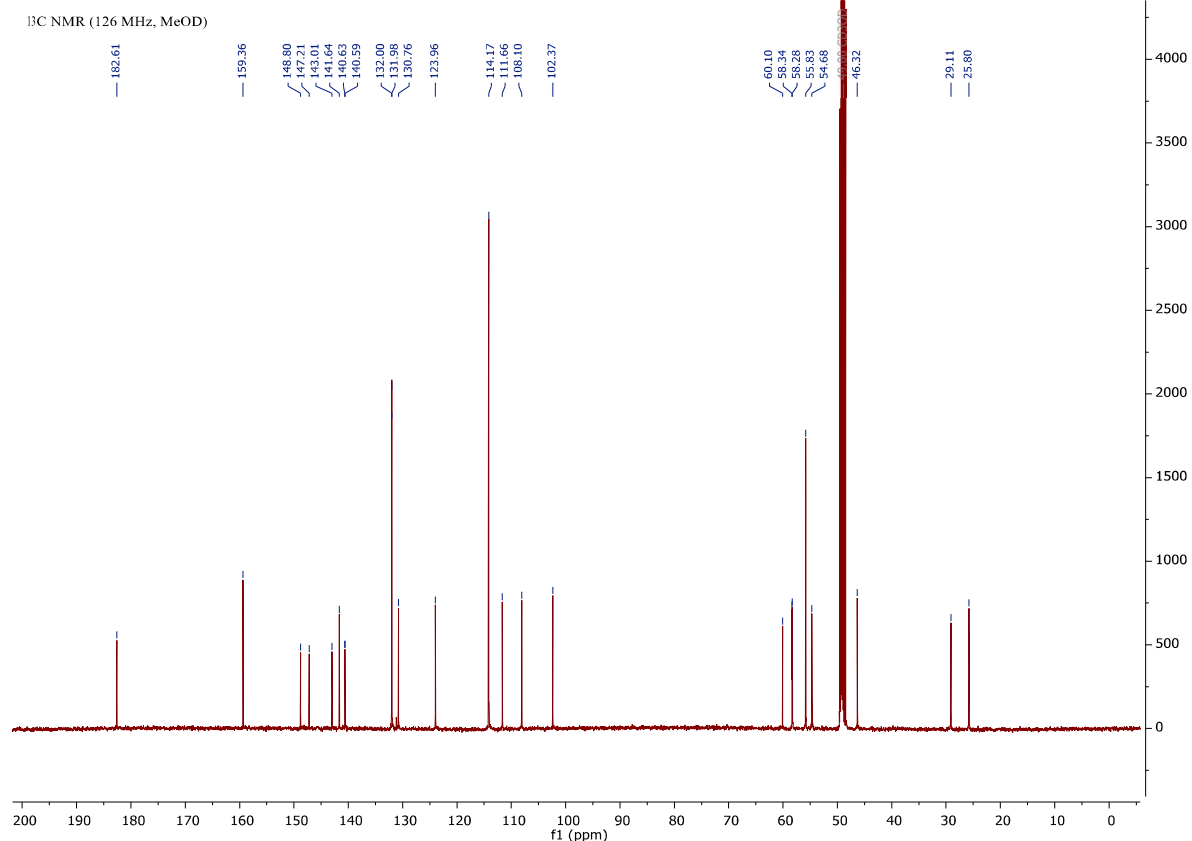
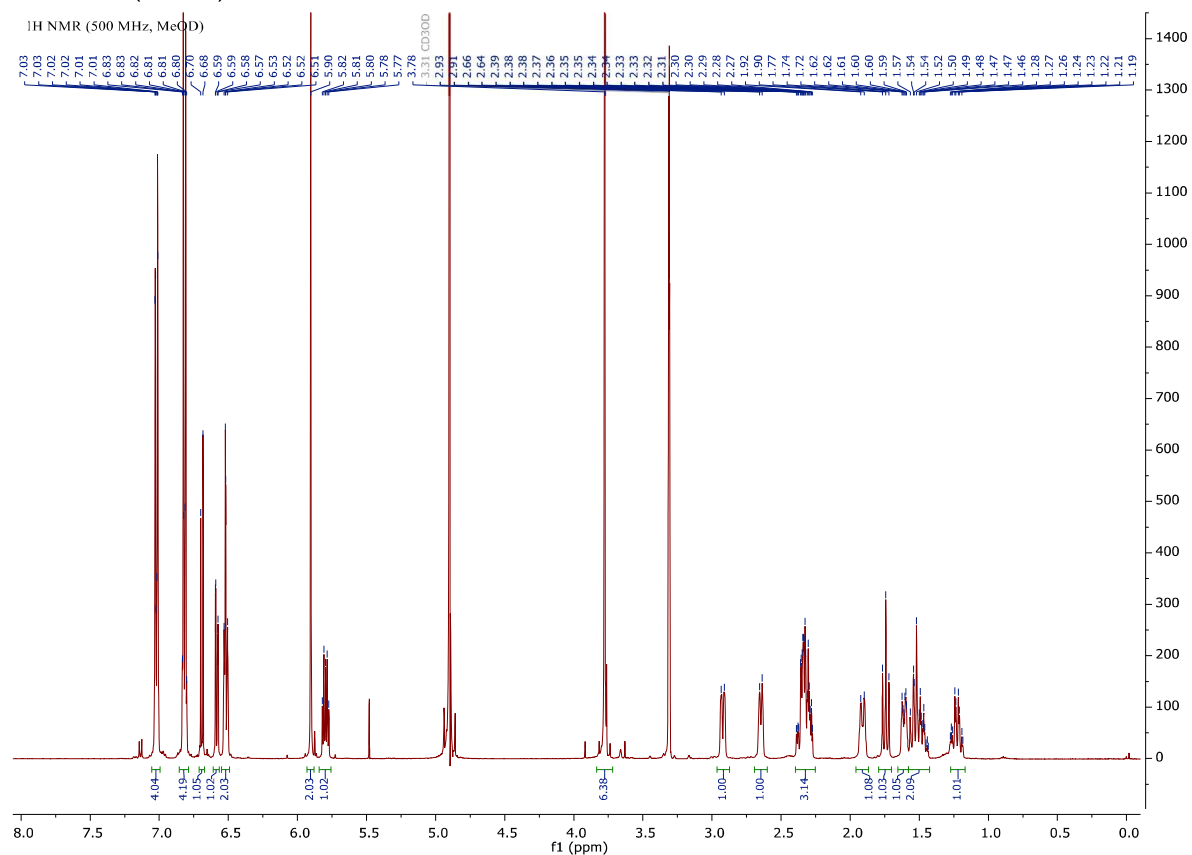
Table of contents:

1. List of the ^1H NMR and ^{13}C NMR data of synthesized compounds *rac-7a–l*.

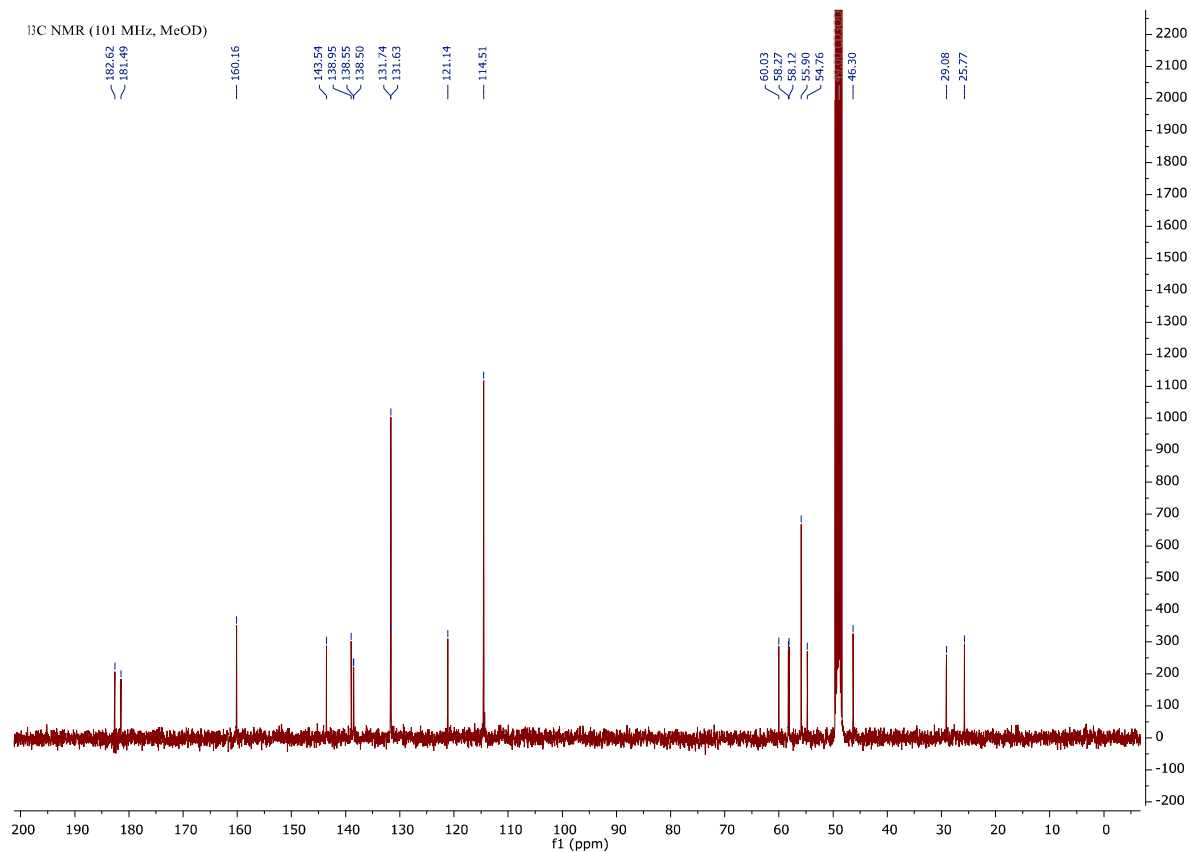
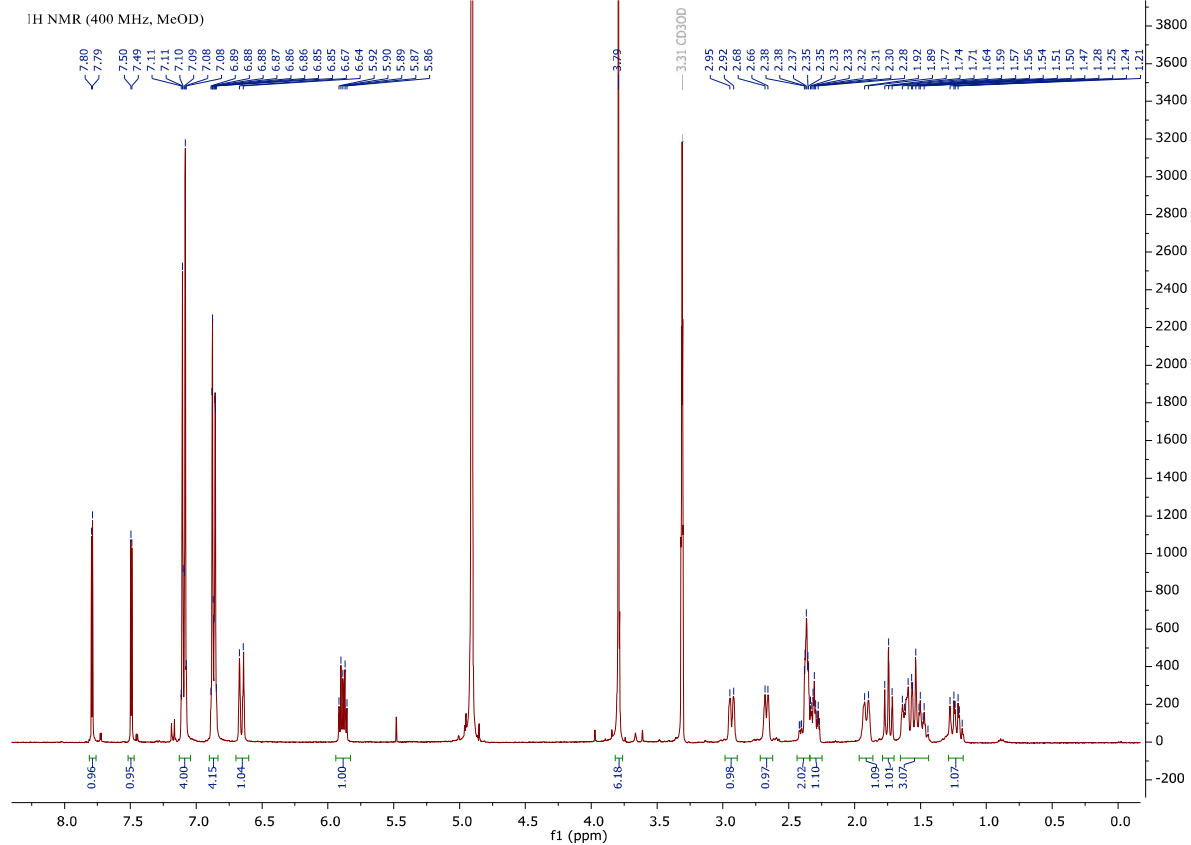
1.1. (Z)-1-[4,4,4-Tris(4-methoxyphenyl)but-2-en-1-yl]piperidine-3-carboxylic acid, (*rac-7a*)



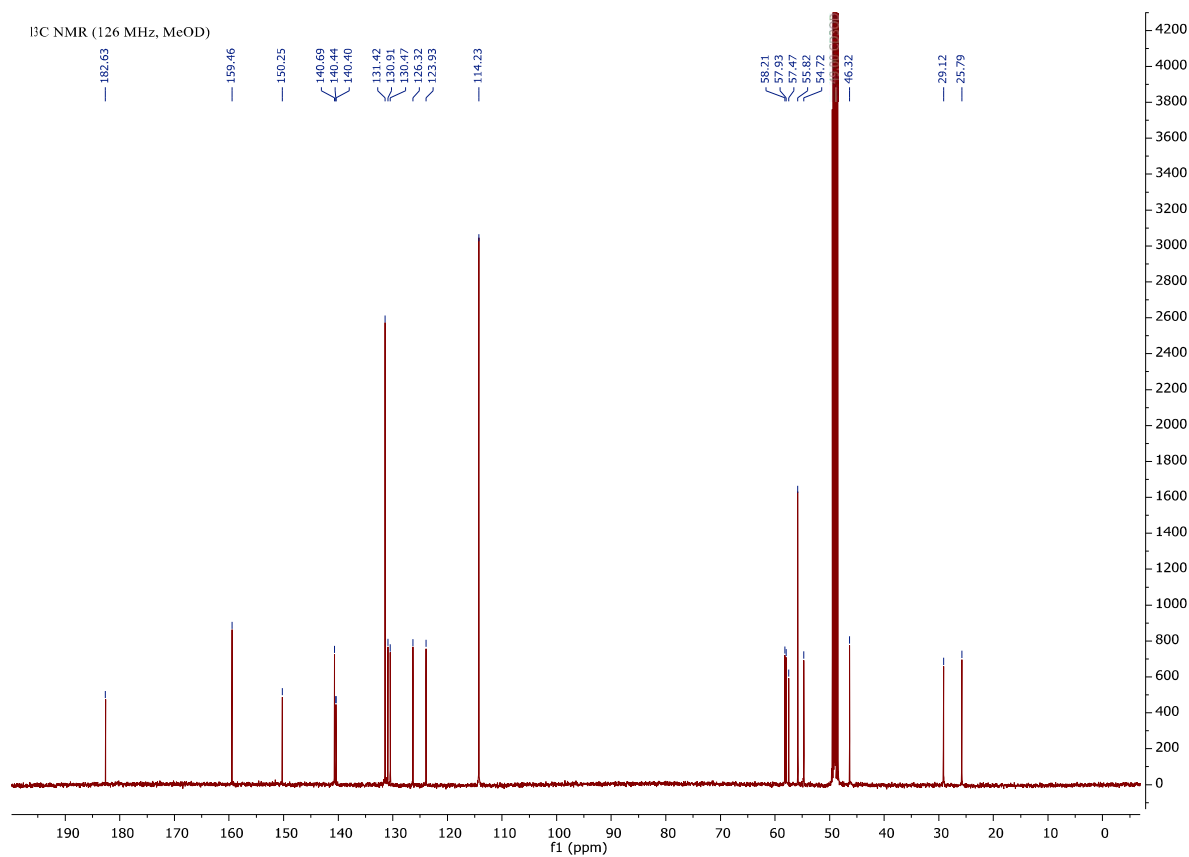
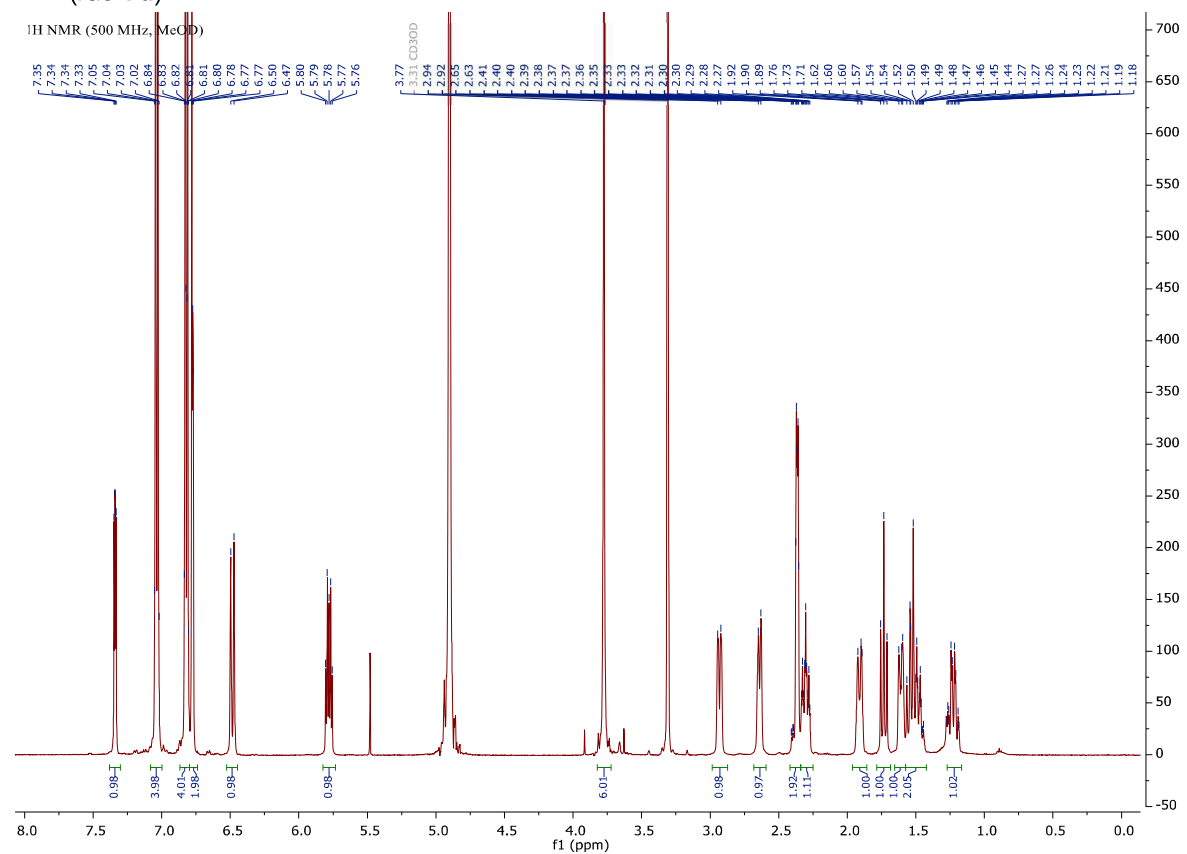
1.2. (Z)-1-[4-(Benzo[d][1,3]dioxol-5-yl)-4,4-bis(4-methoxyphenyl)but-2-en-1-yl]piperidine-3-carboxylic acid, (*rac*-**7b**)



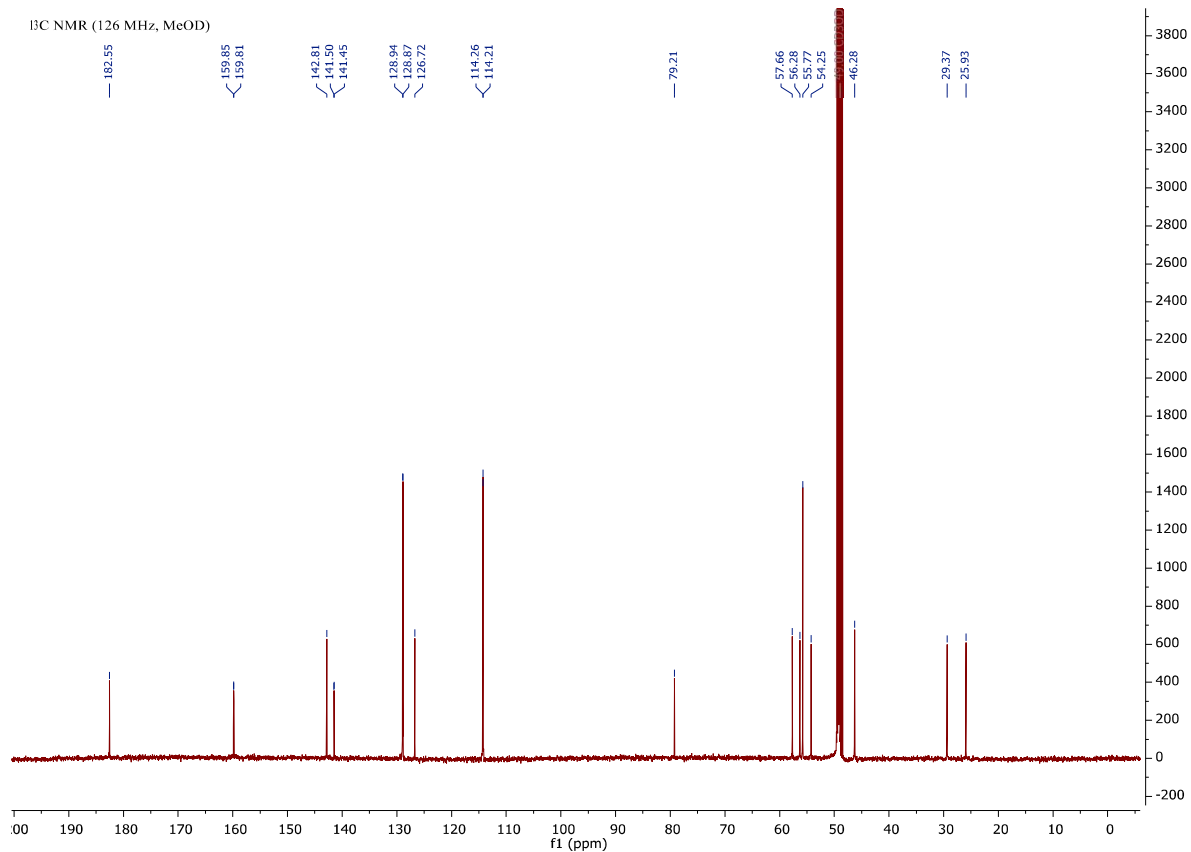
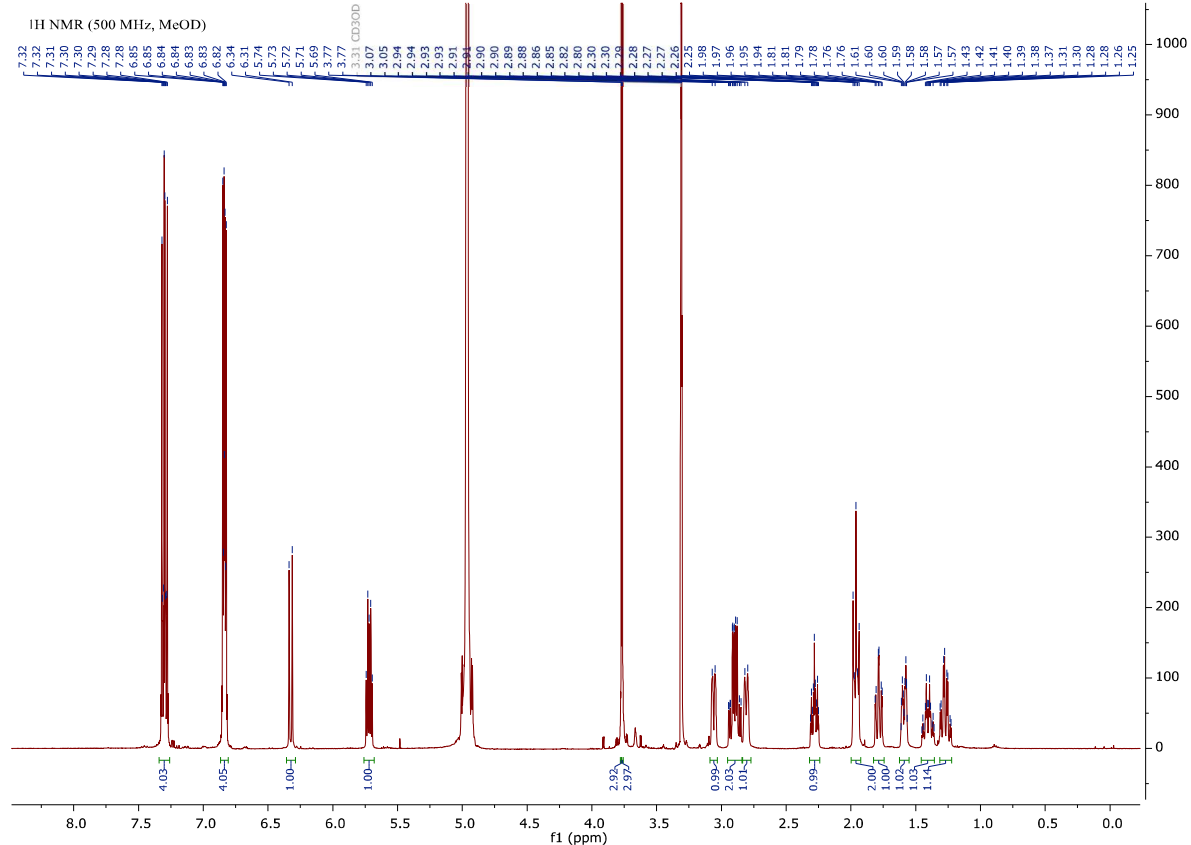
1.3. (Z)-1-[4,4-Bis(4-methoxyphenyl)-4-(thiazol-2-yl)but-2-en-1-yl]piperidine-3-carboxylic acid, (rac-7c)



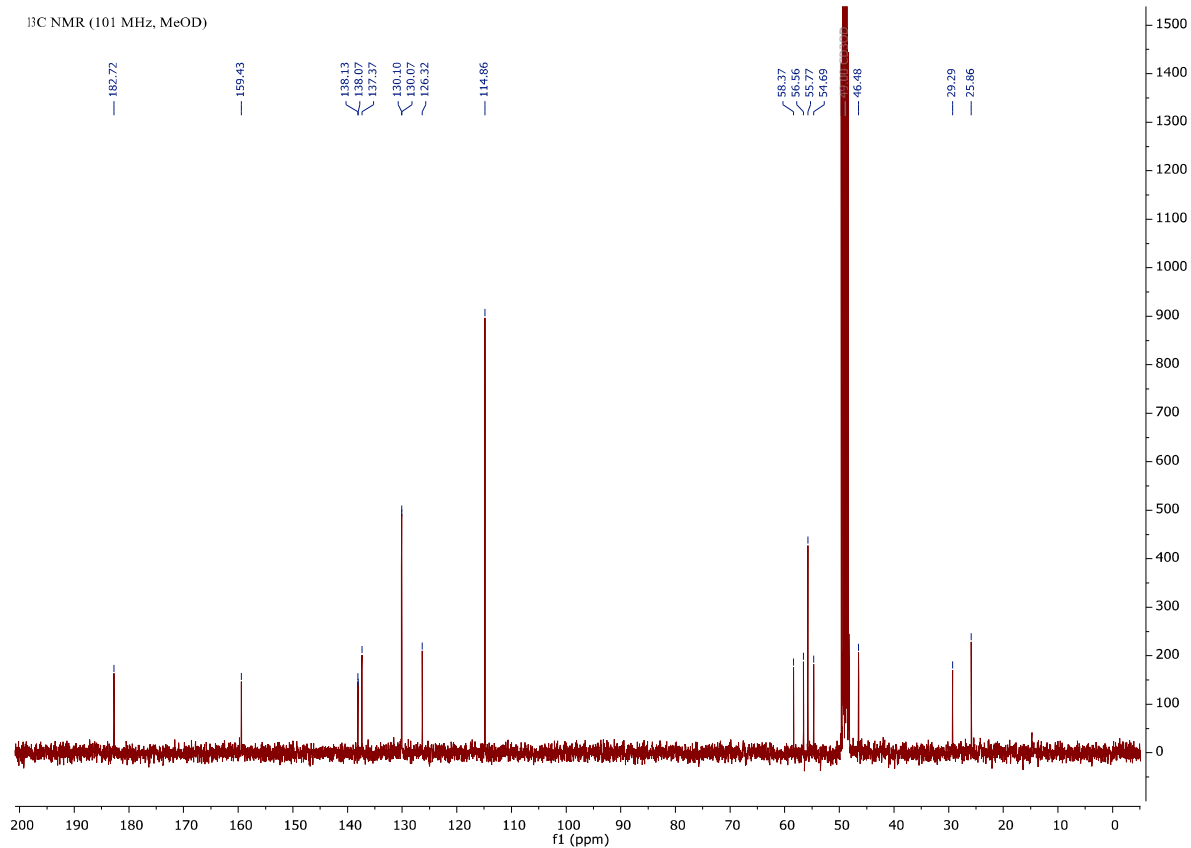
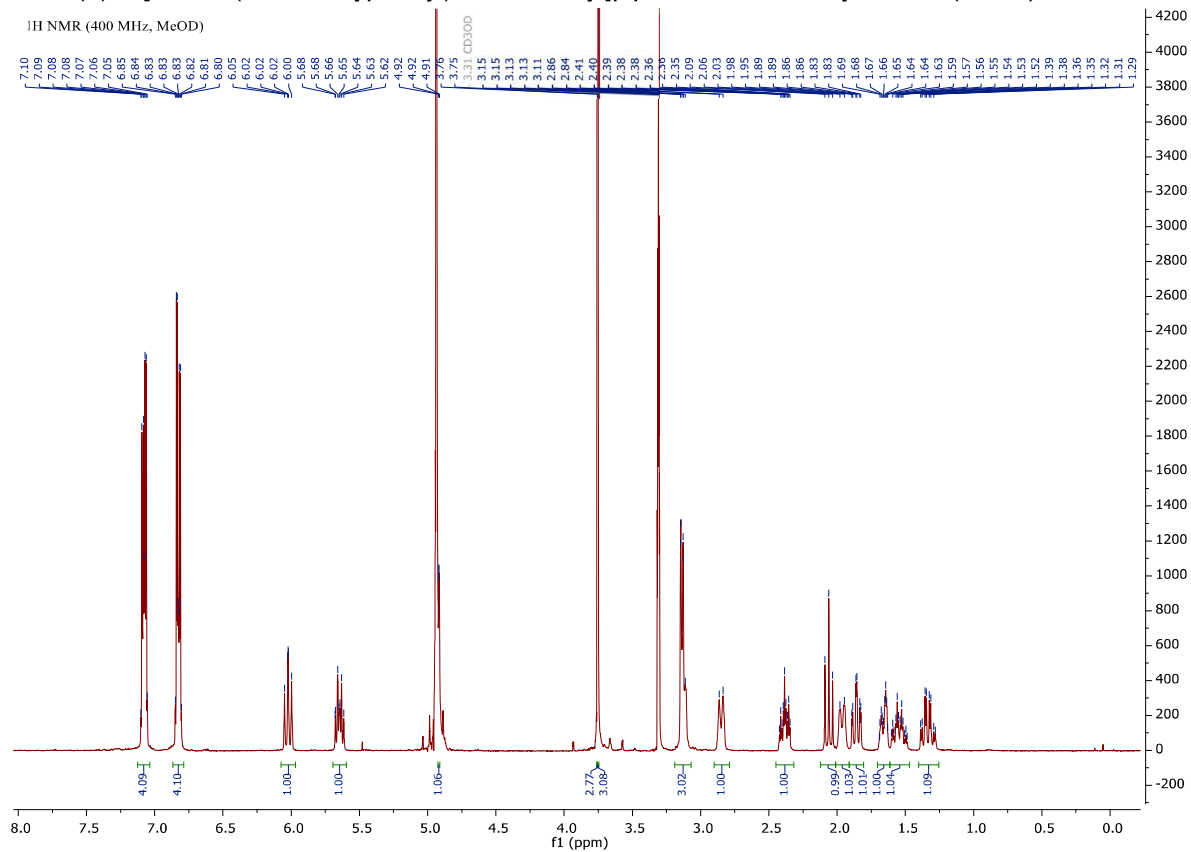
1.4. (Z)-1-[4,4-Bis(4-methoxyphenyl)-4-(thiophen-3-yl)but-2-en-1-yl]piperidine-3-carboxylic acid, (rac-7d)



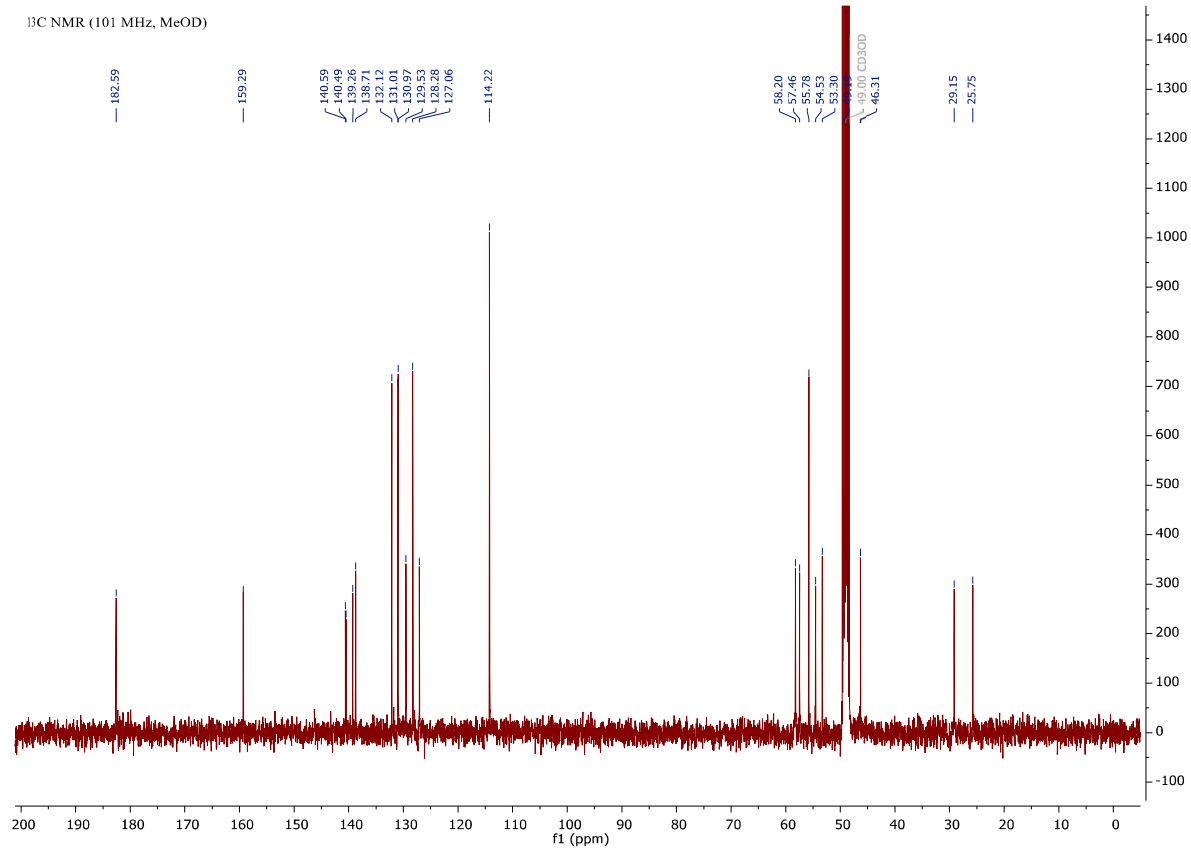
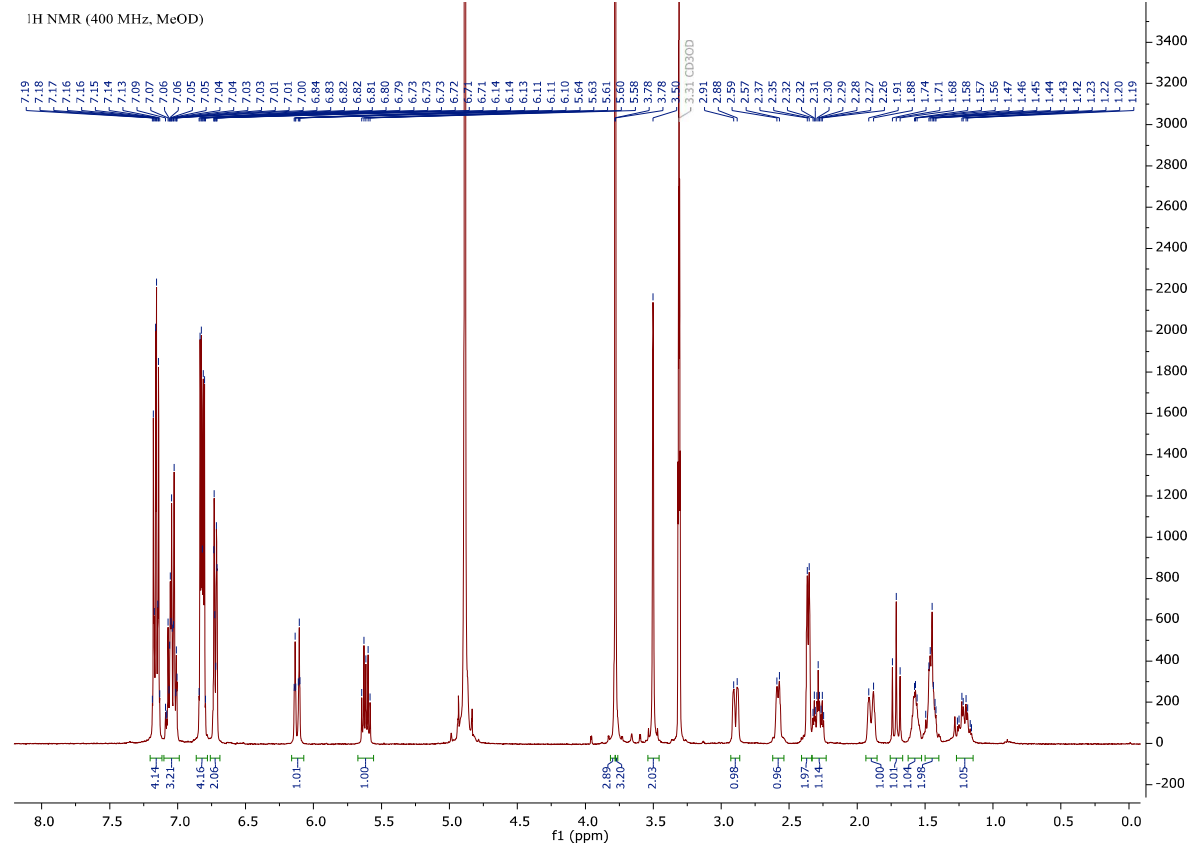
1.5. (Z)-1-[4-Hydroxy-4,4-bis(4-methoxyphenyl)but-2-en-1-yl]piperidine-3-carboxylic acid, (*rac-7e*)



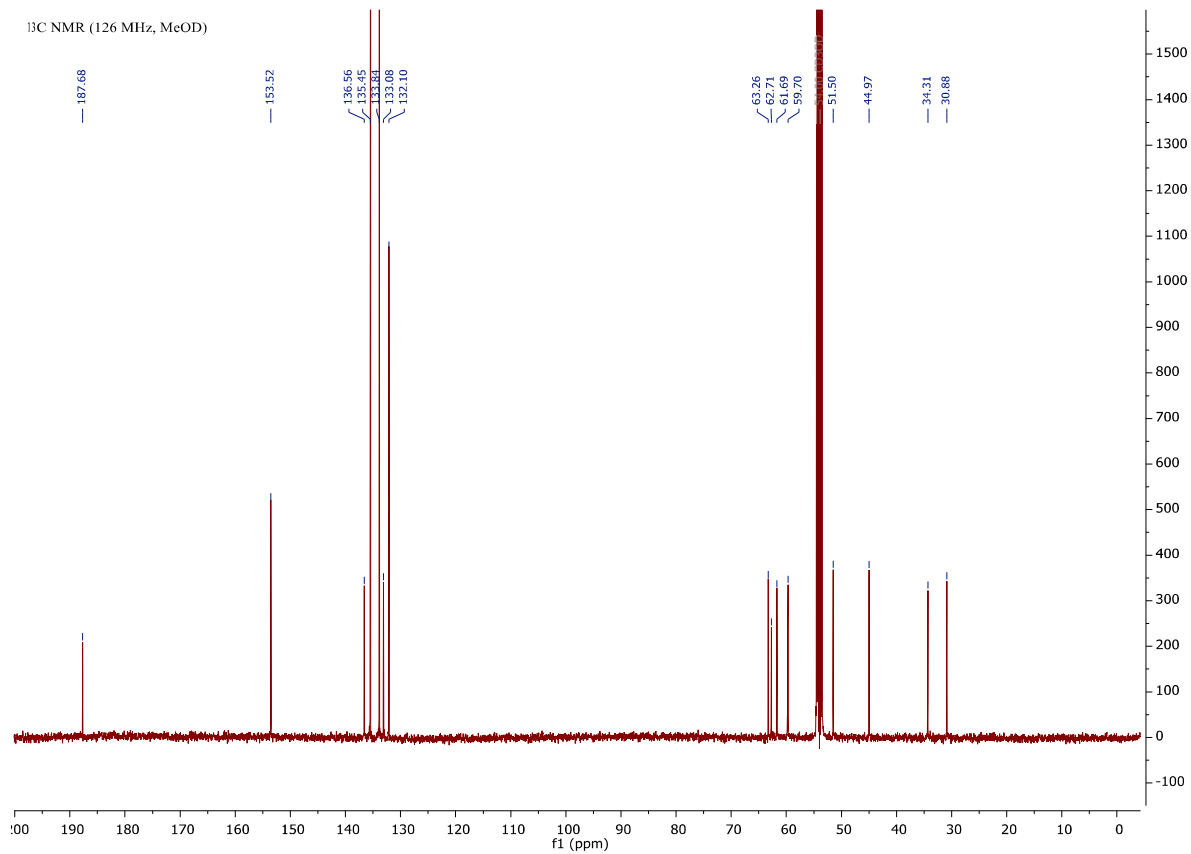
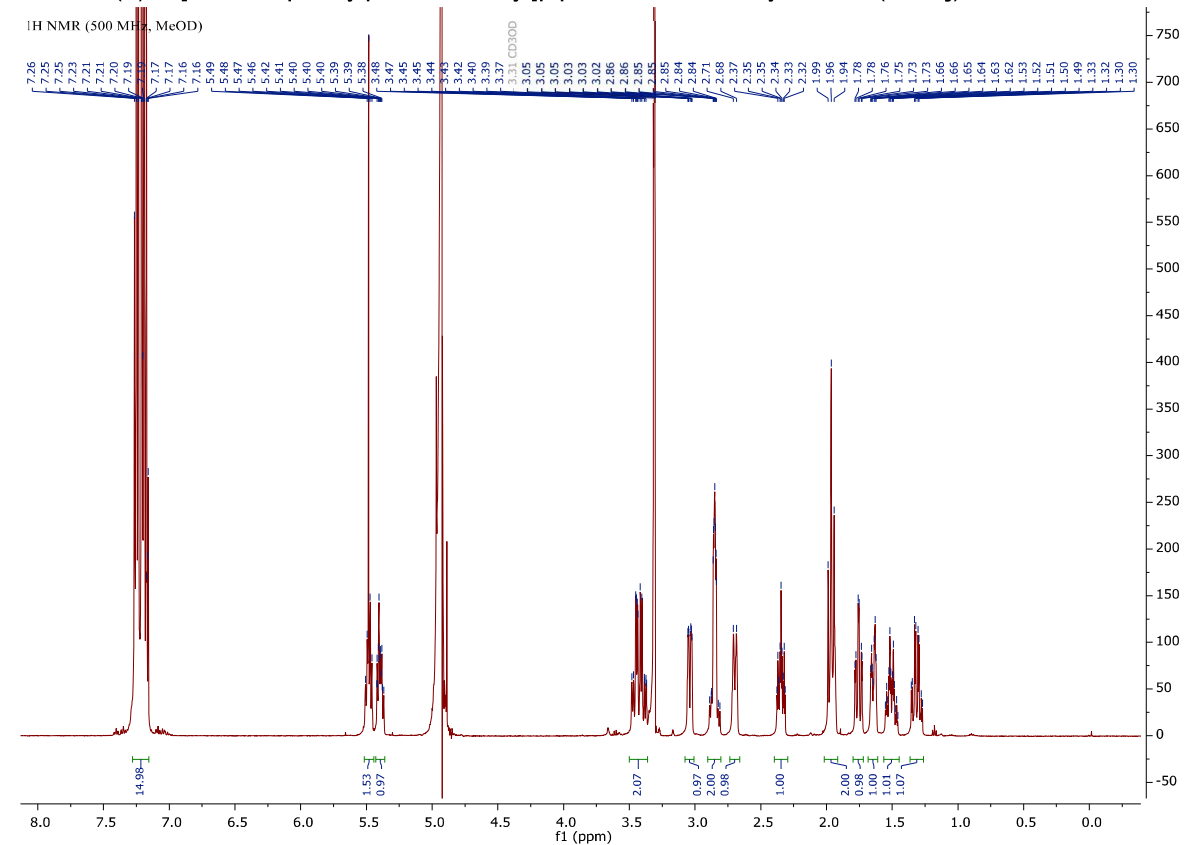
1.6. (Z)-1-[4,4-Bis(4-methoxyphenyl)but-2-en-1-yl]piperidine-3-carboxylic acid, (*rac*-7f)



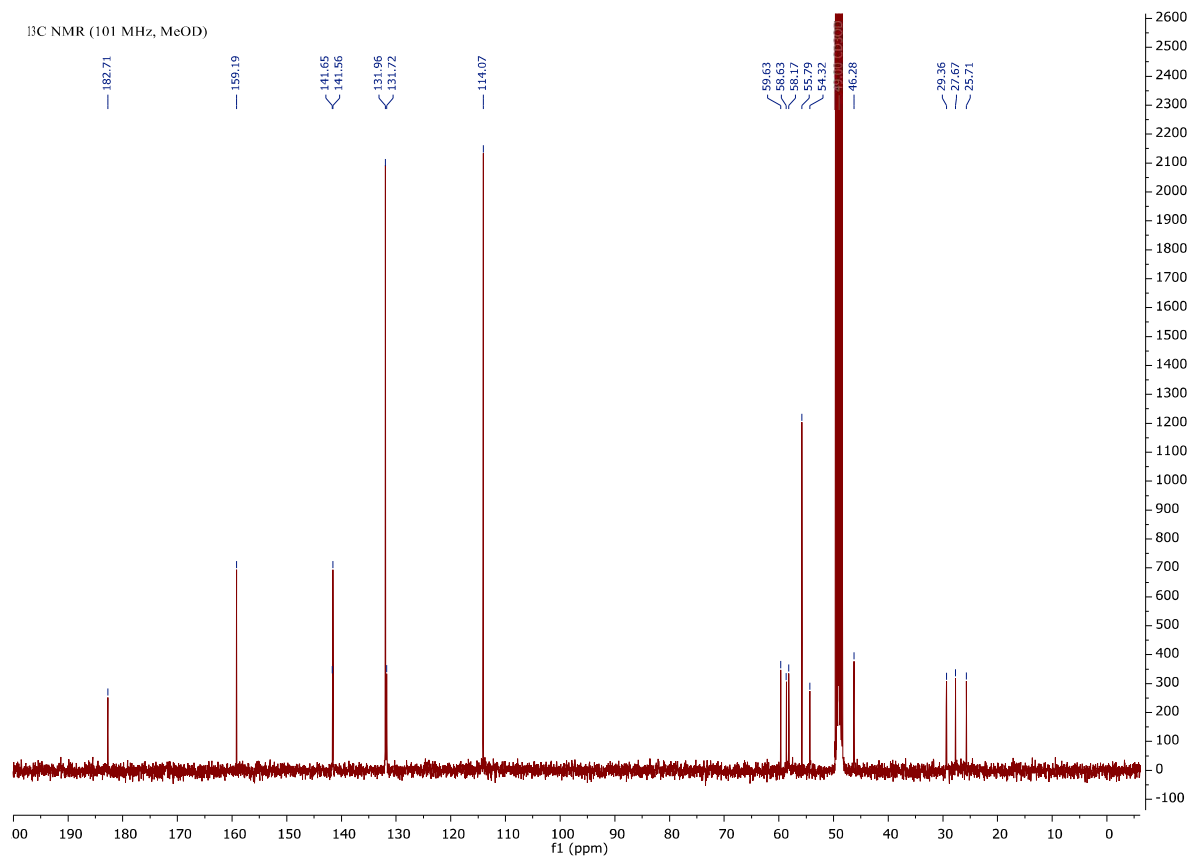
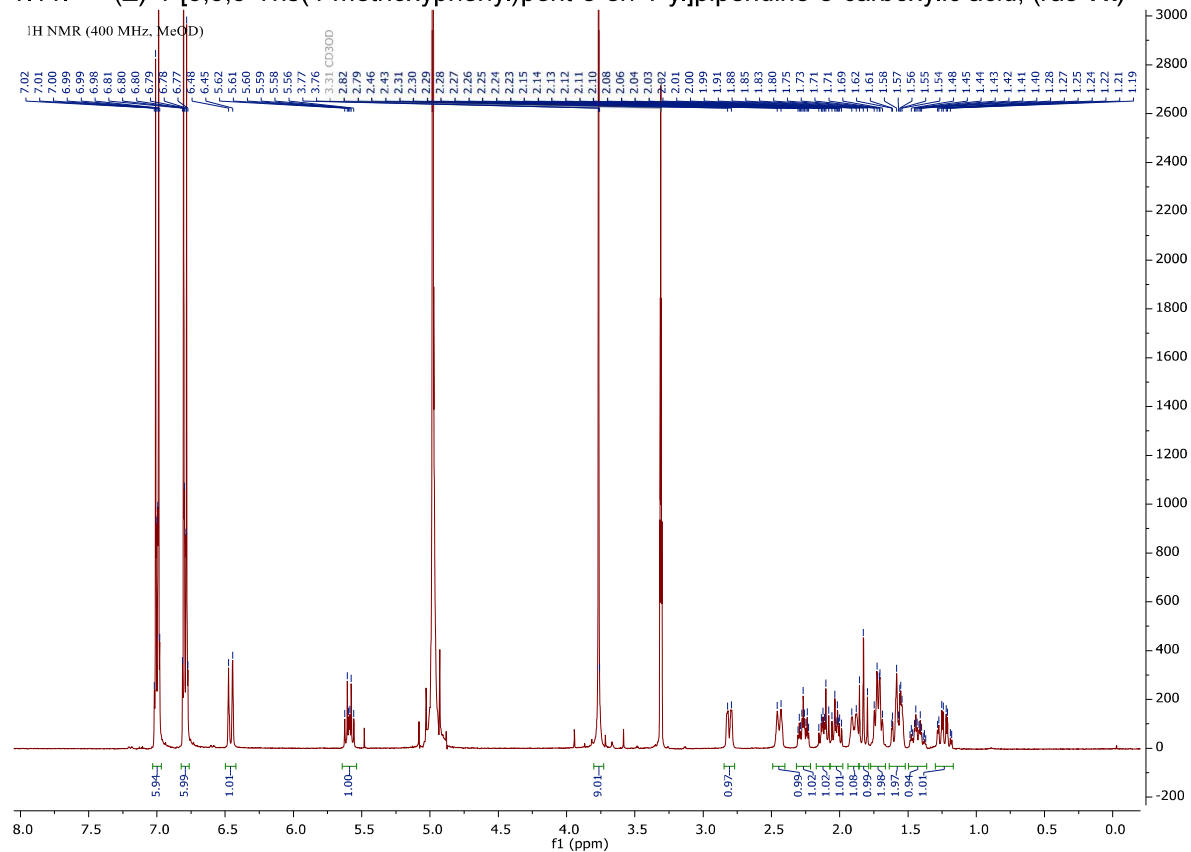
1.8. (Z)-1-[4,4-Bis(4-methoxyphenyl)-5-phenylpent-2-en-1-yl]piperidine-3-carboxylic acid, (*rac*-7h)



1.10. (Z)-1-[5,5,5-Triphenylpent-2-en-1-yl]piperidine-3-carboxylic acid, (*rac*-7j)



1.11. (Z)-1-[5,5,5-Tris(4-methoxyphenyl)pent-3-en-1-yl]piperidine-3-carboxylic acid, (rac-7k)



1.12. (Z)-1-[5,5,5-Triphenylpent-3-en-1-yl]piperidine-3-carboxylic acid, (*rac*-7I)

